Part IV

TWO-FERMION PRODUCTION IN ELECTRON–POSITRON COLLISIONS

Conveners: Michael Kobel[1,a] and Zbigniew Wąs[2]

Working group: C. Ainsley[3], A. Arbuzov[4,5], S. Arcelli[6], D. Bardin[7], I. Boyko[7], D. Bourilkov[8,b], P. Christova[7,9], J. Fujimoto[10], M. Grünewald[11], T. Ishikawa[10], M. Jack[12], S. Jadach[13,2], L. Kalinovskaya[7], Y. Kurihara[10], A. Leike[14], R. Mcpherson[15], M-N. Minard[16,c], G. Montagna[17,18], M. Moretti[19,20], T. Munehisa[21], O. Nicrosini[18,17], A. Olchevski[7,22,d], F. Piccinini[18,17], B. Pietrzyk[16], W. Płaczek[23], S. Riemann[12], T. Riemann[12], G. Taylor[24,e], Y. Shimizu[10], M. Skrzypek[2], S. Spagnolo[25], B.F.L. Ward[13,26]

[1] Physikalisches Institut, Universität Bonn, Germany

[2] Institute of Nuclear Physics, ul. Kawiory 26a, 30-055, Cracow, Poland

[3] High Energy Physics Group, Cavendish Laboratory, University of Cambridge, UK

[4] DFT, Università di Torino; INFN, Sezione di Torino; via Giuria 1, I-10125 Torino, Italy

[5] BLTPh, Joint Institute for Nuclear Research, Dubna, 141980, Russia

[6] EPHEPG, Department of Physics and Astronomy, University of Maryland, USA

[7] LNP, JINR, RU-141980, Dubna, Russia

[8] Institute for Particle Physics, ETH Zurich, Switzerland

[9] Faculty of Physics, Bishop Preslavsky University, Shoumen, Bulgaria

[10] High Energy Accelerator Research Organization (KEK), Tsukuba, Ibaraki 305-0801, Japan

[11] Humboldt University Berlin, Germany

[12] DESY, D-15738 Zeuthen, Germany

[13] Department of Physics and Astronomy The University of Tennessee, Knoxville, Tennessee 37996-1200, USA

[14] Sektion Physik, Ludwig-Maximilians-Universität München, Germany

[15] Department of Physics and Astronomy, TRIUMF, University of Victoria, Canada

[16] LAPP, IN2P3-CNRS, F-74941 Annecy-le-Vieux, France

[17] Dipartimento di Fisica Nucleare e Teorica, Università di Pavia, Italy

[18] INFN, Sezione di Pavia, Italy

[19] Dipartimento di Fisica, Università di Ferrara, Italy

[20] INFN, Sezione di Ferrara, Italy

[21] Yamanashi University, Kofu, Yamanashi 400-8510, Japan

[22] EP Division, CERN, CH-1211 Geneva 23, Switzerland

[23] Institute of Computer Science, Jagellonian University, Cracow, Poland

[24] SCIPP Natural Sciences II, University of California, USA

[25] Rutherford Appleton Laboratory, UK

[26] SLAC, Stanford University, Stanford, California 94309, USA.

[a] Coordinator for OPAL Collab., [b] Coordinator for L3 Collab., [c] Doordinator for ALEPH Collab.,

[d] Coordinator for DELPHI Collab., [e] Experimental coordinator for $\nu\bar{\nu}\gamma$ channels.

1 INTRODUCTION

At LEP2 the two-fermion production has the highest cross section of all hard processes. At LEP1 it serves as the unique reaction to study the properties of the Z boson and it had a very distinct two-body character, as the photon initial state emission (ISR) was highly suppressed. At LEP2, far above the Z pole, the ISR is strong and frequent, the radiative tail of the Z develops to such an extent that the ISR QED radiative corrections are several times as large as the Born cross sections. Another important fact is that one needs to account for the production of secondary real fermion-anti-fermion pairs (usually light and soft) due to the radiation of off-shell photons and Z bosons from the initial- or final-state. This makes the task of the 'signal definition', that is what we really mean by the two-fermion final state, rather nontrivial, in other words there is the question of the separation between the radiative corrections to two-fermion production and the genuine four-fermion production. This aspect of the two-fermion process was highlighted in the discussion of the LEP Electroweak Group and also in the presentations in the beginning of the current workshop. One aim of the workshop therefore was to come up with a 2-fermion signal definition, which is applicable to all 2-fermion final states, and suited equally well for theoretical predictions and experimental measurements.

The other topics which emerged as important theoretical issues for the work in two-fermion group were the question of the reliability of the existing QED calculations, especially of the so called initial-final state interference, and the question of the reliability of the pure electroweak corrections. The outstanding performance of the machine gave LEP experiments sizable samples of events with one and two explicitly (tagged) photons which are very useful for searches of the phenomena beyond the Standard Model (SM). The evaluation of the rates of these events from QED was high on the agenda of our work from the beginning.

The layout of our chapter reflects to a large extent the evolution of the work of our two-fermion group. In general we pursued two ways of collecting, evaluating and improving theoretical calculations for two-fermion precess. On one hand, we collected all available theoretical calculations, as implemented in Monte Carlo (MC) and semi-analytical programs (codes) and we applied them to get predictions for all cross sections, asymmetries, etc. measured in LEP2 experiments, which were identified in first place, with the help of our experimental coordinators, one for each LEP collaboration. All codes bear their own theoretical error specification and applicability range. This what we call the 'wide-range comparisons' of many codes for many observables has given us confidence into individual error specifications, or has led to some questions to be solved either within this workshop or beyond. On the other hand, the alternative path was followed of the so called 'tuned-comparisons' or 'theme-comparisons' which either concentrated on the more detailed comparisons of 2-3 codes, usually concentrating just on one theoretical problem and trying to reduce just one source of the theoretical errors, for example from QED effects. The prominent part of the 'theme-comparisons' was the study on the effects of the secondary pair production process.

Having this in mind the outline of the report is not surprising. In the first section we amass the rich list of processes and measurable quantities for all 2-fermion channels, that is the Bhabha process, the quark-, μ-, τ-pair channels, without and with tagged photons which are one pillar of the 'wide-range comparisons'. Another pillar is the third section in which all theoretical calculations/codes are collected – each of them includes its individual total theoretical error and range of applicability. In the second section we present the harvest of the wide-range comparisons, summarizing in a quantitative way results of them, channel per channel.

The 'theme-comparisons' are located in the fourth section and their subset related to secondary pair production was important enough to be awarded the status of the separate fifth section.

In the last section we summarize all important results and list the problems in two-fermion production which are still left out for further work.

2 EXPERIMENTAL OBSERVABLES AND THEORETICAL PRECISION REQUIREMENTS

This section collects specifications of the quantities measured in the two-fermion process at LEP2 which we call for short 'observables', and we also try for each listed observable to define the necessary precision level of the theoretical prediction, keeping in mind the total experimental error which will be achieved at the end of LEP2 operation, for data combined for all four LEP experiments.

The great diversity of these observables is a distinct feature of the two-fermion process, as compared to the WW channel or QCD studies, see other sections. It is partly due to the fact that various final states like muon-pairs, tau-pairs, quark-pairs, neutrino-pair with gamma and the Bhabha process have very different experimental characteristics, different methods of measurement and each of them comes in two versions, accepting Z radiative return or rejecting it. Furthermore, the two-fermion process cannot be experimentally completely disentangled from the four-fermion process, multiplying again the possible option for defining the *two-fermion observables.* On top of that there are still (and will be) differences between the ways the four experiments define and measure their cross-sections, asymmetries and distributions.

In this section we make a sort of 'frontal attack' on the problem of defining what is measured as a two-fermion process at LEP2, by doing the most complete list of two-fermion observables used in LEP2 data analysis. The primary aim of this is to help theorists to understand what is really measured in LEP2 and what are the ultimate precision targets in the LEP2 data. However, such an exhaustive list can also be useful for experimental collaborations when combining data from four LEP collaborations.

We never had a hope to have a complete theoretical prediction and full discussion of theoretical errors for all this impressive list of two-fermion observables. It is not even necessary as some of them are quite similar, and some of them are rather difficult to implement for the average theorist. In the process of scrutinizing various theoretical calculations we use only part of these observables, mostly of the 'simplified type'. The simplified observables are also necessary because semi-analytical programs can provide predictions only for them and not for the realistic ones. (MC event generators have no such limitations.) Another role of simplified observables is that they are prototypes of the observables used for combining data from the four LEP collaborations.

For the so called 'tuned comparisons' which were made for instance among $\mathcal{KK}$MC and ZFITTER or between BHWIDE and LABSMC the authors of these codes have used their own, even more simple kinematic cuts, tailored specifically to these tests. They are not discussed in this section.

The observables which *include* the Z resonance in the phase space, that is Z-*inclusive,* and which *exclude* the Z resonance, that is Z-*exclusive,* we usually denote them using the short-hand notation 'inclusive observables' and 'exclusive observables' instead of the full 'Z-inclusive' and 'Z-exclusive'. We hope that this will not lead to confusion, and wherever necessary we shall expand to the full terminology.

For the purpose of our main aim, that is of establishing theoretical errors for the *typical two-fermion observables* this section contains too much information. We think, however, that it is a valuable asset of this report and we decided to keep it to the full extent, accepting that only some of them will be really used in the actual *theoretical* studies.

2.1 Precision requirements for theoretical predictions

One of the most important ingredient of the observable definition is its precision tag. Obviously the higher precision the more complicated the study of its theoretical uncertainties will be. Also more of the details of experimental cuts will be needed to estimate the theoretical systematic errors.

The following rule of thumb with respect to the errors obtained for the data taken at $\sqrt{s} = 189\,\mathrm{GeV}$ was suggested for estimating the required precision in cases where there is no better information available.

1. The experimental statistical error is decreased by factor of $\sqrt{12} \simeq 3.5$ with respect to present (summer 1999) one for the single collaboration. We still expect statistics to grow by factor of 3 and combination of all 4 experiments makes the total statistics a factor of 12 bigger.

2. The experimental systematic error can be expected to go down by a factor of 2 (may be 3) due to improvements and partial non-correlations among experiments.

3. The above estimates of the experimental statistical and systematic error should be added in quadrature.

4. The required precision should be $1/3$ of that to assure that theoretical effects will not deteriorate experimental results (will not increase an error) by more than 10%.

The demand of a maximum of 10% increase of the final experimental overall error due to theoretical uncertainties is not an over-demand. It is equivalent to a decrease in running time of experiments by 20% in cases when the statistical error dominates. A similar 10% deterioration of an overall detection performance would occur only after a 30% decrease in data taking for measurements where the statistical and systematic errors are similar in size. Having this in mind and also an enormous effort of so many people over so many years, not mentioning the costs, may even lead to the conclusion that our rule for precision requirements from theory is not strict enough.

In general as inclusive (incl.) we understand the cross section for $\sqrt{s'/s} > 0.1$ and as exclusive (excl.) for $\sqrt{s'/s} > 0.85$. For Bhabha excl_1 denotes $|\cos\theta| < 0.9$ and excl_2 denotes $|\cos\theta| < 0.7$. For asymmetries the (absolute) error tag can be obtained from the one of thecross section multiplying it by $0.01\cdot\sqrt{2}$ and dropping the % symbol.

The following precision tags can be assumed if explicit numbers do not overrule them in the text:

1. cross sections for $q\bar{q}$ final states: incl. 0.11%, excl. 0.23%

2. cross sections for e^-e^+ final states: excl_1 0.13%, excl_2 0.21%

3. cross sections and asymmetries for $\mu^-\mu^+$ final states: incl. 0.41%, excl. 0.53%

4. cross sections and asymmetries for $\tau^-\tau^+$ final states: incl. 0.44%, excl. 0.61%

5. searches background cross sections from quarks and tagged hard photons 0.3%

6. searches background cross sections from leptons and tagged hard photons:
   single photons 1.5%, multiple photons 5%

7. searches background cross sections from neutrinos and tagged hard photons
   single photons 0.5%, multiple photons 2%

These numbers serve as a starting point for the definition of precision tags required from complete theoretical calculations. For separate ingredients such as interferences pair corrections etc, the physical precision tag must be even more strict, to assure that their combination will not overcome the required tag. Finally the tag for technical tests must be set another factor of few smaller.

2.2 General comments on observable definition

In the following chapters the observables will be defined. For more details see respectively: ALEPH [1], DELPHI [2] for all observables, for ($f\bar{f}(\gamma)$) processes L3 [3–6], OPAL [7–9]; for ($\ell\bar{\ell}+\gamma$) [10, 11]; and for ($\nu\bar{\nu}+\gamma$) [12–14].

The main groups of observables are formed by physics processes, they are later divided into *realistic* and *idealized* ones corresponding to different stages of experimental analysis. Finally specific solutions adopted by experiments are placed in the subsections. Some points which could be extracted from the observables definition like a glossary or the approach to the extra pair are discussed at the beginning of the chapter to avoid unnecessary repetition.

The purpose of the list of observables is to review all necessary conditions for calculation of theoretical predictions. More explanatory examples are given later in the section.

2.3 Notation

In definition of observables we will use some short-hand notations to make it easier. Let us illustrate just a few of them.

- E_{cm}: centre of mass energy.
- θ_γ: The polar angle of particle γ with respect to the electron beam.
- $|\cos\theta_{f/\bar{f}}| < 0.9$: The polar angle of both particles f and $\bar{f}$ must satisfy the cut.
- E_γ: The energy of particle γ.
- $x_\gamma = 2E_\gamma/E_{cm}$: The energy fraction of particle γ.
- N_{trk}: Number of charged tracks in the event.
- $\mathrm{a}col(e^+e^-)$: The collinearity angle between particles e^+ and e^-.
- A_{FB}: forward-backward asymmetry constructed on the basis of final state charged particles.
- $M_{prop-}(f\bar{f})$: invariant mass of the s-channel propagator, with ISR/FSR interference subtracted.
- $M_{prop+}(f\bar{f})$: invariant mass of the s-channel propagator, with ISR/FSR interference not subtracted. In this case, the propagator mass is ambiguous for the interference contribution, so this part is actually evaluated using the $f\bar{f}$ invariant mass excluding radiative photons.
- $M_{inv}(f\bar{f})$: invariant mass of f and $\bar{f}$ - all other particles such as collinear photons are excluded. For realistic observables, this is determined from the reconstructed 4-momenta of the two particles.
- $M_{ang}(f\bar{f})$: invariant mass determined from the measured polar angles of particles f and $\bar{f}$ with respect to the electron beam. These are taken from jet angles in case of hadrons. This calculation is based on four-momentum conservation assuming that only one radiative photon is present. If no photon is seen in the detector, this radiative photon is assumed to go along the beam axis. If an energetic, isolated photon is seen in the detector, then its reconstructed polar angle is used.
- $M_{kine}(f\bar{f})$: invariant mass determined from a kinematic fit. This uses 4-momentum conservation to improve the mass estimate based on the reconstructed 4-momenta of the f and $\bar{f}$.
- s'_{L3} for $\mu^+\mu^-$ or $\tau^+\tau^-$ from observed ISR photon (E more than 10 GeV, $|\cos\theta_\gamma| < 0.985$, separation to nearest fermion more than 10 degrees), *or* from fermion angles assuming photon escapes along the beam pipe

- s'_{L3} for $q\bar{q}$: to reconstruct the effective centre-of-mass energy two different methods are used. For the first one, all events are reclustered into two jets using the JADE algorithm. A single ISR photon is assumed to be emitted along the beam axis and to result in a missing momentum vector. From the polar angles of the jets, θ_1 and θ_2, the photon energy can be estimated. The second method uses the clustered jets ($y_{\rm cut} = 0.01$) obtained using the JADE algorithm. A kinematic fit is performed on the jets and the missing four-momentum vector using different hypotheses for the emitted ISR photons. The missing energy is attributed to zero, one or two ISR photons. From the differences given by the two methods, systematic errors on the effective centre-of-mass energy reconstruction are calculated. When an isolated energetic photon (energy larger than 10 GeV) is detected, the energy and momentum of this photon are added to the undetected ISR photons.

- $s'_{\rm OPAL}$ for $\rm q\overline{q}$: from a series of kinematic fits using observed ISR photons ($|\cos\theta_\gamma| < 0.985$, isolated with less than 1 GeV energy flow in a cone of half angle 0.2 rad around them) plus hadronic jets. The fits allow zero, one or two additional photons emitted close to the beam direction. s' is taken from the fit with the lowest number of extra photons giving an acceptable χ^2.

2.4 Additional pair treatment

ALEPH

Apart from the cuts listed for realistic observables, no additional requirement is added to reject events with real or virtual pair emission, their contribution is taken in account for efficiency calculation. The main rejection to 4-fermions process is due to invariant mass cuts associated to the topological cut on the event shape. For a two-fermion final state they are considered as backgrounds and their residual contribution estimated from Monte-Carlo four-fermion events for which both fermion pair invariant mass $\rm f\overline{f}$ or $\rm f'\overline{f'}$ are above 65 GeV. This excludes from the signal definition the 4-fermions arising from virtual Z or W contribution, but not the contribution from virtual photon. The above requirement are valid for hadronic, muon pairs and tau pairs. Note that for ALEPH the pair contribution is kept both in realistic and idealized observables.

DELPHI

In the case of idealized observables it is assumed that theoretical predictions should not include either real or virtual pair corrections. These are subtracted from the data with the help of the Monte Carlo. The appropriate systematic error is to be discussed with the help of Monte Carlo program or programs. Monte Carlo predictions for idealized observables with pair corrections excluded are required as well as for realistic observables with pair corrections included. In the case of realistic observables implicit cuts on additional fermion pairs are given, where appropriate, with the sufficient detail for DELPHI observables. Exceptions are $\nu\bar{\nu}\gamma$ observables, where events are required to have no jets/leptons (ch) within the DELPHI acceptance, that is of energy $E_{ch} > 0.5$ GeV and $|\cos\theta_{ch}| < 0.97$.

L3

Let us define first the cut on the secondary pairs for idealized observables:

- We assume that all the phase space for the secondary pairs is included and integrated over, however contribution form resonant diagrams from 4-fermion processes etc. must be subtracted from the data first by means of Monte Carlo.

For the secondary pair cut to be used for realistic L3 observables our aim was to describe it in a form as brief as possible. In particular we accept ambiguities which may lead to differences much smaller than precision tag. The cut off on the secondary pair is performed in the following way:

- The invariant mass of the primary pair must be at least 60 GeV for qq, 75 GeV for $\mu\mu/\tau\tau$. The invariant mass is determined from collinearity of primary pair and other tracks under assumption

that missing is only single photon (collinear to the beam). The primary pair means lepton same-flavor anti-lepton or two jets, of highest energies.

- cut on invariant mass of the secondary pair to be smaller than invariant mass of the primary pair is not explicitly required, but it is in practice through the selection targets on the 2 highest energy jets to form the primary pair, seen in the detector.

- The W and Z-pair production background is reduced by applying the following cuts. Semi-leptonic W-pair decays are rejected by requiring the transverse energy imbalance to be smaller than 0.3 $E_{\rm vis}$. The background from hadronic W(Z)-pair decays is reduced by rejecting events with at least four jets each with energy larger than 15 GeV. The jets are obtained using the JADE algorithm with a fixed jet resolution parameter $y_{\rm cut} = 0.01$. The remaining part of the 4-fermion processes due to W and Z contributions remain and must be subtracted later with the help of Monte Carlo of well established theoretical uncertainty.

- For Bhabha there is no explicit cut on primary mass, but implicit cut on secondary pair is present through the collinearity cut. The primary electrons are selected as the two highest in energy clusters which are matched to charged tracks. Note that in this way we allow the presence of photon(s) which is harder than one or both of the final state e^+e^-.

- $M_{inv}(e^+e^-)$ ($L3$) and electron clusters definitions: In L3 electrons are considered dressed, absorbing photons (or extra pairs) in a half-cone 2.5 deg, all these can be seen as detector coverage is larger than used phase space.

- our definition is not practical for primary pair being neutrinos. Then, instead we request veto cut, no visible charged energy deposits above 1 GeV and $\cos_{\theta_X} < 0.97$.

OPAL

To define our strategy for additional pair treatment let us recall the main points from the Ref. [7]. No additional cuts, apart those listed for the respective observables, are applied to reject events with pair emission. In general, we compare our measurements with analytical predictions including pair emission. This means that pair emission via virtual photons from both the initial and final state must be included in efficiency calculations, and be excluded from background estimates. In order to perform the separation, we ignore interference between s- and t-channel diagrams contributing to the same four-fermion final state, and generate separate Monte Carlo samples for the different diagrams for each final state. For a two-fermion final state $\mathrm{f\bar{f}}$ we then include as signal those four-fermion events arising from s-channel processes for which $m_{\mathrm{f\bar{f}}} > m_{\mathrm{f'\bar{f}'}}$, $m_{\mathrm{f'\bar{f}'}} < 70$ GeV and $m_{inv}(\mathrm{f\bar{f}})/\sqrt{s} > 0.1$ ($m_{inv}(\mathrm{f\bar{f}})/\sqrt{s} > 0.85$ in the non-radiative case). This kinematic classification closely models the desired classification of $\mathrm{f\bar{f}f'\bar{f}'}$ in terms of intermediate bosons, in that pairs arising from virtual photons are generally included as signal whereas those arising from virtual Z bosons are not. All events arising from s-channel processes failing the above cuts, together with those arising from the t-channel process (Zee) and two-photon processes are regarded as background. Four-fermion processes involving WW or single W production are also background in all cases. The overall efficiency, ϵ, is calculated as

$$\epsilon = \left(1 - \frac{\sigma_{\mathrm{f\bar{f}f'\bar{f}'}}}{\sigma_{\rm tot}}\right)\epsilon_{\mathrm{f\bar{f}}} + \frac{\sigma_{\mathrm{f\bar{f}f'\bar{f}'}}}{\sigma_{\rm tot}}\epsilon_{\mathrm{f\bar{f}f'\bar{f}'}} \qquad (1)$$

where $\epsilon_{\mathrm{f\bar{f}}}$, $\epsilon_{\mathrm{f\bar{f}f'\bar{f}'}}$ are the efficiencies derived from the two-fermion and four-fermion signal Monte Carlo events respectively, $\sigma_{\mathrm{f\bar{f}f'\bar{f}'}}$ is the generated four-fermion cross-section, and $\sigma_{\rm tot}$ is the total cross-section from the analytical prediction (e.g. ZFITTER) including pair emission. Using this definition of efficiency, effects of cuts on soft pair emission in the four-fermion generator are correctly summed with vertex corrections involving virtual pairs. The inclusion of the four-fermion part of the signal produces negligible changes to the efficiencies for hadronic events and for lepton pairs with $\sqrt{s'_{OPAL}/s} > 0.85$.

The efficiencies for lepton pairs with $\sqrt{s'_{OPAL}/s} > 0.10$ are decreased by about 0.5%. The discussion in the above paragraph applies to hadronic, muon pair and tau pair final states. In the case of electron pairs, the situation is slightly different. In principle the t-channel process with a second fermion pair arising from the conversion of a virtual photon emitted from an initial- or final-state electron should be included as signal. As this process is not included in any program we use for comparison we simply ignore such events: they are not included as background as this would underestimate the cross-section.

2.5 Realistic $e^+e^- \to q\bar{q}(\gamma)$ observables

ALEPH

1. **Inclusive Selection: Aleph1** Event clustered into jets with JADE algorithm until $(M_{jet-jet}/E_{cm})^2 > 0.008$. Low mass jets with high electromagnetic energy fraction are assumed to be radiative photons. Non-photon jets then cluster together until only two left, corresponding to the $q\bar{q}$ system. Then

   (a) **Aleph1a** $M_{inv}(q\bar{q}) > 50$ GeV (excluding photon jets),

   (b) **Aleph1b** $M_{ang}(q\bar{q}) > 0.1E_{cm}$.

2. **Exclusive Selection: Aleph2** Same as inclusive selection, then following extra cuts,

   (a) **Aleph2a** $M_{inv}(q\bar{q}) > 0.7E_{cm}$ (excluding photon jets),

   (b) **Aleph2b** $M_{ang}(q\bar{q}) > 0.9E_{cm}$,

   (c) **Aleph2c** $|\cos\theta_{q/\bar{q}}| < 0.95$,

   (d) **Aleph2d** Event thrust > 0.85.

DELPHI

Events were retained if they contained at least 7 charged tracks and if the charged energy was greater than 15 % of the collision energy. In addition, the quantity $E_{rad} = \sqrt{E_F^2 + E_B^2}$, where E_F and E_B stand for the total energy seen in the Forward and Backward electromagnetic calorimeters, was required to be less than 90% of the beam energy.

3. **Inclusive Selection: Delphi1** $M_{\rm ang}(q\bar{q}) > 75$ GeV

4. **Exclusive Selection: Delphi2** $M_{\rm ang}(q\bar{q})/\sqrt{s} > 0.85$

L3

Events are selected by restricting the visible energy, $E_{\rm vis}$, to $0.4 < E_{\rm vis}/\sqrt{s} < 2.0$. The longitudinal energy imbalance must satisfy $|E_{\rm long}|/E_{\rm vis} < 0.7$. These cuts account for a large reduction of the two-photon background. In order to reject background originating from lepton pair events, more than 18 calorimetric clusters with an energy larger than 300 MeV are requested.

5. **Inclusive Selection 1: LT1** $\sqrt{s'_{\rm L3}/s} > 0.10$

6. **Inclusive Selection 2: LT2** $\sqrt{s'_{\rm L3}} > 60$ GeV

7. **Exclusive Selection: LT3** $\sqrt{s'_{\rm L3}/s} > 0.85$

OPAL

Events are required to have at least 7 electromagnetic clusters and at least 5 tracks. The total energy deposited in the electromagnetic calorimeter has to be at least 14% of the centre-of-mass energy. The

energy balance R_{bal} along the beam direction has to satisfy $R_{bal} \equiv \mid \Sigma(E_{clus} \cdot \cos\theta) \mid / \Sigma E_{clus} < 0.75$, where the sum runs over all clusters in the electromagnetic calorimeter, θ is the polar angle, and E_{clus} is the energy of each cluster. Events selected as W-pair candidates according to the criteria of [15] are rejected.

8. **Inclusive Selection: OPAL1** $\sqrt{s'_{OPAL}/s} > 0.10$
9. **Exclusive Selection: OPAL2** $\sqrt{s'_{OPAL}/s} > 0.85$

2.6 Idealized $e^+e^- \to q\bar{q}(\gamma)$ observables

ALEPH

10. **Inclusive Selection: IAleph1** $M_{prop+}(q\bar{q})/E_{cm} > 0.1$.
11. **Exclusive Selection: IAleph2** $M_{prop+}(q\bar{q})/E_{cm} > 0.9$ and $|\cos\theta_q| < 0.95$.

DELPHI

12. **Inclusive Selection: IDelphi1** $M_{prop+}(q\bar{q})/E_{cm} > 0.1$ and $|\cos\theta_q| < 1.0$.
13. **Exclusive Selection: IDelphi2** $M_{prop+}(q\bar{q})/E_{cm} > 0.85$ and $|\cos\theta_q| < 1.0$.

L3

14. **Inclusive Selection 1: ILT1** $M_{prop-}(q\bar{q})/E_{cm} > 0.10$ and $|\cos\theta_q| < 1.0$.
15. **Inclusive Selection 2: ILT2** $M_{prop-}(q\bar{q}) > 60$ GeV and $|\cos\theta_q| < 1.0$.
16. **Exclusive Selection: ILT3** $M_{prop-}(q\bar{q})/E_{cm} > 0.85$ and $|\cos\theta_q| < 1.0$.

OPAL

17. **Inclusive Selection: IOpal1** $M_{prop-}(q\bar{q})/E_{cm} > 0.10$ and $|\cos\theta_q| < 1.0$.
18. **Exclusive Selection: IOpal2** $M_{prop-}(q\bar{q})/E_{cm} > 0.85$ and $|\cos\theta_q| < 1.0$.

2.7 Realistic $e^+e^- \to e^+e^-(\gamma)$ observables

ALEPH

19. **Exclusive Selection 1: Aleph3** $2 \le N_{trk} \le 8$. Two of tracks must be identified as electrons, have $|\cos\theta| < 0.95$ and opposite charge. The scalar sum of their momenta should exceed $0.3E_{cm}$. The sum of their energies including photons within 20° of each tracks should exceed $0.4E_{cm}$. Then $M_{inv}(e^+e^-) > 80$ GeV (reconstructed from track momenta), $M_{ang}(e^+e^-) > 0.9E_{cm}$ (where radiative photons reconstructed as for $q\bar{q}$ selection), and $-0.9 < \cos\theta^*_{e^-} < 0.9$.
20. **Exclusive Selection 2: Aleph4** Same as exclusive selection 1, but $-0.9 < \cos\theta^*_{e^-} < 0.7$.

DELPHI

21. **Exclusive Selection: Delphi3** The electron and positron were required to be in the polar angle range $44^\circ < \theta < 136^\circ$ and the non-radiative events were selected by asking the collinearity to be smaller than 20°.

L3

The electron and positron are required to be in the polar angle range $44^\circ < \theta < 136^\circ$ or $20^\circ < \theta < 160^\circ$ and non-radiative events are selected by asking the collinearity to be smaller than 20° OR $M_{inv}(e^+e^-)/E_{cm} > 0.85$.

22. **Exclusive Selection 1: LT4** $M_{inv}(e^+e^-)/E_{cm} > 0.85$ and $|\cos\theta_{e^+/e^-}| < 0.71934$.
23. **Exclusive Selection 2: LT5** $\mathrm{a}col(e^+e^-) < 25^\circ$ and $|\cos\theta_{e^+/e^-}| < 0.71934$.
24. **Exclusive Selection 3: LT6** $\mathrm{a}col(e^+e^-) < 25^\circ$ and $|\cos\theta_{e^+/e^-}| < 0.94$.
25. **Inclusive Selection 1: LT7** $\mathrm{a}col(e^+e^-) < 120^\circ$ and $|\cos\theta_{e^+/e^-}| < 0.71934$.
26. **Inclusive Selection 2: LT8** $M_{inv}(e^+e^-)/E_{cm} > 0.10$ and $|\cos\theta_{e^+/e^-}| < 0.94$.

OPAL

Events selected as electron pairs are required to have at least two and not more than eight clusters in the electromagnetic calorimeter, and not more than eight tracks in the central tracking chambers. At least two clusters must have an energy exceeding 20% of the beam energy, and the total energy deposited in the electromagnetic calorimeter must be at least 50% of the centre-of-mass energy. For the inclusive selection and the exclusive selection 1, at least two of the three highest energy clusters must each have an associated central detector track. If all three clusters have an associated track, the two highest energy clusters are chosen to be the electron and positron. For the large acceptance exclusive selection 2, no requirement is placed on the association of tracks to clusters, but the requirement on the total electromagnetic energy is increased to 70% of the centre-of-mass energy.

27. **Inclusive Selection: Opal3** $\mathrm{acol}(e^+e^-) < 170^\circ$ and $|\cos\theta_{e^+/e^-}| < 0.9$.
28. **Exclusive Selection 1: Opal4** $\mathrm{acol}(e^+e^-) < 10^\circ$ and $|\cos\theta_{e^-}| < 0.7$.
29. **Exclusive Selection 2: Opal5** $\mathrm{acol}(e^+e^-) < 10^\circ$ and $|\cos\theta_{e^+/e^-}| < 0.96$.

2.8 Idealized $e^+e^- \to e^+e^-(\gamma)$ observables

ALEPH

30. **Exclusive Selection 1: IAleph3** $M_{inv}(e^+e^-)/E_{cm} > 0.9$ and $-0.9 < \cos\theta^*_{e^-} < 0.9$.
31. **Exclusive Selection 2: IAleph4** $M_{inv}(e^+e^-)/E_{cm} > 0.9$ and $-0.9 < \cos\theta^*_{e^-} < 0.7$.

DELPHI

32. **Exclusive Selection: IDelphi4** $M_{inv}(e^+e^-)/E_{cm} > 0.85$ and $|\cos\theta_{e^+/e^-}| < 0.7$.

L3

33. **Exclusive Selection 1: ILT4** $M_{inv}(e^+e^-)/E_{cm} > 0.85$ and $|\cos\theta_{e^+/e^-}| < 0.71934$.
34. **Exclusive Selection 2: ILT5** $\mathrm{a}col(e^+e^-) < 25^\circ$ and $|\cos\theta_{e^+/e^-}| < 0.71934$.
35. **Exclusive Selection 3: ILT6** $\mathrm{a}col(e^+e^-) < 25^\circ$ and $|\cos\theta_{e^+/e^-}| < 0.94$.
36. **Inclusive Selection 1: ILT7** $\mathrm{a}col(e^+e^-) < 120^\circ$ and $|\cos\theta_{e^+/e^-}| < 0.71934$.
37. **Inclusive Selection 2: ILT8** $M_{inv}(e^+e^-)/E_{cm} > 0.10$ and $|\cos\theta_{e^+/e^-}| < 0.94$.

OPAL

38. **Inclusive Selection: IOpal3** $\mathrm{acol}(e^+e^-) < 170^\circ$ and $|\cos\theta_{e^+/e^-}| < 0.9$.

39. **Exclusive Selection 1: IOpal4** $\mathrm{acol}(e^+e^-) < 10^\circ$ and $|\cos\theta_{e^-}| < 0.7$.

40. **Exclusive Selection 2: IOpal5** $\mathrm{acol}(e^+e^-) < 10^\circ$ and $|\cos\theta_{e^+/e^-}| < 0.96$.

2.9 Realistic $e^+e^- \to \mu^+\mu^-(\gamma)$ observables

ALEPH

41. **Inclusive Selection: Aleph5** $2 \le N_{trk} \le 8$. Two tracks must be identified as muons, have $p > 6$ GeV, $|\cos\theta| < 0.95$ and opposite charge. The scalar sum of their momenta should exceed 60 GeV. Photons are identified from jets clustered with JADE algorithm until $(M_{jet-jet}/E_{cm})^2 > 0.008$. Then $M_{ang}(\mu^+\mu^-)/E_{cm} > 0.10$ (where radiative photons reconstructed as for $q\bar{q}$ selection).

42. **Exclusive Selection: Aleph6** Same as inclusive selection, then following extra cuts, $M_{ang}(\mu^+\mu^-)$ $/E_{cm} > 0.9E_{cm}$ (where radiative photons reconstructed as for $q\bar{q}$ selection) and $M_{inv}(\mu^+\mu^-) > 0.74$ (excluding photons).

DELPHI

An event was required to have two identified muons in the polar angle range $20^\circ \le \theta_\mu \le 160^\circ$ and the highest muon momentum of at least $30\ GeV/c$. $M_{inv}(\mu^+\mu^-)$ was calculated from a kinematic fit, where four different topologies were investigated for each event: i) no photon radiated, ii) one photon radiated along the beam line, iii) one seen and one unseen photon in any direction, iv) a single unseen photon in any direction. The seen photon fit was performed if a neutral energy deposit greater than $5\ GeV$ was measured in the electromagnetic calorimeters.

43. **Inclusive Selection: Delphi4** $M_{inv}(\mu^+\mu^-) > 75$ GeV

44. **Exclusive Selection: Delphi5** $M_{inv}(\mu^+\mu^-)/E_{cm} > 0.85$

L3

An event must have two identified muons in the polar angle range $20^\circ \le \theta_\mu \le 160^\circ$ and the highest muon momentum should exceed 35 GeV. The effective centre-of-mass energy for each event is determined assuming the emission of a single ISR photon. In case the photon is found in the detector ($|\cos\theta_\gamma| < 0.985$) it is required to have an energy, E_γ, larger than 15 GeV in the electromagnetic calorimeter and an angular separation to the nearest muon of more than 10 degrees. Otherwise the photon is assumed to be emitted along the beam axis and its energy is calculated from the polar angles of the outgoing muons.

45. **Inclusive Selection: LT9** $M_{ang}(\mu^+\mu^-) > 75$ GeV

46. **Exclusive Selection: LT10** $M_{ang}(\mu^+\mu^-)/E_{cm} > 0.85$

OPAL

$N_{trk} \ge 2$. A pair of tracks is taken as muon pair candidate, if both tracks are identified as muons, have $p > 6$ GeV, $|\cos\theta| < 0.95$ and are separated by 320 mrad in azimuthal angle ϕ. If more than one pair of tracks satisfies the above conditions, the pair with the largest scalar momentum sum is chosen. The event is rejected if more than one other track has a transverse momentum greater than 0.7 GeV. Finally, E_{vis}, defined as the scalar sum of the two muon momenta plus the energy of the highest energy cluster in the electromagnetic calorimeter ($|\cos\theta| < 0.985$), has to be larger than $0.35\sqrt{s} + 0.5M_z^2/\sqrt{s}$. For photon to be used in definition of M_{ang} it has to be separated at least by 200 mrad from charged muons.

47. **Inclusive Selection: Opal6** $M_{ang}(\mu^+\mu^-)/E_{cm} > 0.10$ and $M_{inv}(\mu^+\mu^-) > 70$ GeV, if $0.35\sqrt{s} < E_{vis} - 0.5M_z^2/\sqrt{s} < 0.75\sqrt{s}$.

48. **Exclusive Selection: Opal7** $M_{ang}(\mu^+\mu^-)/E_{cm} > 0.85$ and $M_{inv}(\mu^+\mu^-) > \sqrt{M_Z^2 + 0.1s}$.

2.10 Idealized $e^+e^- \to \mu^+\mu^-(\gamma)$ observables

ALEPH

49. **Inclusive Selection: IAleph5** $M_{inv}(\mu^+\mu^-)/E_{cm} > 0.1$ and $|\cos\theta_{\mu^-}| < 0.95$.

50. **Exclusive Selection: IAleph6** $M_{inv}(\mu^+\mu^-)/E_{cm} > 0.9$ and $|\cos\theta_{\mu^-}| < 0.95$.

DELPHI

51. **Inclusive Selection: IDelphi5** $M_{inv}(\mu^+\mu^-) > 75$ GeV and $|\cos\theta_{\mu^-}| < 0.95$.

52. **Exclusive Selection: IDelphi6** $M_{inv}(\mu^+\mu^-)/E_{cm} > 0.85$ and $|\cos\theta_{\mu^-}| < 0.95$.

L3

53. **Inclusive Selection: ILT9** $M_{inv}(\mu^+\mu^-) > 75$ GeV and $|\cos\theta_{\mu^-}| < 0.90$.

54. **Exclusive Selection 1: ILT10** $M_{inv}(\mu^+\mu^-)/E_{cm} > 0.85$ and $|\cos\theta_{\mu^-}| < 0.90$.

55. **Exclusive Selection 2: ILT11** $M_{inv}(\mu^+\mu^-)/E_{cm} > 0.85$ and $|\cos\theta_{\mu^-}| < 1.0$.

OPAL

56. **Inclusive Selection: IOpal6** $M_{prop-}(\mu^+\mu^-)/\sqrt{s} > 0.10$ and $|\cos\theta_{\mu^-}| < 0.95$.

57. **Inclusive Selection: IOpal7** $M_{prop-}(\mu^+\mu^-)/\sqrt{s} > 0.10$ and $|\cos\theta_{\mu^-}| < 1.00$.

58. **Exclusive Selection: IOpal8** $M_{prop-}(\mu^+\mu^-)/\sqrt{s} > 0.85$ and $|\cos\theta_{\mu^-}| < 0.95$.

59. **Exclusive Selection: IOpal9** $M_{prop-}(\mu^+\mu^-)/\sqrt{s} > 0.85$ and $|\cos\theta_{\mu^-}| < 1.00$.

2.11 Realistic $e^+e^- \to \tau^+\tau^-(\gamma)$ observables

ALEPH

60. **Inclusive Selection: Aleph7** Two identified τ candidates with $M_{inv}(\tau^+\tau^-) > 25$ GeV and $\mathrm{a}col(\tau^+\tau^-) < 250$ mrad in plane perpendicular to beam axis. Then $M_{ang}(\tau^+\tau^-) > 0.1E_{cm}$ (where radiative photons are reconstructed as for $q\bar{q}$ selection).

61. **Exclusive Selection: Aleph8** Same as inclusive selection, then following extra cut $M_{ang}(\tau^+\tau^-) > 0.9E_{cm}$ (where radiative photons reconstructed as for $q\bar{q}$ selection) and $|\cos\theta_{\tau^-}| < 0.95$.

DELPHI

The leading track in each hemisphere was required to lie in the polar angle range $|\cos\theta| < 0.94$, and the observed charged particle multiplicity was requested to be unity in one hemisphere and no more than five in the other. At least one of the leading tracks was required to have momentum greater than $0.025 \times \sqrt{s}$. Full description of the cuts can be found in Ref. [2]. The $M_{ang}(\tau^+\tau^-)$ was calculated from fermion directions estimated by leading tracks.

62. **Inclusive Selection: Delphi6** $M_{ang}(\tau^+\tau^-) > 75$ GeV

63. **Exclusive Selection: Delphi7** $M_{ang}(\tau^+\tau^-)/E_{cm} > 0.85$

L3

Tau leptons are identified as narrow, low multiplicity jets, containing from one to five charged particles. Tau jets are formed by matching the energy depositions in the electromagnetic and hadron calorimeters with tracks in the central tracker and the muon spectrometer. Two tau jets of at least 3.5 GeV are required to lie within the polar angular range $|\cos\theta| < 0.92$. To reject background from two photon processes the most energetic jet must have an energy larger than 20 GeV. The reconstruction of the effective centre-of-mass energy follows the procedure described in the muon subsection, using the polar angles of the two tau jets. Full description of the cuts can be found in Ref. [4].

64. **Inclusive Selection: LT11** $M_{ang}(\tau^+\tau^-) > 75$ GeV

65. **Exclusive Selection: LT12** $M_{ang}(\tau^+\tau^-)/E_{cm} > 0.85$

OPAL

Tau-pair candidates are events with exactly two charged, low multiplicity cones with 35° half-angle.

- The event is rejected if it was selected as a μ pair.
- $N_{trk} < 7$, where N_{trk} is the number of tracks in the central detector.
- $N_{trk} + N_{clus} < 16$, where N_{clus} is the number of ECAL clusters.
- $|\cos\theta_{\tau^+\tau^-}| < 0.90$, where $|\cos\theta_\tau|$ is the cosine of the respective cone axis.
- $0.02 < R_{shw} < 0.7$, where R_{shw} is the summed ECAL energy scaled by the centre-of-mass energy.
- $R_{trk} < 0.8$, where R_{trk} is the scalar sum of track momenta scaled by the centre-of-mass energy.
- $R_{shw} > 0.2$ or $R_{trk} > 0.2$.
- $R_{shw} + R_{trk} < 1.05(1.10)$, for $|\cos\theta| > 0.7$ (< 0.7),where $|\cos\theta|$ is the average of the two tau cones.
- $|\cos\theta_{p^{ECAL}_{missing}}| < 0.99$, where $\cos\theta_{p^{ECAL}_{missing}}$ is the cosine of the direction of missing momentum calculated using the ECAL.
- $p_t^{ECAL} > 0.015\sqrt{s}$ where p_t^{ECAL} is the sum of the transverse ECAL energy.
- Events are rejected if $0.9 < E/p < 1.1$ in both cones.
- Using the values of θ_τ, the expected energy of each lepton is calculated assuming that the final state consists only of two leptons plus a single unobserved photon along the beam direction. We then require that $0.02 < \sqrt{(X_{E1}^2 + X_{E2}^2)} < 0.8$, and $\sqrt{(X_{P1}^2 + X_{P2}^2)} < 0.8$, where $X_{E1,E2}$ are the total electromagnetic calorimeter energies in each tau cone normalized to the expected value calculated above, and $X_{P1,P2}$ are the scalar sums of track momenta in the two tau cones, also normalized to the expected values.
- $\theta_{\text{acollinearity}} < 180^\circ - 2\tan^{-1}\left(\frac{2M_Z\sqrt{s}}{s-M_Z^2}\right) + 10^\circ$. This cut is placed 10° degrees above the expected radiative return peak.

- $\theta_{\mathrm{acoplanarity}} < 30^{\circ}$.

66. **Inclusive Selection: Opal8** $M_{ang}(\tau^+\tau^-)/\sqrt{s} > 0.10$.
67. **Exclusive Selection: Opal9** $M_{ang}(\tau^+\tau^-)/\sqrt{s} > 0.85$.

2.12 Idealized $e^+e^- \to \tau^+\tau^-(\gamma)$ observables

ALEPH

68. **Inclusive Selection: IAleph7** $M_{inv}(\tau^+\tau^-)/E_{cm} > 0.1$ and $|\cos\theta_{\tau^-}| < 0.95$.
69. **Exclusive Selection: IAleph8** $M_{inv}(\tau^+\tau^-)/E_{cm} > 0.9$ and $|\cos\theta_{\tau^-}| < 0.95$.

DELPHI

70. **Inclusive Selection: IDelphi7** $M_{inv}(\tau^+\tau^-) > 75$ GeV and $|\cos\theta_{\tau^-}| < 0.95$.
71. **Exclusive Selection: IDelphi8** $M_{inv}(\tau^+\tau^-)/E_{cm} > 0.85$ and $|\cos\theta_{\tau^-}| < 0.95$.

L3

72. **Inclusive Selection: ILT12** $M_{inv}(\tau^+\tau^-) > 75$ GeV and $|\cos\theta_{\tau^-}| < 0.92$.
73. **Exclusive Selection 1: ILT13** $M_{inv}(\tau^+\tau^-)/E_{cm} > 0.85$ and $|\cos\theta_{\tau^-}| < 0.92$.
74. **Exclusive Selection 2: ILT14** $M_{inv}(\tau^+\tau^-)/E_{cm} > 0.85$ and $|\cos\theta_{\tau^-}| < 1.0$.

OPAL

75. **Inclusive Selection 1: IOpal10** $M_{prop-}(\tau^+\tau^-)/\sqrt{s} > 0.10$ and $|\cos\theta_{\tau^-}| < 0.90$.
76. **Inclusive Selection 2: IOpal11** $M_{prop-}(\tau^+\tau^-)/\sqrt{s} > 0.10$ and $|\cos\theta_{\tau^-}| < 1.00$.
77. **Exclusive Selection: IOpal12** $M_{prop-}(\tau^+\tau^-)/\sqrt{s} > 0.85$ and $|\cos\theta_{\tau^-}| < 0.90$.
78. **Exclusive Selection: IOpal13** $M_{prop-}(\tau^+\tau^-)/\sqrt{s} > 0.85$ and $|\cos\theta_{\tau^-}| < 1.00$.

2.13 $\mathrm{q\overline{q}}\gamma$ observables

This section contains precision requirements for regions of phase space selected in searches for anomalous neutral gauge couplings (ZZγ,Z$\gamma\gamma$), especially for the visible $\gamma + Z \to \gamma + \mathrm{q\overline{q}}$ final state. The prominent Standard Model process populating this region is the radiative return to the Z. Numerical results are not provided, we expect uncertainties for initial state bremsstrahlung contributions to be similar to the one in case of leptons, however the additional, often dominant uncertainties due to interplay of the final state QCD interaction and photon emission, are not discussed in our section.

L3

79. **Total Cross-Section LT13** Hadronic events are selected by asking for more than 6 charged tracks and more than 11 calorimetric clusters. The transverse and longitudinal energy imbalances should be below 15 and 20% respectively. A photon with $14^{\circ} < \theta_{\gamma} < 166^{\circ}$ and energy $80\ \mathrm{GeV} < \sqrt{s - 2E_{\gamma}\sqrt{s}} < 110$ GeV is required. The precision tag is 0.3–0.4%.

OPAL

80. **Total Cross-Section Opal10** Events are selected with two jets and one visible photon, fulfilling a 3C kinematic fit, allowing an additional photon of at most 5% of the beam energy to be radiated along the beam pipe. The relevant phase space is defined by

    (a) $E_\gamma > 50$ GeV

    (b) $15^\circ < \theta_\gamma < 165^\circ$

    (c) angle between photon and closest jet, $\alpha_{\gamma-jet} > 30^\circ$.

    The required precision tag for the radiative return cross-section in this phase space for a LEP-combined analysis is 0.3%. It assumes uncorrelated experimental systematics and is dominated by the experimental statistics. For fully correlated experimental systematics the precision tag is 0.4%. Currently, the predictions of the $\mathcal{KK}$MC and PYTHIA generators in this phase space differ by 15%.

81. **Differential Cross-Section Opal11** Selected Events in the above phase space are subjected to a maximum likelihood fit in the differential distributions of $E_\gamma, \cos\theta_\gamma$, and $\cos\theta_q^\star$, which is the angle of the final state quark-jets in the Z rest frame. Precision tag: The ratio between the rate of events within $|\cos\theta_\gamma| < 0.7$ and the boundary of the acceptance has to be known within about 1%. The discrepancy between $\mathcal{KK}$MC and PYTHIA in the region $|\cos\theta_\gamma| < 0.7$ is currently at level of 30% (stat. significance 2σ).

2.14 $\ell\bar{\ell}\gamma$ observables

This final state is primarily used to search for single (one photon) or pair (two photons) production of excited leptons. In principle, the radiative return peak in $M_{\ell\ell}$ can be rejected in these searches, which is not possible in the anomalous neutral coupling analyses (see above). In practice, however, experimental resolution and further (final state) radiation reduce the power of such an anticut. Therefore both topologies (including and omitting the anticut) need to be studied.

ALEPH

Photons are required to have at least 15 GeV and $|\cos\theta_\gamma|$ <0.95. Leptons are also required to have $|\cos\theta_l|$ <0.95, they are identified from oppositely charged jet clustered from charged tracks (at most 3) with at least one jet above 5 GeV. The angle between the 2 jets being at least 30 degree and the photon candidate at least 10 degree from the charged jet.

- **$\ell\bar{\ell}$ plus one photon**
  Two leptons of same type are required accompanied of at least one photon. The two most energetic leptons and the most energetic photon are considered.

  82. **eeγ ALEPH-11** Two tracks are identified as electron and the sum of charged energy greater than 0.6*E_{cm}. Expected precision tag 1.4%
  83. $\mu\mu\gamma$ **ALEPH-12** Two muons have to be identified and charged energy greater than $0.6 * E_{cm}$. Precision tag 1.5%
  84. $\tau\tau\gamma$ **ALEPH-13** At least a 3-prong tau jet candidate in the event is required. Precision tag 1.7%

- **$\ell\bar{\ell}$ plus two photons**
  Two electrons (or muons or taus) have to be identified and 2-photon jet identified Isolation cut on the 4 angles between photon and lepton required to be at least 20 degree. The 2 reconstructed lepton–gamma masses have to agree within 5 GeV/c**2

85. **ee$\gamma\gamma$ ALEPH-14** Precision tag 3%.
86. $\mu\mu\gamma\gamma$ **ALEPH-15** Precision tag 5%.
87. $\tau\tau\gamma\gamma$ **ALEPH-16** Precision tag 8%.

DELPHI

Events with a visible energy above $0.2\sqrt{s}$ in the region $|\cos\theta| < 0.9397$ and not more than 6 charged tracks are selected. Photons are required to have an energy above 5 GeV and $|\cos\theta| < 0.9848$. The total charged (neutral) energy in a 15° cone around the photon is required to be below 1 GeV (2 GeV). Charged particles are clustered into jets. Jets are required to have $|\cos\theta| < 0.9063$ and the most energetic to have an energy above 5 GeV. In three- or four-body topologies the energies are rescaled by imposing energy momentum conservation and using the measured angles. An improved energy resolution is obtained. Compatibility between the measured and rescaled energies is required.

- $\ell\overline{\ell}$ **plus one photon** The energy of the photon is required to be above 10 GeV. Events with one photon and one or two jets in the final state are considered. This accounts for situations in which one of the leptons was lost in the beam pipe or has very low momentum (close to the kinematic limit). The expected backgrounds and thus the further selections and the efficiencies are very dependent on the lepton flavour.

  88. **eeγ DELPHI8**
  At least one jet identified as an electron and the other not identified as a muon, the most energetic jet with $E > 10$ GeV. One photon with $|\cos\theta| < 0.7660$. If only one jet is found the angle between the jet and the photon must be in the between 100° and 179°. Precision tag: 1.4%
  89. $\mu\mu\gamma$ **DELPHI9**
  At least one jet identified as a muon and no jets identified as electrons, the most energetic jet with $E > 10$ GeV. Precision tag: 1.6%
  90. $\tau\tau\gamma$ **DELPHI10**
  The most energetic jet with $E > 10$ GeV. One photon with $|\cos\theta| < 0.94$. Tau events are selected by requiring a difference between the measured and the rescaled energy of the jets, expected due to the presence of neutrinos. If only one jet is found the angle between the jet and the photon must be between 100° and 179°. Precision tag: 1.8%

- $\ell\overline{\ell}$ **plus two photons**

  Two jets and two photons in the event. Compatibility between two reconstructed $\ell\gamma$ masses is required. The relevant quantity is the minimum of the electron-photon invariant mass differences ($\Delta m_{\ell\gamma}$). The statistical error of the selection clearly dominates.

  91. **ee$\gamma\gamma$ DELPHI11**
  $\Delta m_{e\gamma} < 15$ GeV/c^2. Precision tag: 5%
  92. $\mu\mu\gamma\gamma$ **DELPHI12**
  $\Delta m_{\mu\gamma} < 10$ GeV/c^2 Precision tag: 6%
  93. $\tau\tau\gamma\gamma$ **DELPHI13**
  $\Delta m_{\tau\gamma} < 10$ GeV/c^2 Precision tag: 6%

L3

Hadronic events are rejected by requiring less than 8 charged tracks. Photons are required to have at least 15 GeV and $|\cos\theta_\gamma|$ <0.97. Leptons are required to have the same flavor and $|\cos\theta_l|$ <0.94. They are identified from oppositely charged tracks/low multiplicity jets(for tau).

- $\ell\overline{\ell}$ **plus one photon**
  At least one lepton accompanied by at most one hard photon. The second lepton may be in the beam pipe. The photon is required to have at least 20 GeV and $|\cos\theta_\gamma|$ <0.75. One mass (lγ) should be greater than 70 GeV.

  94. **ee**γ **LT14** Expected precision tag 1.2%
  95. $\mu\mu\gamma$ **LT15** Precision tag 1.5%
  96. $\tau\tau\gamma$ **LT16** Precision tag 1.8%

- $\ell\overline{\ell}$ **plus two photons**
  one phon (or muon or tau) and 2 photons seen. The photons are required to have at least 15 GeV and one should be in $|\cos\theta_\gamma|$ <0.75, the second in $|\cos\theta_\gamma|$ <0.94. The difference of the 2 reconstructed lepton-gamma masses should be below 10 GeV and their sum above 100 GeV.

  97. **ee**$\gamma\gamma$ **LT17** Precision tag 4%.
  98. $\mu\mu\gamma\gamma$ **LT18** Precision tag 6%.
  99. $\tau\tau\gamma\gamma$ **LT19** Precision tag 6%.

OPAL

Photon candidates are required to have an energy exceeding 5% of the beam energy, and have to lie within $|\cos\theta_\gamma| < 0.95$. Leptons are also identified within $|\cos\theta_\ell| < 0.95$ and are required to have $p_t > 1$ GeV. Photons, electrons, and muons are required to be isolated by at least 20 degree from the nearest charged track of momentum larger than 1 GeV.

- $\ell\overline{\ell}$ **plus one photon**
  There must be at least two identified leptons of the same type and at least one photon. The two most energetic leptons and the most energetic photon are used in the analysis. Their energy sum is called E_{vis} in the following. The precision tag assumes uncorrelated experimental systematics. Both, uncorrelated systematics, and expected statistical precision of the LEP combined result contribute to about equal parts to the precision tag. For correlated experimental systematics the required theoretical precision is loosened by about 0.9%.

  100. **ee**γ **w/o rad return rejection Opal12**
     - $E_{vis} > 1.6 E_{\rm beam}$
     - $|\cos\theta_\gamma| < 0.70$
     - $|\cos\theta_e| < 0.70$ for at least one electron.

     Precision tag: 1.3%
  101. **ee**γ **with rad return rejection Opal13**
     - $E_{vis} > 1.6 E_{\rm beam}$
     - $|\cos\theta_\gamma| < 0.70$
     - $|\cos\theta_e| < 0.70$ for at least one electron.
     - reject events with 85 GeV $< M_{ee} <$ 95 GeV

     Precision tag: 1.4%
  102. $\mu\mu\gamma$ **w/o rad return rejection Opal14**
     - $E_{vis} > 1.6 E_{\rm beam}$

     Precision tag: 1.5%

103. $\mu\mu\gamma$ **with rad return rejection Opal15**
   - $E_{vis} > 1.6E_{\rm beam}$
   - reject events with 85 GeV $< M_{\mu\mu} <$ 95 GeV

   Precision tag: 1.7%

104. $\tau\tau\gamma$ **w/o rad return rejection Opal16**
   - $0.8E_{\rm beam} < E_{vis} > 1.9E_{\rm beam}$

   Precision tag: 1.4%

105. $\tau\tau\gamma$ **with rad return rejection Opal17**
   - $0.8E_{\rm beam} < E_{vis} < 1.9E_{\rm beam}$
   - reject events with 85 GeV $< M_{\tau\tau} <$ 95 GeV

   Precision tag: 1.5%

- $\ell\overline{\ell}$ **plus two photons**
  There must be at least two identified leptons of the same type and at least two photons. The two most energetic leptons and the two most energetic photons are used in the analysis. Their energy sum is called E_{vis} in the following. The precision tag is dominated by the statistical error of the selection.

106. **ee**$\gamma\gamma$ **w/o rad return rejection Opal18**
   - $E_{vis} > 1.6E_{\rm beam}$
   - minimum opening angle among all electron-photon combinations $|\cos\alpha^{e\gamma}_{\rm min}| < 0.90$.

   Precision tag: 3%

107. **ee**$\gamma\gamma$ **with rad return rejection Opal19**
   - $E_{vis} > 1.6E_{\rm beam}$
   - minimum opening angle among all electron-photon combinations $|\cos\alpha^{e\gamma}_{\rm min}| < 0.90$.
   - reject events with 85 GeV $< M_{ee} <$ 95 GeV

   Precision tag: 3%

108. $\mu\mu\gamma\gamma$ **w/o rad return rejection Opal20**
   - $E_{vis} > 1.6E_{\rm beam}$

   Precision tag: 5%

109. $\mu\mu\gamma\gamma$ **with rad return rejection Opal21**
   - $E_{vis} > 1.6E_{\rm beam}$
   - reject events with 85 GeV $< M_{\mu\mu} <$ 95 GeV

   Precision tag: 6%

110. $\tau\tau\gamma\gamma$ **w/o rad return rejection Opal22**
   - $0.8E_{\rm beam} < E_{vis} > 1.9E_{\rm beam}$

   Precision tag: 5%

111. $\tau\tau\gamma\gamma$ **with rad return rejection Opal23**
   - $0.8E_{\rm beam} < E_{vis} < 1.9E_{\rm beam}$
   - reject events with 85 GeV $< M_{\tau\tau} <$ 95 GeV

   Precision tag: 6%

2.15 $\nu\bar{\nu}\gamma$ observables

The observables listed below do not include any cut to eliminate the regions of phase space dominated by the radiative return to the Z. Such events are usually selected by a cut on the mass of the invisible system. For such an extended observable the required precision tag should simply be scaled according to the somewhat decreased statistics. In general, *fully exclusive* predictions with help of the full multi-dimensional distributions of photon(s) energies and directions are needed with a precision comparable to that of the total cross section.

ALEPH

112. **Nu1** Single photon and missing energy: Exactly one photon with $|\cos\theta_\gamma| < 0.95$ and $P_t > 0.0375 * E_{cm}$. No other photon with $|\cos\theta_\gamma| < 0.9997$ and $E_\gamma > 1$ GeV.

113. **Nu2** Two or more photons and missing energy: Two or more photons, each with $E_\gamma > 1$ GeV and $|\cos\theta_\gamma| < 0.95$. The transverse momentum of the multi-photon system must be such that $\Sigma P_t > 0.0375 * (E_{cm} - \Sigma E)$. No other photon with $|\cos\theta_\gamma|$ between 0.95 and 0.9997, and $E_\gamma > 1$ GeV.

DELPHI

114. Single photon and missing energy: Require exactly one observed photon with energy requirement varying with polar angle

    (a) **Nu11** Very forward (or backward): $3.8^\circ < \theta < 6.5^\circ$, $x_\gamma > 0.3$ or $x_\gamma > (9.2 - \theta)/9$

    (b) **Nu12** Forward (or backward): $12^\circ < \theta < 32^\circ$, $x_\gamma > 0.2$

    (c) **Nu13** Barrel: $45^\circ < \theta < 90^\circ$, $x_\gamma > 0.06$

    No additional photons with $E_\gamma > 0.8$ GeV and $\theta > 38$ mrad unless they are within 3°, 15° and 20° from the primary photon for the very forward, forward and barrel regions, respectively.

115. Two or more photons and missing energy **Nu14**: Two or more photons with $E_\gamma > 0.05 * E_{beam}$ and $|\cos\theta_\gamma| < 0.985$, at least one of which has $|\cos\theta_\gamma| < 0.906$. No additional photon with $E_\gamma > 0.02 * E_{cm}$ and $|\cos\theta_\gamma|$ between 0.985 and 0.9994.

L3

116. Single photon and missing energy: Exactly one photon with $|\cos\theta_\gamma| < 0.97$ and:

    (a) **Nu3** energy and $P_t > 5$ GeV if $14^\circ < \theta$ /endcaps/

    (b) **Nu4g** energy and $P_t > 5$ GeV if $43^\circ < \theta$ /barrel/

    No other photon with $|\cos\theta_\gamma| < 0.9997$ and $E_\gamma > 10$ GeV.

117. Two or more photons and missing energy: each photon with $|\cos\theta_\gamma| < 0.97$ and:

    (a) **Nu5** energy and $P_t > 5$ GeV if $14^\circ < \theta$ (endcaps)

    (b) **Nu6** energy and $P_t > 1$ GeV if $43^\circ < \theta$ (barrel)

    The transverse momentum of the multi-photon system must be greater than 5 GeV and the collinearity greater than 2.5° No other photon with $|\cos\theta_\gamma| < 0.9997$ and $E_\gamma > 10$ GeV.

118. Single photon and missing energy**Nu7** : The maximum energy photon must have $|\cos\theta_\gamma| < 0.9660$ and $P_t > 0.05 * E_{beam}$. There may be at most ONE additional photon with $E_\gamma > 0.3$ GeV and $|\cos\theta_\gamma| < 0.9848$.

119. Two or more photons and missing energy: Two or more photons each with

    (a) **Nu8** $E_\gamma > 0.05 * E_{beam}$ and $|\cos\theta_\gamma| < 0.9660$,

    (b) **Nu9** $E_\gamma > 1.75$ GeV, $|\cos\theta_\gamma| < 0.8$ and the sum of their $P_t > 0.05 * E_{beam}$

    (c) **Nu10** $E_\gamma > 1.75$ GeV, $|\cos\theta_\gamma| < 0.966$ and the sum of their $P_t > 0.05 * E_{beam}$

3 DISCUSSION OF NUMERICAL RESULTS FOR IDEALIZED AND REALISTIC OBSERVABLES

In this section we compare numerical results from all MC and semi-analytical programs available in in our working group.

The aim of this exercise is two-fold:

- to check if these codes give meaningful predictions. Usually they do but it can be a nontrivial test, we also check in this way the applicability range of the codes.
- to probe the error specifications declared by the authors of the codes in the Section 4

In order to make the comparison meaningful we defined a common input. In general we took physical parameters from the latest publication of world averages in the PDG. For the Higggs mass we took $M_H = 120$ GeV.

For the QCD coupling the average $\alpha_S(M_Z)$ was used as an input. The value of $\Delta\alpha^{(5)}_{had}(M_Z) = 0.027782 \pm 0.000254$ is not present in PDG, and this value was taken from Ref. [16]. It contains updates of the analysis of Ref. [17]. For additional discussion on this subject see Section 3.1.

3.1 Hadronic low energy vacuum polarisation

Vacuum polarization makes about 6% correction to the value of α_{QED} at s = m_Z^2. The leptonic part of this contribution is known with excellent precision [18]. The quark part, however, is more difficult since the quark masses are not unambiguously defined and there is no general agreement that the pertubartive QCD can be use for reliable calculations. Several reevaluations of the hadronic contribution to the QED vacuum polarization have been performed to determine the effective QED coupling $\alpha(M_Z^2)$ [17, 19–30]. They are compared on Fig. 1. The results marked with * are obtained using a dispersion integral of R_{had}

$$R_{had} = \frac{\sigma(e^+e^- \to hadrons)}{\sigma(e^+e^- \to \mu^+\mu^-)}$$

measured experimentally. The uncertainties are dominated by the precision of measurement of $\sigma(e^+e^- \to hadrons)$ at the e^+e^- centre-of-mass energies below 5 GeV. The values not marked with * are obtained by using perturbative QCD in this region.

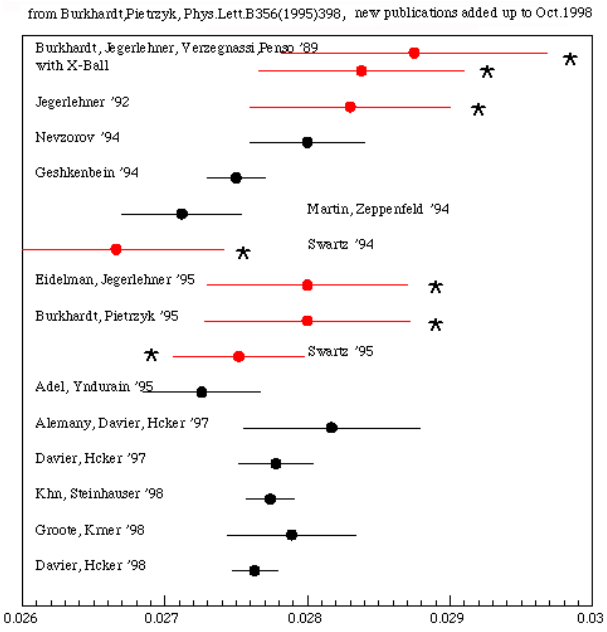

Fig. 1: Results of calculations of the hadronic contribution to the QED vacuum polarization. The results marked with * are obtained using a dispersion integral of R_{had} measured experimentally.

Table 1: α^{-1}(s) using results of calculations of Ref. [20].

$\sqrt{s}$ (GeV)	α^{-1}(s)
80.364	129.08 ± 0.09
91.1871	128.89 ± 0.09
161	128.07 ± 0.09
172	127.98 ± 0.09
183	127.89 ± 0.09
186	127.86 ± 0.09
192	127.82 ± 0.09
196	127.79 ± 0.09
200	127.76 ± 0.09
205	127.72 ± 0.09

The values of hadronic contributions presented in Fig. 1 are in good agreement. The precision of calculations using a dispersion integral of R_{had} measured experimentally is sufficient for the precision required at LEP2. The values of the effective QED coupling $\alpha(s)$ at different centre of mass are given in Table 1.

3.2 Discussion of numerical results for $q\bar{q}(\gamma)$ observables

There is good (0.1% or better) agreement between $\mathcal{KK}$MC and ZFITTER with pair corrections switched off, in all available entries in Table 2. For the observables where predictions from $\mathcal{KK}$MC are missing it is due to experimental treatment of the interference correction, which requires more runs of the Monte Carlo for every entry. The level of agreement is consistent with the predictions of the systematic theoretical uncertainties from the program authors. We can thus conclude that the systematic error from the QED/electroweak sector for these processes is indeed smaller than 0.2%. If pair effects

and their uncetrainty is taken into account as discussed in Section 5.5.11 the total uncertainty from the QED/electroweak sector is 0.26%.

Table 2: Numerical predictions from theoretical calculations of the following idealized observables in $q\bar{q}(\gamma)$ final states; *cross-sections*. The last field of the table shows relative deviation (multiplied by 100) with respect to the first calculation.

obs.	program	ene	value and error estimate	δ ratio
IAleph1	ZFITTER v6.30	189.0	$9.8387{\cdot}10^{1}$ $+5.22{\cdot}10^{-3}$ $-4.80{\cdot}10^{-2}$	
	ZF6.30 no pair	189.0	$9.6865{\cdot}10^{1}$ $+5.22{\cdot}10^{-3}$ $-5.11{\cdot}10^{-3}$	-1.55
	ZFITTER v6.30	206.0	$7.9133{\cdot}10^{1}$ $+6.58{\cdot}10^{-3}$ $-4.25{\cdot}10^{-2}$	
	ZF6.30 no pair	206.0	$7.7853{\cdot}10^{1}$ $+6.56{\cdot}10^{-3}$ $-2.83{\cdot}10^{-3}$	-1.62
IAleph2	ZFITTER v6.30	189.0	$1.9370{\cdot}10^{1}$ $+1.02{\cdot}10^{-2}$ $-1.66{\cdot}10^{-3}$	
	ZF6.30 no pair	189.0	$1.9400{\cdot}10^{1}$ $+8.28{\cdot}10^{-3}$ $-1.66{\cdot}10^{-3}$	0.16
	ZFITTER v6.30	206.0	$1.5456{\cdot}10^{1}$ $+8.52{\cdot}10^{-3}$ $-8.30{\cdot}10^{-4}$	
	ZF6.30 no pair	206.0	$1.5481{\cdot}10^{1}$ $+6.98{\cdot}10^{-3}$ $-8.31{\cdot}10^{-4}$	0.16
IDelphi1	ZFITTER v6.30	189.0	$9.6865{\cdot}10^{1}$ $+5.22{\cdot}10^{-3}$ $-5.11{\cdot}10^{-3}$	
	ZF6.30 no pair	189.0	$9.6865{\cdot}10^{1}$ $+5.22{\cdot}10^{-3}$ $-5.11{\cdot}10^{-3}$	0.00
	ZFITTER v6.30	206.0	$7.7853{\cdot}10^{1}$ $+6.56{\cdot}10^{-3}$ $-2.83{\cdot}10^{-3}$	
	ZF6.30 no pair	206.0	$7.7853{\cdot}10^{1}$ $+6.56{\cdot}10^{-3}$ $-2.83{\cdot}10^{-3}$	0.00
IDelphi2	ZFITTER v6.30	189.0	$2.2001{\cdot}10^{1}$ $+1.43{\cdot}10^{-3}$ $-1.88{\cdot}10^{-3}$	
	ZF6.30 no pair	189.0	$2.2001{\cdot}10^{1}$ $+1.43{\cdot}10^{-3}$ $-1.88{\cdot}10^{-3}$	0.00
	ZFITTER v6.30	206.0	$1.7540{\cdot}10^{1}$ $+1.39{\cdot}10^{-3}$ $-9.43{\cdot}10^{-4}$	
	ZF6.30 no pair	206.0	$1.7540{\cdot}10^{1}$ $+1.39{\cdot}10^{-3}$ $-9.43{\cdot}10^{-4}$	0.00
ILT1	ZFITTER v6.30	189.0	$9.8429{\cdot}10^{1}$ $+5.20{\cdot}10^{-3}$ $-4.80{\cdot}10^{-2}$	
	ZF6.30 no pair	189.0	$9.6906{\cdot}10^{1}$ $+5.20{\cdot}10^{-3}$ $-5.11{\cdot}10^{-3}$	-1.55
	KKMC 4.13	189.0	$9.6911{\cdot}10^{1}$ $\pm 2.54{\cdot}10^{-2}$	-1.54
	ZFITTER v6.30	206.0	$7.9167{\cdot}10^{1}$ $+6.58{\cdot}10^{-3}$ $-4.25{\cdot}10^{-2}$	
	ZF6.30 no pair	206.0	$7.7886{\cdot}10^{1}$ $+6.56{\cdot}10^{-3}$ $-2.83{\cdot}10^{-3}$	-1.62
	KKMC 4.13	206.0	$7.7907{\cdot}10^{1}$ $\pm 1.99{\cdot}10^{-2}$	-1.59
ILT2	ZFITTER v6.30	189.0	$9.6751{\cdot}10^{1}$ $+6.74{\cdot}10^{-3}$ $-4.39{\cdot}10^{-2}$	
	ZF6.30 no pair	189.0	$9.5273{\cdot}10^{1}$ $+6.74{\cdot}10^{-3}$ $-5.11{\cdot}10^{-3}$	-1.53
	KKMC 4.13	189.0	$9.5259{\cdot}10^{1}$ $\pm 2.54{\cdot}10^{-2}$	-1.54
	ZFITTER v6.30	206.0	$7.7847{\cdot}10^{1}$ $+8.01{\cdot}10^{-3}$ $-3.92{\cdot}10^{-2}$	
	ZF6.30 no pair	206.0	$7.6602{\cdot}10^{1}$ $+7.98{\cdot}10^{-3}$ $-2.83{\cdot}10^{-3}$	-1.60
	KKMC 4.13	206.0	$7.6609{\cdot}10^{1}$ $\pm 1.98{\cdot}10^{-2}$	-1.59
ILT3	ZFITTER v6.30	189.0	$2.2080{\cdot}10^{1}$ $+3.34{\cdot}10^{-3}$ $-1.88{\cdot}10^{-3}$	
	ZF6.30 no pair	189.0	$2.2100{\cdot}10^{1}$ $+1.43{\cdot}10^{-3}$ $-1.88{\cdot}10^{-3}$	0.09
	KKMC 4.13	189.0	$2.2096{\cdot}10^{1}$ $\pm 1.82{\cdot}10^{-2}$	0.08
	ZFITTER v6.30	206.0	$1.7603{\cdot}10^{1}$ $+2.95{\cdot}10^{-3}$ $-9.43{\cdot}10^{-4}$	
	ZF6.30 no pair	206.0	$1.7620{\cdot}10^{1}$ $+1.39{\cdot}10^{-3}$ $-9.44{\cdot}10^{-4}$	0.10
	KKMC 4.13	206.0	$1.7616{\cdot}10^{1}$ $\pm 1.43{\cdot}10^{-2}$	0.07
IOpal1	ZFITTER v6.30	189.0	$9.8429{\cdot}10^{1}$ $+5.20{\cdot}10^{-3}$ $-4.80{\cdot}10^{-2}$	
	ZF6.30 no pair	189.0	$9.6906{\cdot}10^{1}$ $+5.20{\cdot}10^{-3}$ $-5.11{\cdot}10^{-3}$	-1.55
	KKMC 4.13	189.0	$9.6911{\cdot}10^{1}$ $\pm 2.54{\cdot}10^{-2}$	-1.54
	ZFITTER v6.30	206.0	$7.9167{\cdot}10^{1}$ $+6.58{\cdot}10^{-3}$ $-4.25{\cdot}10^{-2}$	
	ZF6.30 no pair	206.0	$7.7886{\cdot}10^{1}$ $+6.56{\cdot}10^{-3}$ $-2.83{\cdot}10^{-3}$	-1.62
	KKMC 4.13	206.0	$7.7907{\cdot}10^{1}$ $\pm 1.99{\cdot}10^{-2}$	-1.59
IOpal2	ZFITTER v6.30	189.0	$2.2080{\cdot}10^{1}$ $+3.34{\cdot}10^{-3}$ $-1.88{\cdot}10^{-3}$	
	ZF6.30 no pair	189.0	$2.2100{\cdot}10^{1}$ $+1.43{\cdot}10^{-3}$ $-1.88{\cdot}10^{-3}$	0.09
	KKMC 4.13	189.0	$2.2096{\cdot}10^{1}$ $\pm 1.82{\cdot}10^{-2}$	0.08
	ZFITTER v6.30	206.0	$1.7603{\cdot}10^{1}$ $+2.95{\cdot}10^{-3}$ $-9.43{\cdot}10^{-4}$	
	ZF6.30 no pair	206.0	$1.7620{\cdot}10^{1}$ $+1.39{\cdot}10^{-3}$ $-9.44{\cdot}10^{-4}$	0.10
	KKMC 4.13	206.0	$1.7616{\cdot}10^{1}$ $\pm 1.43{\cdot}10^{-2}$	0.07

Some improvements in $\mathcal{KK}$MC and ZFITTER with respective to published versions to obtain that level of agreements were needed. Especially the question of choice of input parameters had to be revisited. See the Section 4.5 and 4.13 describing the programs and section on comparisons 5.4 for details. We can conclude that in all cases the overall QED uncertainty in quark channels are below the experimental precision tag. The effect due to pairs can not be neglected but even if it is included in a rather approximate way, this would be enough. We do not expect the appropriate uncertainty to be sizable enough to affect the experimental studies in any case.

Finally let us point that we were not addressing any questions related to uncertainties of final state QCD interactions, see report of the QCD working group in this report [31]. The QCD FSR corrections are implemented in $\mathcal{KK}$MC and ZFITTER as an overall K-factor taking into account all available higher orders, however, they do not take into account any kinematic cuts on real gluons. That is why their predictions for realistic observables are of the partial use only.

3.3 Discussion of numerical results for observables in $e^+e^-(\gamma)$ final states

Tuned BHWIDE LABSMC comparisons

Certain tuned comparisons of the BHWIDE and LABSMC programs were performed for the $e^+e^-(\gamma)$ observables. First, at the Born level an agreement was found between the predictions of the two programs (after adjusting the EW parameters) at the level of 0.1% (stat. errors). Then, cross-checks of the pure QED contribution to the Bhabha process were performed, i.e. of only the γ-exchange contribution with the pure QED corrections (photonic corrections only – no pairs). Here, the two programs differ up to 0.4% (the predictions of BHWIDE are in most cases lower than the ones of LABSMC). These differences can be explained by the different treatments of higher order QED corrections in the two programs: the YFS exponentiation in BHWIDE versus the structure function formalism in LABSMC. The biggest differences are for the observables with a direct cut on the 'bare' invariant mass $M_{inv}(e^+e^-)$. For such observables FSR plays an important role and the differences in the higher order FSR implementation in the two programs may be the reason for these discrepancies. The agreement for other observables is at the level of 0.1%.

Further comparisons

All idealized observables are computed with LABSMC and BHWIDE, for realistic observables only LABSMC results are available for OPAL. It would be very desirable to compare the MC codes with semi-analytic programs like TOPAZ0 that, unfortunately, did not contribute to the present Workshop.

At 189 GeV the agreement between BHWIDE and LABSMC is better than the following:

Type of observ.	Barrel	Endcaps
Real. obs.	1.4%	0.2%
Ideal. obs.	1.4-2.4%	0.1-0.6%

This is true for both cases: high-energy events and observable where Z-return is included. This does not contradicts the BHWIDE estimate that the precision in the barrel region is equal to or better than 1.5%, and can be after tests reduced to 0.5%. For the endcaps the precision is better or equal 0.5%, which is due to the dominant photon exchange in the t-channel when the forward region is included. The remaining differences between BHWIDE and LABSMC, as seen in Tables 3, 4, for the full Bhabha process come from non-QED contributions/corrections and are under investigation. At present our estimate of systematic error must remain at 2% for the barrel region and 0.5% for endcap.

The differences in case of observables with explicitly tagged photons, ($l\bar{l}\gamma$ final states) are, as expected bigger, but still at the 3% level.

For **DELPHI8** and **LT14** one of the electrons can be lost in the beam pipe. BHWIDE doesn't describe such configurations (both e^+, e^- are required to be detected) - that is why BHWIDE does not provide any results for these observables. OPAL's realistic observables: **Opal3**, **Opal4**, **Opal5**, are not implemented with BHWIDE also.

Table 3: Numerical predictions from theoretical calculations of the following realistic observables in $e^+e^-(\gamma)$ final states; *cross-sections*. The last field of the table shows relative deviation (multiplied by 100) with respect to the first calculation.

obs.	program	ene	value and error estimate	δ ratio
Aleph3	LABSMC no pair	189.0	$9.9101 \cdot 10^{1} \pm 1.65 \cdot 10^{-2}$	
	BHWIDE	189.0	$9.9232 \cdot 10^{1} \pm 2.71 \cdot 10^{-2}$	0.13
	LABSMC no pair	200.0	$8.8608 \cdot 10^{1} \pm 1.47 \cdot 10^{-2}$	
	BHWIDE	200.0	$8.8753 \cdot 10^{1} \pm 2.28 \cdot 10^{-2}$	0.16
	LABSMC no pair	206.0	$8.3566 \cdot 10^{1} \pm 1.39 \cdot 10^{-2}$	
	BHWIDE	206.0	$8.3709 \cdot 10^{1} \pm 2.10 \cdot 10^{-2}$	0.17
Aleph4	LABSMC no pair	189.0	$2.0475 \cdot 10^{1} \pm 7.51 \cdot 10^{-3}$	
	BHWIDE	189.0	$2.0410 \cdot 10^{1} \pm 1.03 \cdot 10^{-2}$	-0.32
	LABSMC no pair	200.0	$1.8230 \cdot 10^{1} \pm 6.69 \cdot 10^{-3}$	
	BHWIDE	200.0	$1.8204 \cdot 10^{1} \pm 8.60 \cdot 10^{-3}$	-0.14
	LABSMC no pair	206.0	$1.7159 \cdot 10^{1} \pm 6.29 \cdot 10^{-3}$	
	BHWIDE	206.0	$1.7143 \cdot 10^{1} \pm 8.00 \cdot 10^{-3}$	-0.09
Delphi3	LABSMC no pair	189.0	$2.3192 \cdot 10^{1} \pm 7.99 \cdot 10^{-3}$	
	BHWIDE	189.0	$2.2869 \cdot 10^{1} \pm 1.09 \cdot 10^{-2}$	-1.39
	LABSMC no pair	200.0	$2.0635 \cdot 10^{1} \pm 7.11 \cdot 10^{-3}$	
	BHWIDE	200.0	$2.0373 \cdot 10^{1} \pm 9.20 \cdot 10^{-3}$	-1.27
	LABSMC no pair	206.0	$1.9421 \cdot 10^{1} \pm 6.70 \cdot 10^{-3}$	
	BHWIDE	206.0	$1.9179 \cdot 10^{1} \pm 8.40 \cdot 10^{-3}$	-1.25
LT4	LABSMC no pair	189.0	$2.2142 \cdot 10^{1} \pm 7.81 \cdot 10^{-3}$	
	BHWIDE	189.0	$2.1862 \cdot 10^{1} \pm 1.07 \cdot 10^{-2}$	-1.27
	LABSMC no pair	200.0	$1.9700 \cdot 10^{1} \pm 6.95 \cdot 10^{-3}$	
	BHWIDE	200.0	$1.9474 \cdot 10^{1} \pm 9.00 \cdot 10^{-3}$	-1.15
	LABSMC no pair	206.0	$1.8543 \cdot 10^{1} \pm 6.54 \cdot 10^{-3}$	
	BHWIDE	206.0	$1.8332 \cdot 10^{1} \pm 8.30 \cdot 10^{-3}$	-1.14
LT5	LABSMC no pair	189.0	$2.3452 \cdot 10^{1} \pm 8.03 \cdot 10^{-3}$	
	BHWIDE	189.0	$2.3110 \cdot 10^{1} \pm 1.10 \cdot 10^{-2}$	-1.46
	LABSMC no pair	200.0	$2.0873 \cdot 10^{1} \pm 7.16 \cdot 10^{-3}$	
	BHWIDE	200.0	$2.0590 \cdot 10^{1} \pm 9.20 \cdot 10^{-3}$	-1.35
	LABSMC no pair	206.0	$1.9647 \cdot 10^{1} \pm 6.74 \cdot 10^{-3}$	
	BHWIDE	206.0	$1.9385 \cdot 10^{1} \pm 8.50 \cdot 10^{-3}$	-1.33
LT6	LABSMC no pair	189.0	$1.9768 \cdot 10^{2} \pm 2.33 \cdot 10^{-2}$	
	BHWIDE	189.0	$1.9738 \cdot 10^{2} \pm 3.83 \cdot 10^{-2}$	-0.15
	LABSMC no pair	200.0	$1.7673 \cdot 10^{2} \pm 2.08 \cdot 10^{-2}$	
	BHWIDE	200.0	$1.7650 \cdot 10^{2} \pm 3.22 \cdot 10^{-2}$	-0.13
	LABSMC no pair	206.0	$1.6664 \cdot 10^{2} \pm 1.96 \cdot 10^{-2}$	
	BHWIDE	206.0	$1.6644 \cdot 10^{2} \pm 2.97 \cdot 10^{-2}$	-0.12
LT7	LABSMC no pair	189.0	$2.4981 \cdot 10^{1} \pm 8.29 \cdot 10^{-3}$	
	BHWIDE	189.0	$2.4550 \cdot 10^{1} \pm 1.19 \cdot 10^{-2}$	-1.73
	LABSMC no pair	200.0	$2.2145 \cdot 10^{1} \pm 7.37 \cdot 10^{-3}$	
	BHWIDE	200.0	$2.1767 \cdot 10^{1} \pm 9.90 \cdot 10^{-3}$	-1.71
	LABSMC no pair	206.0	$2.0795 \cdot 10^{1} \pm 6.93 \cdot 10^{-3}$	
	BHWIDE	206.0	$2.0450 \cdot 10^{1} \pm 9.00 \cdot 10^{-3}$	-1.66
LT8	LABSMC no pair	189.0	$2.0661 \cdot 10^{2} \pm 2.38 \cdot 10^{-2}$	
	BHWIDE	189.0	$2.0692 \cdot 10^{2} \pm 4.01 \cdot 10^{-2}$	0.15
	LABSMC no pair	200.0	$1.8460 \cdot 10^{2} \pm 2.13 \cdot 10^{-2}$	
	BHWIDE	200.0	$1.8484 \cdot 10^{2} \pm 3.37 \cdot 10^{-2}$	0.13
	LABSMC no pair	206.0	$1.7406 \cdot 10^{2} \pm 2.01 \cdot 10^{-2}$	
	BHWIDE	206.0	$1.7423 \cdot 10^{2} \pm 3.10 \cdot 10^{-2}$	0.10
Opal3	LABSMC no pair	189.0	$1.0978 \cdot 10^{2} \pm 1.74 \cdot 10^{-2}$	
	LABSMC no pair	200.0	$9.7930 \cdot 10^{1} \pm 1.55 \cdot 10^{-2}$	
	LABSMC no pair	206.0	$9.2231 \cdot 10^{1} \pm 1.46 \cdot 10^{-2}$	
Opal4	LABSMC no pair	189.0	$2.0337 \cdot 10^{1} \pm 7.48 \cdot 10^{-3}$	
	LABSMC no pair	200.0	$1.8088 \cdot 10^{1} \pm 6.66 \cdot 10^{-3}$	
	LABSMC no pair	206.0	$1.7036 \cdot 10^{1} \pm 6.27 \cdot 10^{-3}$	
Opal5	LABSMC no pair	189.0	$3.0546 \cdot 10^{2} \pm 2.90 \cdot 10^{-2}$	
	LABSMC no pair	200.0	$2.7299 \cdot 10^{2} \pm 2.59 \cdot 10^{-2}$	
	LABSMC no pair	206.0	$2.5744 \cdot 10^{2} \pm 2.44 \cdot 10^{-2}$	

Table 4: Numerical predictions from theoretical calculations of the following idealized observables in $e^+e^-(\gamma)$ final states; *cross-sections*. The last field of the table shows relative deviation (multiplied by 100) with respect to the first calculation.

obs.	program	ene	value and error estimate	δ ratio
IAleph3	LABSMC no pair	189.0	$8.7693 \cdot 10^{1} \pm 1.55 \cdot 10^{-2}$	
	BHWIDE	189.0	$8.7187 \cdot 10^{1} \pm 2.60 \cdot 10^{-2}$	-0.58
	LABSMC no pair	200.0	$7.8259 \cdot 10^{1} \pm 1.39 \cdot 10^{-2}$	
	BHWIDE	200.0	$7.7826 \cdot 10^{1} \pm 2.19 \cdot 10^{-2}$	-0.55
	LABSMC no pair	206.0	$7.3692 \cdot 10^{1} \pm 1.30 \cdot 10^{-2}$	
	BHWIDE	206.0	$7.3329 \cdot 10^{1} \pm 2.01 \cdot 10^{-2}$	-0.49
IAleph4	LABSMC no pair	189.0	$1.8080 \cdot 10^{1} \pm 7.05 \cdot 10^{-3}$	
	BHWIDE	189.0	$1.7739 \cdot 10^{1} \pm 9.70 \cdot 10^{-3}$	-1.89
	LABSMC no pair	200.0	$1.6065 \cdot 10^{1} \pm 6.28 \cdot 10^{-3}$	
	BHWIDE	200.0	$1.5786 \cdot 10^{1} \pm 8.10 \cdot 10^{-3}$	-1.73
	LABSMC no pair	206.0	$1.5126 \cdot 10^{1} \pm 5.91 \cdot 10^{-3}$	
	BHWIDE	206.0	$1.4850 \cdot 10^{1} \pm 7.50 \cdot 10^{-3}$	-1.82
IDelphi4	LABSMC no pair	189.0	$1.8582 \cdot 10^{1} \pm 7.15 \cdot 10^{-3}$	
	BHWIDE	189.0	$1.8266 \cdot 10^{1} \pm 9.80 \cdot 10^{-3}$	-1.70
	LABSMC no pair	200.0	$1.6517 \cdot 10^{1} \pm 6.37 \cdot 10^{-3}$	
	BHWIDE	200.0	$1.6257 \cdot 10^{1} \pm 8.20 \cdot 10^{-3}$	-1.57
	LABSMC no pair	206.0	$1.5549 \cdot 10^{1} \pm 5.99 \cdot 10^{-3}$	
	BHWIDE	206.0	$1.5294 \cdot 10^{1} \pm 7.50 \cdot 10^{-3}$	-1.64
ILT4	LABSMC no pair	189.0	$2.0744 \cdot 10^{1} \pm 7.56 \cdot 10^{-3}$	
	BHWIDE	189.0	$2.0408 \cdot 10^{1} \pm 1.05 \cdot 10^{-2}$	-1.62
	LABSMC no pair	200.0	$1.8447 \cdot 10^{1} \pm 6.73 \cdot 10^{-3}$	
	BHWIDE	200.0	$1.8167 \cdot 10^{1} \pm 8.80 \cdot 10^{-3}$	-1.52
	LABSMC no pair	206.0	$1.7361 \cdot 10^{1} \pm 6.33 \cdot 10^{-3}$	
	BHWIDE	206.0	$1.7096 \cdot 10^{1} \pm 8.10 \cdot 10^{-3}$	-1.53
ILT5	LABSMC no pair	189.0	$2.3509 \cdot 10^{1} \pm 8.04 \cdot 10^{-3}$	
	BHWIDE	189.0	$2.3175 \cdot 10^{1} \pm 1.10 \cdot 10^{-2}$	-1.42
	LABSMC no pair	200.0	$2.0919 \cdot 10^{1} \pm 7.16 \cdot 10^{-3}$	
	BHWIDE	200.0	$2.0645 \cdot 10^{1} \pm 9.20 \cdot 10^{-3}$	-1.31
	LABSMC no pair	206.0	$1.9688 \cdot 10^{1} \pm 6.74 \cdot 10^{-3}$	
	BHWIDE	206.0	$1.9435 \cdot 10^{1} \pm 8.50 \cdot 10^{-3}$	-1.28
ILT6	LABSMC no pair	189.0	$1.9814 \cdot 10^{2} \pm 2.34 \cdot 10^{-2}$	
	BHWIDE	189.0	$1.9788 \cdot 10^{2} \pm 3.84 \cdot 10^{-2}$	-0.13
	LABSMC no pair	200.0	$1.7710 \cdot 10^{2} \pm 2.08 \cdot 10^{-2}$	
	BHWIDE	200.0	$1.7691 \cdot 10^{2} \pm 3.23 \cdot 10^{-2}$	-0.11
	LABSMC no pair	206.0	$1.6697 \cdot 10^{2} \pm 1.96 \cdot 10^{-2}$	
	BHWIDE	206.0	$1.6682 \cdot 10^{2} \pm 2.98 \cdot 10^{-2}$	-0.09
ILT7	LABSMC no pair	189.0	$2.5083 \cdot 10^{1} \pm 8.31 \cdot 10^{-3}$	
	BHWIDE	189.0	$2.4692 \cdot 10^{1} \pm 1.20 \cdot 10^{-2}$	-1.56
	LABSMC no pair	200.0	$2.2227 \cdot 10^{1} \pm 7.38 \cdot 10^{-3}$	
	BHWIDE	200.0	$2.1885 \cdot 10^{1} \pm 9.90 \cdot 10^{-3}$	-1.54
	LABSMC no pair	206.0	$2.0868 \cdot 10^{1} \pm 6.94 \cdot 10^{-3}$	
	BHWIDE	206.0	$2.0557 \cdot 10^{1} \pm 9.10 \cdot 10^{-3}$	-1.49
ILT8	LABSMC no pair	189.0	$2.0748 \cdot 10^{2} \pm 2.39 \cdot 10^{-2}$	
	BHWIDE	189.0	$2.0684 \cdot 10^{2} \pm 4.01 \cdot 10^{-2}$	-0.31
	LABSMC no pair	200.0	$1.8529 \cdot 10^{2} \pm 2.13 \cdot 10^{-2}$	
	BHWIDE	200.0	$1.8477 \cdot 10^{2} \pm 3.36 \cdot 10^{-2}$	-0.28
	LABSMC no pair	206.0	$1.7468 \cdot 10^{2} \pm 2.01 \cdot 10^{-2}$	
	BHWIDE	206.0	$1.7416 \cdot 10^{2} \pm 3.10 \cdot 10^{-2}$	-0.30
IOpal3	LABSMC no pair	189.0	$1.1047 \cdot 10^{2} \pm 1.74 \cdot 10^{-2}$	
	BHWIDE	189.0	$1.1000 \cdot 10^{2} \pm 2.91 \cdot 10^{-2}$	-0.43
	LABSMC no pair	200.0	$9.8585 \cdot 10^{1} \pm 1.56 \cdot 10^{-2}$	
	BHWIDE	200.0	$9.8137 \cdot 10^{1} \pm 2.44 \cdot 10^{-2}$	-0.45
	LABSMC no pair	206.0	$9.2852 \cdot 10^{1} \pm 1.46 \cdot 10^{-2}$	
	BHWIDE	206.0	$9.2463 \cdot 10^{1} \pm 2.24 \cdot 10^{-2}$	-0.42
IOpal4	LABSMC no pair	189.0	$1.9662 \cdot 10^{1} \pm 7.36 \cdot 10^{-3}$	
	BHWIDE	189.0	$2.0109 \cdot 10^{1} \pm 1.02 \cdot 10^{-2}$	2.27
	LABSMC no pair	200.0	$1.7485 \cdot 10^{1} \pm 6.55 \cdot 10^{-3}$	
	BHWIDE	200.0	$1.7913 \cdot 10^{1} \pm 8.50 \cdot 10^{-3}$	2.45
	LABSMC no pair	206.0	$1.7080 \cdot 10^{1} \pm 6.28 \cdot 10^{-3}$	
	BHWIDE	206.0	$1.6861 \cdot 10^{1} \pm 7.90 \cdot 10^{-3}$	-1.28
IOpal5	LABSMC no pair	189.0	$3.0671 \cdot 10^{2} \pm 2.91 \cdot 10^{-2}$	
	BHWIDE	189.0	$3.0692 \cdot 10^{2} \pm 4.77 \cdot 10^{-2}$	0.07
	LABSMC no pair	200.0	$2.7412 \cdot 10^{2} \pm 2.59 \cdot 10^{-2}$	
	BHWIDE	200.0	$2.7441 \cdot 10^{2} \pm 4.01 \cdot 10^{-2}$	0.11
	LABSMC no pair	206.0	$2.5851 \cdot 10^{2} \pm 2.44 \cdot 10^{-2}$	
	BHWIDE	206.0	$2.5876 \cdot 10^{2} \pm 3.70 \cdot 10^{-2}$	0.10

3.3.1 Some comments on results for $e^+e^-(\gamma)$

The issue of extrapolations is especially important in cases when theoretical uncertainties are not fully under control.

In the case of L3 and OPAL selections, predictions for the realistic observables agree with the idealistic ones at 3%. No large extrapolations are thus needed. This is due to use of collinearity cuts in both cases. The only exception is the pair **LT4-ILT4**, where the difference is around 6%. This is due to the use of an invariant mass cut, where realistic observables sum electron energies with the energies of photons close by.

In the cases of ALEPH and DELPHI the differences between idealistic and realistic observables are larger (more than 20%). Here one of the, idealized observable – realistic observable, pair uses the invariant mass cut and the other an collinearity cut (or mass from the angles). This leads to larger extrapolations. The results presented here favor the use of collinearity cuts in all cases (for both types of observables).

The precision tags set by experimental considerations are: 0.21% barrel, 0.13% endcap. The precision tag for the barrel is not met by the theoretical calculation. A sizable factor of *ten* is still missing. This will reduce the sensitivity of searches for new phenomena like:

- contact interactions [32],
- low scale gravity effects [33],
- sneutrinos,
- non-zero size of the electrons [32].

The precision tag in the endcaps is closer to being met. Even the precision of or below 0.5%, if confirmed, will largely improve results like the measurement of the running of the fine-structure constant, which are limited by the theoretical uncertainty [6].

As an example of the effects of theoretical uncertainties in the Bhabha channel let us use as an example the contact interactions. The expected precision for the measurement in the barrel detector (44-136°) for four LEP experimental combined, and 600 pb^{-1} at $\sim$ 200 GeV (average) energy is about 0.45% (statistical) for the cross-section. The systematic error should be lower. The 0.0026 statistical error is expected for A_{fb}, here systematic error can be a bit higher.

The numerical results for the limits on contact interactions are summarized in the Table 5:

Table 5: Limits for Contact Interaction models at 95% CL expected from combined data of large-angle Bhabha scattering (barrel) at LEP2 /rough estimate/

Theoretical error:	2%	1%	0.5%
Contact Interaction Model	Sensitivity [TeV]	Sensitivity [TeV]	Sensitivity [TeV]
LL	7.6	9.3	10.6
RR	7.5	9.2	10.4
LR	9.3	10.7	11.8
VV	16.1	19.5	22.0
AA	12.1	12.1	12.2

Running of α_{QED}

In the following L3 paper [6], the cross section for Bhabha scattering from 20 to 36° at 189 GeV was measured to be $\sigma = 145.6 \pm 0.9(stat.) \pm 0.8(sys.) \pm 2.2(theory)\ pb$. This can be converted to a measurement of the running of the fine-structure constant between the Q^2 of the luminosity monitor and the endcap calorimeter:

$$\frac{1}{\alpha}(-12.25\ \mathrm{GeV}^2) - \frac{1}{\alpha}(-3434\ \mathrm{GeV}^2) = 3.80 \pm 0.61(exp.) \pm 1.14(theory)$$

or total error on $\frac{1}{\alpha}$ of 1.29 dominated by the theory uncertainty of BHWIDE taken to be 1.5%. The running is established at 3 sigma level. A LEP combined measurement can reduce the statistical error by factor more than 3 and the systematic error by factor of about two.

Clearly the theory uncertainty is the key for improvement. As a result of the MC workshop the theory uncertainty seems to be reduced to 0.5%, but not yet matching the experimental precision. This gives a promise to measure the running of α in this range with a precision on $\frac{1}{\alpha}$ of 0.3 (4 times more precise than now).

3.4 Discussion of numerical results for observables in $\mu^+\mu^-(\gamma)$ and $\tau^+\tau^-(\gamma)$ final states

This comparison is essential for the workshop because it tests theoretical uncertainties on different strategies of moving from raw data, realistic observables, to hard physics parameters with the intermediate step of idealized observables. That is the strategy actually in use by all experiments. The size of effects such as QED interferences in context of truly complicated analyses including sophisticated cuts should be documented. The results can serve as a benchmark for old simulations also.

The group of realistic observables in Table 6 includes comparisons of the old KORALZ Monte Carlo with $\mathcal{KK}$MC. As one can see the differences were in all cases due to the interference correction and new method of exponentiation[1], other effects such as different way of implementing electroweak corrections were not important. Differences between results from $\mathcal{KK}$MC option EEX2 and KORALZ were always below 0.25%, which is no surprise as exponentiation in KORALZ is quite similar to the option EEX2 for $\mathcal{KK}$MC. The CEEX2 option of $\mathcal{KK}$MC includes better scheme of exponentiation and in particular effects due to interference.

The comparisons for τ and μ leptons idealized observables (Tables 7,8 include calculations performed with the help of $\mathcal{KK}$MC and ZFITTER programs. Almost everywhere the differences between $\mathcal{KK}$MC and ZFITTER predictions are below 0.4%, which is the precision tag of experiments (See also Section 5.4 and 5.3.8). The exception are the cases with the intermediate cut on M_{inv}. Here the differences are slightly larger, up to 0.6%, but also acceptable. The effect due to pairs can not be neglected but even if included in a rather approximate way would be enough. The interference effect and the effect of CEEX exponentiation combined with respect to EEX are sizable also and should be taken into account. The three classes of effects as can be seen from the tables are respectively up to 1.3 and 1.6% thus respectively 3 to 4 times the experimental precision tag.

We can conclude that in all cases the overall theoretical uncertainty in μ and τ channels are 0.4%, just below (or very close to) the experimental precision tag. Therefore, we do not expect the overall QED uncertainty in these channels to be sizable enough to affect the experimental studies in any case now. This comfortable situation for the experimental analyses is the result of better understanding reached in comparisons which have been performed recently, in particular, in the framework of this workshop.

[1] Note that in the case of the observables with the tagged photons (see Table 9) the pattern of differences is more complicated and $\mathcal{KK}$MC CEEX2 results do not coincide with KORALZ.

Table 6: Numerical predictions from theoretical calculations of the following realistic observables in $\mu^+\mu^-(\gamma)$ final states; *cross-sections and symmetries.* The last field of the table shows relative deviation (multiplied by 100) with respect to the first calculation.

obs. σ	program	ene	value and error estimate	comments	δ ratio
Aleph5	KKMC 4.14	189.0	$6.1354{\cdot}10^{0}$ $\pm 4.49{\cdot}10^{-3}$	CEEX2	
	KKMC 4.14	189.0	$6.0640{\cdot}10^{0}$ $\pm 3.96{\cdot}10^{-3}$	EEX2	-1.16
	KORALZ 4.04	189.0	$6.0633{\cdot}10^{0}$ $\pm 2.50{\cdot}10^{-3}$		-1.17
	KKMC 4.14	206.0	$4.9465{\cdot}10^{0}$ $\pm 3.53{\cdot}10^{-3}$	CEEX2	
	KKMC 4.14	206.0	$4.8857{\cdot}10^{0}$ $\pm 3.11{\cdot}10^{-3}$	EEX2	-1.23
	KORALZ 4.04	206.0	$4.8794{\cdot}10^{0}$ $\pm 2.07{\cdot}10^{-3}$		-1.36
Aleph6	KKMC 4.14	189.0	$2.6917{\cdot}10^{0}$ $\pm 3.95{\cdot}10^{-3}$	CEEX2	
	KKMC 4.14	189.0	$2.6414{\cdot}10^{0}$ $\pm 3.44{\cdot}10^{-3}$	EEX2	-1.87
	KORALZ 4.04	189.0	$2.6431{\cdot}10^{0}$ $\pm 2.48{\cdot}10^{-3}$		-1.81
	KKMC 4.14	206.0	$2.2245{\cdot}10^{0}$ $\pm 3.13{\cdot}10^{-3}$	CEEX2	
	KKMC 4.14	206.0	$2.1830{\cdot}10^{0}$ $\pm 2.73{\cdot}10^{-3}$	EEX2	-1.87
	KORALZ 4.04	206.0	$2.1814{\cdot}10^{0}$ $\pm 2.03{\cdot}10^{-3}$		-1.94
Delphi4	KKMC 4.14	189.0	$5.7129{\cdot}10^{0}$ $\pm 4.39{\cdot}10^{-3}$	CEEX2	
	KKMC 4.14	189.0	$5.6471{\cdot}10^{0}$ $\pm 3.88{\cdot}10^{-3}$	EEX2	-1.15
	KORALZ 4.04	189.0	$5.6477{\cdot}10^{0}$ $\pm 2.59{\cdot}10^{-3}$		-1.14
	KKMC 4.14	206.0	$4.6121{\cdot}10^{0}$ $\pm 3.45{\cdot}10^{-3}$	CEEX2	
	KKMC 4.14	206.0	$4.5558{\cdot}10^{0}$ $\pm 3.05{\cdot}10^{-3}$	EEX2	-1.22
	KORALZ 4.04	206.0	$4.5504{\cdot}10^{0}$ $\pm 2.14{\cdot}10^{-3}$		-1.34
Delphi5	KKMC 4.14	189.0	$2.7945{\cdot}10^{0}$ $\pm 3.95{\cdot}10^{-3}$	CEEX2	
	KKMC 4.14	189.0	$2.7474{\cdot}10^{0}$ $\pm 3.46{\cdot}10^{-3}$	EEX2	-1.68
	KORALZ 4.04	189.0	$2.7498{\cdot}10^{0}$ $\pm 2.50{\cdot}10^{-3}$		-1.60
	KKMC 4.14	206.0	$2.3129{\cdot}10^{0}$ $\pm 3.13{\cdot}10^{-3}$	CEEX2	
	KKMC 4.14	206.0	$2.2737{\cdot}10^{0}$ $\pm 2.75{\cdot}10^{-3}$	EEX2	-1.69
	KORALZ 4.04	206.0	$2.2727{\cdot}10^{0}$ $\pm 2.06{\cdot}10^{-3}$		-1.74
LT9	KKMC 4.14	189.0	$5.8226{\cdot}10^{0}$ $\pm 4.40{\cdot}10^{-3}$	CEEX2	
	KKMC 4.14	189.0	$5.7536{\cdot}10^{0}$ $\pm 3.88{\cdot}10^{-3}$	EEX2	-1.19
	KORALZ 4.04	189.0	$5.7533{\cdot}10^{0}$ $\pm 2.57{\cdot}10^{-3}$		-1.19
	KKMC 4.14	206.0	$4.6980{\cdot}10^{0}$ $\pm 3.46{\cdot}10^{-3}$	CEEX2	
	KKMC 4.14	206.0	$4.6395{\cdot}10^{0}$ $\pm 3.05{\cdot}10^{-3}$	EEX2	-1.24
	KORALZ 4.04	206.0	$4.6331{\cdot}10^{0}$ $\pm 2.12{\cdot}10^{-3}$		-1.38
LT10	KKMC 4.14	189.0	$2.9972{\cdot}10^{0}$ $\pm 4.01{\cdot}10^{-3}$	CEEX2	
	KKMC 4.14	189.0	$2.9512{\cdot}10^{0}$ $\pm 3.51{\cdot}10^{-3}$	EEX2	-1.54
	KORALZ 4.04	189.0	$2.9519{\cdot}10^{0}$ $\pm 2.55{\cdot}10^{-3}$		-1.51
	KKMC 4.14	206.0	$2.4743{\cdot}10^{0}$ $\pm 3.18{\cdot}10^{-3}$	CEEX2	
	KKMC 4.14	206.0	$2.4361{\cdot}10^{0}$ $\pm 2.78{\cdot}10^{-3}$	EEX2	-1.55
	KORALZ 4.04	206.0	$2.4342{\cdot}10^{0}$ $\pm 2.09{\cdot}10^{-3}$		-1.62
Opal6	KKMC 4.14	189.0	$6.5402{\cdot}10^{0}$ $\pm 4.85{\cdot}10^{-3}$	CEEX2	
	KKMC 4.14	189.0	$6.4707{\cdot}10^{0}$ $\pm 4.17{\cdot}10^{-3}$	EEX2	-1.06
	KORALZ 4.04	189.0	$6.4733{\cdot}10^{0}$ $\pm 2.38{\cdot}10^{-3}$		-1.02
	KKMC 4.14	206.0	$5.3040{\cdot}10^{0}$ $\pm 3.83{\cdot}10^{-3}$	CEEX2	
	KKMC 4.14	206.0	$5.2437{\cdot}10^{0}$ $\pm 3.29{\cdot}10^{-3}$	EEX2	-1.14
	KORALZ 4.04	206.0	$5.2402{\cdot}10^{0}$ $\pm 1.97{\cdot}10^{-3}$		-1.20
Opal7	KKMC 4.14	189.0	$2.9571{\cdot}10^{0}$ $\pm 4.05{\cdot}10^{-3}$	CEEX2	
	KKMC 4.14	189.0	$2.9143{\cdot}10^{0}$ $\pm 3.54{\cdot}10^{-3}$	EEX2	-1.45
	KORALZ 4.04	189.0	$2.9206{\cdot}10^{0}$ $\pm 2.54{\cdot}10^{-3}$		-1.23
	KKMC 4.14	206.0	$2.4516{\cdot}10^{0}$ $\pm 3.21{\cdot}10^{-3}$	CEEX2	
	KKMC 4.14	206.0	$2.4158{\cdot}10^{0}$ $\pm 2.81{\cdot}10^{-3}$	EEX2	-1.46
	KORALZ 4.04	206.0	$2.4196{\cdot}10^{0}$ $\pm 2.09{\cdot}10^{-3}$		-1.31

obs. A_{FB}	program	ene	value and error estimate	comments	δ ratio
Aleph5	KKMC 4.14	189.0	0.3191 ± 0.0007	CEEX2	
	KKMC 4.14	189.0	0.3205 ± 0.0007	EEX2	0.15
	KORALZ 4.04	189.0	0.3218 ± 0.0007		0.27
	KKMC 4.14	206.0	0.3187 ± 0.0007	CEEX2	
	KKMC 4.14	206.0	0.3204 ± 0.0007	EEX2	0.16
	KORALZ 4.04	206.0	0.3219 ± 0.0007		0.31
Aleph6	KKMC 4.14	189.0	0.5513 ± 0.0015	CEEX2	
	KKMC 4.14	189.0	0.5513 ± 0.0015	EEX2	0.00
	KORALZ 4.04	189.0	0.5530 ± 0.0009		0.18
	KKMC 4.14	206.0	0.5370 ± 0.0014	CEEX2	
	KKMC 4.14	206.0	0.5370 ± 0.0014	EEX2	0.00
	KORALZ 4.04	206.0	0.5379 ± 0.0009		0.10
Delphi4	KKMC 4.14	189.0	0.3341 ± 0.0007	CEEX2	
	KKMC 4.14	189.0	0.3355 ± 0.0007	EEX2	0.15
	KORALZ 4.04	189.0	0.3366 ± 0.0007		0.25
	KKMC 4.14	206.0	0.3326 ± 0.0007	CEEX2	
	KKMC 4.14	206.0	0.3343 ± 0.0007	EEX2	0.17
	KORALZ 4.04	206.0	0.3353 ± 0.0007		0.27
Delphi5	KKMC 4.14	189.0	0.5476 ± 0.0014	CEEX2	
	KKMC 4.14	189.0	0.5476 ± 0.0014	EEX2	0.01
	KORALZ 4.04	189.0	0.5495 ± 0.0009		0.20
	KKMC 4.14	206.0	0.5334 ± 0.0014	CEEX2	
	KKMC 4.14	206.0	0.5334 ± 0.0014	EEX2	0.00
	KORALZ 4.04	206.0	0.5345 ± 0.0009		0.11
LT9	KKMC 4.14	189.0	0.3284 ± 0.0007	CEEX2	
	KKMC 4.14	189.0	0.3299 ± 0.0007	EEX2	0.15
	KORALZ 4.04	189.0	0.3311 ± 0.0007		0.27
	KKMC 4.14	206.0	0.3270 ± 0.0007	CEEX2	
	KKMC 4.14	206.0	0.3286 ± 0.0007	EEX2	0.16
	KORALZ 4.04	206.0	0.3300 ± 0.0007		0.30
LT10	KKMC 4.14	189.0	0.5372 ± 0.0013	CEEX2	
	KKMC 4.14	189.0	0.5372 ± 0.0013	EEX2	0.00
	KORALZ 4.04	189.0	0.5392 ± 0.0009		0.21
	KKMC 4.14	206.0	0.5247 ± 0.0013	CEEX2	
	KKMC 4.14	206.0	0.5247 ± 0.0013	EEX2	0.00
	KORALZ 4.04	206.0	0.5258 ± 0.0009		0.11
Opal6	KKMC 4.14	189.0	0.3285 ± 0.0007	CEEX2	
	KKMC 4.14	189.0	0.3297 ± 0.0007	EEX2	0.12
	KORALZ 4.04	189.0	0.3309 ± 0.0007		0.24
	KKMC 4.14	206.0	0.3276 ± 0.0007	CEEX2	
	KKMC 4.14	206.0	0.3290 ± 0.0007	EEX2	0.14
	KORALZ 4.04	206.0	0.3301 ± 0.0007		0.26
Opal7	KKMC 4.14	189.0	0.5525 ± 0.0014	CEEX2	
	KKMC 4.14	189.0	0.5526 ± 0.0014	EEX2	0.00
	KORALZ 4.04	189.0	0.5539 ± 0.0009		0.14
	KKMC 4.14	206.0	0.5376 ± 0.0013	CEEX2	
	KKMC 4.14	206.0	0.5377 ± 0.0013	EEX2	0.01
	KORALZ 4.04	206.0	0.5385 ± 0.0009		0.09

Table 7: Numerical predictions from theoretical calculations of the following idealized observables in $\mu^+\mu^-(\gamma)$ final states; *cross-sections and asymmetries*. The last field of the table shows relative deviation (multiplied by 100) with respect to the first calculation.

obs. σ	program	ene	value and error estimate	δ ratio
tAleph5	ZFITTER v6.30	189.0	$6.8388 \cdot 10^{0} \pm 5.88 \cdot 10^{-5}$ $-2.52 \cdot 10^{-2}$	
	ZF6.30 no pair	189.0	$6.7562 \cdot 10^{0} \pm 5.73 \cdot 10^{-5}$ $-2.24 \cdot 10^{-2}$	-1.21
	KKMC 4.14	189.0	$6.7663 \cdot 10^{0} \pm 4.59 \cdot 10^{-3}$	-1.06
	ZFITTER v6.30	206.0	$5.5642 \cdot 10^{0} \pm 4.54 \cdot 10^{-5}$ $-2.21 \cdot 10^{-2}$	
	ZF6.30 no pair	206.0	$5.4944 \cdot 10^{0} \pm 4.42 \cdot 10^{-5}$ $-1.96 \cdot 10^{-2}$	-1.26
	KKMC 4.14	206.0	$5.5095 \cdot 10^{0} \pm 3.62 \cdot 10^{-3}$	-0.98
tAleph6	ZFITTER v6.30	189.0	$2.6693 \cdot 10^{0} \pm 1.32 \cdot 10^{-3}$ $-1.46 \cdot 10^{-2}$	
	ZF6.30 no pair	189.0	$2.6736 \cdot 10^{0} \pm 1.06 \cdot 10^{-3}$ $-1.46 \cdot 10^{-2}$	0.16
	KKMC 4.14	189.0	$2.6727 \cdot 10^{0} \pm 3.95 \cdot 10^{-3}$	0.13
	ZFITTER v6.30	206.0	$2.2060 \cdot 10^{0} \pm 1.12 \cdot 10^{-3}$ $-1.25 \cdot 10^{-2}$	
	ZF6.30 no pair	206.0	$2.2097 \cdot 10^{0} \pm 9.00 \cdot 10^{-4}$ $-1.25 \cdot 10^{-2}$	0.17
	KKMC 4.14	206.0	$2.2108 \cdot 10^{0} \pm 3.13 \cdot 10^{-3}$	0.22
lDelphi5	ZFITTER v6.30	189.0	$6.2713 \cdot 10^{0} \pm 5.45 \cdot 10^{-5}$ $-1.76 \cdot 10^{-2}$	
	ZF6.30 no pair	189.0	$6.2713 \cdot 10^{0} \pm 5.45 \cdot 10^{-5}$ $-1.76 \cdot 10^{-2}$	0.00
	KKMC 4.14	189.0	$6.2981 \cdot 10^{0} \pm 4.55 \cdot 10^{-3}$	0.43
	ZFITTER v6.30	206.0	$5.1205 \cdot 10^{0} \pm 4.20 \cdot 10^{-5}$ $-1.56 \cdot 10^{-2}$	
	ZF6.30 no pair	206.0	$5.1205 \cdot 10^{0} \pm 4.20 \cdot 10^{-5}$ $-1.56 \cdot 10^{-2}$	0.00
	KKMC 4.14	206.0	$5.1462 \cdot 10^{0} \pm 3.59 \cdot 10^{-3}$	0.50
lDelphi6	ZFITTER v6.30	189.0	$2.8452 \cdot 10^{0} \pm 1.13 \cdot 10^{-3}$ $-1.16 \cdot 10^{-2}$	
	ZF6.30 no pair	189.0	$2.8452 \cdot 10^{0} \pm 1.13 \cdot 10^{-3}$ $-1.16 \cdot 10^{-2}$	0.00
	KKMC 4.14	189.0	$2.8474 \cdot 10^{0} \pm 4.02 \cdot 10^{-3}$	0.08
	ZFITTER v6.30	206.0	$2.3521 \cdot 10^{0} \pm 9.55 \cdot 10^{-4}$ $-1.00 \cdot 10^{-2}$	
	ZF6.30 no pair	206.0	$2.3521 \cdot 10^{0} \pm 9.55 \cdot 10^{-4}$ $-1.00 \cdot 10^{-2}$	0.00
	KKMC 4.14	206.0	$2.3570 \cdot 10^{0} \pm 3.19 \cdot 10^{-3}$	0.21
lLT9	ZFITTER v6.30	189.0	$5.7496 \cdot 10^{0} \pm 4.91 \cdot 10^{-5}$ $-1.78 \cdot 10^{-2}$	
	ZF6.30 no pair	189.0	$5.6872 \cdot 10^{0} \pm 4.77 \cdot 10^{-5}$ $-1.63 \cdot 10^{-2}$	-1.09
	KKMC 4.14	189.0	$5.7136 \cdot 10^{0} \pm 4.22 \cdot 10^{-3}$	-0.63
	ZFITTER v6.30	206.0	$4.6790 \cdot 10^{0} \pm 3.75 \cdot 10^{-5}$ $-1.59 \cdot 10^{-2}$	
	ZF6.30 no pair	206.0	$4.6259 \cdot 10^{0} \pm 3.64 \cdot 10^{-5}$ $-1.45 \cdot 10^{-2}$	-1.14
	KKMC 4.14	206.0	$4.6505 \cdot 10^{0} \pm 3.33 \cdot 10^{-3}$	-0.61
lLT10	ZFITTER v6.30	189.0	$2.6247 \cdot 10^{0} \pm 1.28 \cdot 10^{-3}$ $-1.07 \cdot 10^{-2}$	
	ZF6.30 no pair	189.0	$2.6275 \cdot 10^{0} \pm 1.04 \cdot 10^{-3}$ $-1.07 \cdot 10^{-2}$	0.11
	KKMC 4.14	189.0	$2.6306 \cdot 10^{0} \pm 3.73 \cdot 10^{-3}$	0.22
	ZFITTER v6.30	206.0	$2.1688 \cdot 10^{0} \pm 1.08 \cdot 10^{-3}$ $-9.18 \cdot 10^{-3}$	
	ZF6.30 no pair	206.0	$2.1712 \cdot 10^{0} \pm 8.83 \cdot 10^{-4}$ $-9.18 \cdot 10^{-3}$	0.11
	KKMC 4.14	206.0	$2.1759 \cdot 10^{0} \pm 2.96 \cdot 10^{-3}$	0.33
lLT11	ZFITTER v6.30	189.0	$3.0747 \cdot 10^{0} \pm 4.42 \cdot 10^{-4}$ $-1.25 \cdot 10^{-2}$	
	ZF6.30 no pair	189.0	$3.0779 \cdot 10^{0} \pm 1.70 \cdot 10^{-4}$ $-1.25 \cdot 10^{-2}$	0.10
	KKMC 4.14	189.0	$3.0786 \cdot 10^{0} \pm 4.39 \cdot 10^{-3}$	0.13
	ZFITTER v6.30	206.0	$2.5428 \cdot 10^{0} \pm 3.73 \cdot 10^{-4}$ $-1.07 \cdot 10^{-2}$	
	ZF6.30 no pair	206.0	$2.5456 \cdot 10^{0} \pm 1.44 \cdot 10^{-4}$ $-1.07 \cdot 10^{-2}$	0.11
	KKMC 4.14	206.0	$2.5511 \cdot 10^{0} \pm 3.49 \cdot 10^{-3}$	0.33
tOpal6	ZFITTER v6.30	189.0	$6.8232 \cdot 10^{0} \pm 5.89 \cdot 10^{-5}$ $-2.53 \cdot 10^{-2}$	
	ZF6.30 no pair	189.0	$6.7403 \cdot 10^{0} \pm 5.74 \cdot 10^{-5}$ $-2.25 \cdot 10^{-2}$	-1.21
	KKMC 4.14	189.0	$6.7519 \cdot 10^{0} \pm 4.06 \cdot 10^{-3}$	-1.04
	ZFITTER v6.30	206.0	$5.5544 \cdot 10^{0} \pm 4.55 \cdot 10^{-5}$ $-2.22 \cdot 10^{-2}$	
	ZF6.30 no pair	206.0	$5.4843 \cdot 10^{0} \pm 4.43 \cdot 10^{-5}$ $-1.97 \cdot 10^{-2}$	-1.26
	KKMC 4.14	206.0	$5.4964 \cdot 10^{0} \pm 3.20 \cdot 10^{-3}$	-1.04
tOpal7	ZFITTER v6.30	189.0	$7.7155 \cdot 10^{0} \pm 6.85 \cdot 10^{-5}$ $-3.14 \cdot 10^{-3}$	
	ZF6.30 no pair	189.0	$7.6261 \cdot 10^{0} \pm 6.69 \cdot 10^{-5}$ $-1.45 \cdot 10^{-4}$	-1.16
	KKMC 4.14	189.0	$7.6407 \cdot 10^{0} \pm 4.35 \cdot 10^{-3}$	-0.97
	ZFITTER v6.30	206.0	$6.3271 \cdot 10^{0} \pm 6.21 \cdot 10^{-5}$ $-2.82 \cdot 10^{-3}$	
	ZF6.30 no pair	206.0	$6.2515 \cdot 10^{0} \pm 6.08 \cdot 10^{-5}$ $-1.05 \cdot 10^{-4}$	-1.20
	KKMC 4.14	206.0	$6.2689 \cdot 10^{0} \pm 3.43 \cdot 10^{-3}$	-0.92
tOpal8	ZFITTER v6.30	189.0	$2.9620 \cdot 10^{0} \pm 1.46 \cdot 10^{-3}$ $-5.56 \cdot 10^{-5}$	
	ZF6.30 no pair	189.0	$2.9649 \cdot 10^{0} \pm 1.20 \cdot 10^{-3}$ $-5.57 \cdot 10^{-5}$	0.10
	KKMC 4.14	189.0	$2.9682 \cdot 10^{0} \pm 3.57 \cdot 10^{-3}$	0.21
	ZFITTER v6.30	206.0	$2.4506 \cdot 10^{0} \pm 1.23 \cdot 10^{-3}$ $-4.45 \cdot 10^{-5}$	
	ZF6.30 no pair	206.0	$2.4531 \cdot 10^{0} \pm 1.01 \cdot 10^{-3}$ $-4.46 \cdot 10^{-5}$	0.10
	KKMC 4.14	206.0	$2.4579 \cdot 10^{0} \pm 2.83 \cdot 10^{-3}$	0.30
tOpal9	ZFITTER v6.30	189.0	$3.1930 \cdot 10^{0} \pm 4.56 \cdot 10^{-4}$ $-5.95 \cdot 10^{-5}$	
	ZF6.30 no pair	189.0	$3.1962 \cdot 10^{0} \pm 1.74 \cdot 10^{-4}$ $-5.95 \cdot 10^{-5}$	0.10
	KKMC 4.14	189.0	$3.1982 \cdot 10^{0} \pm 3.78 \cdot 10^{-3}$	0.16
	ZFITTER v6.30	206.0	$2.6428 \cdot 10^{0} \pm 3.84 \cdot 10^{-4}$ $-4.78 \cdot 10^{-5}$	
	ZF6.30 no pair	206.0	$2.6455 \cdot 10^{0} \pm 1.48 \cdot 10^{-4}$ $-4.78 \cdot 10^{-5}$	0.10
	KKMC 4.14	206.0	$2.6507 \cdot 10^{0} \pm 3.00 \cdot 10^{-3}$	0.30

obs. A_{FB}	program	ene	value and error estimate	δ ratio
tAleph5	ZFITTER v6.30	189.0	0.2920 $\pm$0.0011 $-$0.0000	
	ZF6.30 no pair	189.0	0.2955 $\pm$0.0010 $-$0.0000	0.36
	KKMC 4.14	189.0	0.2999 $\pm$0.0007	0.79
	ZFITTER v6.30	206.0	0.2909 $\pm$0.0012 $-$0.0000	
	ZF6.30 no pair	206.0	0.2946 $\pm$0.0011 $-$0.0000	0.37
	KKMC 4.14	206.0	0.2988 $\pm$0.0007	0.79
tAleph6	ZFITTER v6.30	189.0	0.5738 $\pm$0.0001 $-$0.0002	
	ZF6.30 no pair	189.0	0.5729 $\pm$0.0001 $-$0.0001	-0.09
	KKMC 4.14	189.0	0.5694 $\pm$0.0017	-0.45
	ZFITTER v6.30	206.0	0.5589 $\pm$0.0001 $-$0.0002	
	ZF6.30 no pair	206.0	0.5580 $\pm$0.0001 $-$0.0001	-0.09
	KKMC 4.14	206.0	0.5558 $\pm$0.0016	-0.32
lDelphi5	ZFITTER v6.30	189.0	0.3224 $\pm$0.0010 $-$0.0000	
	ZF6.30 no pair	189.0	0.3224 $\pm$0.0010 $-$0.0000	0.00
	KKMC 4.14	189.0	0.3234 $\pm$0.0008	0.09
	ZFITTER v6.30	206.0	0.3193 $\pm$0.0010 $-$0.0000	
	ZF6.30 no pair	206.0	0.3193 $\pm$0.0010 $-$0.0000	0.00
	KKMC 4.14	206.0	0.3201 $\pm$0.0007	0.09
lDelphi6	ZFITTER v6.30	189.0	0.5694 $\pm$0.0000 $-$0.0001	
	ZF6.30 no pair	189.0	0.5694 $\pm$0.0000 $-$0.0001	0.00
	KKMC 4.14	189.0	0.5669 $\pm$0.0016	-0.25
	ZFITTER v6.30	206.0	0.5541 $\pm$0.0001 $-$0.0001	
	ZF6.30 no pair	206.0	0.5541 $\pm$0.0001 $-$0.0001	0.00
	KKMC 4.14	206.0	0.5532 $\pm$0.0015	-0.10
lLT9	ZFITTER v6.30	189.0	0.3134 $\pm$0.0010 $-$0.0000	
	ZF6.30 no pair	189.0	0.3168 $\pm$0.0010 $-$0.0000	0.34
	KKMC 4.14	189.0	0.3176 $\pm$0.0008	0.42
	ZFITTER v6.30	206.0	0.3105 $\pm$0.0011 $-$0.0000	
	ZF6.30 no pair	206.0	0.3141 $\pm$0.0010 $-$0.0000	0.36
	KKMC 4.14	206.0	0.3149 $\pm$0.0008	0.44
lLT10	ZFITTER v6.30	189.0	0.5523 $\pm$0.0000 $-$0.0002	
	ZF6.30 no pair	189.0	0.5517 $\pm$0.0000 $-$0.0001	-0.06
	KKMC 4.14	189.0	0.5494 $\pm$0.0016	-0.29
	ZFITTER v6.30	206.0	0.5374 $\pm$0.0001 $-$0.0002	
	ZF6.30 no pair	206.0	0.5369 $\pm$0.0001 $-$0.0001	-0.06
	KKMC 4.14	206.0	0.5358 $\pm$0.0015	-0.16
lLT11	ZFITTER v6.30	189.0	0.5873 $\pm$0.0001 $-$0.0001	
	ZF6.30 no pair	189.0	0.5867 $\pm$0.0001 $-$0.0000	-0.06
	KKMC 4.14	189.0	0.5839 $\pm$0.0017	-0.34
	ZFITTER v6.30	206.0	0.5717 $\pm$0.0002 $-$0.0001	
	ZF6.30 no pair	206.0	0.5711 $\pm$0.0001 $-$0.0000	-0.06
	KKMC 4.14	206.0	0.5702 $\pm$0.0016	-0.16
tOpal6	ZFITTER v6.30	189.0	0.2890 $\pm$0.0011 $-$0.0000	
	ZF6.30 no pair	189.0	0.2925 $\pm$0.0010 $-$0.0000	0.36
	KKMC 4.14	189.0	0.2952 $\pm$0.0006	0.62
	ZFITTER v6.30	206.0	0.2871 $\pm$0.0012 $-$0.0000	
	ZF6.30 no pair	206.0	0.2907 $\pm$0.0011 $-$0.0000	0.37
	KKMC 4.14	206.0	0.2939 $\pm$0.0006	0.69
tOpal7	ZFITTER v6.30	189.0	0.2807 $\pm$0.0002 $-$0.0000	
	ZF6.30 no pair	189.0	0.2839 $\pm$0.0001 $-$0.0000	0.33
	KKMC 4.14	189.0	0.2862 $\pm$0.0006	0.56
	ZFITTER v6.30	206.0	0.2771 $\pm$0.0002 $-$0.0000	
	ZF6.30 no pair	206.0	0.2804 $\pm$0.0001 $-$0.0000	0.34
	KKMC 4.14	206.0	0.2832 $\pm$0.0006	0.62
tOpal8	ZFITTER v6.30	189.0	0.5535 $\pm$0.0000 $-$0.0002	
	ZF6.30 no pair	189.0	0.5530 $\pm$0.0000 $-$0.0001	-0.05
	KKMC 4.14	189.0	0.5510 $\pm$0.0014	-0.25
	ZFITTER v6.30	206.0	0.5377 $\pm$0.0000 $-$0.0002	
	ZF6.30 no pair	206.0	0.5372 $\pm$0.0000 $-$0.0001	-0.05
	KKMC 4.14	206.0	0.5368 $\pm$0.0013	-0.09
tOpal9	ZFITTER v6.30	189.0	0.5683 $\pm$0.0001 $-$0.0001	
	ZF6.30 no pair	189.0	0.5677 $\pm$0.0001 $-$0.0000	-0.06
	KKMC 4.14	189.0	0.5658 $\pm$0.0014	-0.25
	ZFITTER v6.30	206.0	0.5520 $\pm$0.0001 $-$0.0000	
	ZF6.30 no pair	206.0	0.5515 $\pm$0.0001 $-$0.0000	-0.06
	KKMC 4.14	206.0	0.5513 $\pm$0.0013	-0.07

Table 8: Numerical predictions from theoretical calculations of the following idealized observables in $\tau^+\tau^-(\gamma)$ final states; *cross-sections and asymmetries*. The last field of the table shows relative deviation (multiplied by 100) with respect to the first calculation.

obs. σ	program	ene	value and error estimate	δ ratio
tAlcph7	ZFITTER v6.30	189.0	$6.8336 \cdot 10^{0} \quad +5.86 \cdot 10^{-5} \quad -2.52 \cdot 10^{-2}$	
	ZF6.30 no pair	189.0	$6.7510 \cdot 10^{0} \quad +5.71 \cdot 10^{-5} \quad -2.25 \cdot 10^{-2}$	-1.21
	KKMC 4.13	189.0	$6.7622 \cdot 10^{0} \quad \pm 2.62 \cdot 10^{-3}$	-1.05
	ZFITTER v6.30	206.0	$5.5636 \cdot 10^{0} \quad +4.53 \cdot 10^{-5} \quad -2.22 \cdot 10^{-2}$	
	ZF6.30 no pair	206.0	$5.4938 \cdot 10^{0} \quad +4.41 \cdot 10^{-5} \quad -1.97 \cdot 10^{-2}$	-1.26
	KKMC 4.13	206.0	$5.5008 \cdot 10^{0} \quad \pm 2.85 \cdot 10^{-3}$	-1.13
tAlcph8	ZFITTER v6.30	189.0	$2.7580 \cdot 10^{0} \quad +1.37 \cdot 10^{-3} \quad -8.43 \cdot 10^{-3}$	
	ZF6.30 no pair	189.0	$2.7624 \cdot 10^{0} \quad +1.10 \cdot 10^{-3} \quad -8.43 \cdot 10^{-3}$	0.16
	KKMC 4.13	189.0	$2.7627 \cdot 10^{0} \quad \pm 2.28 \cdot 10^{-3}$	0.17
	ZFITTER v6.30	206.0	$2.2794 \cdot 10^{0} \quad +1.16 \cdot 10^{-3} \quad -7.28 \cdot 10^{-3}$	
	ZF6.30 no pair	206.0	$2.2832 \cdot 10^{0} \quad +9.35 \cdot 10^{-4} \quad -7.28 \cdot 10^{-3}$	0.16
	KKMC 4.13	206.0	$2.2823 \cdot 10^{0} \quad \pm 2.49 \cdot 10^{-3}$	0.13
tDelphi7	ZFITTER v6.30	189.0	$6.3354 \cdot 10^{0} \quad +5.56 \cdot 10^{-5} \quad -1.79 \cdot 10^{-2}$	
	ZF6.30 no pair	189.0	$6.3354 \cdot 10^{0} \quad +5.56 \cdot 10^{-5} \quad -1.79 \cdot 10^{-2}$	0.00
	KKMC 4.13	189.0	$6.3562 \cdot 10^{0} \quad \pm 2.60 \cdot 10^{-3}$	0.33
	ZFITTER v6.30	206.0	$5.1704 \cdot 10^{0} \quad +4.29 \cdot 10^{-5} \quad -1.59 \cdot 10^{-2}$	
	ZF6.30 no pair	206.0	$5.1704 \cdot 10^{0} \quad +4.29 \cdot 10^{-5} \quad -1.59 \cdot 10^{-2}$	0.00
	KKMC 4.13	206.0	$5.1851 \cdot 10^{0} \quad \pm 2.84 \cdot 10^{-3}$	0.28
tDelphi8	ZFITTER v6.30	189.0	$2.9164 \cdot 10^{0} \quad +1.17 \cdot 10^{-3} \quad -6.49 \cdot 10^{-3}$	
	ZF6.30 no pair	189.0	$2.9164 \cdot 10^{0} \quad +1.17 \cdot 10^{-3} \quad -6.49 \cdot 10^{-3}$	0.00
	KKMC 4.13	189.0	$2.9211 \cdot 10^{0} \quad \pm 2.32 \cdot 10^{-3}$	0.16
	ZFITTER v6.30	206.0	$2.4111 \cdot 10^{0} \quad +1.00 \cdot 10^{-3} \quad -5.61 \cdot 10^{-3}$	
	ZF6.30 no pair	206.0	$2.4111 \cdot 10^{0} \quad +1.00 \cdot 10^{-3} \quad -5.61 \cdot 10^{-3}$	0.00
	KKMC 4.13	206.0	$2.4133 \cdot 10^{0} \quad \pm 2.54 \cdot 10^{-3}$	0.09
ILT12	ZFITTER v6.30	189.0	$6.0350 \cdot 10^{0} \quad +5.27 \cdot 10^{-5} \quad -1.87 \cdot 10^{-2}$	
	ZF6.30 no pair	189.0	$5.9695 \cdot 10^{0} \quad +5.13 \cdot 10^{-5} \quad -1.71 \cdot 10^{-2}$	-1.09
	KKMC 4.13	189.0	$5.9913 \cdot 10^{0} \quad \pm 2.49 \cdot 10^{-3}$	-0.72
	ZFITTER v6.30	206.0	$4.9149 \cdot 10^{0} \quad +4.04 \cdot 10^{-5} \quad -1.67 \cdot 10^{-2}$	
	ZF6.30 no pair	206.0	$4.8591 \cdot 10^{0} \quad +3.93 \cdot 10^{-5} \quad -1.52 \cdot 10^{-2}$	-1.14
	KKMC 4.13	206.0	$4.8749 \cdot 10^{0} \quad \pm 2.71 \cdot 10^{-3}$	-0.81
ILT13	ZFITTER v6.30	189.0	$2.7782 \cdot 10^{0} \quad +1.36 \cdot 10^{-3} \quad -6.20 \cdot 10^{-3}$	
	ZF6.30 no pair	189.0	$2.7811 \cdot 10^{0} \quad +1.12 \cdot 10^{-3} \quad -6.20 \cdot 10^{-3}$	0.10
	KKMC 4.13	189.0	$2.7870 \cdot 10^{0} \quad \pm 2.21 \cdot 10^{-3}$	0.32
	ZFITTER v6.30	206.0	$2.2961 \cdot 10^{0} \quad +1.15 \cdot 10^{-3} \quad -5.36 \cdot 10^{-3}$	
	ZF6.30 no pair	206.0	$2.2986 \cdot 10^{0} \quad +9.47 \cdot 10^{-4} \quad -5.36 \cdot 10^{-3}$	0.11
	KKMC 4.13	206.0	$2.3019 \cdot 10^{0} \quad \pm 2.42 \cdot 10^{-3}$	0.25
ILT14	ZFITTER v6.30	189.0	$3.1514 \cdot 10^{0} \quad +4.59 \cdot 10^{-4} \quad -7.01 \cdot 10^{-3}$	
	ZF6.30 no pair	189.0	$3.1546 \cdot 10^{0} \quad +1.83 \cdot 10^{-4} \quad -7.01 \cdot 10^{-3}$	0.10
	KKMC 4.13	189.0	$3.1606 \cdot 10^{0} \quad \pm 2.53 \cdot 10^{-3}$	0.29
	ZFITTER v6.30	206.0	$2.6064 \cdot 10^{0} \quad +3.90 \cdot 10^{-4} \quad -6.06 \cdot 10^{-3}$	
	ZF6.30 no pair	206.0	$2.6091 \cdot 10^{0} \quad +1.59 \cdot 10^{-4} \quad -6.06 \cdot 10^{-3}$	0.11
	KKMC 4.13	206.0	$2.6108 \cdot 10^{0} \quad \pm 2.77 \cdot 10^{-3}$	0.17
tOpal10	ZFITTER v6.30	189.0	$6.1509 \cdot 10^{0} \quad +5.16 \cdot 10^{-5} \quad -2.34 \cdot 10^{-2}$	
	ZF6.30 no pair	189.0	$6.0744 \cdot 10^{0} \quad +5.02 \cdot 10^{-5} \quad -2.08 \cdot 10^{-2}$	-1.24
	KKMC 4.13	189.0	$6.0820 \cdot 10^{0} \quad \pm 2.18 \cdot 10^{-3}$	-1.12
	ZFITTER v6.30	206.0	$4.9889 \cdot 10^{0} \quad +3.94 \cdot 10^{-5} \quad -2.05 \cdot 10^{-2}$	
	ZF6.30 no pair	206.0	$4.9242 \cdot 10^{0} \quad +3.83 \cdot 10^{-5} \quad -1.82 \cdot 10^{-2}$	-1.30
	KKMC 4.13	206.0	$4.9283 \cdot 10^{0} \quad \pm 2.37 \cdot 10^{-3}$	-1.21
tOpal11	ZFITTER v6.30	189.0	$7.7067 \cdot 10^{0} \quad +6.83 \cdot 10^{-5} \quad -3.13 \cdot 10^{-3}$	
	ZF6.30 no pair	189.0	$7.6175 \cdot 10^{0} \quad +6.67 \cdot 10^{-5} \quad -1.42 \cdot 10^{-4}$	-1.16
	KKMC 4.13	189.0	$7.6339 \cdot 10^{0} \quad \pm 2.48 \cdot 10^{-3}$	-0.95
	ZFITTER v6.30	206.0	$6.3200 \cdot 10^{0} \quad +7.70 \cdot 10^{-5} \quad -2.81 \cdot 10^{-3}$	
	ZF6.30 no pair	206.0	$6.2446 \cdot 10^{0} \quad +7.57 \cdot 10^{-5} \quad -1.05 \cdot 10^{-4}$	-1.19
	KKMC 4.13	206.0	$6.2569 \cdot 10^{0} \quad \pm 2.71 \cdot 10^{-3}$	-1.00
tOpal12	ZFITTER v6.30	189.0	$2.7412 \cdot 10^{0} \quad +1.36 \cdot 10^{-3} \quad -5.18 \cdot 10^{-5}$	
	ZF6.30 no pair	189.0	$2.7439 \cdot 10^{0} \quad +1.12 \cdot 10^{-3} \quad -5.19 \cdot 10^{-5}$	0.10
	KKMC 4.13	189.0	$2.7487 \cdot 10^{0} \quad \pm 1.92 \cdot 10^{-3}$	0.28
	ZFITTER v6.30	206.0	$2.2670 \cdot 10^{0} \quad +1.15 \cdot 10^{-3} \quad -4.14 \cdot 10^{-5}$	
	ZF6.30 no pair	206.0	$2.2693 \cdot 10^{0} \quad +9.49 \cdot 10^{-4} \quad -4.14 \cdot 10^{-5}$	0.10
	KKMC 4.13	206.0	$2.2726 \cdot 10^{0} \quad \pm 2.10 \cdot 10^{-3}$	0.25
tOpal13	ZFITTER v6.30	189.0	$3.1927 \cdot 10^{0} \quad +4.70 \cdot 10^{-4} \quad -5.95 \cdot 10^{-5}$	
	ZF6.30 no pair	189.0	$3.1959 \cdot 10^{0} \quad +1.89 \cdot 10^{-4} \quad -5.95 \cdot 10^{-5}$	0.10
	KKMC 4.13	189.0	$3.1995 \cdot 10^{0} \quad \pm 2.16 \cdot 10^{-3}$	0.21
	ZFITTER v6.30	206.0	$2.6426 \cdot 10^{0} \quad +3.98 \cdot 10^{-4} \quad -4.78 \cdot 10^{-5}$	
	ZF6.30 no pair	206.0	$2.6453 \cdot 10^{0} \quad +1.61 \cdot 10^{-4} \quad -4.78 \cdot 10^{-5}$	0.10
	KKMC 4.13	206.0	$2.6467 \cdot 10^{0} \quad \pm 2.37 \cdot 10^{-3}$	0.16

obs. A_{FB}	program	ene	value and error estimate	δ ratio
tAlcph7	ZFITTER v6.30	189.0	0.2926 +0.0011 −0.0000	
	ZF6.30 no pair	189.0	0.2962 +0.0010 −0.0000	0.36
	KKMC 4.13	189.0	0.3007 ±0.0004	0.80
	ZFITTER v6.30	206.0	0.2909 +0.0012 −0.0000	
	ZF6.30 no pair	206.0	0.2946 +0.0011 −0.0000	0.37
	KKMC 4.13	206.0	0.2991 ±0.0005	0.82
tAlcph8	ZFITTER v6.30	189.0	0.5731 +0.0001 −0.0002	
	ZF6.30 no pair	189.0	0.5722 +0.0000 −0.0001	-0.09
	KKMC 4.13	189.0	0.5704 ±0.0010	-0.26
	ZFITTER v6.30	206.0	0.5582 +0.0001 −0.0002	
	ZF6.30 no pair	206.0	0.5573 +0.0001 −0.0001	-0.09
	KKMC 4.13	206.0	0.5558 ±0.0012	-0.23
tDelphi7	ZFITTER v6.30	189.0	0.3200 +0.0010 −0.0000	
	ZF6.30 no pair	189.0	0.3200 +0.0010 −0.0000	0.00
	KKMC 4.13	189.0	0.3217 ±0.0004	0.17
	ZFITTER v6.30	206.0	0.3169 +0.0010 −0.0000	
	ZF6.30 no pair	206.0	0.3169 +0.0010 −0.0000	0.00
	KKMC 4.13	206.0	0.3182 ±0.0006	0.13
tDelphi8	ZFITTER v6.30	189.0	0.5689 +0.0000 −0.0001	
	ZF6.30 no pair	189.0	0.5689 +0.0000 −0.0001	0.00
	KKMC 4.13	189.0	0.5685 ±0.0009	-0.04
	ZFITTER v6.30	206.0	0.5537 +0.0000 −0.0001	
	ZF6.30 no pair	206.0	0.5537 +0.0000 −0.0001	0.00
	KKMC 4.13	206.0	0.5534 ±0.0012	-0.02
ILT12	ZFITTER v6.30	189.0	0.3137 +0.0010 −0.0000	
	ZF6.30 no pair	189.0	0.3172 +0.0010 −0.0000	0.35
	KKMC 4.13	189.0	0.3189 ±0.0004	0.52
	ZFITTER v6.30	206.0	0.3108 +0.0011 −0.0000	
	ZF6.30 no pair	206.0	0.3144 +0.0010 −0.0000	0.36
	KKMC 4.13	206.0	0.3158 ±0.0006	0.50
ILT13	ZFITTER v6.30	189.0	0.5590 +0.0000 −0.0002	
	ZF6.30 no pair	189.0	0.5584 +0.0000 −0.0001	-0.06
	KKMC 4.13	189.0	0.5584 ±0.0009	-0.07
	ZFITTER v6.30	206.0	0.5440 +0.0000 −0.0002	
	ZF6.30 no pair	206.0	0.5434 +0.0000 −0.0001	-0.06
	KKMC 4.13	206.0	0.5434 ±0.0012	-0.06
ILT14	ZFITTER v6.30	189.0	0.5867 +0.0001 −0.0001	
	ZF6.30 no pair	189.0	0.5862 +0.0001 −0.0000	-0.06
	KKMC 4.13	189.0	0.5857 ±0.0009	-0.10
	ZFITTER v6.30	206.0	0.5712 +0.0001 −0.0001	
	ZF6.30 no pair	206.0	0.5706 +0.0001 −0.0000	-0.06
	KKMC 4.13	206.0	0.5699 ±0.0012	-0.13
tOpal10	ZFITTER v6.30	189.0	0.2876 +0.0011 −0.0000	
	ZF6.30 no pair	189.0	0.2912 +0.0011 −0.0000	0.36
	KKMC 4.13	189.0	0.2951 ±0.0004	0.75
	ZFITTER v6.30	206.0	0.2860 +0.0012 −0.0000	
	ZF6.30 no pair	206.0	0.2897 +0.0011 −0.0000	0.38
	KKMC 4.13	206.0	0.2939 ±0.0005	0.79
tOpal11	ZFITTER v6.30	189.0	0.2809 +0.0002 −0.0000	
	ZF6.30 no pair	189.0	0.2842 +0.0001 −0.0000	0.33
	KKMC 4.13	189.0	0.2869 ±0.0003	0.61
	ZFITTER v6.30	206.0	0.2773 +0.0002 −0.0000	
	ZF6.30 no pair	206.0	0.2807 +0.0001 −0.0000	0.34
	KKMC 4.13	206.0	0.2832 ±0.0004	0.59
tOpal12	ZFITTER v6.30	189.0	0.5370 +0.0000 −0.0002	
	ZF6.30 no pair	189.0	0.5365 +0.0000 −0.0001	-0.05
	KKMC 4.13	189.0	0.5366 ±0.0008	-0.04
	ZFITTER v6.30	206.0	0.5217 +0.0000 −0.0002	
	ZF6.30 no pair	206.0	0.5212 +0.0000 −0.0001	-0.05
	KKMC 4.13	206.0	0.5210 ±0.0010	-0.07
tOpal13	ZFITTER v6.30	189.0	0.5682 +0.0001 −0.0001	
	ZF6.30 no pair	189.0	0.5676 +0.0001 −0.0000	-0.06
	KKMC 4.13	189.0	0.5675 ±0.0008	-0.07
	ZFITTER v6.30	206.0	0.5519 +0.0001 −0.0000	
	ZF6.30 no pair	206.0	0.5514 +0.0001 −0.0000	-0.06
	KKMC 4.13	206.0	0.5507 ±0.0010	-0.13

One should note that, for example, for the dimuon channel where expected ultimate experimental error on the cross section measurement from four LEP experiments is about 1.2% the decrease of theory uncertainty from 1% to the present 0.4–0.5% is roughly equivalent to the additional year of LEP running.

In some of the analyses performed with the two-fermion LEP data (like the fits for searches extra dimension gravity) the sensitivity depends on the differential distribution over the fermion production angle. The question of theoretical uncertainties in such differential distributions was, at least approximately, addressed by comparing forward-backward asymmetry values with different angular cuts. The agreement between different calculations in these quantities satisfies the experimental requirements also.

Realistic τ observables

Numerical results for τ-lepton realistic observables are not collected. This is not only due to complexity, but also due to relative similarity to the easier μ-lepton case. The remaining, rather historical issue is the spin implementation in KORALZ. It can be of some concern for those analysis which rely on simulation with that program. The eventual cross check of this aspect is rather easy; it should follow exactly the same procedure as presented in Table 6.

3.5 Discussion of numerical results for $l^+l^-\gamma$ observables

One can see (Table 9) that in all cases KORALZ and $\mathcal{KK}$MC (options CEEX2 IFIoff, EEX2 EEX3) give results which are similar within requested precision tags. Different choices of the exponentiation etc., lead to effects at the level of 1 to 2%. As the case of the $\mathcal{KK}$MC and the matrix element CEEX2 is expected to be the best, and the typical numerical size of the pair effects does not exceed the precision tag, we can conclude that all effects, except those of the interference correction (difference between $\mathcal{KK}$MC results, option CEEX2 and CEEX2 IFIoff), are well under sufficient control since a rather long time for this group of observables. The size of the interference correction is however sizable, as expected, depending on selection it can vary from 0 to nearly 20% and definitely must be taken into account in comparison of data with theoretical predictions. Comparisons with other possible calculations of interference corrections, like in single photon mode of KORALZ, or as in Ref. [34] for two hard photons, were not performed for the observables as in Table 9.

The predictions of KORALZ due to the older exponentiation used (which is similar to EEX2) should coincide with $\mathcal{KK}$MC EEX2 results. One can see that it is not always the case. This may indicate e.g. deficiencies of the way how electroweak corrections are implemented in KORALZ. The method designed for LEP1 works still quite good, but in configurations with massive bremsstrahlung, such as radiative return to Z, limits become visible. These differences are important to evaluate other places where similar systematic error may play a role, that is $\nu\bar{\nu}\gamma$ and $\tau^+\tau^-(\gamma)$ final states in case of observables including radiative return to Z.

For the observables from $e^+e^-\gamma$ the differences between the two available codes were at 3% maximum. For the moment this can be used as the estimate of theoretical uncertainty. It is consistent with the 2% estimation from LABSMC.

3.6 Discussion of numerical results for $\nu\bar{\nu}\gamma$ observables

Events where one or more photons are accompanied by missing energy are the characteristic signature of many new physics processes. For example, in the framework of both the MSSM and GMSB models of supersymmetry, neutralino pair production can give rise to events where one or two photons are accompanied by missing energy. This final state may also be produced in theories where quantum gravity is propagating in extra spatial dimensions. In such theories, gravitons may be produced copiously in association with a photon. The graviton subsequently escapes detection giving rise to the photon and missing energy signature. Such events can also be used to study the trilinear WWγ vertex and thereby

Table 9: Numerical predictions from theoretical calculations of the following realistic observables in $l^+l^-\gamma$ final states; *cross-sections*. The last field of the table shows relative deviation (multiplied by 100) with respect to the first calculation.

obs.	program	ene	value and error estimate	comments	δ ratio
ALEPH-11	LABSMC no pair	189.0	$3.7557 \cdot 10^{0} \pm 3.22 \cdot 10^{-3}$		
	BHWIDE	189.0	$3.6330 \cdot 10^{0} \pm 6.70 \cdot 10^{-3}$		-3.27
	LABSMC no pair	200.0	$3.3771 \cdot 10^{0} \pm 2.88 \cdot 10^{-3}$		
	BHWIDE	200.0	$3.2945 \cdot 10^{0} \pm 5.50 \cdot 10^{-3}$		-2.45
	LABSMC no pair	206.0	$3.1927 \cdot 10^{0} \pm 2.71 \cdot 10^{-3}$		
	BHWIDE	206.0	$3.0946 \cdot 10^{0} \pm 4.70 \cdot 10^{-3}$		-3.07
DELPHI8	LABSMC no pair	189.0	$4.4705 \cdot 10^{0} \pm 3.51 \cdot 10^{-3}$		
	LABSMC no pair	200.0	$4.0981 \cdot 10^{0} \pm 3.17 \cdot 10^{-3}$		
	LABSMC no pair	206.0	$3.9101 \cdot 10^{0} \pm 3.01 \cdot 10^{-3}$		
LT14	LABSMC no pair	189.0	$2.7800 \cdot 10^{0} \pm 2.77 \cdot 10^{-3}$		
	LABSMC no pair	200.0	$2.5884 \cdot 10^{0} \pm 2.52 \cdot 10^{-3}$		
	LABSMC no pair	206.0	$2.4896 \cdot 10^{0} \pm 2.40 \cdot 10^{-3}$		
Opal12	LABSMC no pair	189.0	$1.0097 \cdot 10^{0} \pm 1.67 \cdot 10^{-3}$		
	BHWIDE	189.0	$9.7750 \cdot 10^{-1} \pm 4.60 \cdot 10^{-3}$		-3.19
	LABSMC no pair	200.0	$8.9901 \cdot 10^{-1} \pm 1.49 \cdot 10^{-3}$		
	BHWIDE	200.0	$8.7700 \cdot 10^{-1} \pm 4.00 \cdot 10^{-3}$		-2.45
	LABSMC no pair	206.0	$8.4595 \cdot 10^{-1} \pm 1.40 \cdot 10^{-3}$		
	BHWIDE	206.0	$8.2040 \cdot 10^{-1} \pm 3.70 \cdot 10^{-3}$		-3.02
Opal13	LABSMC no pair	189.0	$8.7387 \cdot 10^{-1} \pm 1.55 \cdot 10^{-3}$		
	BHWIDE	189.0	$8.4600 \cdot 10^{-1} \pm 3.90 \cdot 10^{-3}$		-3.19
	LABSMC no pair	200.0	$7.8068 \cdot 10^{-1} \pm 1.38 \cdot 10^{-3}$		
	BHWIDE	200.0	$7.5790 \cdot 10^{-1} \pm 3.30 \cdot 10^{-3}$		-2.92
	LABSMC no pair	206.0	$7.3532 \cdot 10^{-1} \pm 1.30 \cdot 10^{-3}$		
	BHWIDE	206.0	$7.1080 \cdot 10^{-1} \pm 3.00 \cdot 10^{-3}$		-3.33
ALEPH-14	BHWIDE	189.0	$5.5000 \cdot 10^{-3} \pm 5.00 \cdot 10^{-4}$		
	BHWIDE	200.0	$5.1000 \cdot 10^{-3} \pm 3.00 \cdot 10^{-4}$		
	BHWIDE	206.0	$4.6000 \cdot 10^{-3} \pm 3.00 \cdot 10^{-4}$		
LT17	BHWIDE	189.0	$1.3700 \cdot 10^{-2} \pm 6.00 \cdot 10^{-4}$		
	BHWIDE	200.0	$1.2500 \cdot 10^{-2} \pm 5.00 \cdot 10^{-4}$		
	BHWIDE	206.0	$1.2300 \cdot 10^{-2} \pm 5.00 \cdot 10^{-4}$		
Opal18	BHWIDE	189.0	$8.5300 \cdot 10^{-2} \pm 1.70 \cdot 10^{-3}$		
	BHWIDE	200.0	$7.5200 \cdot 10^{-2} \pm 1.30 \cdot 10^{-3}$		
	BHWIDE	206.0	$6.9600 \cdot 10^{-2} \pm 1.20 \cdot 10^{-3}$		
Opal19	BHWIDE	189.0	$7.7600 \cdot 10^{-2} \pm 1.50 \cdot 10^{-3}$		
	BHWIDE	200.0	$6.9300 \cdot 10^{-2} \pm 1.20 \cdot 10^{-3}$		
	BHWIDE	206.0	$6.4900 \cdot 10^{-2} \pm 1.10 \cdot 10^{-3}$		
ALEPH-12	KKMC 4.14	189.0	$3.9198 \cdot 10^{-1} \pm 7.56 \cdot 10^{-4}$	CEEX2	
	KKMC 4.14	189.0	$4.2566 \cdot 10^{-1} \pm 7.66 \cdot 10^{-4}$	CEEX2 IFIoff	8.59
	KKMC 4.14	189.0	$4.3236 \cdot 10^{-1} \pm 7.71 \cdot 10^{-4}$	EEX2	10.30
	KKMC 4.14	189.0	$4.3210 \cdot 10^{-1} \pm 7.70 \cdot 10^{-4}$	EEX3	10.23
	KORALZ 4.04	189.0	$4.2770 \cdot 10^{-1} \pm 1.16 \cdot 10^{-3}$		9.11
	KKMC 4.14	206.0	$1.6967 \cdot 10^{-1} \pm 5.18 \cdot 10^{-4}$	CEEX2	
	KKMC 4.14	206.0	$1.9697 \cdot 10^{-1} \pm 5.35 \cdot 10^{-4}$	CEEX2 IFIoff	16.09
	KKMC 4.14	206.0	$1.9879 \cdot 10^{-1} \pm 5.37 \cdot 10^{-4}$	EEX2	17.16
	KKMC 4.14	206.0	$1.9877 \cdot 10^{-1} \pm 5.37 \cdot 10^{-4}$	EEX3	17.15
	KORALZ 4.04	206.0	$1.9850 \cdot 10^{-1} \pm 7.25 \cdot 10^{-4}$		16.99
ALEPH-15	KKMC 4.14	189.0	$2.1482 \cdot 10^{-3} \pm 4.14 \cdot 10^{-5}$	CEEX2	
	KKMC 4.14	189.0	$2.2307 \cdot 10^{-3} \pm 4.05 \cdot 10^{-5}$	CEEX2 IFIoff	3.84
	KKMC 4.14	189.0	$2.1427 \cdot 10^{-3} \pm 3.55 \cdot 10^{-5}$	EEX2	-0.26
	KKMC 4.14	189.0	$2.0841 \cdot 10^{-3} \pm 3.53 \cdot 10^{-5}$	EEX3	-2.98
	KORALZ 4.04	189.0	$2.1251 \cdot 10^{-3} \pm 8.39 \cdot 10^{-5}$		-1.08
	KKMC 4.14	206.0	$1.6532 \cdot 10^{-3} \pm 4.45 \cdot 10^{-5}$	CEEX2	
	KKMC 4.14	206.0	$1.7860 \cdot 10^{-3} \pm 7.52 \cdot 10^{-5}$	CEEX2 IFIoff	8.03
	KKMC 4.14	206.0	$1.6686 \cdot 10^{-3} \pm 2.79 \cdot 10^{-5}$	EEX2	0.93
	KKMC 4.14	206.0	$1.6142 \cdot 10^{-3} \pm 2.77 \cdot 10^{-5}$	EEX3	-2.36
	KORALZ 4.04	206.0	$1.6542 \cdot 10^{-3} \pm 6.71 \cdot 10^{-5}$		0.06
DELPHI9	KKMC 4.14	189.0	$1.0711 \cdot 10^{0} \pm 1.17 \cdot 10^{-3}$	CEEX2	
	KKMC 4.14	189.0	$1.1386 \cdot 10^{0} \pm 1.18 \cdot 10^{-3}$	CEEX2 IFIoff	6.30
	KKMC 4.14	189.0	$1.1520 \cdot 10^{0} \pm 1.18 \cdot 10^{-3}$	EEX2	7.56
	KKMC 4.14	189.0	$1.1504 \cdot 10^{0} \pm 1.18 \cdot 10^{-3}$	EEX3	7.41
	KORALZ 4.04	189.0	$1.1516 \cdot 10^{0} \pm 1.82 \cdot 10^{-3}$		7.52
	KKMC 4.14	206.0	$8.6262 \cdot 10^{-1} \pm 9.15 \cdot 10^{-4}$	CEEX2	
	KKMC 4.14	206.0	$9.1859 \cdot 10^{-1} \pm 9.26 \cdot 10^{-4}$	CEEX2 IFIoff	6.49
	KKMC 4.14	206.0	$9.3087 \cdot 10^{-1} \pm 9.22 \cdot 10^{-4}$	EEX2	7.91
	KKMC 4.14	206.0	$9.2927 \cdot 10^{-1} \pm 9.22 \cdot 10^{-4}$	EEX3	7.73
	KORALZ 4.04	206.0	$9.2807 \cdot 10^{-1} \pm 1.48 \cdot 10^{-3}$		7.59

obs.	program	ene	value and error estimate	comments	δ ratio
DELPHI12	KKMC 4.14	189.0	$1.1896 \cdot 10^{-2} \pm 1.06 \cdot 10^{-4}$	CEEX2	
	KKMC 4.14	189.0	$1.2985 \cdot 10^{-2} \pm 1.09 \cdot 10^{-4}$	CEEX2 IFIoff	9.16
	KKMC 4.14	189.0	$1.2951 \cdot 10^{-2} \pm 1.06 \cdot 10^{-4}$	EEX2	8.87
	KKMC 4.14	189.0	$1.2762 \cdot 10^{-2} \pm 1.05 \cdot 10^{-4}$	EEX3	7.28
	KORALZ 4.04	189.0	$1.2740 \cdot 10^{-2} \pm 2.05 \cdot 10^{-4}$		7.10
	KKMC 4.14	206.0	$8.9173 \cdot 10^{-3} \pm 8.09 \cdot 10^{-5}$	CEEX2	
	KKMC 4.14	206.0	$9.7636 \cdot 10^{-3} \pm 8.64 \cdot 10^{-5}$	CEEX2 IFIoff	9.49
	KKMC 4.14	206.0	$9.6816 \cdot 10^{-3} \pm 8.03 \cdot 10^{-5}$	EEX2	8.57
	KKMC 4.14	206.0	$9.5247 \cdot 10^{-3} \pm 8.00 \cdot 10^{-5}$	EEX3	6.81
	KORALZ 4.04	206.0	$9.4411 \cdot 10^{-3} \pm 1.60 \cdot 10^{-4}$		5.87
LT15	KKMC 4.14	189.0	$4.3261 \cdot 10^{-1} \pm 7.07 \cdot 10^{-4}$	CEEX2	
	KKMC 4.14	189.0	$4.6135 \cdot 10^{-1} \pm 7.27 \cdot 10^{-4}$	CEEX2 IFIoff	6.64
	KKMC 4.14	189.0	$4.6345 \cdot 10^{-1} \pm 7.23 \cdot 10^{-4}$	EEX2	7.13
	KKMC 4.14	189.0	$4.6352 \cdot 10^{-1} \pm 7.23 \cdot 10^{-4}$	EEX3	7.14
	KORALZ 4.04	189.0	$4.6300 \cdot 10^{-1} \pm 1.21 \cdot 10^{-3}$		7.03
	KKMC 4.14	206.0	$3.6073 \cdot 10^{-1} \pm 5.65 \cdot 10^{-4}$	CEEX2	
	KKMC 4.14	206.0	$3.8588 \cdot 10^{-1} \pm 5.83 \cdot 10^{-4}$	CEEX2 IFIoff	6.97
	KKMC 4.14	206.0	$3.8825 \cdot 10^{-1} \pm 5.81 \cdot 10^{-4}$	EEX2	7.63
	KKMC 4.14	206.0	$3.8815 \cdot 10^{-1} \pm 5.81 \cdot 10^{-4}$	EEX3	7.60
	KORALZ 4.04	206.0	$3.9020 \cdot 10^{-1} \pm 1.00 \cdot 10^{-3}$		8.17
LT18	KKMC 4.14	189.0	$4.7264 \cdot 10^{-3} \pm 5.71 \cdot 10^{-5}$	CEEX2	
	KKMC 4.14	189.0	$5.0399 \cdot 10^{-3} \pm 5.92 \cdot 10^{-5}$	CEEX2 IFIoff	6.63
	KKMC 4.14	189.0	$4.9062 \cdot 10^{-3} \pm 5.59 \cdot 10^{-5}$	EEX2	3.80
	KKMC 4.14	189.0	$4.9198 \cdot 10^{-3} \pm 5.62 \cdot 10^{-5}$	EEX3	4.09
	KORALZ 4.04	189.0	$5.0060 \cdot 10^{-3} \pm 1.29 \cdot 10^{-4}$		5.92
	KKMC 4.14	206.0	$3.6632 \cdot 10^{-3} \pm 4.46 \cdot 10^{-5}$	CEEX2	
	KKMC 4.14	206.0	$3.9542 \cdot 10^{-3} \pm 4.65 \cdot 10^{-5}$	CEEX2 IFIoff	7.94
	KKMC 4.14	206.0	$3.8426 \cdot 10^{-3} \pm 4.40 \cdot 10^{-5}$	EEX2	4.90
	KKMC 4.14	206.0	$3.8417 \cdot 10^{-3} \pm 4.41 \cdot 10^{-5}$	EEX3	4.87
	KORALZ 4.04	206.0	$3.8309 \cdot 10^{-3} \pm 1.02 \cdot 10^{-4}$		4.58
Opal14	KKMC 4.14	189.0	$5.8425 \cdot 10^{-1} \pm 8.89 \cdot 10^{-4}$	CEEX2	
	KKMC 4.14	189.0	$6.4295 \cdot 10^{-1} \pm 9.60 \cdot 10^{-4}$	CEEX2 IFIoff	10.05
	KKMC 4.14	189.0	$6.5139 \cdot 10^{-1} \pm 9.64 \cdot 10^{-4}$	EEX2	11.49
	KKMC 4.14	189.0	$6.5164 \cdot 10^{-1} \pm 9.64 \cdot 10^{-4}$	EEX3	11.54
	KORALZ 4.04	189.0	$6.4707 \cdot 10^{-1} \pm 1.41 \cdot 10^{-3}$		10.75
	KKMC 4.14	206.0	$4.6775 \cdot 10^{-1} \pm 6.91 \cdot 10^{-4}$	CEEX2	
	KKMC 4.14	206.0	$5.1427 \cdot 10^{-1} \pm 7.45 \cdot 10^{-4}$	CEEX2 IFIoff	9.95
	KKMC 4.14	206.0	$5.2153 \cdot 10^{-1} \pm 7.48 \cdot 10^{-4}$	EEX2	11.50
	KKMC 4.14	206.0	$5.2175 \cdot 10^{-1} \pm 7.48 \cdot 10^{-4}$	EEX3	11.55
	KORALZ 4.04	206.0	$5.1632 \cdot 10^{-1} \pm 1.14 \cdot 10^{-3}$		10.38
Opal15	KKMC 4.14	189.0	$3.1255 \cdot 10^{-1} \pm 7.52 \cdot 10^{-4}$	CEEX2	
	KKMC 4.14	189.0	$3.7040 \cdot 10^{-1} \pm 8.46 \cdot 10^{-4}$	CEEX2 IFIoff	18.51
	KKMC 4.14	189.0	$3.7294 \cdot 10^{-1} \pm 8.48 \cdot 10^{-4}$	EEX2	19.32
	KKMC 4.14	189.0	$3.7333 \cdot 10^{-1} \pm 8.48 \cdot 10^{-4}$	EEX3	19.45
	KORALZ 4.04	189.0	$3.7106 \cdot 10^{-1} \pm 1.09 \cdot 10^{-3}$		18.72
	KKMC 4.14	206.0	$2.5805 \cdot 10^{-1} \pm 5.96 \cdot 10^{-4}$	CEEX2	
	KKMC 4.14	206.0	$3.0380 \cdot 10^{-1} \pm 6.65 \cdot 10^{-4}$	CEEX2 IFIoff	17.73
	KKMC 4.14	206.0	$3.0610 \cdot 10^{-1} \pm 6.67 \cdot 10^{-4}$	EEX2	18.62
	KKMC 4.14	206.0	$3.0642 \cdot 10^{-1} \pm 6.67 \cdot 10^{-4}$	EEX3	18.75
	KORALZ 4.04	206.0	$3.0499 \cdot 10^{-1} \pm 8.91 \cdot 10^{-4}$		18.19
Opal20	KKMC 4.14	189.0	$3.1979 \cdot 10^{-2} \pm 1.64 \cdot 10^{-4}$	CEEX2	
	KKMC 4.14	189.0	$3.5019 \cdot 10^{-2} \pm 1.74 \cdot 10^{-4}$	CEEX2 IFIoff	9.51
	KKMC 4.14	189.0	$3.4397 \cdot 10^{-2} \pm 1.66 \cdot 10^{-4}$	EEX2	7.56
	KKMC 4.14	189.0	$3.4416 \cdot 10^{-2} \pm 1.67 \cdot 10^{-4}$	EEX3	7.62
	KORALZ 4.04	189.0	$3.4896 \cdot 10^{-2} \pm 3.39 \cdot 10^{-4}$		9.12
	KKMC 4.14	206.0	$2.5259 \cdot 10^{-2} \pm 1.30 \cdot 10^{-4}$	CEEX2	
	KKMC 4.14	206.0	$2.7679 \cdot 10^{-2} \pm 1.53 \cdot 10^{-4}$	CEEX2 IFIoff	9.58
	KKMC 4.14	206.0	$2.7030 \cdot 10^{-2} \pm 1.27 \cdot 10^{-4}$	EEX2	7.01
	KKMC 4.14	206.0	$2.7035 \cdot 10^{-2} \pm 1.27 \cdot 10^{-4}$	EEX3	7.03
	KORALZ 4.04	206.0	$2.6789 \cdot 10^{-2} \pm 2.69 \cdot 10^{-4}$		6.06
Opal21	KKMC 4.14	189.0	$1.9285 \cdot 10^{-2} \pm 1.33 \cdot 10^{-4}$	CEEX2	
	KKMC 4.14	189.0	$2.2261 \cdot 10^{-2} \pm 1.49 \cdot 10^{-4}$	CEEX2 IFIoff	15.44
	KKMC 4.14	189.0	$2.1739 \cdot 10^{-2} \pm 1.43 \cdot 10^{-4}$	EEX2	12.73
	KKMC 4.14	189.0	$2.1779 \cdot 10^{-2} \pm 1.43 \cdot 10^{-4}$	EEX3	12.94
	KORALZ 4.04	189.0	$2.1960 \cdot 10^{-2} \pm 2.69 \cdot 10^{-4}$		13.87
	KKMC 4.14	206.0	$1.5516 \cdot 10^{-2} \pm 1.10 \cdot 10^{-4}$	CEEX2	
	KKMC 4.14	206.0	$1.7853 \cdot 10^{-2} \pm 1.39 \cdot 10^{-4}$	CEEX2 IFIoff	15.06
	KKMC 4.14	206.0	$1.7316 \cdot 10^{-2} \pm 1.11 \cdot 10^{-4}$	EEX2	11.60
	KKMC 4.14	206.0	$1.7342 \cdot 10^{-2} \pm 1.11 \cdot 10^{-4}$	EEX3	11.77
	KORALZ 4.04	206.0	$1.7228 \cdot 10^{-2} \pm 2.16 \cdot 10^{-4}$		11.03

Table 10: Numerical predictions from theoretical calculations of the following realistic observables in $\nu\bar{\nu}\gamma$ final states. The last field of the table shows relative deviation (multiplied by 100) with respect to the first calculation.

obs.	program	ene	value and error estimate	δ ratio
Nu1	NUNUGPV	189.0	$3.2559{\cdot}10^{0}$ $\pm 2.00{\cdot}10^{-3}$	
	grcnunugam	189.0	$3.1800{\cdot}10^{0}$ $\pm 1.00{\cdot}10^{-3}$	-2.33
	KORALZ 4.04	189.0	$3.2244{\cdot}10^{0}$ $\pm 4.34{\cdot}10^{-3}$	-0.97
	NUNUGPV	200.0	$2.8711{\cdot}10^{0}$ $\pm 1.80{\cdot}10^{-3}$	
	grcnunugam	200.0	$2.7930{\cdot}10^{0}$ $\pm 1.00{\cdot}10^{-3}$	-2.72
	KORALZ 4.04	200.0	$2.8414{\cdot}10^{0}$ $\pm 3.90{\cdot}10^{-3}$	-1.03
	NUNUGPV	206.0	$2.6986{\cdot}10^{0}$ $\pm 1.70{\cdot}10^{-3}$	
	grcnunugam	206.0	$2.6190{\cdot}10^{0}$ $\pm 1.00{\cdot}10^{-3}$	-2.95
	KORALZ 4.04	206.0	$2.6742{\cdot}10^{0}$ $\pm 3.70{\cdot}10^{-3}$	-0.90
Nu2	NUNUGPV	189.0	$2.0900{\cdot}10^{-1}$ $\pm 1.20{\cdot}10^{-3}$	
	grcnunugam	189.0	$2.1100{\cdot}10^{-1}$ $\pm 5.00{\cdot}10^{-4}$	0.96
	KORALZ 4.04	189.0	$2.1733{\cdot}10^{-1}$ $\pm 1.20{\cdot}10^{-3}$	3.98
	NUNUGPV	200.0	$1.8730{\cdot}10^{-1}$ $\pm 1.20{\cdot}10^{-3}$	
	grcnunugam	200.0	$1.8770{\cdot}10^{-1}$ $\pm 5.00{\cdot}10^{-4}$	0.21
	KORALZ 4.04	200.0	$1.9278{\cdot}10^{-1}$ $\pm 1.07{\cdot}10^{-3}$	2.93
	NUNUGPV	206.0	$1.7870{\cdot}10^{-1}$ $\pm 2.70{\cdot}10^{-3}$	
	grcnunugam	206.0	$1.7760{\cdot}10^{-1}$ $\pm 5.00{\cdot}10^{-4}$	-0.62
	KORALZ 4.04	206.0	$1.8309{\cdot}10^{-1}$ $\pm 1.02{\cdot}10^{-3}$	2.46
Nu11	NUNUGPV	189.0	$8.8950{\cdot}10^{-1}$ $\pm 9.00{\cdot}10^{-4}$	
	grcnunugam	189.0	$9.1900{\cdot}10^{-1}$ $\pm 3.00{\cdot}10^{-3}$	3.32
	KORALZ 4.04	189.0	$9.1767{\cdot}10^{-1}$ $\pm 2.42{\cdot}10^{-3}$	3.17
	NUNUGPV	200.0	$7.8120{\cdot}10^{-1}$ $\pm 8.00{\cdot}10^{-4}$	
	grcnunugam	200.0	$8.1400{\cdot}10^{-1}$ $\pm 2.00{\cdot}10^{-3}$	4.20
	KORALZ 4.04	200.0	$8.1236{\cdot}10^{-1}$ $\pm 2.17{\cdot}10^{-3}$	3.99
	NUNUGPV	206.0	$7.3220{\cdot}10^{-1}$ $\pm 8.00{\cdot}10^{-4}$	
	grcnunugam	206.0	$7.7200{\cdot}10^{-1}$ $\pm 5.00{\cdot}10^{-3}$	5.44
	KORALZ 4.04	206.0	$7.6398{\cdot}10^{-1}$ $\pm 2.06{\cdot}10^{-3}$	4.34
Nu12	NUNUGPV	189.0	$1.7784{\cdot}10^{0}$ $\pm 3.80{\cdot}10^{-3}$	
	grcnunugam	189.0	$1.7680{\cdot}10^{0}$ $\pm 1.00{\cdot}10^{-3}$	-0.58
	KORALZ 4.04	189.0	$1.8442{\cdot}10^{0}$ $\pm 3.37{\cdot}10^{-3}$	3.70
	NUNUGPV	200.0	$1.5657{\cdot}10^{0}$ $\pm 2.90{\cdot}10^{-3}$	
	grcnunugam	200.0	$1.5760{\cdot}10^{0}$ $\pm 1.00{\cdot}10^{-3}$	0.66
	KORALZ 4.04	200.0	$1.6235{\cdot}10^{0}$ $\pm 3.02{\cdot}10^{-3}$	3.69
	NUNUGPV	206.0	$1.4697{\cdot}10^{0}$ $\pm 3.80{\cdot}10^{-3}$	
	grcnunugam	206.0	$1.4890{\cdot}10^{0}$ $\pm 1.00{\cdot}10^{-3}$	1.31
	KORALZ 4.04	206.0	$1.5215{\cdot}10^{0}$ $\pm 2.86{\cdot}10^{-3}$	3.52
Nu13	NUNUGPV	189.0	$1.7235{\cdot}10^{0}$ $\pm 1.90{\cdot}10^{-3}$	
	grcnunugam	189.0	$1.6840{\cdot}10^{0}$ $\pm 1.00{\cdot}10^{-3}$	-2.29
	KORALZ 4.04	189.0	$1.8045{\cdot}10^{0}$ $\pm 3.35{\cdot}10^{-3}$	4.70
	NUNUGPV	200.0	$1.5281{\cdot}10^{0}$ $\pm 1.60{\cdot}10^{-3}$	
	grcnunugam	200.0	$1.5110{\cdot}10^{0}$ $\pm 1.00{\cdot}10^{-3}$	-1.12
	KORALZ 4.04	200.0	$1.6033{\cdot}10^{0}$ $\pm 3.01{\cdot}10^{-3}$	4.92
	NUNUGPV	206.0	$1.4413{\cdot}10^{0}$ $\pm 1.50{\cdot}10^{-3}$	
	grcnunugam	206.0	$1.4330{\cdot}10^{0}$ $\pm 1.00{\cdot}10^{-3}$	-0.58
	KORALZ 4.04	206.0	$1.5179{\cdot}10^{0}$ $\pm 2.87{\cdot}10^{-3}$	5.31
Nu14	NUNUGPV	189.0	$1.9770{\cdot}10^{-1}$ $\pm 5.00{\cdot}10^{-4}$	
	grcnunugam	189.0	$1.9600{\cdot}10^{-1}$ $\pm 2.00{\cdot}10^{-3}$	-0.86
	KORALZ 4.04	189.0	$2.0121{\cdot}10^{-1}$ $\pm 1.15{\cdot}10^{-3}$	1.78
	NUNUGPV	200.0	$1.7360{\cdot}10^{-1}$ $\pm 5.00{\cdot}10^{-4}$	
	grcnunugam	200.0	$1.7200{\cdot}10^{-1}$ $\pm 1.00{\cdot}10^{-3}$	-0.92
	KORALZ 4.04	200.0	$1.7534{\cdot}10^{-1}$ $\pm 1.02{\cdot}10^{-3}$	1.00
	NUNUGPV	206.0	$1.6280{\cdot}10^{-1}$ $\pm 6.00{\cdot}10^{-4}$	
	grcnunugam	206.0	$1.6100{\cdot}10^{-1}$ $\pm 1.00{\cdot}10^{-3}$	-1.11
	KORALZ 4.04	206.0	$1.6323{\cdot}10^{-1}$ $\pm 9.66{\cdot}10^{-4}$	0.26
Nu3	NUNUGPV	189.0	$4.2913{\cdot}10^{0}$ $\pm 2.80{\cdot}10^{-3}$	
	grcnunugam	189.0	$4.2390{\cdot}10^{0}$ $\pm 3.00{\cdot}10^{-3}$	-1.22
	KORALZ 4.04	189.0	$4.2885{\cdot}10^{0}$ $\pm 4.89{\cdot}10^{-3}$	-0.07
	NUNUGPV	200.0	$3.8532{\cdot}10^{0}$ $\pm 2.60{\cdot}10^{-3}$	
	grcnunugam	200.0	$3.7880{\cdot}10^{0}$ $\pm 3.00{\cdot}10^{-3}$	-1.69
	KORALZ 4.04	200.0	$3.8451{\cdot}10^{0}$ $\pm 4.43{\cdot}10^{-3}$	-0.21
	NUNUGPV	206.0	$3.6546{\cdot}10^{0}$ $\pm 2.50{\cdot}10^{-3}$	
	grcnunugam	206.0	$3.5890{\cdot}10^{0}$ $\pm 2.00{\cdot}10^{-3}$	-1.79
	KORALZ 4.04	206.0	$3.6529{\cdot}10^{0}$ $\pm 4.22{\cdot}10^{-3}$	-0.05

obs.	program	ene	value and error estimate	δ ratio
Nu4g	NUNUGPV	189.0	$1.9218{\cdot}10^{0}$ $\pm 1.30{\cdot}10^{-3}$	
	grcnunugam	189.0	$1.9110{\cdot}10^{0}$ $\pm 2.00{\cdot}10^{-3}$	-0.56
	KORALZ 4.04	189.0	$1.9398{\cdot}10^{0}$ $\pm 3.46{\cdot}10^{-3}$	0.94
	NUNUGPV	200.0	$1.7276{\cdot}10^{0}$ $\pm 1.20{\cdot}10^{-3}$	
	grcnunugam	200.0	$1.7080{\cdot}10^{0}$ $\pm 1.00{\cdot}10^{-3}$	-1.13
	KORALZ 4.04	200.0	$1.7430{\cdot}10^{0}$ $\pm 3.13{\cdot}10^{-3}$	0.89
	NUNUGPV	206.0	$1.6406{\cdot}10^{0}$ $\pm 1.20{\cdot}10^{-3}$	
	grcnunugam	206.0	$1.6200{\cdot}10^{0}$ $\pm 1.00{\cdot}10^{-3}$	-1.26
	KORALZ 4.04	206.0	$1.6611{\cdot}10^{0}$ $\pm 2.99{\cdot}10^{-3}$	1.25
Nu5	NUNUGPV	189.0	$1.1600{\cdot}10^{-1}$ $\pm 3.00{\cdot}10^{-4}$	
	grcnunugam	189.0	$1.1750{\cdot}10^{-1}$ $\pm 2.00{\cdot}10^{-4}$	1.29
	KORALZ 4.04	189.0	$1.1850{\cdot}10^{-1}$ $\pm 8.83{\cdot}10^{-4}$	2.15
	NUNUGPV	200.0	$1.0550{\cdot}10^{-1}$ $\pm 3.00{\cdot}10^{-4}$	
	grcnunugam	200.0	$1.0680{\cdot}10^{-1}$ $\pm 2.00{\cdot}10^{-4}$	1.23
	KORALZ 4.04	200.0	$1.0779{\cdot}10^{-1}$ $\pm 8.03{\cdot}10^{-4}$	2.17
	NUNUGPV	206.0	$1.0070{\cdot}10^{-1}$ $\pm 4.00{\cdot}10^{-4}$	
	grcnunugam	206.0	$1.0180{\cdot}10^{-1}$ $\pm 2.00{\cdot}10^{-4}$	1.09
	KORALZ 4.04	206.0	$1.0247{\cdot}10^{-1}$ $\pm 7.66{\cdot}10^{-4}$	1.75
Nu6	NUNUGPV	189.0	$5.4200{\cdot}10^{-2}$ $\pm 3.00{\cdot}10^{-4}$	
	grcnunugam	189.0	$5.5000{\cdot}10^{-2}$ $\pm 2.00{\cdot}10^{-4}$	1.48
	KORALZ 4.04	189.0	$5.6543{\cdot}10^{-2}$ $\pm 6.11{\cdot}10^{-4}$	4.32
	NUNUGPV	200.0	$4.8700{\cdot}10^{-2}$ $\pm 4.00{\cdot}10^{-4}$	
	grcnunugam	200.0	$4.9000{\cdot}10^{-2}$ $\pm 2.00{\cdot}10^{-4}$	0.62
	KORALZ 4.04	200.0	$4.9965{\cdot}10^{-2}$ $\pm 5.48{\cdot}10^{-4}$	2.60
	NUNUGPV	206.0	$4.6700{\cdot}10^{-2}$ $\pm 5.00{\cdot}10^{-4}$	
	grcnunugam	206.0	$4.6300{\cdot}10^{-2}$ $\pm 1.00{\cdot}10^{-4}$	-0.86
	KORALZ 4.04	206.0	$4.7053{\cdot}10^{-2}$ $\pm 5.21{\cdot}10^{-4}$	0.76
Nu7	NUNUGPV	189.0	$4.6140{\cdot}10^{0}$ $\pm 1.40{\cdot}10^{-2}$	
	grcnunugam	189.0	$4.6650{\cdot}10^{0}$ $\pm 6.00{\cdot}10^{-3}$	1.11
	KORALZ 4.04	189.0	$4.5109{\cdot}10^{0}$ $\pm 5.00{\cdot}10^{-3}$	-2.24
	NUNUGPV	200.0	$4.0710{\cdot}10^{0}$ $\pm 1.00{\cdot}10^{-2}$	
	grcnunugam	200.0	$4.1850{\cdot}10^{0}$ $\pm 6.00{\cdot}10^{-3}$	2.80
	KORALZ 4.04	200.0	$4.0540{\cdot}10^{0}$ $\pm 4.52{\cdot}10^{-3}$	-0.42
	NUNUGPV	206.0	$3.8600{\cdot}10^{0}$ $\pm 1.30{\cdot}10^{-3}$	
	grcnunugam	206.0	$3.9650{\cdot}10^{0}$ $\pm 7.00{\cdot}10^{-3}$	2.72
	KORALZ 4.04	206.0	$3.8534{\cdot}10^{0}$ $\pm 4.31{\cdot}10^{-3}$	-0.17
Nu8	NUNUGPV	189.0	$1.6320{\cdot}10^{-1}$ $\pm 6.00{\cdot}10^{-4}$	
	grcnunugam	189.0	$1.6450{\cdot}10^{-1}$ $\pm 4.00{\cdot}10^{-4}$	0.80
	KORALZ 4.04	189.0	$1.7074{\cdot}10^{-1}$ $\pm 1.06{\cdot}10^{-3}$	4.62
	NUNUGPV	200.0	$1.4410{\cdot}10^{-1}$ $\pm 8.00{\cdot}10^{-4}$	
	grcnunugam	200.0	$1.4850{\cdot}10^{-1}$ $\pm 3.00{\cdot}10^{-4}$	3.05
	KORALZ 4.04	200.0	$1.4912{\cdot}10^{-1}$ $\pm 9.44{\cdot}10^{-4}$	3.49
	NUNUGPV	206.0	$1.3490{\cdot}10^{-1}$ $\pm 8.00{\cdot}10^{-4}$	
	grcnunugam	206.0	$1.4230{\cdot}10^{-1}$ $\pm 3.00{\cdot}10^{-4}$	5.49
	KORALZ 4.04	206.0	$1.3915{\cdot}10^{-1}$ $\pm 8.92{\cdot}10^{-4}$	3.15
Nu9	NUNUGPV	189.0	$7.2200{\cdot}10^{-2}$ $\pm 2.00{\cdot}10^{-4}$	
	grcnunugam	189.0	$7.4700{\cdot}10^{-2}$ $\pm 3.00{\cdot}10^{-4}$	3.46
	KORALZ 4.04	189.0	$7.4208{\cdot}10^{-2}$ $\pm 7.00{\cdot}10^{-4}$	2.78
	NUNUGPV	200.0	$6.4800{\cdot}10^{-2}$ $\pm 3.00{\cdot}10^{-4}$	
	grcnunugam	200.0	$6.7000{\cdot}10^{-2}$ $\pm 2.00{\cdot}10^{-4}$	3.40
	KORALZ 4.04	200.0	$6.6175{\cdot}10^{-2}$ $\pm 6.31{\cdot}10^{-4}$	2.12
	NUNUGPV	206.0	$6.1500{\cdot}10^{-2}$ $\pm 3.00{\cdot}10^{-4}$	
	grcnunugam	206.0	$6.3500{\cdot}10^{-2}$ $\pm 2.00{\cdot}10^{-4}$	3.25
	KORALZ 4.04	206.0	$6.2656{\cdot}10^{-2}$ $\pm 6.00{\cdot}10^{-4}$	1.88
Nu10	NUNUGPV	189.0	$2.4670{\cdot}10^{-1}$ $\pm 1.50{\cdot}10^{-3}$	
	grcnunugam	189.0	$2.5330{\cdot}10^{-1}$ $\pm 6.00{\cdot}10^{-4}$	2.68
	KORALZ 4.04	189.0	$2.5040{\cdot}10^{-1}$ $\pm 1.28{\cdot}10^{-3}$	1.50
	NUNUGPV	200.0	$2.2130{\cdot}10^{-1}$ $\pm 1.80{\cdot}10^{-3}$	
	grcnunugam	200.0	$2.2800{\cdot}10^{-1}$ $\pm 5.00{\cdot}10^{-4}$	3.03
	KORALZ 4.04	200.0	$2.2332{\cdot}10^{-1}$ $\pm 1.15{\cdot}10^{-3}$	0.91
	NUNUGPV	206.0	$2.1020{\cdot}10^{-1}$ $\pm 1.90{\cdot}10^{-3}$	
	grcnunugam	206.0	$2.1620{\cdot}10^{-1}$ $\pm 5.00{\cdot}10^{-4}$	2.85
	KORALZ 4.04	206.0	$2.1185{\cdot}10^{-1}$ $\pm 1.10{\cdot}10^{-3}$	0.78

to search for anomalous couplings. The Standard Model background for such searches comes from two processes: radiative returns to the Z resonance, with the Z decaying to neutrinos, and t-channel W exchange with the photon(s) radiated from the beam electrons or the W.

The large integrated luminosity provide by LEP at high energies allows such searches to be performed with high precision. At the end of the LEP2 running period each experiment will have around 1800 single photon and missing energy events and close to 90 events with two photons and missing energy. When the data from the four experiments are combined the single photon cross section will be measured with a statistical precision of around 1.2%. The combined systematic uncertainties from the photon selection efficiency and luminosity measurement is expected to be around 0.5%. Clearly, to have a negligible contribution to the overall cross section measurement, and hence to the search for new physics, the theoretical uncertainty on the SM background prediction must also be at the 0.5% level. Much less precision is required for the two photon and missing energy channel, where the combined statistical uncertainty at the end of LEP2 will be around 5%. The precision required of the theoretical estimate of the SM background in this case is only 2%. For this final state the other sources of experimental systematic uncertainty are negligible.

The level of precision which is now being achieved by LEP is impressive. The initial estimate of the total integrated luminosity of LEP2 was only half what was finally achieved. Furthermore, techniques for combining the data from the photon and missing energy searches of all four experiments have been developed in the framework of the LEP SUSY Working Group. That is why, the required precision is so much higher than the 2% level which was though to be sufficient until now.

There were three independent Monte Carlo programs available for comparison of numerical results. The main sources of differences between the results of these calculations were expected to arise from the following effects:

1. Although the cuts are (supposed to be) the same for all programs, the input parameters were not set to the same values, we are not performing 'tuned comparisons'; this means in particular that we have to expect discrepancies of about 2% due to the different renormalization schemes implemented, as was for instance shown by the Japanese group in Ref. [35].

2. The QED corrections arising from missing non-log terms are expected to lead to a theoretical uncertainty of about 1-2%.

Taken these two effects into account, the size of the observed discrepancies[2] is essentially what was expected.

The comparison of observable between the different Monte Carlo programs may be summarized as follows:
• In the worst case the difference between the programs is at the level of 4-5%,
• Moreover, when the event selections are particularly clear/simple: and there are no sharp cuts (no selection of narrow bands in angular dependences, as in **Nu13** or cuts on soft photons **Nu13**) the level of agreement is better. This could arise as a result of systematic differences between the codes simply via different implementations of *very complicated* cuts. More likely, this could be explained by the different way how hard matrix elements and/or soft photons are treated in some corners of the phase space.
• This explanation seems to be supported by the following two plots 2, representing the missing mass spectrum for one and two photon events compared between KORALZ and NUNUGPV with cuts as for observables **Nu1** and **Nu2**. The KORALZ predictions tend to be higher than NUNUGPV for the part of the spectrum of missing mass smaller or comparable to Z and lower for events of large missing mass (which have relatively soft photons).

[2]The observable **Nu4g** was an exception, until the cut on the energy of the trigger photon was increased from previous 1 GeV to present 5 GeV. This may be good starting point for further investigation.

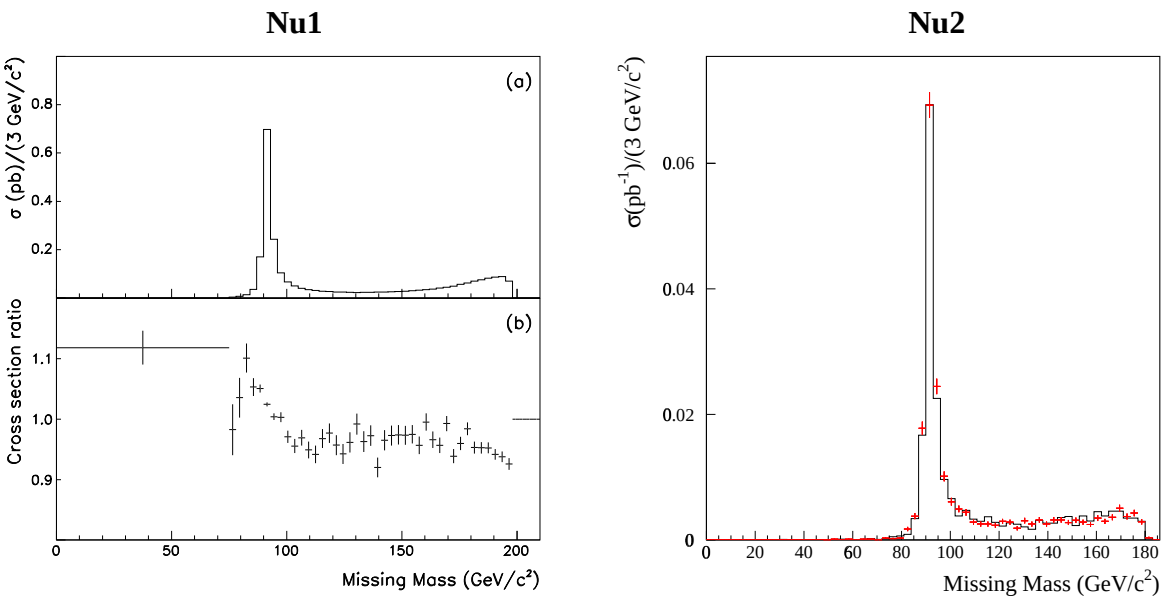

Fig. 2: *Left side:* Missing mass distribution from the NUNUGPV Monte Carlo: part (a); and ratio of KORALZ to NUNUGPV predictions: part (b). Plot was made for centre-of-mass energy of 206 GeV and selection cuts as defined for observable **Nu1**.
Right side: Missing mass distribution from the nunugpv Monte Carlo (histogram) and KORALZ (error bars) for centre-of- mass energy of 189 GeV and selection cuts as defined for observable **Nu2**.

• On the other hand the implementation of W contribution of $e^+e^- \to \nu_e\bar{\nu}_e\gamma$ channel in KORALZ is affected by approximation.

3.6.1 Conclusions for $\nu\bar{\nu}\gamma$

In the case of relatively *simple* observables (no selection of narrow bands in angular dependences or cuts on soft photons) agreement was found at the level 2–3% for both the single- and double- photon observables otherwise differences of around 3–5% are observed. Single- and double-tagged photon observables provide rather similar pattern of agreements and differences. It is possible that the contributions of electroweak box diagrams and pair corrections, which have not yet been fully studied, may introduce theoretical uncertainty of around 2–3%. This should not affect our estimate of the final theoretical uncertainty of around 4% for *simple* observables and 5% otherwise.

As an example of what this level of theoretical uncertainty may mean in practice let us use the search for TeV scale quantum gravity propagating in two extra dimensions. The combined LEP limit on the mass scale associated with this new physics at the end of LEP2 would be (assuming no hint of a signal)

1.23 TeV for 0.4% theoretical syst

1.21 TeV for 1.2% theoretical syst

1.12 TeV for 5.0% theoretical syst

For this topology the cross section for the new physics varies as $(1/M)^4$. The current (preliminary) limit from the ALEPH data taken up till now is 1.10 TeV. From the point of view of this analysis, until further theoretical developments will become available with the systematic error reduced below 4–5%, there is little point in analyzing the final years data nor, indeed in combining the results of the four LEP experiments.

4 MONTE CARLO AND SEMI-ANALYTICAL CODES AND THEIR OWN ERROR SPECIFICATIONS

In this section we present the Monte Carlo and the semi-analytical codes used in the work of our working group. The last subsection in the description of each code represents the theoretical error specification of each calculation, as seen by the authors of the codes. They are the starting point for the comparisons in our working group. Throughout the comparisons of the codes and discussion among the authors of the codes we could verify these statements, improve the understanding of the problems and add more value to them.But first of all we need to define our starting point. And this is to be done here in this section.

4.1 Presentation of the program BHWIDE

1) Authors:	**S. Jadach, W. Płaczek and B.F.L. Ward**
2) Program:	**BHWIDE v.1.10, December 1998**
3) Can be obtained from	`http://enigma.phys.utk.edu/pub/BHWIDE/`
4) Reference to main description	[36]
5) Reference to example	[37]
6) advertisement	

In this subsection, we briefly describe our Monte Carlo (MC) event generator for large angle Bhabha (LABH) scattering called `BHWIDE` and discuss some important cross-checks of the program.

`BHWIDE` is based on the YFS exclusive exponentiation procedure [38], where all the IR singularities are summed-up to infinite order and canceled out properly in the so-called YFS form factor. The remaining non-IR residuals, $\bar{\beta}_n^{(l)}$, corresponding to the emission of n-real photons, are calculated perturbatively up to a given order l, where $l \geq n$, and $(l-n)$ is a number of loops in the $\bar{\beta}_n^{(l)}$ calculation. In `BHWIDE` an arbitrary number n of real photons with non-zero p_T are generated according to the YFS MC method of Ref. [39]. The non-IR residuals $\bar{\beta}_n^{(l)}$ are calculated up to $\mathcal{O}(\alpha)$, i.e. $\bar{\beta}_0^{(1)}$ and $\bar{\beta}_1^{(1)}$ corresponding to zero-real (one-loop) and one-real (zero-loop) photons, respectively, are included. In $\bar{\beta}_0^{(1)}$ we implemented two libraries of the $\mathcal{O}(\alpha)$ virtual EW corrections: **(1)** the older one of Refs. [40, 41], which is not up to date but can be useful for some tests/cross-checks, and **(2)** the more recent one of Ref. [42]. When the genuine weak corrections are switched off (or numerically negligible) they are equivalent. In $\bar{\beta}_0^{(1)}$ we implemented two independent matrix elements for single-hard-photon radiation: **(1)** our calculation [36] in terms of helicity amplitudes, and **(2)** the formula of CALKUL [43] for the squared matrix element. We have checked that the above two representations agree numerically up to at least 6 digits on an event-by-event basis.

The MC algorithm of `BHWIDE` is based on the algorithm of the program `BHLUMI` for small angle Bhabha scattering [39], however with some important extensions: **(1)** QED interferences between the electron and positron lines ('up-down' interferences) had to be reintroduced as they are important in LABH; **(2)** the full YFS form factor for the $2 \to 2$ process, including all s-, t- and u-channels, was implemented [36]; **(3)** the exact $\mathcal{O}(\alpha)$ matrix element for the full Bhabha process was included. The multi-photon radiation is generated at the low-level MC stage as for the t-channel process, while the s-channel as well as all interferences are reintroduced through appropriate MC weights. This means that the program is more efficient when the t-channel contribution is dominant, as e.g. at LEP2 energies; however, it proved to work well also near the Z resonance.

The program is written in `FORTRAN77` and is particularly suited for use under the `Unix` operating system[3] for which a special directory structure has been created with useful `Makefile`'s for easy

[3]However, it can be used, in principle, on any operating system with a `FORTRAN77` compiler.

compiling and linking. The program runs in three stages: (1) initialization – where all input parameters are read and transmitted to the program as well as all necessary initializations are performed, (2) event generation – here a single event is generated, and (3) finalization – final bookkeeping for a generated event statistics is done and some useful information is provided (printed-out). There are two main modes of event generation: one can generate either variable weight events (useful for various tests) or constant (=1) weight events (useful for apparatus MC simulations). Various input parameter options, to be set by the user, allow to choose between different contributions/corrections to the cross section, such as weak corrections (two libraries), vacuum polarization (three parametrizations), etc. Other input parameters allow to specify the necessary ingredients for the cross section calculation and the event generation, such as the CMS energy, physical parameters (masses, widths, etc.), phase space cuts, etc. For each generated event, four-momenta of the final state electron, positron and all radiative photons are provided. In the variable-weight-event mode they are supplemented with the main (best) event weight as well a vector of weights corresponding to various models/approximations. In the finalization stage, the total cross section corresponding to the generated event sample is calculated and provided (printed-out) together with some other useful information.

4.2 Error specifications of BHWIDE

So far, several tests/cross-checks of the program have been performed, see e.g. Ref. [44]. First comparisons with other MC programs for LABH were done during the LEP2 Workshop in 1995 [37]. They showed a general agreement of `BHWIDE` with most of those programs within 2% at LEP2 energies. At that time such a level of precision was expected to be sufficient for LEP2. Discrepancies between various calculations can be explained by the fact that most of the programs were designed for LEP1 where the Z s-channel contribution was dominant, while at the LEP2 energy range the t-channel γ exchange dominates. Thus, the physical features of the Bhabha process at LEP1 and LEP2 are very different. Recently, a more detailed study of the theoretical precision of `BHWIDE` has been carried out [45]. Comparisons have been made with the MC programs: `OLDBIS` [39] (a modernized version of the program `OLDBAB` [46]) and `BHLUMI` [47], and the semi-analytic code `ALIBABA` [42]. Tests were done at $\mathcal{O}(\alpha)$ and with higher order corrections for various cuts – by starting from the pure t-channel γ-exchange and switching on gradually other contributions/corrections. This study shows that at $\mathcal{O}(\alpha)$ `BHWIDE` agrees with `OLDBIS` within 0.1% for the pure QED process, while `ALIBABA` differs by up to 0.3%. When higher order corrections are included, `BHWIDE` is generally within 1% of `BHLUMI` (0.5% in the forward region: $\cos\theta_e > 0.7$) for the pure t-channel γ-exchange process and within 1.2% of `ALIBABA` for all kinds of contributions/corrections. From these test we have estimated the overall theoretical precision of `BHWIDE` at 1.5% for the LEP2 energy range. We expect that by making some improvements of the program (e.g. modifying the 'reduction procedures' for the matrix element calculations, including $\mathcal{O}(\alpha^2)$ LL corrections) and performing some new cross-checks (e.g. with the program LABSMC [48]) we can reduce this precision to $\sim 0.5\%$. Further improvements of the theoretical precision can be made, in our opinion, with the help of the `KK` MC program [49] after implementing in it the e^+e^- channel.

4.3 Presentation of the program KORALZ

1) Author:	**S. Jadach, B.F.L. Ward and Z. Wąs**
2) Program:	**KORALZ v.4.04,**
3) Can be obtained from	Library of Computer Physics Communication, or from the author (`z.was@cern.ch`) upon request
4) Reference to main description	[50] and references therein.
5) Reference to example, use:	[51, 52]

Initially the KORALZ event generator was written [53] to simulate τ-pair production and decay for LEP1 physics at the first order of QED bremsstrahlung without any exponentiation. Only longitudinal τ spin effects were included. Later [54, 55], longitudinal beam polarization was included and higher order QED effects were incorporated using powerful exponentiation techniques [56, 57] of initial state bremsstrahlung first, but later of final state bremsstrahlung as well. The interference of initial and final state bremsstrahlung was always neglected, except as a parallel mode of operation at the single bremsstrahlung level. This assumption was good at the peak of the Z resonance, due to suppression of the correction due to Z life-time, and the estimation of the error based on the single bremsstrahlung calculations was sufficient [52, 58]. At that time a quite complete system of tests and cross-checks was developed for the effects due to corrections of initial state bremsstrahlung using dedicated methods based on comparison of semi-analytical results and the Monte Carlo [59] using importance sampling. Tests at the technical precision of 10^{-4} and better could be obtained. In general the total precision of 0.2% was achievable for quite a range spectrum of observables for $\mu^+\mu^-$ or $\tau^+\tau^-$ final states. The $\nu\bar{\nu}\gamma$ final states were also introduced [60] using the assumption that the t-channel W-exchange forms a contribution which is rather small so that, in particular, the $W-W-\gamma$ interaction can be completely neglected.

The use of KORALZ at LEP2 energies impedes substantial improvement of precision. For $\mu^+\mu^-$ or $\tau^+\tau^-$ it is mainly due to the lack of interference effects in exponentiation. For $\nu\bar{\nu}\gamma$ final states it is due to the approximate treatment of t-channel W-exchange. Even though the $W-W-\gamma$ interaction was included, the method explained in Ref. [51] is not enough for the single photon observables and any precision meant to be better than 1-2%. For double photon observables precision decreases even further as the matrix element for the two photon configuration is approximate to the pragmatic order α^2 only.

Electroweak corrections are implemented in KORALZ using the reduced Born method. This means that the effects of electroweak corrections beyond the crude Born level are implemented at the leading-log level only. Recently, the final version of KORALZ was published and documented [50]. That version uses DIZET version 6.05, however, for the sake of tests versions with the up to date DIZET library may be maintained.

Use of the program is expected to be gradually replaced by $\mathcal{KK}$MCMonte Carlo which already at present is superior in all applications (for the time being except $\nu\bar{\nu}\gamma$ final states) and at all energy ranges as far as precision is concerned. Some tools for studying anomalous effects in $\tau\tau\gamma$ final states [61], $\nu\bar{\nu}\gamma$ [62], and leptoquarks [63] are available at present for KORALZ only. A number of flags, to be set by the user, allow the user to switch between different options and perform specific comparisons and investigations, e.g. for calculation of the program physical precision.

The program uses the following libraries: YFS 3.4 [57] for multiple photon bremsstrahlung, TAUOLA [64] for τ-lepton decay and PHOTOS [65] for radiative corrections in τ-lepton decays.

4.4 Error specifications of KORALZ

The main purpose of the program was to serve the Monte Carlo simulation for LEP1 observables. The program was adapted to become useful at LEP2 energies, but it was known that the backbone of its construction is not best suited for that purpose. Also, as the new program $\mathcal{KK}$MCwas developed in parallel. The effort to push the limits of the KORALZ program precision were not exploited.

Let us recall the main points and present crude estimates of the related systematic errors.

• The electroweak section of the program is functionally equivalent to the one used in $\mathcal{KK}$MCand based now on the DIZET part of ZFITTER. The related contribution to the systematic error can be thus taken as 0.15%.

• There is no pair correction included, as the size of pair effects is typically of order of 1.5%; the appropriate contribution has to be calculated independently with the help of a semianalytical program or other means. In case of non-idealized observables, this leads to an uncertainty which we can estimate as 0.4% (0.2% for idealized ones).

• The similar situation holds for the QED initial-final state interference which is not included in the program also and affects observables for all final states including charged fermions. At LEP2 the interference effects are at 1-2% level for photon non-tagging observables. For non-neutrino final states and observables where one or more photons are tagged the uncertainty is bigger (5 to 20%) and $\mathcal{KK}$MC should be used.

• The matrix element is limited to pragmatic second-order. The related uncertainty is about 0.1% for observables where photons are not tagged, about 0.2% for single photon tagged observables, but can be more for observables where more than one photon are tagged.

• In KORALZ exponentiation is based on the relatively old algorithm [57] (with some later improvements but of incomplete tests only) and 1 (0.2)% uncertainty for observables including (not including) radiative return to Z should be added due to that point. This is especially important for $\nu\bar{\nu}\gamma$ observables.

• For $\nu\bar{\nu}\gamma$ final states some rather simple approximations are used in implementation of the contribution of t-channel W-exchange and the $W-W-\gamma$ coupling. It was shown in Ref. [51] that the corresponding uncertainty is not exceeding 1 or 2% for observables including single tagged photons. For double tagged photons we expect the related contribution to uncertainty to be of order of 3-10% depending on the average requested p_T of the second hardest photon.

The final numbers for uncertainties for observables can be obtained as the sum in quadrature of the above uncertainties. It will be calculated at the end of the workshop as the individual contributions can still change thanks to the comparisons, in particular with $\mathcal{KK}$MC.

4.5 Presentation of the program $\mathcal{KK}$MC

1) Author:	**S. Jadach, B.F.L. Ward and Z. Wąs**
2) Program:	**$\mathcal{KK}$MC v.4.13 and v.4.14**
3) Can be obtained from	Library of Computer Physics Communication, or from http://home.cern.ch/jadach,
4) Reference to main description	[49]
5) Reference to example, use:	[66]

$\mathcal{KK}$MC is the Monte Carlo event generator providing weighted and constant weight events for $e^+e^- \to f + \bar{f} + n\gamma, f = \mu, \tau, d, u, s, c, b$ within the complete phase space. Technical description and users guide of the version 4.13 can be found in Ref. [49] while physics content and numerical results are contained in Ref. [66]. The current version with minor improvements which was used during this workshop is 4.14. It will be publicly available at the time of publishing this report. In the following we describe the main features of the program and we discuss in a detail the critical issue of the overall technical and physical precision of the program, stressing that, although it can be viewed from outside as a monolithic single code, in reality almost every vital aspect/component of its total precision is relies on the comparison with another independent code, quite often with several other ones. Since this aspect was highlighted in the discussion during the workshop, we elaborate on this at some length.

4.5.1 QED in $\mathcal{KK}$MC

The QED part the program does not rely for the photon emission, on the structure functions (SF) or the parton shower (PS) model but rather on the new Coherent Exclusive Exponentiation (CEEX) [66, 67] which is an extension of the Yennie-Frautschi-Suura (YFS) exponentiation [38]. This older Exclusive Exponentiation (EEX) [56], more closely related to the original YFS formulation, the same as in KORALZ, is kept as an option in $\mathcal{KK}$MC, for tests of precision and for the purpose of the backward compat-

ibility. The CEEX matrix element in $\mathcal{KK}$MC is entirely based on spin amplitudes, which helps to treat exactly spin effects and to include the QED initial-final state interference. CEEX is based entirely on Feynman diagram calculations and the present version includes the complete $\mathcal{O}(\alpha^2)$ for ISR and almost complete $\mathcal{O}(\alpha^2)$ for FSR[4]. It is important to realize that the ISR calculation in $\mathcal{KK}$MC is the first $\mathcal{O}(\alpha^2)$ independent calculation since the work by Burghers, Berends and Van Neerven (BBVN) [68] [5]. On the contrary, semi-analytical programs like ZFITTER, TOPAZ0 [69] or $\mathcal{KK}$sem rely on the SF's (called also radiator functions) which are derived from BBVN, as far as the $\mathcal{O}(\alpha^2)$ sub-leading terms are concerned. For the real photon emissions CEEX employs the Weyl-spinor methods of Kleiss and Stirling [70]. The 2-loop virtual corrections are derived from Ref. [71] and one-loop corrections to single photon emission are from Refs. [68, 72] and were also cross checked independently by our collaborators [73].

4.5.2 Electroweak corrections

The complete $\mathcal{O}(\alpha)$ electroweak corrections with higher order extensions are included with help of the DIZET library [74], the same version as that used in ZFITTER 6.30 [75]. The complex electroweak form-factors (EWFFs), dependent on s and t variables, are calculated by DIZET and used in the construction of the CEEX matrix element. In order to speed up calculations they are stored in the look-up tables (using a finite grid in the s and t variables) and interpolated. The basic uncertainty of EW corrections in $\mathcal{KK}$MC is therefore the same as that of DIZET/ZFITTER (but this is not true of the QED corrections). We have good reasons to believe that our CEEX matrix element offers a better way of combining EW corrections with QED corrections than that used in the semianalytical codes like ZFITTER, basically because in $\mathcal{KK}$MC it is done at the amplitude level, using Feynman diagrams instead of the SF's. The QCD FSR corrections are taken also from DIZET, keeping properly track of their s-dependence (through look-up tables and interpolation).

4.5.3 Spin effects

Complete spin effects are included for the decaying τ-pairs and for beam polarizations in an exact way, valid from the τ threshold up to multi-TeV linear collider energies. Due to the use of the improved Kleiss-Stirling spinor technique, the appropriate Wigner rotation of the spin amplitudes is done in the rest frame of the outgoing fermions and of the beam electrons [76]. For τ channel the program implements spin-sensitive τ-decays using TAUOLA [64] for τ-lepton decay and PHOTOS [65] for radiative corrections in τ-lepton decays.

4.5.4 Virtual pairs in $\mathcal{KK}$MC

The effect of virtual initial and final state pairs is optionally added to the F_1 electric form-factor, see Feynman diagram of Fig. 4.15, using an old well-known formula [77]

$$F_1^{pair}(s) = \sum_f \left\{ -\frac{1}{36}L_f^3 + \frac{19}{72}L_f^2 + (\frac{1}{18}\pi^2 - \frac{265}{216})L_f + C_F \right\}, \tag{2}$$

$$C_F = \begin{cases} \frac{383}{108} - \frac{11}{6}\frac{\pi^2}{6}, & m_f = m_F, \\ -\frac{1}{3}\zeta(3) + \frac{3355}{1296} - \frac{19}{18}\frac{\pi^2}{6}, & m_f \gg m_F. \end{cases} \tag{3}$$

$$L_f = \log\frac{s}{m_f^2}, \tag{4}$$

[4]For FSR the 2-γ and 1-γ real matrix element are exact, while the 1-loop corrections to the $1-\gamma$ real matrix element is still in the LL approximation. This in principle should be good enough, at the precision level of $\sim 0.1\%$.

[5]BBVN calculated $\mathcal{O}(\alpha^2)$ ISR also directly from Feynman rules. The resulting inclusive/integrated distributions they have cross-checked with the renormalization group techniques, down to the second order next-to-leading logarithmic (NLL) term.

with m_f denoting the mass of virtual fermion in the fermion loop and m_F mass of the fermion flowing through the vertex (typically an electron). The two cases correspond to correction due to identical and heavy fermion in the virtual loop.

Technically, virtual pairs in the initial and final state are added in $\mathcal{KK}$MC as alternative weights: `WtList(213)` represents the case with Virtual Pairs and IFI on, `WtList(263)` represents the case with Virtual Pairs and IFI off. Masses m_f are taken 0.2 GeV for $f = d, u, s$ and PDG values for the rest. Changing m_f of light quarks by factor two induces only $\delta\sigma_{virt}/\sigma = 0.04\%$!

This option should be used in conjunction with adding the signal contribution of real pairs via a full 4-fermion Monte Carlo generator, like KORALW. Concerning the proper cancellation of the virtual pairs mass-logs from $\mathcal{KK}$MC and from KORALW, there should be no technical (precision) problems, especially for the precision level 0.1% required for LEP2. The main complication will be a proper matching of these mass-logs in the presence of the QED bremsstrahlung. Here, the loading-logarithmic approximation and renormalization group will be used as a guide, as usual. For the moment we use effective-quark masses instead of dispersion relations, because we do not see clear indication that it is really necessary to use the latter method at the 0.1% level. However, if it turns out to be necessary, it is possible to introduce $R_{had}(s)$ in both $\mathcal{KK}$MC and KORALW.

Summarizing, this new feature will allow the use of $\mathcal{KK}$MC together with the KORALW Monte Carlo, according to the scheme already suggested in Ref. [78], to produce predictions for the observables with the real/virtual pair contribution.

4.5.5 Recent improvements not yet documented elsewhere updates

In version 4.14 the QCD FSR corrections to the final states of quarks were cross checked and some necessary modifications were introduced.

The F_1 form-factor – the virtual correction factor corresponding to initial and final state emission of non-singlet and singlet pairs was introduced, see above.

Note also that $\mathcal{KK}$MC is expected to take over all functionality of the `KORALZ` event generator. The most important feature of `KORALZ` which is still missing in $\mathcal{KK}$MC is the neutrino channel.

4.6 Error specifications of $\mathcal{KK}$MC

4.6.1 Technical precision

The overall technical precision due to phase space integration is estimated to be 0.02% in terms of the typical total cross section with Z-exclusive or Z-inclusive cuts. The basic test of the normalization of the phase space integration is the following: we do not cut on photon transverse momenta, but only on the total photon energy through $s' = M^2_{inv}(f\bar{f}) > s'_{\min}$ and downgrade the ISR or ISR+FSR matrix element without ISR$\otimes$FSR interference to most the simple CEEX $\mathcal{O}(\alpha^0)$ case, that is the product of the real photon soft-factor times the YFS/Sudakov form-factor and $\sigma_{\rm Born}(s')$, with s' shifted due to ISR. For this simplified QED model we integrate analytically over the phase space, keeping for ISR the terms of $\mathcal{O}(\alpha, L\alpha, L\alpha^2, L^2\alpha^2, L^3\alpha^3)$, that is enough terms to reach 0.01% precision even for Z-inclusive cuts, and for FSR we limit ourselves to $\mathcal{O}(\alpha, L\alpha, L^2\alpha^2)$, also enough for this precision tag[6]. Within such a simplified QED model we compare a very high statistics MC run ($\sim 10^9$ events) with the analytical formula and we get agreement, see Ref. [49], better than 0.02%. The possible loophole in this estimate of precision is that it may break down when we cut the transverse momenta of the real photons, or switch to a more sophisticated QED model. The second is very unlikely as the phase space and the actual SM model matrix element are separated into completely separate modules in the program. The question of the cut transverse momenta of the real photons requires further discussion. Here, it has to be stressed

[6]We see that for ISR and $\sigma_{\rm Born}(s') = const$ switching off the $\mathcal{O}(L\alpha^2, L^3\alpha^3)$ terms changes results only by 0.01%.

that in our MC the so-called big-logarithm

$$L = \ln\left(\frac{s}{m_f^2}\right) - 1 \tag{5}$$

is the *result of the phase space integration* and if this integration were not correct then we would witness the breakdown of the infrared (IR) cancellation and the fermion mass cancellation for FSR. We do not see anything like that at the 0.02% precision level. In addition there is a wealth of comparison with many *independent codes* of the phase space integration for $n_\gamma = 1, 2, 3$ real photons, with and without cuts on photon p_T. It should be remembered that the multi-photon phase space integration module/code in $\mathcal{KK}$MC is unchanged since last 10 years. For ISR it is based on YFS2 algorithm of Ref. [56] and for FSR on YFS3 algorithm of Ref. [57], these modules/codes were part of the KORALZ [55] multi-photon MC from the very beginning, already at the time of the LEP1 1989 workshop [79], and they were continuously tested since then. The phase space integration for $n_\gamma = 1$ was tested very early by the authors of YFS2/YFS3 against the older MC programs MUSTRAAL [80] and KORALB [81] and with analytical calculations, at the precision level $< 0.1\%$, with and without cuts on photon p_T. The phase space integration for $n_\gamma = 2, 3$ with cuts on photon p_T was tested very many times over the years by the authors of the YFS2/YFS3/KORALZ and independently by all four LEP collaborations, using other integration programs like COMPHEP, GRACE and other ones, in the context of the search of the anomalous 2γ and 3γ events. Another important series of tests was done in Ref. [60] for ISR $n_\gamma = 1, 2$ photons (with cuts sensitive to p_T of photons), comparing KORALZ/YFS2 with the MC of Ref. [82] for the $\nu\bar{\nu}\gamma(\gamma)$ final states. Typically, these tests, in which QED matrix element was programmed in several independent ways, showed agreement at the level of 10% for the cross section for $n_\gamma = 2$ which was of order 0.1% of the Born, or 0.2-0.5% for $n_\gamma = 1$ which was of order 1% of the Born, so they never invalidated our present technical precision of 0.02% in terms of Born cross section (or total cross section in terms of Z-inclusive cut).

We conclude therefore that the technical precision of $\mathcal{KK}$MC due to phase space integration is 0.02% of the integrated cross section, for any cuts on photon energies Z-inclusive and Z-exclusive, stronger than[7] $M_{inv}(f\bar{f}) > 0.1\sqrt{s}$ and any mild cut on the transverse photon energies due to any typical realistic experimental cuts. For the cross sections with a single photon tagged it is about 0.2-0.5% and with two photon tagged it is $\sim 10\%$ of the corresponding integrated cross section. These conclusions are based on the comparisons with at least six other independent codes.

4.6.2 Physical precision of pure QED ISR and FSR

In the following we shall discuss mainly the physical precision of $\mathcal{KK}$MC, that is the magnitude of the missing higher orders in the QED/SM matrix element implemented in $\mathcal{KK}$MC. This will also include the technical precision of the matrix element implementation not related to phase space integration discussed previously.

As we already mentioned, in $\mathcal{KK}$MC we have also the older EEX-type matrix element, similar to the one of KORALZ/YFS2 and BHLUMI. Its crucial role in establishing physical precision is that of 'second line of defense' because it has its own estimate of the physical and technical precisions (unrelated to phase space integration) which are factor 2 worse than for CEEX, but a very solid and independent one. The basic test of the EEX matrix element is based again on the comparison with the analytical integration over the photon phase space, this time within the $\mathcal{O}(\alpha, L\alpha, L^2\alpha^2)$ only, but with the additional bonus that the analytical integration is exact in the soft limit. Furthermore, the EEX matrix element is split into about six pieces, so called $\bar{\beta}$-functions and each of them is cross-checked separately. The comparison is done for ISR and FSR separately, taking $\sigma_{\rm Born}(s') = const$ in addition to the normal one with Z resonance. Since some of $\bar{\beta}$-functions like $\bar{\beta}_{1,2}$ are concentrated in the region of the phase space with $n_\gamma = 1, 2$ real hard photons, their separate tests provide an independent non-trivial cross-check of the

[7] It downgrades to 0.5% for $M_{inv}(\mu\bar{\mu}) \leq 2m_\mu$, i.e. full phase space.

phase space integration. The above detailed tests lead for $\sigma_{\rm Born}(s') = const$ to differences between MC and analytical results $< 0.1\%$, vanishing to zero for strong cuts on total photon energy. This is our basic estimate of the technical precision of the implementation of the EEX (unrelated to phase space integration).

There is an eternal ongoing discussion how to estimate the physical precision. Our approach is the conservative one, just take the difference of the two consecutive perturbative calculations at hand[8]. In order to be not over-conservative we usually take half of such a difference, which means that we assume that the convergence of the perturbative expansion is like $(1/2)^n$ at least, which is not a bad assumption for QED where $2L_e\alpha/\pi \sim 0.07$ and $1/L = 0.05$.

In the case of EEX we check the differences of EEX3-EEX2 and EEX2-EEX1, where EEX1= $\mathcal{O}(\alpha, L\alpha)_{\rm EEX}$, EEX2= $\mathcal{O}(\alpha, L\alpha, L^2\alpha^2)_{\rm EEX}$ and EEX3= $\mathcal{O}(\alpha, L\alpha, L^2\alpha^2, L^3\alpha^3)_{\rm EEX}$. We find (1/2) (EEX2-EEX1) $\sim 0.1\%$ for Z-exclusive cuts and $\sim 0.5\%$ for Z-inclusive cuts, and this we take as a physical precision of the EEX2 and EEX3 QED matrix element (no ISR$\otimes$FSR interf.). The difference (1/2) (EEX3-EEX2) is generally negligible $< 0.1\%$ for any cuts.

Having fortified our position on the physical precision of EEX, how do we proceed to determine physical precision of CEEX matrix element? We can compare with EEX2 or EEX3 and in this way we get a handle on the $\mathcal{O}(L\alpha)$ ISR which is missing in EEX2 and $\mathcal{O}(L^3\alpha^3)$ missing in CEEX (which is negligible, however). The other possibility is to look into differences of CEEX2= $\mathcal{O}(\alpha, L\alpha, L^2\alpha^2, L\alpha^2)_{\rm CEEX}$ and CEEX1= $\mathcal{O}(\alpha, L\alpha)_{\rm CEEX}$. We did both and we treat the latter difference (1/2)(CEEX2$-$CEEX1) as our basic source of the physical precision and the former CEEX2$-$EEX3 as an additional cross-check. In Ref. [66] we have found (1/2)(CEEX2$-$CEEX1) to be for both Z-exclusive and Z-inclusive observables below 0.2%. The difference CEEX2$-$EEX3 is rather large, up to 0.8% for Z-inclusive cross section which suggests that the proper inclusion of the $\mathcal{O}(L^1\alpha^2)$ ISR is important and we need in fact the third independent calculation with the complete $\mathcal{O}(L^1\alpha^2)$ ISR. This however is available since long, from BBVN [68]. In Ref. [66] we compared cross section and charge asymmetries from $\mathcal{KK}$MC with semi-analytical calculation based on ISR SF's based on BBVN [68], with added complete $\mathcal{O}(L^3\alpha^3)$ ISR and YFS exponentiation, essentially with the JSW formula of Ref. [83], upgraded with the corresponding FSR SF (in the case FSR is switched on). The above analytical formula is implemented in the $\mathcal{KK}$sem code which is part of the $\mathcal{KK}$MC package. The results of the comparison of the $\mathcal{KK}$sem code and $\mathcal{KK}$MC fully confirms our estimate of 0.2% in the cross section and in charge asymmetry, for Z-exclusive and Z-inclusive cuts, excluding still ISR$\otimes$FSR from consideration.

We may summarize once again how solid is the $\mathcal{O}(L^1\alpha^2)$ ISR: The two-loop $\mathcal{O}(L^1\alpha^2)$ component was already triple-cross-checked at the time of BBVN [68] work, the two-loop $\mathcal{O}(L^1\alpha^2)$ component comes from at least two independent sources [68, 72] and was recently recalculated independently once again[9], while the two real photon emission exact massive matrix element was doubly cross-checked with two independent codes.

On top of that comes the cross check with ZFITTER presented in this report, which from the point of view of QED ISR and FSR (no ISR$\otimes$FSR) is in the same class as BBVN, $\mathcal{KK}$sem while $\mathcal{KK}$MC is rather independent because of the independent full phase space evaluation, and the independent one-loop-one-real and two-real-photon matrix elements.

Summarizing, the physical precision of 0.2% in total cross section and charge asymmetry due to QED ISR and FSR is estimated in a rather solid and conservative way, using many independent codes/calculations, with the triple cross-check being rather the rule than the exception.

[8] One possible pitfall with the above rule is that the difference between the two consecutive perturbative calculations may be accidentally zero for a given value of the cuts, one should therefore vary the values of the cuts before drawing conclusions.

[9] We thank Scott Yost for this valuable cross-check.

4.6.3 Physical precision of QED ISR⊗FSR

The QED ISR⊗FSR is characterized in the separate Section 5.3 of this report so here only mention that the effect of the QED ISR⊗FSR is included in the exponentiated form in our program with help of the new coherent exponentiation technique based entirely on spin amplitudes.

The ISR⊗FSR result of $\mathcal{KK}$MC were debugged/tested first of all by comparing it with the results of $\mathcal{O}(\alpha^1)$ KORALZ without exponentiation, see Ref. [66] where we have found typical agreement $< 0.2\%$ for both Z-exclusive and Z-inclusive cuts. The biggest discrepancy in Ref. [66] was noticed to be 0.4% for the charge asymmetry for a Z-inclusive cut and for the cross section for certain values (far from experimental ones) for the Z-exclusive cut, see also the section on ISR⊗FSR in this report, where we add more comparisons with ZFITTER code. Summarizing, the inclusion of the ISR⊗FSR does not worsen our total theoretical error of 0.2% estimate for the Z-exclusive cuts, while it makes it go to 0.4% level for Z-inclusive cuts. The new comparisons with ZFITTER on ISR⊗FSR presented in section 5.3.8 in this report are consistent with the above estimate.

Note also that the most complete summary/discussion on the subject ISR⊗FSR can be found in the presentation of S.J. at June 1999 meeting of LEPEWG (see transparencies on http://home.cern.ch/jadach).

4.6.4 Physical precision of electroweak corrections

The uncertainty due to pure electroweak corrections is the same as of DIZET, and can be determined for instance by playing with the user options of DIZET, which are available for the user of $\mathcal{KK}$MC. We would like to stress, however, that some physical/technical uncertainties in ZFITTER are really related to the way the EW corrections in ZFITTER are combined with the QED part. In general, the way it is done in $\mathcal{KK}$MC is simpler and these uncertainties are therefore reduced.

4.6.5 Tagged photons

Precision is not less than 1% for observables with a single photon tagged and 3% for observables with double photon tagged.

4.7 Presentation of the program LABSMC

1) Author:	**A.B. Arbuzov**
2) Program:	**LABSMC v.2.05, 5 May 2000**
3) Can be obtained from	the author (`arbuzov@to.infn.it`) upon request
4) Reference to main description	[48]
5) Reference to example	[84]
6) advertisement	

Initially the semi–inclusive `LABSMC` event generator was created [48] to simulate large–angle Bhabha scattering at energies of about a few GeV's at electron positron colliders like VEPP–2M and DAΦNE. The code included the Born level matrix element, the complete set of $\mathcal{O}(\alpha)$ QED RC, and the higher order leading logarithmic RC by means of the electron structure functions. The relevant set of formulae can be found in Ref. [85]. The generation of events is performed using an original algorithm, which combines advantages of semi–analytical programs and Monte Carlo generators.

The structure of our event generator was described in detail in paper [48]. The extension for LEP2 energies is done by introducing electroweak (EW) contributions, such as Z-exchange, into the matrix elements. The third [86] and fourth [87] order leading logarithmic photonic corrections were also

included in the new version. The version of the program under consideration is suited for large–angle scattering. The small–angle version, which incorporates some additional second–order corrections [88], will be described elsewhere.

Starting from the $\mathcal{O}(\alpha^2)$ order the emission of photons is treated semi–inclusively by means of structure functions. Such photons are treated as effective particles, which go at zero angles in respect to the relevant charged particles. The conservation of 4-momenta is fulfilled for each generated event. This feature of the program does not allow to generate realistic events with two photons at large angles.

The code contains:

- the tree level electroweak Born cross section;
- the complete set of $\mathcal{O}(\alpha)$ QED radiative corrections (RC);
- vacuum polarization corrections by leptons, hadrons [17], and W-bosons;
- one–loop electroweak RC according to Ref. [89] by means of DIZET [74] package;
- higher order leading log photonic corrections by means of electron structure functions [86,87,90];
- matrix element for radiative Bhabha scattering with both γ- and Z-exchange [40, 41], vacuum polarization RC, and optionally ISR leading log RC (with exponentiation according to Ref. [90]);
- pair corrections in the $\mathcal{O}(\alpha^2 L^2)$ leading log approximation [91, 92], including the two–photon (multi-peripheral) mechanism of pair production.

A number of flags, to be set by user, allows to switch between different options and perform specific comparisons and investigations. In particular one can switch to generation of only radiative events with visible photons. That allows to avoid technical problems due to low statistics in this case.

The inclusion of the third and fourth order LLA photonic corrections allows not to use exponentiation. A simple estimate [87] shows that the difference between the two treatments at LEP2 is negligible, while the exponentiation requires a specific event generation procedure.

`LABSMC` is a `FORTRAN` program. It works as follows. First, the code makes initialization and reads flags and parameters from a list provided by user. Then it performs an integration (in semi–analytical branch) and generates events. The 4-momenta of generated particles are to be analyzed or recorded in a user subroutine. A certain control of technical precision is provided by comparison of the results from semi–analytical and Monte Carlo branches. Note, that for a case of complicated cuts, which can not be done in the semi–analytical branch, one has to increase the number of generated events to reach the ordered precision.

The accuracy of the code is defined by two main points: technical precision (numerical precision in integrations, errors due to limited statistics, possible bugs *etc.*) and the theoretical uncertainty. Of course, one has than choose the proper, corresponding to his concrete problem, set of flags and parameters.

The technical precision has to be checked and improved, if required, by detailed tests and comparisons with results of other codes. The theoretical uncertainty is defined by: absence of complete set of $\mathcal{O}(\alpha^2 L)$ corrections (for photonic and pair corrections), an uncertainty in definition of vacuum polarization, approximate description of hadronic pair production. There was observed a discrepancy in the treatments of electroweak RC in ZFITTER and ALIBABA [42]. The theoretical uncertainty of the code in description of large–angle Bhabha scattering at LEP2 is estimated now to be of about 0.3%. The corresponding uncertainty for radiative Bhabha scattering with a visible photons is about 2%. But for the latter, we have an additional theoretical systematic uncertainty (about 1%), coming from non–standard radiative corrections [93].

4.7.1 Note about pair corrections in LABSMC

In LABSMC there are included contributions due to pair production according to Ref. [91, 92]. The secondary hadronic pairs are estimated within the leading log approximation.

The double resonant (ZZ) contribution, in which both the primary and secondary pair are produced via virtual Z-bosons, is not taken into account. This contribution will be subtracted from the experimental data by means of some Monte Carlo event generator.

The impact of the multi-peripheral (two–photon) mechanism of pair production and the one of the singlet pairs can be analyzed by means of the program. But the default option is to drop these contributions as in the event generator as well as in the experimental data.

The corrections in per-mil are given in Table 28 of Section 5.5.8. The quantities there were calculated in respect to the cross sections, where all other types of RC have been already applied. There is a simple dependence of the size of corrections on the applied cuts. The most strong cuts on real emission are there, the most large (and negative) effect is coming out. The largest corrections are found for some idealized observables, where also the final state corrections do give a lot.

As concerning the two–photon mechanism, there are visible contributions only for a few event selections (see Table 29 of Section 5.5.8). In the rest of ES the multi-peripheral reaction is cut away by the corresponding sets of conditions. The only large correction to **IOpal3** is because of wide range of allowed collinearity and a very low energy threshold for electrons (1 GeV).

The accuracy on the above numbers for pair corrections can be estimated to be about 20%, which is mainly coming from the uncertainty in the description of secondary hadronic pairs.

4.8 Error specifications of LABSMC

The theoretical uncertainty of `LABSMC` is estimated by the analysis of the following sources of errors.

- A considerably large amount of about 0.10% is coming from the hadronic contribution into vacuum polarization.
- Unknown $\mathcal{O}(\alpha^2 L)$ photonic and pair corrections can give as large as 0.20%. Note, that for small–angle Bhabha at LEP1 we had the corresponding contribution of the order 0.15% [88], and so we can estimate the uncertainty, taking into account that the large log L in the large–angle kinematics is greater.
- The approximate treatment of hadronic pair corrections typically contributes by not more than 0.05%, depending on the concrete event selection. For observables **IAleph3**, **IAleph4**, and **ILT4** we have more: about 0.1%.
- Photonic corrections in high orders $\mathcal{O}(\alpha^3 L^2, \alpha^5 L^5, \ldots)$ are not calculated in the code, but they are really small (0.02%).
- Uncertainties coming from the treatment electroweak constants and loop corrections can give up to 0.2% for the case barrel angular acceptance. For the case with endcaps we have lower contribution from Z-exchange, and the error is less than 0.1%.

Taking into account the limited technical precision, we derive the resulting uncertainty of the code for description of large–angle Bhabha scattering at LEP2 to be of the order 0.3%. As concerning radiative Bhabha with a photon tagged at large angles, the uncertainty is defined by missing $\mathcal{O}(\alpha)$ corrections. It can be estimated to be of about 2%.

4.9 Presentation of the program grc$\nu\nu\gamma$

1. Authors: Y. Kurihara, J. Fujimoto, T. Ishikawa, Y. Shimizu, T. Munehisa
2. Program: grc$\nu\nu\gamma$ v.1.0, 1999.08.20
3. Can be obtained from: `http://www-sc.kek.jp/minami/`
4. Reference to main description: hep-ph/9908422 to be appeared in CPC.
5. Reference to example discussion of the prediction and its systematic uncertainty: hep-ph/9908422 to be appeared in CPC.

   grc$\nu\nu\gamma$ is an event generator which combines the exact matrix elements for $e^+e^- \to \nu\bar{\nu}\gamma(\gamma)$, produced by the GRACE system [94], with QEDPS [95] for ISR. The advantages of these packages are:

   - The exact matrix elements up to the double-photon emission, including the ν_e process, are used. Double-photon emission is practically sufficient for experimental analysis.
   - QEDPS keeps the complete kinematics for the emitted photons and virtual electrons before collisions. It allows a more flexible treatment of the ISR effects in avoiding the double-counting.
   - Besides the above-mentioned pure QED corrections, grc$\nu\nu\gamma$ equips with another class of the electroweak higher order corrections. There is a switch to choose it from the following three schemes; 1) the running coupling constant scheme: the coupling constant of the $fermion$-$fermion$-Z vertex, g_{ffZ}, is determined by the evolution from zero momentum transfer to the mass squared of the $\nu\bar{\nu}$ system, q_Z^2, which differs from one event to another. It varies according to the renormalization group equation (RGE). 2) G_μ scheme [96]: It is such that the weak couplings are determined through the weak-mixing angle, $\sin\theta_W$, which is given by

     $$\sin^2\theta_W = \frac{\pi\alpha(q^2)}{\sqrt{2}G_\mu M_W^2}\frac{1}{1-\Delta r},$$

     where M_W being the W-boson mass and G_μ the muon decay constant. 3) on-shell scheme: the weak couplings are simply fixed by M_W and M_Z though the on-shell relation, $\sin^2\theta_W = 1 - \frac{M_W^2}{M_Z^2}$, where M_Z is the mass of the Z-boson.
   - For the ν_μ case the total cross sections and the hard-photon distributions of grc$\nu\nu\gamma$ are compared with those by the $\mathcal{O}(\alpha)$ calculations [97–99], KORALZ [50] and NUNUGPV [100]. The theoretical error uncertainty for the ISR corrections is under control at the 1% level. The systematics of the G_μ scheme, coming from the double energy scales(M_Z,$\sqrt{s}$) involved in the reaction, is estimated to be around 1%. The energy spectrum of the hard-photons is in a reasonable agreement with KORALZ and NUNUGPV up to the double-photon emission.
   - Concerning ν_e a similar comparison with NUNUGPV has been done, though in this case some programs were lacking complete $\mathcal{O}(\alpha)$.
   - In the package the anomalous coupling of the W-W-γ vertex is implemented. The program includes only those terms which conserve C and P invariance, derived from the following effective Lagrangian [101]:

     $$L_{eff} = -ie[(1+\Delta g_{1\gamma})(W^\dagger_{\mu\nu}W^\mu - W^{\dagger\mu}W_{\mu\nu})A^\nu + (1+\Delta\kappa_\gamma)W^\dagger_\mu W_\nu A^{\mu\nu} + \frac{\lambda_\gamma}{M_W^2}W^\dagger_{\lambda\mu}W^\mu_\nu A^{\lambda\nu}],$$

     where $W_{\mu\nu} = \partial_\mu W_\nu - \partial_\nu W_\mu$, $A_{\mu\nu} = \partial_\mu A_\nu - \partial_\nu A_\mu$. Here $\Delta g_{1\gamma}$, $\Delta\kappa_\gamma$ and λ_γ stand for the anomalous coupling parameters which vanish in the Standard Model.

4.10 Error specifications of grc$\nu\nu\gamma$

- (1) lack of constant term

  One of the intrinsic limitation of the parton shower method is lack of constant terms. It is known that the leading logarithmic solution of the $DGLAP$ equation can reproduce the exact perturbative calculations at LL order except constant terms. For the simple e^+e^- annihilation processes, this effect, so called $K-factor$, is known to be 0.6cannot be better than this accuracy. Though there is no exact estimation of the $K-factor$ for the neutrino pair-production with hard photon(s), we can expect the $K-factor$ for these processes is at the same order as the simple e^+e^- annihilation processes. Then we assign the systematic error of 0.6

- (2) internal consistency

  In the $grc\nu\nu\gamma$, the hard photon is treated using exact matrix elements and the soft photon(s) are treated using QEDPS. It is not necessarily that a definition of the hard photon is the same as those of visible photon given by the experimental requirements. The final result must be independent of the dividing point between hard and soft photons. we checked the stability of the cross sections when the dividing points are varied within a reasonable range. If the experimental requirement is so tight, for example, no additional photons with small energy in very forward region is required, the final result is sensitive for the definition of the soft photon. We assign this dividing-point dependence as a systematic error. This error is much depend on the experimental cuts.

- 3) multi photon limitation

  In the $grc\nu\nu\gamma$, up to two visible photon can be treated. For the experimental requirement as 'two or more photons', we give the results with only two visible photons. The probability to observe third photons is negligible small in general. We estimate the error of this limitation is less than 1.

4.11 Presentation of the program NUNUGPV

Authors: **G. Montagna, M. Moretti, O. Nicrosini and F. Piccinini**

Program: **NUNUGPV v.2.0, July 1998**

Can be obtained from: `http://www.pv.infn.it/~nicrosi/programs/nunugpv/`

The code `NUNUGPV` [100,102] has been developed to simulate events for the signatures single- and multi-photon final states plus missing energy in the Standard Model at LEP and beyond.

Matrix elements

In the program the exact matrix elements are implemented for the reactions

$$e^+e^- \to \nu_i\ \bar{\nu}_i\ n\gamma\ ,$$

with $i = e, \mu, \tau$ and $n = 1, 2, 3$.

The matrix element for single-photon production has been computed by means of helicity amplitude techniques [103], while the amplitudes for multi-photon final states are calculated using the numerical algorithm `ALPHA` [104] for the automatic evaluation of tree-level scattering amplitudes. The contribution of the anomalous couplings Δk_γ and λ_γ to the $WW\gamma$ vertex is included analytically in the matrix element for $e^+e^- \to \nu_e\ \bar{\nu}_e\ \gamma$. Trilinear and quadrilinear anomalous gauge couplings for the processes with more than one photon in the final state have been recently implemented. As an option the program contains also the contribution of a massive neutrino with standard couplings to the Z boson.

Radiative corrections

The phenomenologically relevant Leading Log (LL) QED radiative corrections, due to initial state radiation (ISR), are implemented via the Structure Function (SF) formalism. Due to the presence of a visible photon in the kernel cross section, the inclusion of ISR requires particular care. In order to remove the effects of multiple counting due to the overlap of the phase spaces of pre-emission photons (described by the SF's) and kernel photons (described by the matrix element), the p_t/p_L effects are included in the SF's according to Ref. [102]. The generation of the angular variables at the level of the ISR gives the possibility of rejecting in the event sample those pre-emission photons above the minimum detection angle and threshold energy, thus avoiding 'overlapping effects'. According to such a procedure, the cross section with higher-order QED corrections can be calculated as follows (for the data sample of at least one photon)

$$\sigma^{1\gamma(\gamma)} = \int dx_1 dx_2 dc_\gamma^{(1)} dc_\gamma^{(2)}\, \tilde{D}(x_1, c_\gamma^{(1)}; s)\tilde{D}(x_2, c_\gamma^{(2)}; s)\Theta(cuts) \times \left(d\sigma^{1\gamma} + d\sigma^{2\gamma} + d\sigma^{3\gamma} + ...\right), \quad (6)$$

where $c_\gamma = \cos\vartheta_\gamma$ and $\tilde{D}(x, c_\gamma; s)$ is a proper combination of the collinear SF $D(x, s)$ with an angular factor inspired by the leading behavior $1/(p \cdot k)$ [102] of the pre-emission photons. According to Eq. (6), an 'equivalent' photon is generated for each colliding lepton and accepted as a higher-order ISR contribution if:

- the energy of the equivalent photon is below the threshold for the observed photon $E_{\gamma,min}$, for arbitrary angles;
- or the angle of the equivalent photon is outside the angular acceptance for the observed photons, for arbitrary energies.

Within the angular acceptance of the detected photon(s), the cross section is evaluated by summing the exact matrix elements for the processes $e^+e^- \to \nu\bar{\nu}n\gamma$, $n = 1, 2, 3$ ($d\sigma^{1\gamma}, d\sigma^{2\gamma}, d\sigma^{3\gamma}$).

By means of the above sketched formulation, the signatures that can be handled by the program are:

- exactly one(two) visible photon(s) plus undetected radiation;
- at least one(two) visible photon(s) plus undetected radiation;
- exactly three visible photons with QED corrections in the collinear approximation.

Some improvements for Linear Collider energies have been recently introduced. Predictions for the single-photon signature are possible for polarized electron/positron beams. Simulation of beamsstrahlung can be performed by means of the `circe` library [105]. Both integration and unweighted event generation modes are available. More details on technical and theoretical features can be found in Ref. [100]. Concerning the LEP2 energy regime, the present theoretical accuracy of `NUNUGPV` is at the per cent level, as due to missing $\mathcal{O}(\alpha)$ electroweak corrections.

4.12 Error specifications of NUNUGPV

As discussed in Section 4.11 and in the relevant literature there quoted, the main ingredients NUNUGPV is based upon are

- exact matrix elements for the kernel reaction $e^+e^- \to \nu_i\bar{\nu}_i n\gamma$, with $i = e, \mu, \tau$ and $n = 1, 2, 3$, computed either analytically ($n = 1$) or numerically ($n = 2, 3$);

- convolution of the kernel cross section by means of p_t-dependent structure functions, in order to take into account the huge effect of initial-state radiation, while avoiding double counting in the presence of tagged photons.

The main source of theoretical error is missing non-log $O(\alpha)$ electroweak corrections, which can be estimated to be of the order of $1-2$ %. Pushing the theoretical accuracy at the 0.1 % level would require supplementing the present formulation by a full $O(\alpha)$ calculation, at present not available.

4.13 Presentation of the program ZFITTER with electroweak library DIZET

Authors:	**D. Bardin, P. Christova, M. Jack, L. Kalinovskaya, A. Olchevski, S. Riemann, T. Riemann**
Program:	**ZFITTER v.6.21 (26 July 1999)**
Can be obtained from:	`http://www.ifh.de/~riemann/Zfitter/zf.html` `/afs/cern.ch/user/b/bardindy/public/ZF6_21`
Reference to main description:	[75]
References to examples:	[106–114]
Program development:	The package is permanently updated, user requests are welcome; last update is v.6.30 (xx March 2000)

ZFITTER is a Fortran program, based on a semi-analytical approach to fermion pair production in e^+e^- annihilation at a wide range of centre-of-mass energies, including LEP1 and LEP2 energies. The main body of the program relies on the analytical results presented in Refs. [115–117] for the QED part and in Refs. [74, 118–122] for the electroweak physics part. Some of the formulae used may be found only in Ref. [75].

ZFITTER version v.6.21 was the last one intended for the use at LEP1 energies. The description of this subsection is mostly limited to this version. During the 1999–2000 LEP2 Workshop there was a development which is briefly summarized in Section 4.13.2.

The calculation of realistic observables with potential account of complete $\mathcal{O}(\alpha)$ QED and electroweak corrections plus soft photon exponentiation plus some higher order contributions is made possible with several calculational chains:

- Born cross-sections;
- a fast option: cut on s' or combined cuts on collinearity ξ and minimal energy $E_{\min}$ of the fermions for $\sigma_{\text{T,FB}}$;
- cut on s' (or on $\xi, E_{\min}$) for $d\sigma/d\cos\vartheta$; for $\sigma_{\text{T,FB}}$ additional cut on the production angle of *anti-fermions* ($\cos\vartheta$).

The scattering angle of *fermions* remains unrestricted if the other cut(s) do not impose an implicit restriction.

Numerical integrations are at most one-dimensional and performed with the Simpson method [123, 124]. This makes the code so fast and guarantees any practically needed numerical precision.

ZFITTER calculates:

- Δr – the Standard Model corrections to G_μ;

- M_W – the W boson mass from M_Z, M_H, and fermion masses, and Δr;
- $\Gamma_{Z,W} = \sum_f \Gamma_f$ – total and partial Z and W boson decay widths;
- $d\sigma/d\cos\vartheta$ – differential cross-sections;
- σ_T – total cross-sections;
- A_{FB} – forward-backward asymmetries;
- A_{LR} – left-right asymmetries;
- A_{pol}, A_{FB}^{pol} – final state polarization effects for τ leptons;

Various interfaces allow fits to the experimental data to be performed with different sets of free parameters. There are two options to parameterize the Z boson propagator [125] (see also [126, 127] and the many references therein).

ZFITTER uses pieces of code from other authors ([123, 124, 128–132]). We find it important to mention explicitly that the programming of ZFITTER accumulates the efforts of many theoreticians, whose work went into the code either as default programming or as options to be chosen by many flags. A hopefully complete list (derived from [75]) comprises quite a few references for photonic radiative corrections [68, 86, 90, 107, 133–144] and radiative corrections contributing to the effective Born cross section [18, 145–171]. This is a feature of ZFITTER which makes it very flexible for applications, but also for comparisons with other codes and checks of technical precisions in program development phases. For a systematic presentation of the interplay of the many radiative corrections treated we refer also to [75] and to [172].

ZFITTER is used optionally by other packages, among them are SMATASY [173–175], ZEFIT, [176]. Its electroweak library DIZET is used in KORALZ, [50], $\mathcal{KK}$MC, [49], BHAGENE, [177], and other programs like HECTOR, [178] for the study of ep scattering.

QED initial–final interference:

The exponentiation [179] of initial–final interference (IFI) photonic corrections is implemented in ZFITTER. The exponentiation is done according the procedure developed in Ref. [90]. The base for the construction is the general Yennie–Frautschi–Suura theorem [38]. The resulting formulae are close to the ones of Ref. [180], but the special treatment around the Z-peak is not included in the program now. In the code the IFI option is governed by the flag `INTF`. The effect of the IFI exponentiation was found to be important, especially for forward–backward asymmetry.

The Fortran package DIZET is part of the ZFITTER distribution. It can be used in a stand-alone mode and is regularly used by other programs.

On default, DIZET allows the following calculations:

- by call of subroutine DIZET: W mass and width, Z and W widths;
- by call of subroutine ROKANC: four weak NC form factors, running electromagnetic and strong couplings needed for the composition of effective NC Born cross sections for the production of massless fermions (however, the mass of the top quark appearing in the virtual state of the one-loop diagrams for the process $e^+e^- \to b\bar{b}$ is not ignored);
- by call of subroutine RHOCC: the corresponding form factors and running strong coupling for the composition of effective CC Born cross sections.

If needed, the form factors may be made to contain the contributions from WW and ZZ box diagrams thus ensuring (over a larger energy range than LEP 1) the correct kinematic behavior and gauge invariance.

4.13.1 Pair corrections in ZFITTER

One of particular contributions to the process of electron–positron annihilation is the radiation of secondary pairs. In comparison with the photon radiation, it is relatively small, because it appears only starting from the $\mathcal{O}(\alpha^2)$ order. Nevertheless, the total effect of pair production could reach dozen permil and should be taken into account in the data analysis. The secondary pair can be produced via a virtual photon or Z-boson. The latter case is supposed to be subtracted from the experimental date by means of some Monte Carlo event generator. (The Z boson mediated secondary pair production was also studied with GENTLE/4fan v.2.11, see the description of results in Section 5.5.5.)

Lowest order pair corrections

The complete second order calculation for e^+e^- and $\mu^+\mu^-$ initial state pairs was performed in Ref. [68]. The contribution of hadronic and leptonic pairs (excluding electrons) was considered in paper [137].

The effect of secondary pair production in the final state was calculated in Ref. [181]. It is worth to mention, that the final state pair correction should be realized in a multiplicative way:

$$\sigma = \sigma_{\rm Born}(1+\delta_\gamma)(1+\delta_{\rm FSP}), \tag{7}$$

where δ_γ stands for the initial state (IS) photonic correction, and $\delta_{\rm FSP}$ give the final state (FS) pair one. At LEP2 energies, when the radiative return to the Z-peak is allowed, we have very large values of δ_γ, and the multiplicative treatment provides a correct counting of the simultaneous emission of IS photons and FS pairs. A cut on the invariant mass of the FS secondary pair is allowed by setting parameter `PCUT`.

The pair contribution to the corrected cross section is presented as the integral of the Born cross section with the so–called pair radiator:

$$\mathrm{d}\sigma^{\rm pair} = \int\limits_{z_{\min}}^{1} \mathrm{d}z\ \tilde{\sigma}(zs)H(z) = \sigma(s)(H_\Delta + H_{\rm FSP}) + \int\limits_{z_{\min}}^{1-\Delta} \mathrm{d}z\tilde{\sigma}(zs)H_\Theta(z). \tag{8}$$

Here H_Δ represents the impact of virtual and soft pairs; $H_{\rm FSP}$ stands for the final state pairs. Δ is a *soft-hard separator* ($\Delta \ll 1$), numerical results should not depend on its value.

The singlet channel contribution and the interference of the singlet and non–singlet channels are taken from Ref. [68]. They can be called from ZFITTER optionally (according to the `IPSC` flag value).

A simple estimate of the interference between the ISR and FSR pairs can be done: we can take the initial–final photon interference multiplied by the conversion factor $(\alpha/(3\pi))\ln(s/m_e^2)$. The smallness of the photonic interference and the additional factor provide us the possibility to neglect the initial–final pair interference completely.

Pair production in higher orders

It was observed that the $O(\alpha^2)$ approximation is not enough to provide the desirable precision. Really the interplay of the initial state photon and pair radiation is very important. So, one should consider higher orders. The first exponentiated formula for pair production was suggested in Ref. [90]. The process of one pair production was supplied by emission of arbitrary number of soft photons. This formula gives a good approximation for leading logarithmic corrections close to the Z-peak. But it does not include the important next–to–leading terms, and even the known third order leading logs are not reproduced completely.

In Ref. [142] a phenomenological formula for simultaneous exponentiation of photonic and pair radiation was proposed. The correspondence of the exponentiated formula to the perturbative results was shown there for the case of real hard radiation. Nevertheless, the structure of the radiator function, suggested in Ref. [142], does not allow to check the correspondence for soft and virtual part of the corrections analytically.

An alternative treatment of the higher order corrections due to pair production was suggested in Ref. [144]. In order to account the most important part of the sub–leading corrections we consider the convolution of the $\mathcal{O}(\alpha^2)$ pair radiator with the ordinary $\mathcal{O}(\alpha)$ photonic radiator, proportional to the $P^{(1)}$ splitting function. In this way we receive the main part of the $\mathcal{O}(\alpha^3)$ leading logs, proportional to $P^{(2)}$, and the sub–leading terms enhanced by $\ln(1-z)/(1-z)$, like $L^2\ln(1-z)/(1-z)$ and $L\ln^2(1-z)/(1-z)$. Note that the convolution as well as exponentiation can not give the correct complete sub–leading formula. In fact the convolution gives a part of sub-leading terms coming from the kinematics, where both the pair and the photon are emitted collinearly, while there are other sources for the corrections, like, for instance, emission of a collinear pair and a large–angle photon. But we suppose, that the main terms with enhancements are reproduced correctly, that follows from the general experience in leading log calculations. Note that the same background is under the exponentiation of such terms. For the case of pure photonic radiation this was checked by direct perturbative calculations.

We checked that for real hard emission there is a agreement between the most important terms in the third order contribution to $H_\Theta(z)$ and the corresponding terms in expansion of the exponentiated formula from Ref. [142]. Such a correspondence between the exponentiation and convolution procedures is well known also in the case of pure photonic radiation.

In the same way we derived the expressions both for leptonic and hadronic pairs. In contrast with Ref. [142] we extended the hadronic pair contribution to the third order by means of convolution which takes into account the dynamical interplay between pairs and photons, when they are emitted at the same point, rather than by a static coefficient.

The leading logs, which were not reproduced by the convolution were supplied from Ref. [144]. We estimated also at the fourth order contribution by means of the leading logs (non–singlet channel only):

$$\mathrm{d}\sigma_e^{(4)} = \int \mathrm{d}z\tilde{\sigma}(zs)\left(\frac{\alpha}{2\pi}(L_e-1)\right)^4\left[\frac{1}{12}P^{(3)}(z)+\frac{11}{216}P^{(2)}(z)+\frac{1}{108}P^{(1)}(z)\right]. \tag{9}$$

In the $\mathcal{O}(\alpha^4)$ we keep only the leading logarithmic formula (9) for non–singlet electron pairs.

A good numerical agreement was observed in the treatment of higher order leptonic ISR pairs by means of the convolution [144] and exponentiation [142] (see Table 2 in Ref. [144]). The exponentiated treatment is implemented in ZFITTER also (called by setting `ISPP=4`). The agreement with the exponentiated representation from Ref. [90] is not so good at LEP2 energies.

Numerical illustrations

In Table 11 we present the results for different contributions. The value of correction due to pairs is defined in respect to the cross section for annihilation into hadrons with pure photonic corrections taken into account. The cut–off on both pair and photonic corrections is equal: $z_{\min} = 0.01$ and 0.7225, $s' > z_{\min}\cdot s$. In the FSR column we show the sum of leptonic and hadronic final state pair corrections (`PCUT`=0.99). In the last column the sum of ISR and FSR pairs is given without the contribution of singlet pairs. Centre–of–mass energy is 200 GeV.

As could be seen from the Table, the contribution of singlet pair production becomes important only for small values of $z_{\min}$. In data analysis at LEP, such events are supposed to be extracted from the data together with the two–photon process $e^+e^- \to e^+e^- + \mathrm{hadrons}$. We emphasize, that the procedure should be accurate and well understood, because in fact the events with singlet pairs and multiperiferical production have quite different signatures in the detector. At LEP2 energies the contribution of singlet pairs becomes really important, if the returning to the Z-peak is allowed (for $z_{\min} \lesssim 0.25$).

Table 11: Different contributions to δ.

	ISR pairs					FSR pairs	sum
	e(NS)	e(NS+sing.)	μ	τ	hadr.		
	$z_{\min} = 0.01$						
$\mathcal{O}(\alpha^2)$	6.41	42.00	1.99	0.67	5.49	0.06	14.62
$\mathcal{O}(\alpha^3)$	7.28	42.86	2.19	0.72	6.09	0.06	16.34
$\mathcal{O}(\alpha^4)$	7.24	42.82	2.19	0.72	6.09	0.06	16.30
	$z_{\min} = 0.7225$						
$\mathcal{O}(\alpha^2)$	−0.38	−0.40	−0.11	−0.03	−0.28	−0.29	−1.08
$\mathcal{O}(\alpha^3)$	−0.56	−0.59	−0.17	−0.05	−0.21	−0.30	−1.28
$\mathcal{O}(\alpha^4)$	−0.53	−0.56	−0.17	−0.05	−0.21	−0.30	−1.25

To estimate the uncertainty of our results we look at the relative size of different contributions and at the comparison with the exponentiated formulae. The main source of the uncertainty is the approximate treatment of the hadronic pairs. Another indefiniteness is coming from the sub–sub–leading terms of the third order, which can be received neither by convolution nor by exponentiation, and from the fourth order correction. Our rough estimate for the theoretical uncertainty due to pair production in description of electron–positron annihilation is 0.02% for without returning to the Z-peak. For the returning to the peak at LEP2 we estimate the uncertainty to be at the level of 0.1%.

4.13.2 ZFITTER development after v.6.21

There was a certain development of ZFITTER after version 6.21. On 13 December 1999 we released ZFITTER v.6.23 with an improved treatment of the second order corrections to angular distributions and A_{FB}. The implementation relies on work done by A.B. Arbuzov and will be described in an extended version of Ref. [144].

For this workshop we have created ZFITTER v.6.30, which should be the last version for LEP2. It contains several new important user options.

A new option governed by a new flag `FUNA` is implemented, with:
`FUNA`=0 – old treatment,
`FUNA`=1 – new treatment.
This is a new treatment of the second order ISR QED corrections, in the presence of angular acceptance cuts `ANG0`, `ANG1`, based on a new calculation by A. Arbuzov (to appear as hep-ph report). It is compatible with the use of `ICUT=1,2,3`.

The meaning of flag `INTF` is extended in order to accommodate the new implementation of an exponentiation of IFI QED corrections, also realized by A. Arbuzov (also to appear as hep-ph report):
`INTF`=0,1 – old options,
`INTF`=2 – exponentiated IFI.

Further, final state pair production corrections are implemented (A. Arbuzov). The option is governed by a new flag:
`FSPP`=0 – without FSR pairs,
`FSPP`=1 – with FSR pairs, additive,
`FSPP`=2 – with FSR pairs, multiplicative.
For the FSPP corrections, the cut on the invariant mass of the secondary pair is accessible. In order to accommodate this cut value, the variable SIPP of the
`SUBROUTINE ZUCUTS(INDF,ICUT,ACOL,EMIN,S_PR,ANG0,ANG1,SIPP)`
is now used. Therefore, the meaning of the variable SIPP has been changed. It has nothing to do with

cutting of ISPP; there is no possibility to cut secondary pairs for ISPP, where the primary pair invariant mass cut should be equal to S_PR.

Finally, the new value of flag IPTO=–1 allows to calculate pure virtual pair contributions separately.

ZFITTER v.6.30 should be used together with DIZET v.6.23. Two bugs are fixed in DIZET v.6.23. A bug in the calculation of $\Gamma_{\rm W}$ is fixed (resulting in a 0.3% shift), and another one in the calculation of running α_{em} (of no numerical importance).

Further, an option to fit V_{tb} is implemented to DIZET (D. Bardin, L. Kalinovskaya, A. Olshevsky, March 2000). For this, a main program (interface) zwidthtb6_30.f has to be used together with a standaside DIZET version 6.30; the argument list of that DIZET is changed to accommodate this possibility.

Some more small changes were implemented during this workshop in the result of tuned comparison with $\mathcal{KK}$MC. The range of variation of two flags was extended.

New value WEAK=2 allows to switch off some tiny second order EWRC which do not propagate via DIZET and therefore can't be taken into account by the other codes which use only DIZET. It was proved that the numerical influence of these terms at LEP2 energies is one order of magnitude less than the typical precision tag.

New value CONV=-1 accomodates the choice $\alpha_{em}(0)$ for the γ exchange amplitude allowing the calculation of the 'pure' Born observables, that was used for cross-checks of ISR QED convolution.

The interested reader may find further details on recent program developments at
/afs/cern.ch/user/b/bardindy/public/ZF6_30/
and at
http://www.ifh.de/∼riemann/Zfitter/.

The most important conclusion which emerged from the tuned comparison with $\mathcal{KK}$MC is that at LEP2 energies it is not possible anymore to relay on a simplified treatment of EW boxes realized in ZUTHSM branch of ZFITTER. EW boxes should be considered as a part of EW form factors and due to their angular dependence the only way is to access them via ZUATSM branch of ZFITTER which was already accessible in v.6.21 and was not specially updated during this workshop. However, one should emphasize that the way of using of ZFITTER at LEP1 fails at LEP2 energies completely. In particular, one should use CONV=2 option allowing for *running* of EW form factors under the ISR convolution integral. For more detail see Section 5.4.

Statement on the precision and the systematic errors:

See the other parts of this report, especially Sections 3, 5, and 6.

Statement on limitations:

ZFITTER should not be used for precision calculations of Bhabha cross sections. The corresponding QED corrections have to be recalculated. The effective Born approximation for Bhabha scattering is fixed to LEP 1 kinematics. It is relatively easy to improve the latter, but this has to be done yet.

ZFITTER should be used below $t\bar{t}$ threshold. The implementation of the channel $e^+e^- \to t\bar{t}$ is underway.

4.14 Error specifications of ZFITTER

One should distinguish two main classes of sourses of theoretical errors. First are, so-called *parametric uncertainties, PU's*, which are trivial: propagation of uncertainties of INPUT parameters results for an uncertainties of the predictions. Here we present a study of PU's done with ZFITTER.

It seems reasonable to assume that the only PU's which are worth studying, are those due to uncertainties in:

- the running QED coupling $\alpha(s)$, due to errors in $\Delta\alpha^5_{had}$ for which we use

$$\Delta\alpha^5_{had} = 0.027782 \pm 0.000254; \tag{10}$$

- the pole masses of b and c quarks, for which we adopt

$$M_b = 4.70 \pm 0.15 \text{ GeV}, \qquad M_b = 1.50 \pm 0.25 \text{ GeV}, \tag{11}$$

- the pole masses of the top quark, for which we take, PDG'98 value

$$M_t = 173.8 \pm 5.2 \text{ GeV}, \tag{12}$$

- Higgs boson mass, deserving more explanations.

Conventionally, we use in this report $M_{_H} = 120$ GeV as a preferred value. For its lower limit it is reasonably to take $M_{_H} \approx 100$ GeV as the present lower limit established from direct searches at LEP1. For upper limit we scanned the interval $M_{_H} = 125 - 200$ GeV, because the total (hadronic) cross section shows up a non-monotonic behavior as a function of Higgs mass with a maximum at some value from this interval. Parametric uncertainties due to $M_{_H}$ variation are non-symmetric, since the value $M_{_H} = 120$ GeV is chosen as the preferred value.

For the idealized quark observables we found the following largest variations (in per mil), when we varied five above mentioned input parameters within indicated limits:

$\Delta\alpha^5_{had}$ only	± 0.05
$\Delta\alpha^5_{had}, M_b, M_c$ simultaneously	± 0.07 with negligible contribution from M_c
M_t only	± 1
M_H only	$+0.50 \div -0.85$

One sees that parametric uncertainties due to $\Delta\alpha^5_{had}, M_b, M_c, M_H, M_t$, do not exceed 1 per mil, therefore the measurement of the total hadronic cross section at LEP2 will not contribute to further improvement of top mass and of the upper limit for the Higgs boson mass.

Similar study for muonic idealized observables is summarized in two following tables.
Total cross-section (in per mil):

$\Delta\alpha^5_{had}, M_b, M_c$ simultaneously	± 0.4 with negligible contribution from M_c
M_t only	± 0.45
M_H only	$+0.40 \div -0.60$

Forward–backward asymmetry (in absolute units 10^{-3}):

$\Delta\alpha^5_{had}, M_b, M_c$ simultaneously	± 0.1 with negligible contribution from M_c
M_t only	± 0.15
M_H only	$+0.15 \div -0.21$

For taus, one should expect similar estimates.

Given precision tag of LEP2 measurements, one shouldn't expect that they will add any improvement to our knowledge of input parameters.

4.15 Program GENTLE: tool for the 2-fermion physics

1) Author: **Dmitri Bardin, Jochen Biebel, Michail Bilenky, Dietrich Lehner, Arnd Leike, Alexander Olshevsky, Tord Riemann**

2) Program: **GENTLE/4fan v.2.11, June 2000**

3) Can be obtained from `/afs/cern.ch/user/b/bardindy/public/Gentle2_11/`
`http://www.ifh.de/~riemann/doc/Gentle/gentle.html`

In this section we describe a new version of the code (`GENTLE/4fan v.2.11`), where several features to extract effects of pair production in $2f$ processes have been added. This version is an update of the original `GENTLE/4fan v.2.00` published in Ref. [182] (see also [183]). The results presented in this section use intensively the approach of Ref. [184]. It was extended for a calculation of low-invariant-mass fermionic pairs of the NC24 family. We remind first of all Feynman diagrams describing this family. The NC24 process is a $4f$ process

$$e^+e^- \to f_1\bar{f}_1 f_2 \bar{f}_2 \tag{13}$$

where $f_1 \neq f_2 \neq e$. There are eight diagrams of conversion type, or NC08 sub-set (Fig. 3):

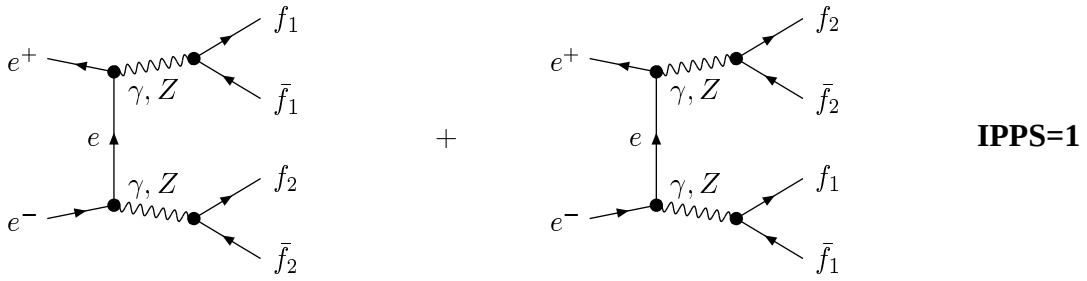

IPPS=1

Fig. 3: The NC08 sub-family of diagrams.

Next, there are eight pair-production-type diagrams (Fig. 4):

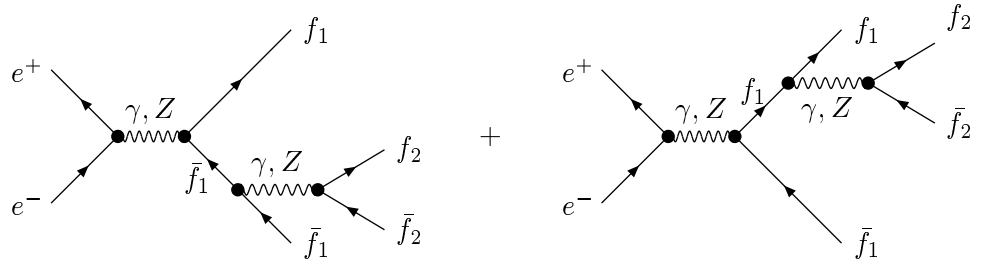

IPPS=2

Fig. 4: Second eight diagrams belonging to the NC24 process.

And finally eight diagrams obtained by interchanging $f_1 \leftrightarrow f_2$ (Fig. 5):

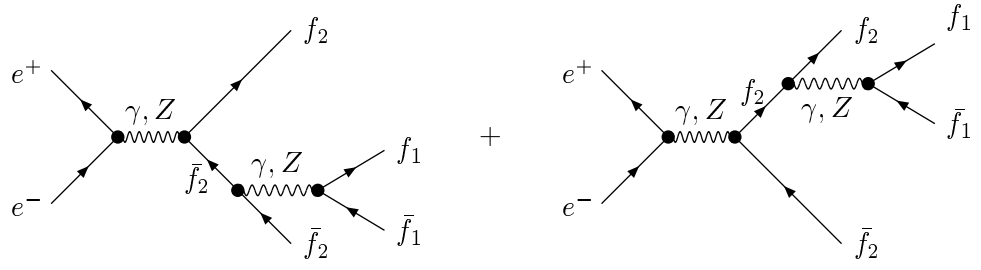

IPPS=3

Fig. 5: Third eight diagrams belonging to the NC24 process.

There is one more diagram with the Higgs boson exchange which is termed the *Higgs signal* or *Higgsstrahlung* contribution

Terminology, notation

These 24 diagrams may be considered as a $4f$ background for a $2f$ process. Their contribution to the $2f$ *signal* could be naturally defined by imposing cuts on the four fermion state. Events surviving cuts mimic the $2f$ process.

To go further on, we have to provide several *definitions.*

The Born approximation for $2f$ process is defined as

$$\text{ISR convolution}\,\{e^+e^- \to f_1\bar{f}_1\}\,, \tag{14}$$

i.e. an ISR convolution of a $2f$ process with $f_1\bar{f}_1$ being termed as a the 'primary pair'.

Relative contribution of $4f$ background processes, Figs 3–4, may be conveniently described in terms of correction due to pair production (PP), which is defined by the ratio

$$\delta_{pairs} = \frac{\text{ISR convolution}\,\{e^+e^- \to f_1\bar{f}_1 f_2\bar{f}_2\}}{\text{ISR convolution}\,\{e^+e^- \to f_1\bar{f}_1\}}\,. \tag{15}$$

In two last equations 'ISR convolution' stands for a rather standard approach

$$\sigma(s) = \int dx H(x,s)\hat{\sigma}[(1-x)s], \tag{16}$$

where $H(x,s)$ is a flux function and $\hat{\sigma}[(1-x)s]$ is a kernel ($4f$ or $2f$) cross-section.

As far as $f_1 \neq f_2$ we have no questions which pair should be considered to be a 'primary' one and which one — a 'secondary'. We may distinguish them by imposing different cuts R_{cut} and P_{cut} on 'primary pair', $f_1\bar{f}_1$ and 'secondary pair' $f_2\bar{f}_2$[10].

The invariant mass cuts are defined as

$$\begin{aligned} R_{cut} &= \frac{M^2_{f_1\bar{f}_1}}{s} \geq 0.01 \text{ inclusive},\ 0.7225 \text{ exclusive}, \\ P_{cut} &= \frac{M^2_{f_2\bar{f}_2}}{s} \leq 10^{-4}, 10^{-3}, 10^{-2}, 10^{-1}, 1 \text{ all values}. \end{aligned} \tag{17}$$

From Eqn.(18) one sees that 'primary' pair is demanded to have large invariant mass, while 'secondary' — small. We also present cut values which were used in this study. For R_{cut} we used two standard LEP2 values: 0.01 (inclusive selection) and 0.7225 (exclusive selection), while for P_{cut} we studied all allowed range ranging from very tight cuts, 10^{-4}, to a no cut situation, $P_{cut} = 1$.

We studied two processes with primary muon and hadron (quark) pairs:

$$\begin{aligned} e^+e^- &\to \mu^+\mu^-, \quad \text{primary muons}, \\ e^+e^- &\to \text{hadrons}, \ \text{primary quarks}. \end{aligned} \tag{18}$$

[10]Some question arises what to do if $f_1 = f_2$, say μ. One may argue that one may distinguish them by requiring that one pair has large invariant mass and another one small. Due to different cuts imposed the effects of Fermi statistics should be negligible. Furthermore, `GENTLE/4fan` allows symmetric treatment of two pairs. Therefore, at least when all 24 diagrams are included everything should be correct (modulo above mentioned interferences contributions) if one treats two muon pairs as two pairs of different particles. Moreover, $\mu\mu$ is only one of eight 4f-channels in $e^+e^- \to \mu\mu$. A similar problem occurs in the consideration of the total hadronic cross-section, where five 4f-channels out of total 40 channels contain identical particles.

Treatment of the secondary pairs deserves special discussion. We may describe them using *fermionic* language similar for description of both 'primary' and 'secondary' pairs, i.e. sum up over all fermion species:

$$e^+e^-, \mu^+\mu^-, \tau^+\tau^-, \text{hadrons} = u, d, c, s, b\text{-pairs}. \tag{19}$$

(NB: Neutrino secondary pairs are presently NOT included; they should and will be!)

This approach suffices, however, a serious drawback. As for primary pairs is concerned fermionic language may be used without questions since pairs is requested to be hard. Even for inclusive selection $M_{f_1\bar{f}_1} \geq 0.2E_{beam} \geq 38$ GeV. On the contrary, secondary pairs are integrated from the production threshold, $2m_f$, up to some typically large cut value $0.1 - 1$. Therefore, we unavoidably cross the region of low lying resonances where a description in terms of quarks fails completely. Fortunately, an adequate language for the description of low-invariant-mass hadronic pairs using a parameterization for the experimentally measured ratio $R = \sigma(e^+e^- \to \text{hadrons})/\sigma(e^+e^- \to \text{muons})$ is elaborated in the literature very well, see e.g. [181].

Virtual pairs

Virtual pairs have to be also added. There are ISR virtual pairs, see Fig. 6, FSR virtual pairs and initial–final interference (IFIPP) virtual pairs. The latter are non-leading (see Ref. [92]) and not included in this study.

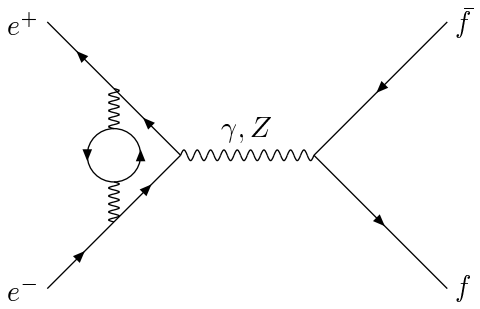

Fig. 6: A typical example of virtual pair correction.

Feynman Diagrams (FD) and their selection with **IPPS, IGONLY** *flags*

In order to study relative contribution of various Feynman diagrams we implemented in the code a 'user options' `IPPS` and `IGONLY` which allows to select sub-groups of diagrams:

IPPS=1 only ISPP is taken into account, see Fig. 3;
IPPS=2 only FSPP with the ordinary meaning of the 'secondary pair', Fig. 4 is included;
IPPS=3 only FSPP of Fig. 5 is accounted for; **IPPS=4** all final pairs, both Fig. 4 and Fig. 5 together with interferences among them are included;
IPPS=5 – IPPS=1$\oplus$ **IPPS=2**;
IPPS=6 – IPPS=1$\oplus$ **IPPS=4**;
IPPS=7 only real IFIPP is considered as a separate contribution;
IPPS=8 all three above sets of 24 diagrams are included;
IGONLY=1 only γ exchanges everywhere;
IGONLY=2 the ordinary secondary pair is produced via γ exchange;
IGONLY=3 all γ and Z exchanges are allowed.

4.16 Program GRC4f: tool for the 2-fermion physics

1) Author: **J. Fujimoto et al.**

2) Program: **GRC4f v 2.1.39,**
`http://is2.kek.jp/ftp/kek/minami/grc4f/`

A more complete references to the GRC4f program can be found in the 4-fermion chapter of this report [183]. Here we address only the features relevant for the generation of a 4-fermion signal and background sample for 2-fermion analyses, i.e. splitting the 4-fermion events in a sample representing pair emission corrections to 2 fermions, and a true 4-fermion background sample.

The GRC4f Monte Carlo package allows the generation of 4-fermion events using Born-level matrix elements (ME), convoluted with ISR photon radiation. It is possible to select the desired set of Feynman diagrams for each final state $\mathrm{f}_1\overline{\mathrm{f}}_1\ \mathrm{f}_2\overline{\mathrm{f}}_2$ by the user. The generation of a signal sample for 2-fermion pair corrections can be done in two ways:

A) Generating a 'signal diagram sample' using only those diagrams, which are considered as signal in the respective definition, and applying the s' (and mass cuts) of the signal definition, to obtain a '4f signal sample'. In addition a second sample with all non-signal diagrams (e.g. MP and ISS) is created, which forms the '4f background sample' together with those events in the signal diagram sample which fail the s' or mass cuts. In this method the (generally small) interferences between signal and background diagrams are neglected in the background subtraction.

B) The '4f signal sample' is obtained from a set of Feynman diagrams, which is larger than the set of signal diagrams. For each MC event a weight w is calculated with the help of the REW99 library [185], which is given by the squared ratio of the matrix elements (ME) summed over all signal diagrams, divided by the sum over all (signal+background) diagrams in the sample.

$$w_{\mathrm{signal}} = \frac{|\sum ME_{\mathrm{signal}}|^2}{|\sum ME_{\mathrm{signal}} + \sum ME_{\mathrm{background}}|^2} \tag{20}$$

where s' or mass cuts can be included in the signal weight, by setting it to zero, if it fails the respective cut. Using the weight $w_{\mathrm{background}} = 1 - w_{\mathrm{signal}}$ one obtains a 4f background sample that accounts for all interference effects between signal and background.

4.17 Program KORALW: tool for the 2-fermion physics

1) Author: **S. Jadach, W. Płaczek, M. Skrzypek, B.F.L. Ward and Z. Wąs**

2) Program: **KORALW 1.42.3**

3) Available at: http://hpjmiady.ifj.edu.pl/programs/programs.html

4) Main references: [186]
[187]
[188]

KORALW allows generation of 4-fermion events. It is described in more detail in the 4-fermion chapter of this report [183]. Here, only the features relevant to 2-fermion pair corrections will be addressed.

It is possible to select in KORALW the desired set of Feynman diagrams for each final state $\mathrm{f}_1\overline{\mathrm{f}}_1$ $\mathrm{f}_2\overline{\mathrm{f}}_2$ by the user. For the moment various approximations of the matrix element have been introduced in KoralW for the $\mu\bar{\mu}\tau\bar{\tau}$ and partly for $\mu\bar{\mu}e\bar{e}$ channels only. These approximations can be activated with the

dip-switch ISWITCH in the routine amp4f in the file ampli4f.grc.all/amp4f.f The available settings are:

- 0: CC03 (old option for WW final states),
- 1: all graphs,
- 2: ISNS$_{\gamma+Z}$,
- 3: FSNS$_{\gamma+Z}$ $\tau\bar{\tau}$ pair to $e\bar{e} \to \mu\bar{\mu}$,
- 4: ISNS$_{\gamma}$ +FSNS$_{\gamma}$ $\tau\bar{\tau}$ pair to $e\bar{e} \to \mu\bar{\mu}$.
- 5: ISNS$_{\gamma}$ $\tau\bar{\tau}$ pair.
- 6: FSNS$_{\gamma+Z}$ $\mu\bar{\mu}$ pair to $e\bar{e} \to \tau\bar{\tau}$,
- negative value: matrix element is calculated for all values of ISWITCH that are declared (set to 1) in ISW4f data statement. The appropriate weights are in this case available as wtset(40+i) with i=1,...,6 as above (note that these weights will be modified along with the principal weight by Coulomb correction and naive QCD, whenever applicable).

For other channels the approximations of matrix element can be introduced in a similar manner in the file ampli4f.grc.all/grc4f_init/selgrf.f Some demo programs are available in the demo.pairs directory, see README file for more information.

Note that the above described extensions of ISWITCH and demo.pairs directory are *not* included in the distribution version 1.42.3 but will be provided as a separate file at the same http location or can be requested from the authors.

5 PHYSICS ISSUES AND DEDICATED STUDIES ON THEORETICAL ERRORS

In the present section we concentrate on two related subjects: the so-called 'tuned comparisons' of the codes done by the authors of the given codes which are critical for the data interpretation at LEP2 energies. At the same time in these comparisons there is some leading 'physics precision theme', in other words they have in mind to clarify a certain aspect of the theoretical errors, like for instance the question of the IRS⊗FSR interference, or secondary pair corrections. The collections of these studies partly represents what we really wanted to be discussed and partly represent the availability of the volunteers who had the time and interest to provide them.

In this section we gather all studies of the above kind except for material on the secondary pair contributions, to which we dedicate the next two sections, although they represent the same class of the workshop activity.

In the section on tuned comparisons of $\mathcal{KK}$MC and ZFITTER some numerical results on the importance of the electroweak boxes is included. We regret that it was not possible to include a more complete numerical study of the electroweak boxes. In order to compensate for that at least partly, we start the present section with a small section explaining what these EW boxes are and what are their properties.

Since most of the studies in the present section concentrate on QED effects, the second small subsection is devoted to methods of QED calculations and then we proceed to two sections which present the tuned comparisons of $\mathcal{KK}$MC and ZFITTER and a dedicated study on IRS⊗FSR interference, also prepared by the $\mathcal{KK}$MC and ZFITTER teams.

5.1 Electroweak boxes

The one-loop *the non-QED* or purely *weak* corrections may be represented as the sum of *dressed* γ and Z exchange amplitudes plus the contribution from *weak box* diagrams, i.e. ZZ and WW boxes, see Fig. 7. The ZZ boxes are separately gauge-invariant.

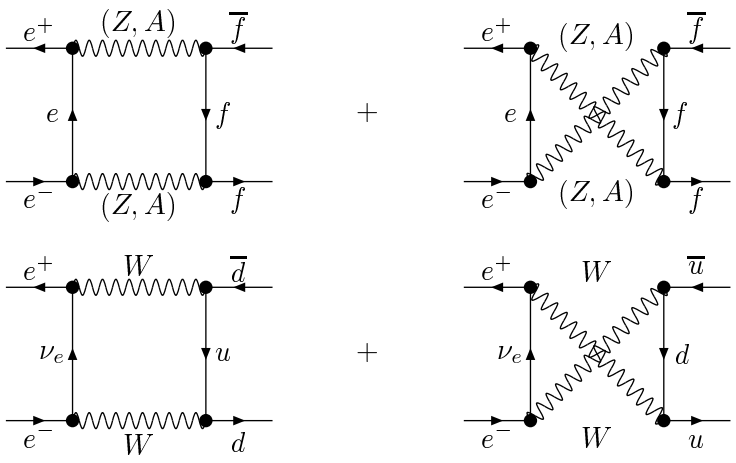

Fig. 7: Full collection of QED and EW boxes.

If external fermion masses are neglected, then the complete one-loop amplitude (OLA) can be described by only four scalar functions and by the running electromagnetic constant $\alpha^{\rm fer}(s)$. Using notation of Refs. [75, 172, 172] one may represent the dressed amplitude in terms of four scalar form factors, $F_{ij}(s,t)$:

$$\begin{aligned}\mathcal{A}^{\rm OLA}_{Z+A} &= \frac{e^2 I_e^{(3)} I_f^{(3)}}{4 s_W^2 c_W^2}\chi_Z(s)\Big\{\gamma_\mu\gamma_+\otimes\gamma_\mu\gamma_+ F_{LL}(s,t) - 4|Q_e|s_W^2\gamma_\mu\otimes\gamma_\mu\gamma_+ F_{QL}(s,t)\\ &\quad -4|Q_f|s_W^2\gamma_\mu\gamma_+\otimes\gamma_\mu F_{LQ}(s,t) + 16|Q_eQ_f|s_W^4\gamma_\mu\otimes\gamma_\mu F_{QQ}(s,t)\Big\}; \qquad (21)\end{aligned}$$

where the $\chi_Z(s)$ denotes the Z boson propagator

$$\chi_Z(s) = \frac{1}{s - M_Z^2 + is\Gamma_Z/M_Z}\,. \qquad (22)$$

The t-dependence is due to the weak boxes. On top of the $\mathcal{A}^{\rm OLA}_{Z+A}$ there is the corrected γ-exchange amplitude, which contains, by construction, only the QED running coupling $\alpha^{\rm fer}(s)$:

$$\mathcal{A}^{\rm OLA}_{A} = \frac{4\pi\alpha^{\rm fer}(s)}{s}\gamma_\mu\otimes\gamma_\mu\,. \qquad (23)$$

The above electroweak boxes are numerically negligible below the WW threshold. At very high energies, $\sim$ 1 TeV they are known to be numerically very large, as was discussed recently in several papers [189–192] in the context of the (im)possible exponentiation of the electroweak corrections (so-called Sudakov double logarithms) in the non-Abelian theories with the spontaneous symmetry breaking. They are therefore part of a rather interesting physical phenomenon. At LEP2 the EW boxes are just rising from nothing to a few per cent level, see later in this section.

EW box corrections are well known and they are theoretically under good control. The only possible issue is the technical precision of their implementation in the MC and other codes. It would therefore be good to make additional tests of the existing codes in this direction.

5.2 Selected aspects of QED calculations

Structure function approach

The basic principles and also details of the structure function approach used in the presented programs are described in Ref. [102] for NUNUGPV and in Refs. [85–87, 90] for LABSMC. The main goal of these approaches is to use the exact matrix element for the given process and one (two ...) extra photons and appropriate phase space whenever they are available and combine them into single prediction using the LL structure function approach for fixing normalizations.

Parton shower approach

The QED radiative correction in the leading-log (LL) approximation can also be obtained using the Monte Carlo method instead of the analytic formulae of the structure function. The details of this method, `QEDPS`, can be found in Ref. [95]. Here we recall that the algorithm can maintain the exact kinematics during the evolution of an electron. This specific feature of the `QEDPS` allows us to apply the `QEDPS` to radiative processes, avoiding a double-counting problem. If one needs to know the precise distributions of the hard photon(s) associated with some kernel process such as neutrino pair-production, one has to use the exact matrix-elements including hard photon(s) with the soft-photon correction. Since the `QEDPS` can provide complete kinematical information about the emitted photons and the virtual electrons, it is easy to separate the soft photons from the parton shower not to go into the visible region. In addition to this simple phase-space separation, the ordering of the electron virtuality is also required. During the evolution of an electron the virtuality is monotonically increasing, which is realized naturally in the `QEDPS` algorithm. A further condition must be imposed on the virtuality of the electron in the matrix-elements after emitting the photon: It should be greater than the virtuality of the electron in the last stage of `QEDPS`. This careful treatment to avoid the double-counting problem allows us precise predictions of radiative photons.

Exponentiation

The exponentiation of QED and its realization in the form of the Monte Carlo is explained already in detail in literature, see Sections 4.5, 4.3 and 4.1 for references; in the following let us concentrate on relatively novel, and essential for establishing the precision required by experiments, subject of initial-final-state interference.

5.3 QED ISR⊗FSR interference in cross section and charge asymmetry

Authors: $\mathcal{KK}$MC and ZFITTER teams.

We start this section with characterizing the ISR⊗FSR interference (IFI) and listing/characterizing the relevant literature and existing tools/codes for calculating IFI. The principal two subsections contain comparisons of $\mathcal{KK}$MC and ZFITTER for the muon channel with ISR+FSR, with and without ISR⊗FSR, for the total cross section and charge asymmetry. Finally we discuss the uncertainty of ISR⊗FSR, as compared to LEP2 precision targets.

5.3.1 Overview of properties of the ISR⊗FSR interference

At LEP2 the QED ISR⊗FSR interference (IFI) is an order of magnitude bigger than at LEP1 because it is not suppressed any more by the factor Γ_Z/M_Z. On the other hand the experimental errors are bigger, so its importance has to be measured in terms of the target precision requirements defined in Section 2.1. All main characteristics if IFI can be understood looking at the leading term in its the first order expression

$$\delta^{\rm IFI}(\cos\theta) = 4Q_eQ_f\frac{\alpha}{\pi}\ \ln\frac{E^\gamma_{\rm max}}{E_{beam}}\ln\frac{1-\cos\theta}{1+\cos\theta} \tag{24}$$

(which is also the θ dependent part of the YFS/Sudakov form-factor). The above factor multiplies the Born differential cross section. We see immediately that:

- IFI is growing for stronger cuts on maximum photon energy $E^\gamma_{\rm max}\to 0$.

- IFI always contributes to A_{FB}, however, not necessarily to the total cross section, unless the Born differential cross section is asymmetric itself. This is true at LEP2, where all muon and quark asymmetries are large.
- IFI is proportional to the charge of the final fermion Q_f, and consequently it is smaller for quarks than for muons. In addition, for quarks the contributions from different channels tend to cancel each other.
- It does not contain logs of fermion masses.

The above facts are illustrated in a more quantitative form in Table 12, where we show the values of the IFI contributions to the $\mu-$ and q-pair channels at two LEP energies. They are calculated with $\mathcal{KK}$MC for unrestricted $\cos\theta$ and a simple cut on the fermion pair invariant mass[11] $M_{f\bar{f}} = \sqrt{s'}$. As we see, the IFI contributions to A_{FB} are the smallest for d, twice as large for u with an alternating sign, and are the largest for μ. They increase for stronger cut on photon energy. Since $A_{FB} \sim 0.6$ for all quarks and μ, consequently the magnitude of the IFI contribution of σ shows the same pattern. For the typical Z-exclusive $v_{\max} = 1 - s'_{min} = 0.2$, looking more closely into numbers, we find for the cross section for muon pairs that the IFI contribution is about 2.4% of σ^μ, that is 6 times bigger than the precision tag 0.4% of Section 2.1. For quarks it is 0.5% of σ^h, that is two times bigger than the precision tag of 0.2% listed in Section 2.1. For the Z-inclusive $v_{\max} = 0.9$ we have the IFI of 0.4% of σ^μ versus the 0.4% precision tag of Section 2.1 and 0.03% of σ^h versus 0.2% precision tag of Section 2.1. There is therefore no doubt that IFI is important for LEP data analysis.

Table 12: The quantitative illustration of the main properties of IFI for q- and μ-pairs at two LEP energies.

f	σ^{IFI}/σ	A_{FB}^{IFI}	f	σ^{IFI}/σ	A_{FB}^{IFI}
	$\sigma(v_{\max})$[pb], $v_{\max} = 0.01$, 189GeV			$\sigma(v_{\max})$[pb], $v_{\max} = 0.01$, 206GeV	
d	0.0194 ± 0.0007	0.0152 ± 0.0065	d	0.0194 ± 0.0009	0.0153 ± 0.0084
u	-0.0452 ± 0.0010	-0.0242 ± 0.0060	u	-0.0442 ± 0.0012	-0.0247 ± 0.0074
s	0.0188 ± 0.0007	0.0149 ± 0.0065	s	0.0191 ± 0.0009	0.0152 ± 0.0084
c	-0.0423 ± 0.0010	-0.0239 ± 0.0058	c	-0.0423 ± 0.0012	-0.0251 ± 0.0071
b	0.0193 ± 0.0007	0.0151 ± 0.0065	b	0.0203 ± 0.0009	0.0149 ± 0.0083
all	-0.0110 ± 0.0008	-0.0051 ± 0.0062	all	-0.0114 ± 0.0010	-0.0057 ± 0.0078
μ	0.0552 ± 0.0017	0.0457 ± 0.0071	μ	0.0564 ± 0.0021	0.0482 ± 0.0085
	ISR$\otimes$FSR, $v_{\max} = 0.20$, 189GeV			ISR$\otimes$FSR, $v_{\max} = 0.20$, 206GeV	
d	0.0080 ± 0.0006	0.0067 ± 0.0051	d	0.0079 ± 0.0008	0.0071 ± 0.0066
u	-0.0197 ± 0.0009	-0.0104 ± 0.0047	u	-0.0193 ± 0.0011	-0.0102 ± 0.0057
s	0.0090 ± 0.0006	0.0070 ± 0.0051	s	0.0078 ± 0.0008	0.0070 ± 0.0066
c	-0.0178 ± 0.0009	-0.0102 ± 0.0046	c	-0.0181 ± 0.0011	-0.0109 ± 0.0056
b	0.0093 ± 0.0006	0.0071 ± 0.0052	b	0.0087 ± 0.0008	0.0068 ± 0.0066
all	-0.0050 ± 0.0007	-0.0024 ± 0.0049	all	-0.0057 ± 0.0009	-0.0025 ± 0.0061
μ	0.0239 ± 0.0014	0.0198 ± 0.0050	μ	0.0238 ± 0.0017	0.0208 ± 0.0061
	ISR$\otimes$FSR, $v_{\max} = 0.30$, 189GeV			ISR$\otimes$FSR, $v_{\max} = 0.30$, 206GeV	
d	0.0066 ± 0.0006	0.0055 ± 0.0049	d	0.0061 ± 0.0008	0.0060 ± 0.0063
u	-0.0163 ± 0.0008	-0.0086 ± 0.0045	u	-0.0163 ± 0.0010	-0.0085 ± 0.0054
s	0.0076 ± 0.0006	0.0059 ± 0.0049	s	0.0067 ± 0.0008	0.0060 ± 0.0063
c	-0.0143 ± 0.0008	-0.0085 ± 0.0044	c	-0.0148 ± 0.0010	-0.0092 ± 0.0054
b	0.0079 ± 0.0006	0.0059 ± 0.0049	b	0.0073 ± 0.0008	0.0057 ± 0.0063
all	-0.0040 ± 0.0007	-0.0020 ± 0.0047	all	-0.0048 ± 0.0009	-0.0021 ± 0.0058
μ	0.0195 ± 0.0013	0.0161 ± 0.0048	μ	0.0194 ± 0.0016	0.0172 ± 0.0058
	ISR$\otimes$FSR, $v_{\max} = 0.90$, 189GeV			ISR$\otimes$FSR, $v_{\max} = 0.90$, 206GeV	
d	0.0008 ± 0.0002	0.0016 ± 0.0012	d	0.0006 ± 0.0002	0.0017 ± 0.0015
u	-0.0023 ± 0.0003	-0.0040 ± 0.0014	u	-0.0027 ± 0.0004	-0.0042 ± 0.0018
s	0.0010 ± 0.0002	0.0018 ± 0.0012	s	0.0005 ± 0.0002	0.0017 ± 0.0015
c	-0.0021 ± 0.0003	-0.0033 ± 0.0014	c	-0.0025 ± 0.0004	-0.0041 ± 0.0018
b	0.0008 ± 0.0002	0.0016 ± 0.0012	b	0.0009 ± 0.0002	0.0015 ± 0.0015
all	-0.0003 ± 0.0002	-0.0005 ± 0.0013	all	-0.0006 ± 0.0003	-0.0007 ± 0.0016
μ	0.0042 ± 0.0006	0.0070 ± 0.0022	μ	0.0043 ± 0.0008	0.0070 ± 0.0026

[11] For realistic cuts the IFI contributions will be slightly smaller, by a factor ~ 0.8.

5.3.2 *Exponentiation of IFI*

In the pure $\mathcal{O}(\alpha^1)$ calculation, see Eq. (24), it has been well known for a long time that the ISR⊗FSR in the integrated cross section and in the charge asymmetry goes to infinity for the strong cuts on photon energy $E^{\gamma}_{\max} \to 0$, clearly an unphysical result. Furthermore, the angular distribution close $\cos\theta = \pm 1$ gets singular behaviour of the kind $\ln((1-\cos\theta)/(1+\cos\theta)$. It is also well known for a long time [38, 193] that summing up properly the soft photon contributions cures both of these problems. This can be schematically demonstrated as

$$1 + \delta^{\rm IFI}(\cos\theta) \to e^{\delta^{\rm IFI}(\cos\theta)} \ . \tag{25}$$

What kind of practical consequence may we expect? For the typical experimental Z-exclusive cut $s' > 0.80s$ and $|\cos\theta < 0.95|$ the effect of the exponentiation will be rather small. Most probably it is equally or more important to convolute properly the ISR⊗FSR with the $\mathcal{O}(L^2\alpha^2)$ ISR.

If Z radiative return is included in the phase space then the situation is more delicate. One hard photon is necessarily emitted and from the real-photon $\mathcal{O}(\alpha^1)$ matrix element we know only that the ISR⊗FSR is suppressed close to and across the Z-peak in s' distribution. Exponentiation in this case means adding into the game a second and more real photons and the $\mathcal{O}(\alpha^2)$ virtual corrections. These additional $\mathcal{O}(\alpha^2)$ and higher corrections are not exactly known/available, and in practice we can only add them in the soft photon approximation. This is probably good enough for the LEP2 precision tag. Such a scenario is already realized in the $\mathcal{KK}$MC, see below.

5.3.3 *Older works on IFI*

In the older literature a rather complete treatment of IFI can be found in Ref. [136], where it is discussed in the soft-photon approximation (no very hard photons), in exponentiated form[12], including Z-resonance and Z-radiative return (not too far from Z). Later works, at the beginning of LEP1 era, see Refs. [59, 115, 116, 194, 195], see also LEP1 proceedings [79] have concentrated mainly on adding hard photons in the game and removing certain approximations in the virtual corrections.

5.3.4 *KORALZ Monte Carlo for IFI*

The KORALZ [55] Monte Carlo offers the most solid benchmark for the $\mathcal{O}(\alpha^1)$ IFI without exponentiation. The $\mathcal{O}(\alpha^1)$ part/option of KORALZ is an improved version of the program of Ref. [80] (exact γ-Z boxes are added). It was well tested to a precision $< 0.1\%$ against analytical calculations in Ref. [59], also far away from Z-resonance. It was also compared with the calculations of Ref. [116]. KORALZ was already used in the first experimental studies of IFI at LEP1, see Refs. [196, 197].

5.3.5 *IFI from $\mathcal{KK}$MC*

The IFI is now implemented in the exponentiated form in the new MC event generator $\mathcal{KK}$MC [49], see Section 4.5. From the IFI point of view $\mathcal{KK}$MC represents the complete $\mathcal{O}(\alpha^1)$ in exponentiated form (Coherent Exclusive Exponentiation), however with some important extensions: (a) it convolutes IFI with the second order ISR (and FSR) and (b) it does have for IFI the exact second order 2-γ matrix element. It misses second order exact virtual corrections relevant for IFI (double boxes), but not completely, they are included in the soft photon approximation.

The IFI numerical results from $\mathcal{KK}$MC were already debugged/tested in Ref. [66] by comparing them with the results of $\mathcal{O}(\alpha^1)$ KORALZ without exponentiation (see above for more details). It was found that the IFI correction to the total cross section and charge asymmetry from $\mathcal{KK}$MC and $\mathcal{O}(\alpha^1)$ KORALZ is about 2% and agrees to within $< 0.2\%$ for the common examples of Z-exclusive cuts, even without a cut on $\cos\theta$. One step further was also made in Ref. [66]: the $\mathcal{KK}$MC results without the

[12] The authors of this paper point out the Yennie-Frautschi-Suura [38] work as a prototype for IFI exponentiation.

ISR⊗FSR were combined with the ISR⊗FSR of KORALZ $\mathcal{O}(\alpha^1)$ ISR[13]. This kind of 'hybrid' $\mathcal{KK}$MC +ISR⊗FSR$_{1-st.ord.}$ result was compared with the exponentiated IFI of standard CEEX over the wide range of photon energy cuts, for the total cross-section and charge asymmetry. Typical agreement of $< 0.2\%$ was found for both Z-exclusive and Z-inclusive cuts. The biggest discrepancy was noticed to be 0.4% for the charge asymmetry for a Z-inclusive cut and for the cross section for certain values (far from the experimental ones) for the Z-exclusive cut.

In Ref. [66] a preliminary comparison was also made for ISR⊗FSR between $\mathcal{KK}$MC and ZFITTER 6.11. Similar patterns of agreements and disagreements were found. This is not surprising, as ZFITTER is also combining the ISR⊗FSR$_{1-st.ord.}$ without exponentiation with the rest of the calculation. The authors of Ref. [66] conclude that there is definitely room for improvement of our understanding of ISR⊗FSR, especially for the Z-inclusive acceptance, but there is no emergency situation[14].

5.3.6 Exponentiated IFI from ZFITTER

The recent version of ZFITTER includes ISR⊗FSR exponentiated according to Greco et al. [193]. We call it in short ZFexp. This option will be available in the future edition of ZFITTER. The first version which we tried in this comparison featured some numerical problems but after extensive tests it now agrees rather well with $\mathcal{KK}$MC. Note that if the ISR⊗FSR is correctly implemented in both programs then we expect the agreement of order 0.1% for any Z-exclusive cuts, in particular the difference between them should not increase for a strong cut.

5.3.7 Semianalytical estimate of soft limit

Before we come to numerical comparisons let us present a simple semi-analytical estimate of the IFI contributions to cross-sections and charge asymmetry in the soft limit, in the case of the exponentiation of IFI. The purpose is two-fold: (a) such expressions are useful in quick testing more complicated programs like $\mathcal{KK}$MC and ZFITTER, (b) they give non-trivial insight into higher orders. The IFI correction to total cross section is

$$\delta_{IFI}(v_{\max}) = \frac{\sigma_{exp} - \sigma_{exp}{}^{\rm NoIFI}}{\sigma_{exp}{}^{\rm NoIFI}} = 1 - 2A_{FB}\kappa \ln v_{\max} + \kappa^2 \ln^2 v_{\max}\Big(\frac{1}{2} + \frac{\pi^2}{6}\Big) + \text{const}, \qquad (26)$$

where $\kappa = 4\frac{\alpha}{\pi}Q_eQ_f$, A_{FB} is Born asymmetry, and $v_{\max} = 1 - s'_{\min}/s \simeq E^{\gamma}_{\max}/E_{beam}$ limits the maximum energy of all soft photons. The constant part is related to non-IR parts of QED boxes. The absence of big mass-logs along with $\ln v_{\max}$ in this formula is not an accident, this is the rigorous result of the proper exponentiation of IFI to infinite order. This gives an argument for the lack of big enhancemet factors like $\ln E^{\gamma}_{\max}/E_{beam}$ in the IFI corrections. Without such enhancement factors IFI at higher orders will always be small, for instance at $\mathcal{O}(\alpha^2)$ it is of order $\kappa\frac{\alpha}{\pi}\ln\frac{s}{m_e^2}$, that is $\sim 0.05\%$. Similarly, one may estimate the IFI correction to A_{FB}:

$$\delta A^{\rm IFI}_{FB}(v_1) = -\kappa \ln v_{\max}\left(2\ln(2) + \frac{3}{4} + 2A_{FB}\right) + \mathcal{O}(\kappa^2 \ln^2 v_{\max}) + \text{const}. \qquad (27)$$

The precision of the above two formulas is 1%. It is enough to test the correctness of the soft limit. Later on in the relevant figures results of the above formula are represented as an additional curve of black dots.

[13]This method was described in Refs. [196, 197] using KORALZ $\mathcal{O}(\alpha^1)$ and KORALZ/YFS3, and used to estimate higher orders to IFI at Z peak.

[14]The more complete summary/discussion on these tests can be also found in the presentation of S.J. at the June 1999 meeting of LEPEWG, see transparencies on http://home.cern.ch/jadach

5.3.8 *Comparisons of $\mathcal{KK}$MC and ZFITTER including IFI*

The material of the present section, on tuned comparisons of $\mathcal{KK}$MC and ZFITTER with IFI switched on, will be continued later in Section 5.4 for the case when IFI is switched off, and can thus be regarded as its extension. All presented numerical results will be for the muon channel with the cut on the effective mass of the muon pair $M_{f\bar{f}} = \sqrt{s'}$, and no restriction on $\cos\theta$. The scattering angle θ is defined[15] as an angle of μ^- with respect to e^-. We shall discuss results for the total cross section first and for the charge asymmetry later on[16].

5.3.9 *IFI in the cross section*

As a warm-up exercise we present in Fig. 8 the comparison of $\mathcal{KK}$MC and ZFITTER for IFI switched off and on. Making the comparison for IFI switched off makes sense because in Section 5.4 the distribution of $M_{f\bar{f}} = \sqrt{s'}$ was not affected by FSR, and now it is. As we see in Fig. 8(a), in the case of no IFI we recover the same level of agreement among $\mathcal{KK}$MC, $\mathcal{KK}$sem and ZFITTER at the level of 0.2% as before. Encouraged by this, we switch on IFI and find in Fig. 8(a) that $\mathcal{KK}$MC and two versions of ZFITTER with and without exponentiation. The latter ZFITTER without exponentiation, let us call ZFstd. As we see, all curves depart for $\mathcal{KK}$sem (which has no IFI) by $\sim 2\%$ for Z-exclusive cuts and $\sim 0.4\%$ for Z-inclusive, and they agree fairly well to within ~ 0.2–0.3%. In the soft limit (the first point in the curves is for $s'_{\rm max} = 0.99s$) ZFstd diverges by 4% from the $\mathcal{KK}$MC and ZFexp.

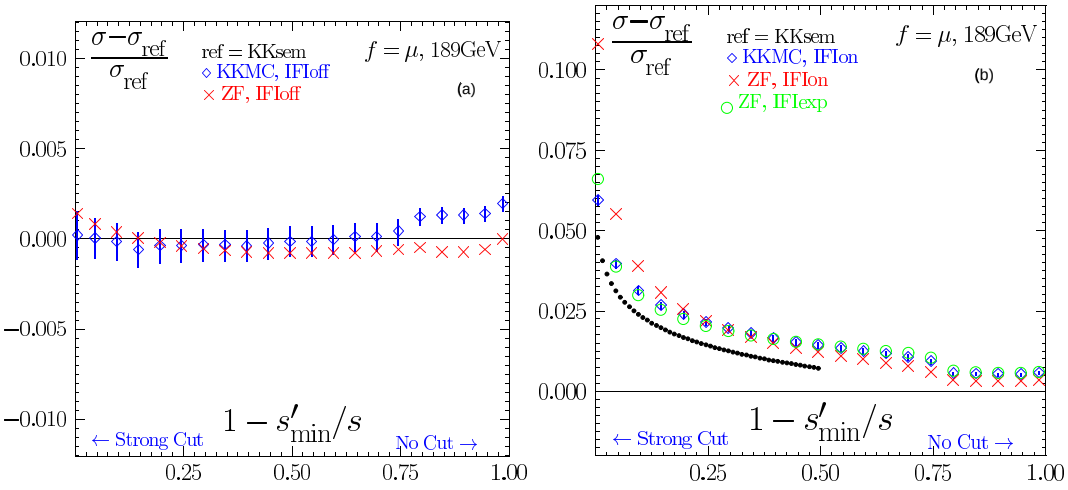

Fig. 8: Comparison of $\mathcal{KK}$MC, $\mathcal{KK}$sem and ZFITTER for cross-section at 189 GeV. The IFI is on/off for $\mathcal{KK}$MC and ZFITTER and off for reference $\mathcal{KK}$sem. Black dots represent Eq. (26).

In the next Fig. 9(a) we look closer into the IFI effect in $\mathcal{KK}$MC and ZFITTER, i.e. into the difference due to switching on IFI in each program (version). In Fig. 9(a) we view the same results plotted as the differences ZFITTER $-$ $\mathcal{KK}$MC. As we see, the difference ZFstd$-\mathcal{KK}$MC is within 0.4% for a wide range of the cuts, including typical Z-exclusive and Z-inclusive cuts, while the difference ZFexp$-\mathcal{KK}$MC is twice smaller, about 0.2% only, again for a wide range of the cuts. In the figures we also show (black dots) the analytical estimate of the IFI exponentiated distribution. The estimate should be valid to within 1% and its main aim is to test the soft photon limit. As we see the soft limit is correctly reproduced for both $\mathcal{KK}$MC and ZFexp, and their difference at $s'_{\rm max} = 0.99s$ is also below 1%.

[15]This angle definition makes little sense for Z radiative return at LEP2 energies where muon pair is very strongly boosted, but we keep it for historical reasons.

[16]However, we should always keep in mind that IFI contributes primarily to A_{FB} and secondarily to σ, as already explained.

5.3.10 *IFI in the charge asymmetry*

In Fig. 10(a) we show the comparison of $\mathcal{KK}$MC and ZFITTER for the charge asymmetry, in the case of IFI switched off. The agreement is within 0.25%, and it should be $< 0.20\%$ in view of the fact

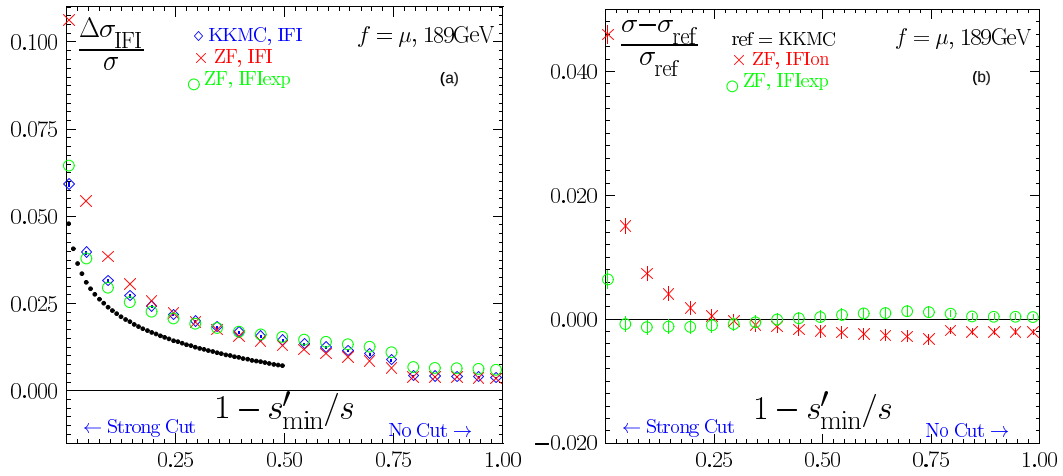

Fig. 9: Comparison of $\mathcal{KK}$MC and ZFITTER for cross-section at 189 GeV. The IFI is on/off for $\mathcal{KK}$MC and ZFITTER. Black dots represent Eq. (26).

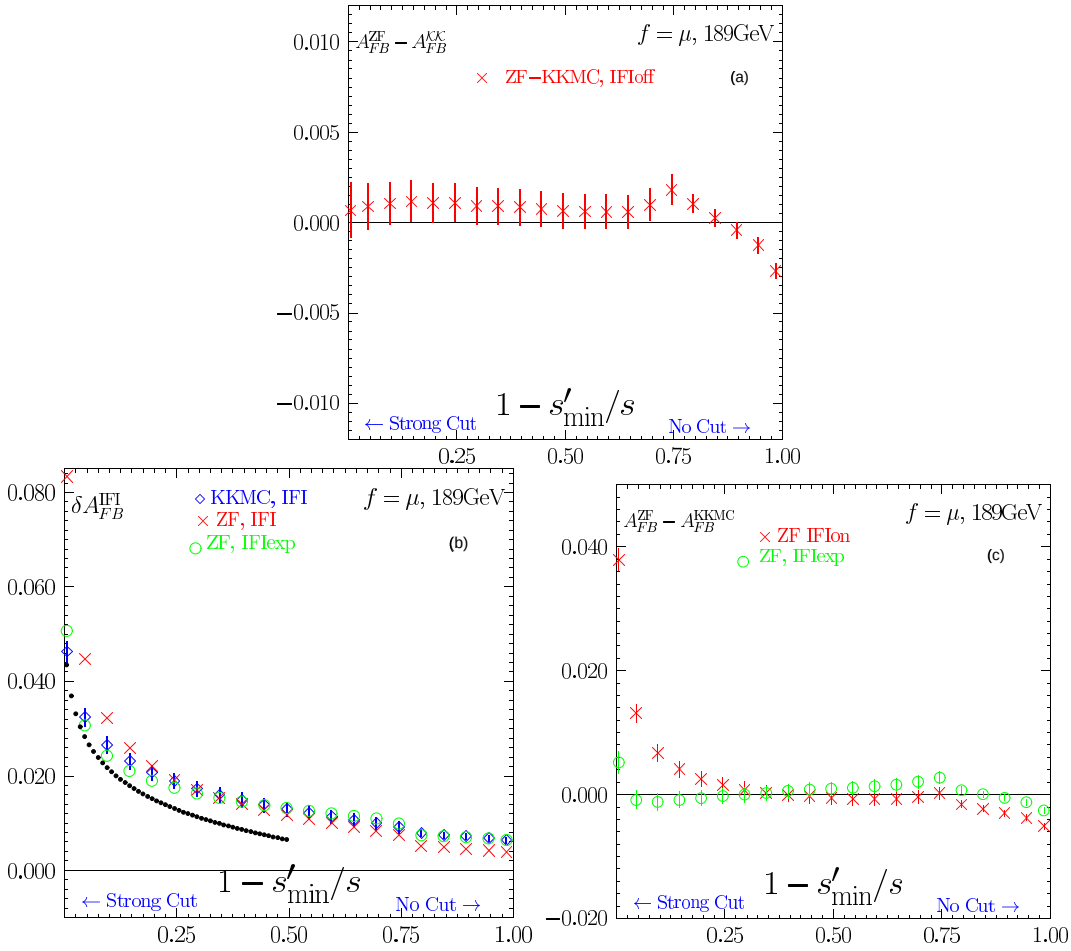

Fig. 10: Comparison of $\mathcal{KK}$MC and ZFITTER for A_{FB} at 189 GeV. Black dots represent Eq. (27).

that $\mathcal{KK}$sem and $\mathcal{KK}$MC agree[17] for A_{FB} to within 0.1%, see Ref. [66]. The quality of the test is also limited by MC statistics.

In the next plot of Fig. 10(b) we look into the IFI effect in the $\mathcal{KK}$MC and in ZFITTER, that is into the difference due to switching on IFI in each program (version). In Fig. 10(c) we view the same results plotted as the difference ZFITTER $-$ $\mathcal{KK}$MC. As we see the the difference ZFstd$-\mathcal{KK}$MC is within 0.4% for a wide range of the cuts, including typical Z-exclusive and Z-inclusive cuts. The difference ZFexp$-\mathcal{KK}$MC is smaller, about 0.25%. This agreement is within the required precision tag of 0.4%–0.5% for A_{FB} in Section 2.1. As for cross sections, we have also included in these plots the analytical estimate of IFI contribution to asymmetry in the soft photon approximation. Results of $\mathcal{KK}$MC agree well with the analytical estimate in the soft limit. And what is also important the exponentiated version of ZFITTER is much closer to $\mathcal{KK}$MC than the older one.

Finally, we include also in Table 13 in a digital form, as a reference benchmark for further studies, a subset of results which were presented visually in Figs. 9 and 10.

Table 13: Cross-sections and asymmetries from $\mathcal{KK}$MC, $\mathcal{KK}$sem and ZFITTER at 189 GeV. The QED ISR$\otimes$FSR interference is switched on/off. No cut on $\cos\theta$. We define $v = 1 - s'/s$.

$v_{\max}$	(a) $\mathcal{KK}$sem Refer.	(b) $\mathcal{O}(\alpha^2)^{\rm IFIoff}_{\rm CEEX}$	(c) ZF IFIoff	(d) $\mathcal{O}(\alpha^2)^{\rm IFIon}_{\rm CEEX}$	(e) ZF IFIon	(f) ZF IFIexp
	$\sigma(\mu^+\mu^-)$, PRIMITIVE, at 189GeV					
$v < 0.01$	1.6714 ± 0.0000	1.6717 ± 0.0022	1.6737 ± 0.0000	1.7706 ± 0.0027	1.8520 ± 0.0000	1.7819 ± 0.0000
$v < 0.10$	2.5200 ± 0.0000	2.5195 ± 0.0026	2.5209 ± 0.0000	2.5987 ± 0.0031	2.6180 ± 0.0000	2.5955 ± 0.0000
$v < 0.20$	2.8484 ± 0.0000	2.8472 ± 0.0027	2.8478 ± 0.0000	2.9160 ± 0.0032	2.9214 ± 0.0000	2.9124 ± 0.0000
$v < 0.30$	3.0618 ± 0.0000	3.0608 ± 0.0028	3.0602 ± 0.0000	3.1214 ± 0.0033	3.1206 ± 0.0000	3.1190 ± 0.0000
$v < 0.40$	3.2284 ± 0.0000	3.2271 ± 0.0028	3.2262 ± 0.0000	3.2812 ± 0.0033	3.2773 ± 0.0000	3.2811 ± 0.0000
$v < 0.50$	3.3748 ± 0.0000	3.3743 ± 0.0029	3.3722 ± 0.0000	3.4228 ± 0.0034	3.4162 ± 0.0000	3.4241 ± 0.0000
$v < 0.60$	3.5215 ± 0.0000	3.5213 ± 0.0029	3.5188 ± 0.0000	3.5649 ± 0.0034	3.5567 ± 0.0000	3.5682 ± 0.0000
$v < 0.70$	3.7223 ± 0.0000	3.7227 ± 0.0029	3.7199 ± 0.0000	3.7618 ± 0.0034	3.7515 ± 0.0000	3.7667 ± 0.0000
$v < 0.80$	6.7047 ± 0.0000	6.7127 ± 0.0032	6.7016 ± 0.0000	6.7410 ± 0.0037	6.7287 ± 0.0000	6.7470 ± 0.0000
$v < 0.90$	7.1472 ± 0.0000	7.1564 ± 0.0032	7.1422 ± 0.0000	7.1849 ± 0.0037	7.1701 ± 0.0000	7.1880 ± 0.0000
$v < 0.99$	7.6171 ± 0.0000	7.6320 ± 0.0032	7.6172 ± 0.0000	7.6599 ± 0.0037	7.6445 ± 0.0000	7.6628 ± 0.0000
	$A_{FB}(\mu^+\mu^-)$, PRIMITIVE, at 189GeV					
$v < 0.01$	0.5656 ± 0.0000	0.5651 ± 0.0015	0.5658 ± 0.0000	0.6113 ± 0.0018	0.6492 ± 0.0000	0.6165 ± 0.0000
$v < 0.10$	0.5666 ± 0.0000	0.5658 ± 0.0012	0.5669 ± 0.0000	0.5923 ± 0.0014	0.5991 ± 0.0000	0.5912 ± 0.0000
$v < 0.20$	0.5678 ± 0.0000	0.5668 ± 0.0011	0.5679 ± 0.0000	0.5874 ± 0.0013	0.5899 ± 0.0000	0.5868 ± 0.0000
$v < 0.30$	0.5694 ± 0.0000	0.5678 ± 0.0010	0.5688 ± 0.0000	0.5851 ± 0.0012	0.5859 ± 0.0000	0.5851 ± 0.0000
$v < 0.40$	0.5715 ± 0.0000	0.5690 ± 0.0010	0.5699 ± 0.0000	0.5839 ± 0.0012	0.5839 ± 0.0000	0.5844 ± 0.0000
$v < 0.50$	0.5745 ± 0.0000	0.5706 ± 0.0010	0.5712 ± 0.0000	0.5835 ± 0.0011	0.5830 ± 0.0000	0.5844 ± 0.0000
$v < 0.60$	0.5791 ± 0.0000	0.5722 ± 0.0009	0.5728 ± 0.0000	0.5836 ± 0.0011	0.5828 ± 0.0000	0.5849 ± 0.0000
$v < 0.70$	0.5864 ± 0.0000	0.5724 ± 0.0009	0.5735 ± 0.0000	0.5823 ± 0.0011	0.5819 ± 0.0000	0.5844 ± 0.0000
$v < 0.80$	0.3513 ± 0.0000	0.3372 ± 0.0005	0.3383 ± 0.0000	0.3450 ± 0.0006	0.3434 ± 0.0000	0.3457 ± 0.0000
$v < 0.90$	0.3103 ± 0.0000	0.3068 ± 0.0005	0.3064 ± 0.0000	0.3139 ± 0.0005	0.3110 ± 0.0000	0.3134 ± 0.0000
$v < 0.99$	0.2850 ± 0.0000	0.2866 ± 0.0004	0.2839 ± 0.0000	0.2930 ± 0.0005	0.2879 ± 0.0000	0.2904 ± 0.0000

5.3.11 Conclusion on the uncertainty of IFI

We have done the same at 206 GeV and all results are practically the same, because IFI depends on CMS energy only very weekly (logarithmically at most).

Summarizing, for the μ-pair total cross section, the uncertainty of the IFI is $\sim 0.2\%$ well within the precision target $\delta\sigma^\mu/\sigma^\mu = 0.4\%$ of Section 2.1 for both Z-inclusive and Z-exclusive cuts. For the μ-pair

[17] We could not include $\mathcal{KK}$sem in the present comparison for A_{FB} because the agreement $\mathcal{KK}$sem - $\mathcal{KK}$MC was obtained for the θ definition in the Z rest frame [66]. Unfortunately ZFITTER cannot use such an angle, and we are forced to the CMS definition of θ.

charge asymmetry the uncertainty of the IFI is $< 0.3\%$, also within the precision target $\delta A_{FB}^{\mu} \sim 0.4$–$0.5\%$ of Section 2.1 for both Z-inclusive and Z-exclusive cuts.

As seen in Table 12, the IFI corrections is a factor 4–5 smaller in the hadronic σ^h than for σ^μ, so by scaling down the $\sim 0.2\%$ uncertainty of the σ^μ, we get something like $\sim 0.05\%$, well below the precision target $\delta\sigma^h/\sigma^h = 0.1$–$0.2\%$ of Section 2.1 for both Z-inclusive and Z-exclusive cuts.

5.4 Tuned comparison of ZFITTER 6.30 and $\mathcal{KK}$MC 4.14

Authors: $\mathcal{KK}$MC and ZFITTER teams.

The main aim of this section is to compare $\mathcal{KK}$MC and ZFITTER for hadronic total cross sections. In order to speed up calculations and make it easier to tune both programs, we have switched off the ISR$\otimes$FSR interference. We included the muon channel in all tests, just as a reference calculation.

Both of the programs ZFITTER [75] and $\mathcal{KK}$MC [49] use the same library of electroweak form-factors (EWFF) DIZET [74]. The advantage is that we can, by comparing these programs, check very well the technical precision of the implementation of EW corrections and the interplay of the EW and QED corrections. However, for these comparisons we can draw little knowledge on the uncertainties of the pure EW corrections in DIZET. For this, one may consult the section on ZFITTER in this report. In the process of comparing $\mathcal{KK}$MC and ZFITTER we have found out that the simple semianalytical program $\mathcal{KK}$sem is very useful, because it agrees always with $\mathcal{KK}$MC but is, of course, much faster. The implementation of EW corrections in $\mathcal{KK}$sem is very similar to that in $\mathcal{KK}$MC, that is it uses the same look-up tables of s- and t-dependent EWFFs[18]. We can use $\mathcal{KK}$sem also because in this section we restrict ourselves to the simplest possible cut $v_{\max} = 1 - s'_{\min}/s$ on the invariant mass of the fermion pair, or the propagator-mass, no cut on $\cos\theta$.

5.4.1 The importance of the EW boxes and of running couplings

Let us begin with emphasizing the fact that the character of the electroweak corrections at LEP2 energies changes dramatically with the onset of the so called 'EW-boxes', that is to say box diagrams with the exchange of the W and Z bosons, see Fig. 7. These genuinely quantum-mechanical contributions, which were negligible on Z resonances, are above 2% in the hadronic cross section at the highest LEP2 energies! That is far bigger than the combined LEP2 experimental error, almost as big as typical QED effects. This point is illustrated by Fig. 11 where we plot the cross section from $\mathcal{KK}$sem and ZFITTER with EW boxes switched off and from $\mathcal{KK}$MC in which EW boxes are switched on[19] (IBOXF=1 in DIZET). As we see, at 206 GeV, for the typical Z-exclusive cut $v_{\max} \sim 0.2$, the EW boxes are the biggest for the u-quark, almost 4%, and after averaging over the five quarks[20] they contribute slightly above 2%. For the muon it is about 1%. We have also checked that at 189 GeV the contribution of the EW boxes is a factor 2 smaller, both for quarks and muons. Most probably the effect of EW boxes is slightly smaller for cross sections with the cut on $\cos\theta$.

We would like therefore to stress that the proper implementation of the EW boxes is of paramount importance for the interpretation of the hadronic total cross section and its energy dependence at the LEP2 energies.

On the other hand, Fig. 11 represents also a nice technical cross-check of the implementation of convolution of the QED ISR structure functions with the effective Born cross section in ZFITTER and $\mathcal{KK}$sem together with the use of DIZET for IBOXF=1. In both programs we used the SFs of Ref. [83]

[18] However, the effective Born distribution $d\sigma/d\cos\theta$ is programmed in $\mathcal{KK}$sem independently and slightly differently, using a subprogram from KORALZ and not the Kleiss-Stirling spinors of $\mathcal{KK}$MC.

[19] We could of course switch on EW boxes in ZFITTER and switch them off in $\mathcal{KK}$MC – the plot is just byproduct of one of our several tests.

[20] The discrepancy for b-quark and Z-inclusive cut $v_{\max} \sim 0.9$ is most probably due to simplified implementation of QCD FSR in $\mathcal{KK}$sem

with the $\mathcal{O}(L^3\alpha^3)$ corrections included. We also checked, by playing with the input flags of ZFITTER, that changing from factorized SFs of Ref. [83] to the additive style of Ref. [198] and Ref. [143] (keeping $\mathcal{O}(L^3\alpha^3)$) has very little influence (typically $< 0.01\%$) on the cross section. The same exercise was done at $\sqrt{s} = 189$ GeV and 206 GeV, and (apart from slight discrepancy for the b-quark for the Z-inclusive cut, which seems to be understood) the agreement was always consistently better than 0.2%.

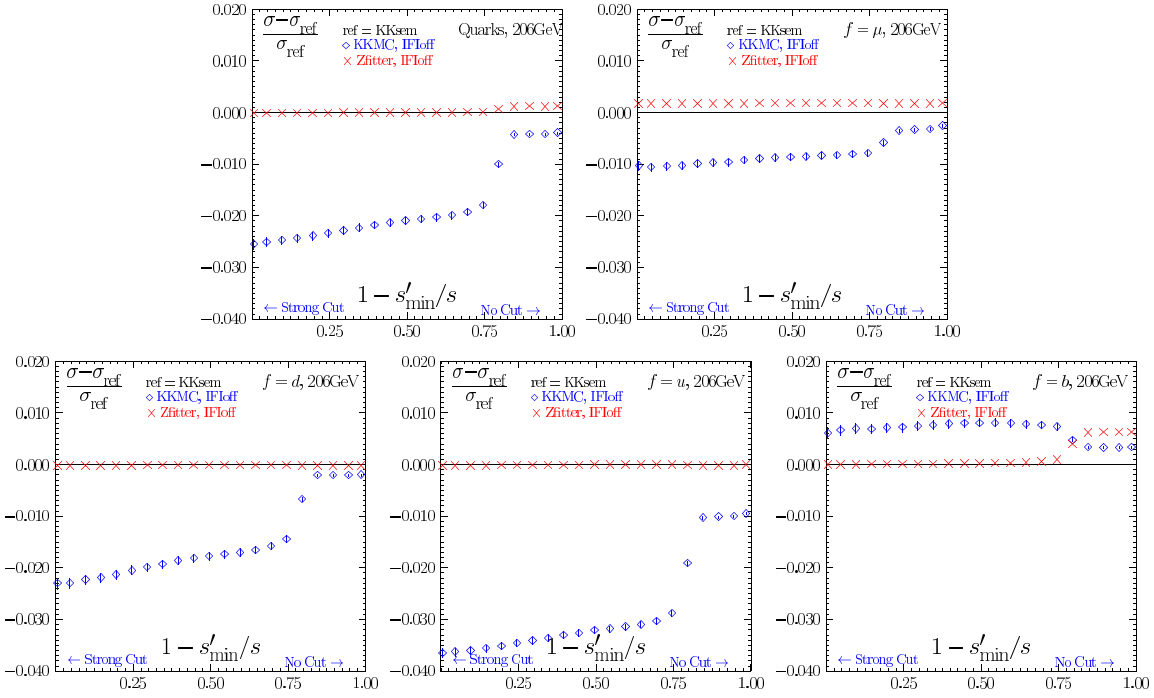

Fig. 11: Electroweak boxes are OFF for ZFITTER and $\mathcal{KK}$sem and ON for $\mathcal{KK}$MC. Cross section from ZFITTER, $\mathcal{KK}$MC and $\mathcal{KK}$sem at 206 GeV for quarks and the muon. The ISR$\otimes$FSR is off. Results are plotted as a function of the cut of the propagator mass $M_{f\bar{f}} = \sqrt{s'}$ with respect to $\mathcal{KK}$sem. No cut on $\cos\theta$. The QED and QCD FSR corrections are included.

5.4.2 All quarks channel by channel and muons, IFI switched off

In the next exercise we switch on EW-boxes and examine the difference between ZFITTER and $\mathcal{KK}$MC for quarks and muons. We keep also $\mathcal{KK}$sem all the time in the game – this has proved to be very useful, because at all stages of our comparisons we could often substitute the comparison among ZFITTER and $\mathcal{KK}$MC by faster comparison among ZFITTER and $\mathcal{KK}$sem, profiting from the fact that the CPU time-consuming comparisons between $\mathcal{KK}$sem and $\mathcal{KK}$MC were already done. The resulting comparison at $\sqrt{s} = 206$ GeV is shown in Fig. 12 and some extract of it also in a numerical form in Table 14. The agreement is very good $< 0.2\%$, for any value of the cut on propagator mass, for each quark, all quarks and the muon (except for the b-quark, Z-inclusive cut, see remarks above). The same kind of agreement we observed for 200 GeV and 189 GeV, see Fig. 13 with the maximum discrepancies for hadrons $< 0.2\%$ and for muons $< 0.3\%$ (a smaller statistical error is needed).

As we have learned during the process of comparisons, the agreement of Fig. 12 was not possible to achieve without setting up properly the user options (flags) of ZFITTER. Flags which were good for LEP1 can not be used at LEP2, in particular one should not use the options for approximate treatment of EW boxes (ZUTHSM interface). One should use instead the ZUATSM interface together with `CONV=2` standing for *running* electroweak couplings.

On the $\mathcal{KK}$MC /$\mathcal{KK}$sem part these problem did not arise, as they use only one method of implementing EW boxes: through s- and t-dependent EWFFs plugged in directly into spin amplitudes, before squaring them.

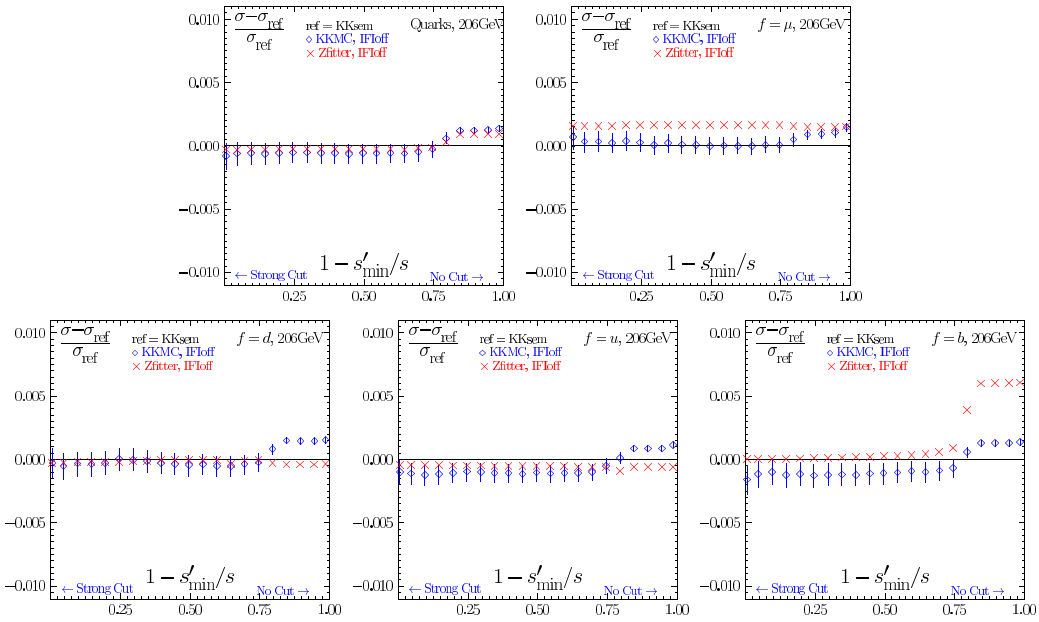

Fig. 12: Total cross-section from ZFITTER, $\mathcal{KK}$MC and $\mathcal{KK}$sem at 206 GeV for quarks and muon. ISR⊗FSR is off. Results plotted as a function of the cut on the propagator mass $M_{prop-} = \sqrt{s'}$ relative to $\mathcal{KK}$sem. (The main result of this section.)

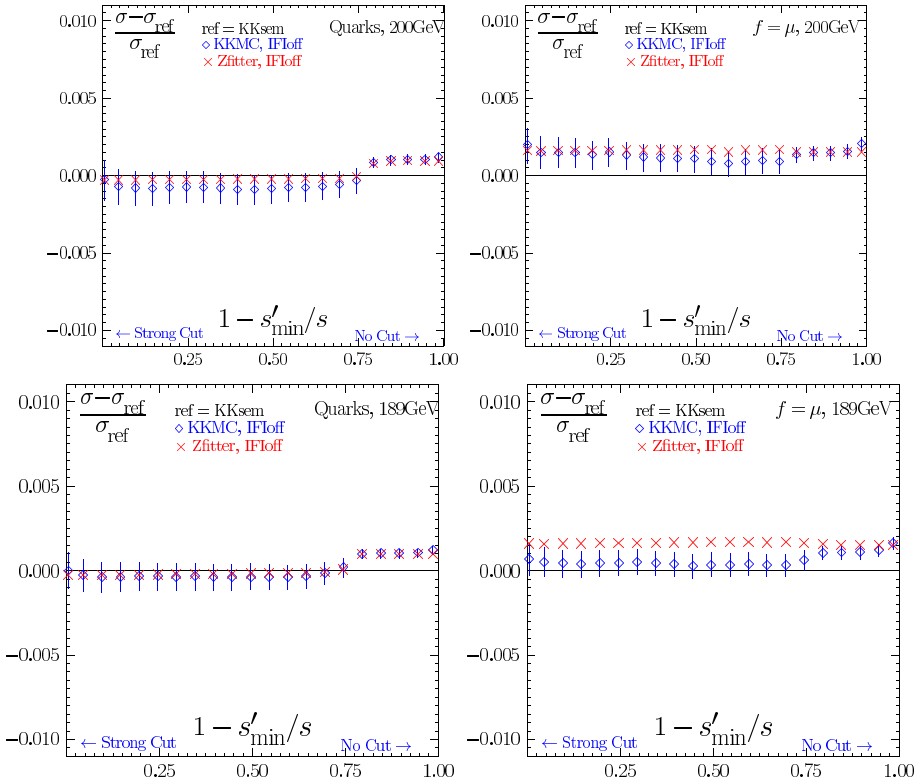

Fig. 13: The same as in Fig. 12 for another $\sqrt{s}$ =189 GeV and 200 GeV.

Table 14: The same results as in Fig. 12, for four values of the cut on the propagator mass, $v_{\max} = 1 - s'_{\min}/s$. The QED and QCD FSR corrections are included in both calculations.

f	(a) $\mathcal{KK}$sem	(b) $\mathcal{O}(\alpha^2)^{\rm intOFF}_{\rm CEEX}$	(c) Zfitter 6.x	(b-a)/a	(c-a)/a
	$\sigma(v_{\max})$[pb], $v_{\max} = 0.10$, 206GeV				
d	2.4763 ± 0.0000	2.4755 ± 0.0024	2.4758 ± 0.0000	-0.0003 ± 0.0010	-0.0002 ± 0.0000
u	4.0358 ± 0.0000	4.0307 ± 0.0032	4.0340 ± 0.0000	-0.0013 ± 0.0008	-0.0004 ± 0.0000
s	2.4763 ± 0.0000	2.4763 ± 0.0024	2.4758 ± 0.0000	0.0000 ± 0.0010	-0.0002 ± 0.0000
c	4.0355 ± 0.0000	4.0346 ± 0.0032	4.0340 ± 0.0000	-0.0002 ± 0.0008	-0.0004 ± 0.0000
b	2.4887 ± 0.0000	2.4862 ± 0.0024	2.4888 ± 0.0000	-0.0010 ± 0.0010	0.0000 ± 0.0000
all	15.5127 ± 0.0000	15.5033 ± 0.0138	15.5083 ± 0.0000	-0.0006 ± 0.0009	-0.0003 ± 0.0000
μ	2.3363 ± 0.0000	2.3370 ± 0.0018	2.3400 ± 0.0000	0.0003 ± 0.0008	0.0016 ± 0.0000
	$\sigma(v_{\max})$[pb], $v_{\max} = 0.20$, 206GeV				
d	2.6991 ± 0.0000	2.6984 ± 0.0025	2.6986 ± 0.0000	-0.0003 ± 0.0009	-0.0002 ± 0.0000
u	4.3887 ± 0.0000	4.3840 ± 0.0033	4.3867 ± 0.0000	-0.0011 ± 0.0008	-0.0004 ± 0.0000
s	2.6991 ± 0.0000	2.6993 ± 0.0025	2.6986 ± 0.0000	0.0000 ± 0.0009	-0.0002 ± 0.0000
c	4.3884 ± 0.0000	4.3872 ± 0.0033	4.3867 ± 0.0000	-0.0003 ± 0.0008	-0.0004 ± 0.0000
b	2.7122 ± 0.0000	2.7090 ± 0.0025	2.7124 ± 0.0000	-0.0012 ± 0.0009	0.0001 ± 0.0000
all	16.8875 ± 0.0000	16.8778 ± 0.0142	16.8831 ± 0.0000	-0.0006 ± 0.0008	-0.0003 ± 0.0000
μ	2.5372 ± 0.0000	2.5381 ± 0.0019	2.5413 ± 0.0000	0.0004 ± 0.0007	0.0016 ± 0.0000
	$\sigma(v_{\max})$[pb], $v_{\max} = 0.70$, 206GeV				
d	3.5101 ± 0.0000	3.5087 ± 0.0027	3.5098 ± 0.0000	-0.0004 ± 0.0008	-0.0001 ± 0.0000
u	5.4587 ± 0.0000	5.4533 ± 0.0035	5.4557 ± 0.0000	-0.0010 ± 0.0006	-0.0005 ± 0.0000
s	3.5100 ± 0.0000	3.5098 ± 0.0027	3.5098 ± 0.0000	-0.0001 ± 0.0008	-0.0001 ± 0.0000
c	5.4581 ± 0.0000	5.4572 ± 0.0035	5.4556 ± 0.0000	-0.0002 ± 0.0006	-0.0005 ± 0.0000
b	3.5169 ± 0.0000	3.5137 ± 0.0027	3.5189 ± 0.0000	-0.0009 ± 0.0008	0.0006 ± 0.0000
all	21.4538 ± 0.0000	21.4427 ± 0.0150	21.4499 ± 0.0000	-0.0005 ± 0.0007	-0.0002 ± 0.0000
μ	3.0802 ± 0.0000	3.0805 ± 0.0020	3.0853 ± 0.0000	0.0001 ± 0.0006	0.0017 ± 0.0000
	$\sigma(v_{\max})$[pb], $v_{\max} = 0.90$, 206GeV				
d	15.5108 ± 0.0000	15.5333 ± 0.0038	15.5050 ± 0.0000	0.0014 ± 0.0002	-0.0004 ± 0.0000
u	15.0845 ± 0.0000	15.0976 ± 0.0042	15.0760 ± 0.0000	0.0009 ± 0.0003	-0.0006 ± 0.0000
s	15.5106 ± 0.0000	15.5324 ± 0.0038	15.5050 ± 0.0000	0.0014 ± 0.0002	-0.0004 ± 0.0000
c	15.0741 ± 0.0000	15.0886 ± 0.0042	15.0740 ± 0.0000	0.0010 ± 0.0003	0.0000 ± 0.0000
b	15.1851 ± 0.0000	15.2043 ± 0.0038	15.2771 ± 0.0000	0.0013 ± 0.0002	0.0061 ± 0.0000
all	76.3651 ± 0.0000	76.4561 ± 0.0198	76.4371 ± 0.0000	0.0012 ± 0.0003	0.0009 ± 0.0000
μ	5.8921 ± 0.0000	5.8975 ± 0.0022	5.9010 ± 0.0000	0.0009 ± 0.0004	0.0015 ± 0.0000

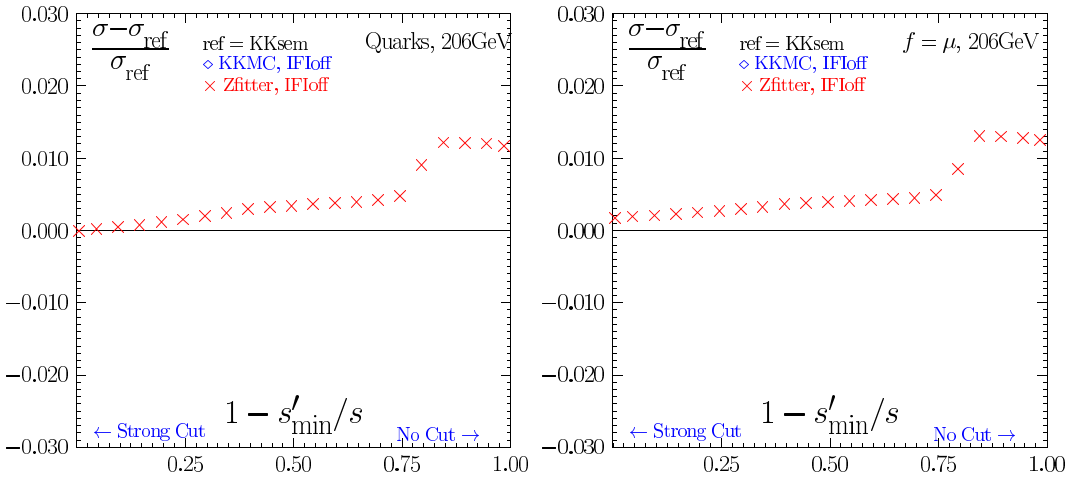

Fig. 14: Illustration of importance of running EWFFs. Plotted is the relative difference of DIZET cross-section with the running of EWFFs switched off and $\mathcal{KK}$sem with the running of EWFFs switched on.

Finally, in Fig. 14, we would like to point out the importance of the running of EWFFs. The effect is at most 0.1% for Z-exclusive cuts, but is very sizeable $\sim$ 1–2% at the Z radiative return! It is a trivial effect but it should not be forgotten. Of course, the running of EWFFs was unimportant at LEP1.

Summarizing, the main result of this section is that of Figs. 12 and 13. It was highly nontrivial to get agreement at the level of $\sim$0.2% of two large codes. These comparisons test strongly the procedures in which pure EW corrections are combined with the QED in both programs and also the reliability of the QED ISR. In particular results of these test do not invalidate the claim of $\mathcal{KK}$MC authors that their program controls ISR at the level of 0.2% for total cross section, both for Z-exclusive and Z-inclusive acceptances. The ISR$\otimes$FSR was excluded from the tests of the present section. They are done in another section of this report dedicated entirely to this type of QED correction.

5.5 Pair effects

Let us concentrate in the present section on another class of corrections which is important for the sub-percent precision tag as demanded by experiments: the *pair corrections.*

Real and virtual secondary fermion pair $f_2\overline{f}_2$ corrections to primary 2-fermion $f_1\overline{f}_1$ final states constitute non-trivial problems, both experimentally and theoretically. The basis of the problems for real pairs is the existence of several classes of Feynman diagrams, all leading to the final state $f_1\overline{f}_1$ $f_2\overline{f}_2$, but not all suitable of being considered as a radiative correction to $f_1\overline{f}_1$ production. The definition of which part of these $f_1\overline{f}_1$ $f_2\overline{f}_2$ processes should be taken as a radiative correction to fermion-pair production is ambiguous. The most useful guidelines for such a definition are therefore its simplicity and generality, and the achievable accuracy of both experimental measurements and theoretical predictions. The precision aims, as discussed earlier in this report, are e.g. for hadrons ($f_1\overline{f}_1$ =qq) of the order 0.2% for the 'exclusive' high s' selection, and 0.1% for the inclusive selection, in order to be negligible with respect to the LEP-combined statistical error of these measurements. This subsection will first discuss basic features of possible 2f+4f signal definitions, identify the most useful choices, and describe their realization in experimental measurements in terms of efficiency determination and background subtraction and their realization in theoretical predictions. Finally a comparison between different choices of signal definitions and different theoretical predictions is performed.

In order to set up a general framework for the analysis of pair corrections we largely follow the approach of Ref. [199]. The key point of the analysis is the separation of pair corrections into two components: *signal* and *background.* We begin by dividing real secondary pair $f_2\overline{f}_2$ contributions to all primary pairs $f_1\overline{f}_1$ except electrons into four groups: (1) Multi-Peripheral **MP**, (2) Initial State Singlet **ISS**, (3) Initial State Non-Singlet **ISNS** and (4) Final State **FS**. We further subdivide groups (3) and (4) into the subgroups **ISNS**$_\gamma$, **ISNS**$_Z$, **FS**$_\gamma$, **FS**$_Z$, where the subscript denotes whether the secondary pair $f_2\overline{f}_2$ is produced via a (virtual) γ or Z boson. If one drops the condition, that for the FS diagrams the primary pair $f_1\overline{f}_1$ has to be that from e^+e^- annihilation, there are in addition two interchanged diagrams which we will denote **SF**$_\gamma$ and **SF**$_Z$, depending again on the boson decaying to $f_2\overline{f}_2$. The group (2) is subdivided into **ISS**$_\gamma$ and **ISS**$_Z$, according to whether the incoming e^+ and e^- exchange a γ or a Z. This nomenclature is summarized in Figs. 15 to 21.

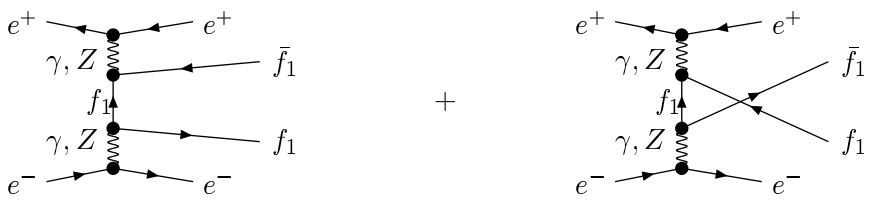

Fig. 15: The multi-peripheral (MP) group of diagrams.

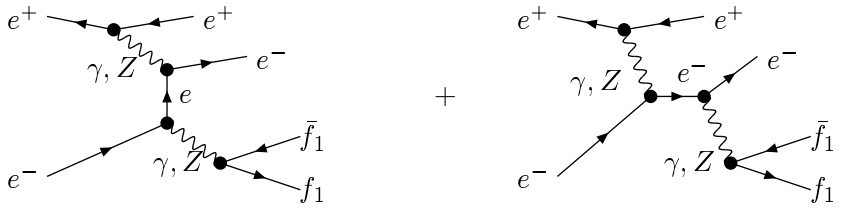

Fig. 16: The eight diagrams of the singlet group ISS_γ and ISS_Z.

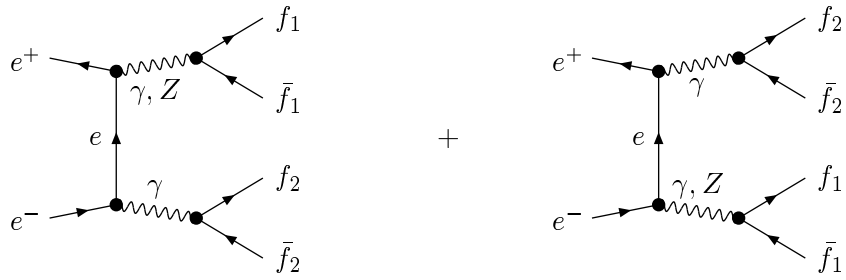

Fig. 17: The subgroup ISNS_γ of the NC08 sub-family of diagrams.

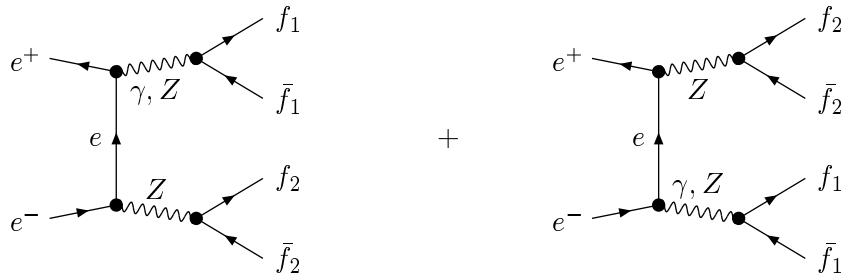

Fig. 18: The subgroup ISNS_Z of the NC08 sub-family of diagrams.

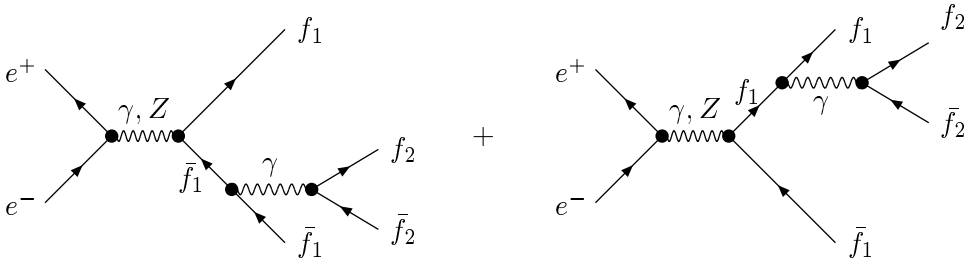

Fig. 19: The four diagrams of subgroup FS_γ belonging to the NC24 process.

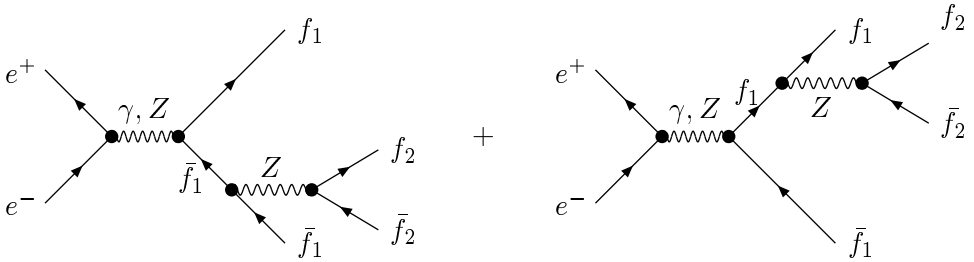

Fig. 20: The four diagrams of subgroup FS_Z belonging to the NC24 process.

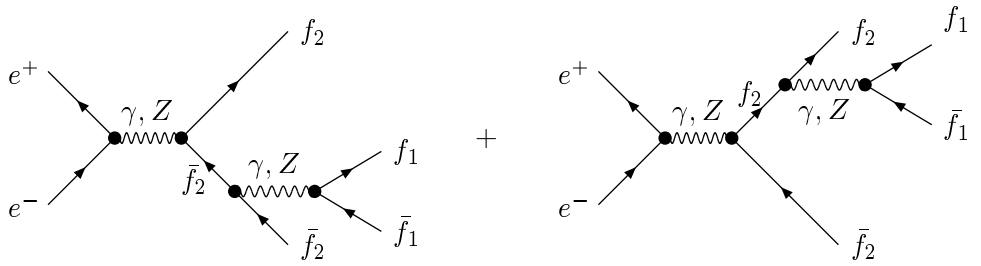

Fig. 21: The eight diagrams of subgroup SF_γ and SF_Z belonging to the NC24 process.

Of course, all of these real pair diagrams come together with their corresponding virtual pairs in vertex corrections. For primary electrons $f_1\bar{f}_1$ = ee similar sets of diagrams can be plotted (not shown here). The main difference from the above diagrams is that the ISNS and FS pairs have now to be attached to both s- and t-channel e^+e^- scattering. The ISNS and FS corrections for t-channel Bhabha scattering are thereby identical to the ISS diagrams in Fig. 16 with the replacement of $f_1\bar{f}_1$ by $f_2\bar{f}_2$. In turn, the singlet ISS diagrams for the t-channel Bhabha process are identical to the MP diagrams in Fig. 15 when the $f\bar{f}$ 1 pair is taken as $e_1^+e_2^-$, and e_1^+ forms the primary pair with the incoming e_1^-. To have the same nomenclature for electrons as for other primary pairs, we keep in the following the terms ISNS, FS and ISS for pair corrections to t-channel Bhabha scattering, even if the corresponding diagrams are identical to the ISS and MP in Figs. 16 and 15, respectively. The pair corrections to the Bhabha process are further discussed in Section 4.7.

Appropriate theoretical calculations for ISNS and ISS pair corrections to primary pairs other than electrons are available in the literature [68, 90, 137, 142, 144] with the precision 0.1% in the LEP2 range [144], matching the required experimental precision. If no cuts are applied on final-state pairs the real+virtual FS contribution can be largely absorbed by evaluating the photonic final-state correction δ_γ using $\alpha_{\rm em}(s)$ instead of $\alpha(0)$, leaving a tiny residual uncertainty of 0.002% of the 2-fermion cross-section at LEP2 energies [181].

Concerning the definition of the 4f signal, there are basically two different approaches

1. **Choosing few (sub)groups of Feynman diagrams as signal definition in such a way that cuts on masses and energies of the secondary $f_2\bar{f}_2$ pairs can be avoided**
   This is a very useful approach for theoretical predictions, since it avoids the calculation of multi-differential cross-sections for the radiated $f_2\bar{f}_2$ pair. It potentially poses problems for experimental measurements since (sub)groups of Feynman diagrams often cannot easily be extracted from full 4-vector four-fermion Monte Carlos like KORALW or GRC4f, and interference of signal and background is possible.

2. **Choosing (nearly) all groups of Feynman diagrams and rejecting the unwanted part of phase space by cuts on masses and/or energies of the radiated $f_2\bar{f}_2$ pair.**
   If the chosen groups match with those of typical 4-fermion generators, this definition is easy to implement in experimental measurements, but can mean considerable calculation and programming work for theoretical predictions.

The discussions in this workshop and in the 2f-LEP2 subgroup of the LEP electroweak working group converged to a proposal for a LEP-wide definition of a 2f+4f signal, which will be detailed below. It is made in such a way that it can nearly equivalently be expressed in both approaches, the definition by diagrams (1), and the definition by cuts (2). Differences between the approaches are below 0.1%, and therefore negligible compared to the experimental accuracy This means that experimentalists could perform a measurement within approach (2), and compare it to a theory prediction with approach (1). The proposal is close to a procedure first used by the OPAL experiment [200], and will be detailed in the following.

5.5.1 2f+4f signal definition by diagrams

The diagram-based choice for a 2f+4f signal definition is

- **DEFINITION 1:** ISNS_γ+FS_γ
  No cuts are applied to the mass of the $\mathrm{f_2\bar{f}_2}$ pair. For the case of ISNS_γ the primary pair is required to pass the cut $s'/s > R_{\rm cut}$, where typical values for $R_{\rm cut}$ at LEP2 are 0.7225 for the 'exclusive' high s' selection and 0.01 for the 'inclusive' selection. The treatment of FS_γ depends on the s' definition. If the s-channel propagator mass is taken $s' = M^2_{\rm prop}$, which is possible only in the absence of initial-final state interference (IFI), no cuts are applied to FS_γ. If one chooses to include IFI in the measurement, one has to define $s' = M^2_{\mathrm{f_1\bar{f}_1}}$, and apply $R_{\rm cut}$ also to FS_γ.

The reasoning for the above choice of diagrams is that the bulk of the phase space of all other diagrams looks kinematically very different from 2-fermion events, and is therefore rejected in most 2-fermion selections. It would make little sense to re-introduce it via efficiency corrections, especially since the modeling of MP and ISS due to poles for forward electrons or positrons is more inaccurate than for other $\mathrm{f_1\bar{f}_1}$ $\mathrm{f_2\bar{f}_2}$ diagrams. In addition MP, ISS (comprising Zee) and $\mathrm{ISNS_Z}$ (comprising ZZ) cover different types of possible new physics contributions, which would hamper the interpretation of 2-fermion cross-section measurements, if they were included in the 2f signal[21].

Predictions for the above signal definition with the definition of $s' = M_{\rm prop-}$ can be obtained easily from (even old versions) of the semianalytical programs ZFITTER and TOPAZ0. For example, in ZFITTER versions up to 5.15 the corresponding full 2f+4f prediction was obtained setting the flags FOT2=3 and INTF=FINR=0. This old pairs treatment is still available in the actual ZFITTER versions using ISPP = -1. For ZFITTER 6.21 onwards the flag setting corresponding to the above definition is INTF = FINR = 0, FSPP = 0, ISPP$\geq$2. In TOPAZ0, version 4.4 the recommended flag setting is ONP=I, for older versions ONP=Y should be used. For both programs the effect of real+virtual pair corrections can be obtained from the difference to flag settings that switch off pairs (ISPP=0 in ZFITTER or ONP=N in TOPAZ0).

After convolution of photon and pair radiation, the s' cut represents a cut on the combined effect of the two. Different s' cuts for photons and pairs would require a rather complicated definition of s'. For the definition $s' = M_{\rm prop-}$ only initial-state photons and pairs have to be modeled. For the definition $s' = M^2_{\mathrm{f_1\bar{f}_1}}$ the FS_γ process is needed explicitly, which is only available from ZFITTER 6.30 onwards, and not available in TOPAZ0. The corresponding flag setting in ZFITTER is INTF=2, FINR=1, FSPP=2 (or 1), and ISPP$\geq$4.

In the diagram-based signal definition there are no pairing ambiguities for four identical fermions, since the pairing is known. The only potential problem remains for the ISNS_γ subprocess $ee \to \gamma^*\gamma^* \to \mathrm{f\bar{f}f'\bar{f}'}$ when both pairs fulfil the s' cut. Such an event is a signal both for a primary pair $\mathrm{f_1\bar{f}_1}$ =$\mathrm{f\bar{f}}$ and $\mathrm{f_1\bar{f}_1}$ =$\mathrm{f'\bar{f}'}$, which is *per se* not a problem. Only if cross-sections of several channels are summed up, like for hadronic final states, can this lead to double counting e.g. the same $\mathrm{u\bar{u}s\bar{s}}$ event could be counted as signal for $\mathrm{f_1\bar{f}_1}$ = $\mathrm{u\bar{u}}$ and $\mathrm{f_1\bar{f}_1}$ = $\mathrm{s\bar{s}}$ in the theory prediction, while it is counted only once by experimental measurements. The amount of such double counting for hadrons depends on the s' cut. Obviously there is no double counting for all $R_{\rm cut} \geq 0.25$ due to phase space. An estimate using fully simulated GRC4f qqqq events shows that at $R_{\rm cut} = 0.01$ the double counting is still below 10^{-4} of the qq cross-section, which makes it truly negligible. Double counting can be fully avoided by imposing an additional cut of $M_{\mathrm{f_1\bar{f}_1}} > M_{\mathrm{f_2\bar{f}_2}}$. It is, however, not possible to apply such a cut in ZFITTER or TOPAZ0, but only in full 4-fermion generators like GRC4f or KORALW.

[21] If an experiment nevertheless chooses to also include ISS_γ in its signal definition, the measurement can be converted to the above definition correcting for the contribution of ISS_γ, which can be obtained from TOPAZ0 [69] by selecting OSING='SP" or from ZFITTER versions 6.21 onwards, calculating the correction from the difference between IPSC=3 and IPSC=0 with flag ISPP=2

5.5.2 2f+4f signal definition by cuts

The cut-based choice for a 4f signal definition is

- **DEFINITION 2: ISNS+FS**, with a cut $M_{\mathrm{f_2\bar{f}_2}} < M_{\max}$
  In this case the meaning of ISNS and FS is ISNS=ISNS$_\gamma$+ISNS$_\mathrm{Z}$ and FS=FS$_\gamma$+FS$_\mathrm{Z}$+SF$_\gamma$+SF$_\mathrm{Z}$. This definition corresponds to using all $\mathrm{f_1\bar{f}_1}$ $\mathrm{f_2\bar{f}_2}$ diagrams with the exception of MP and ISS. Both pairs, if passing the s' cut, can be taken as the primary pair. In order to suppress e.g. the unwanted contribution from ZZ final states, a mass cut on the secondary pair is added. It will be shown below that due to a plateau in the pair cross-section between the $\gamma*$ peak at low $\mathrm{f_2\bar{f}_2}$ masses and the Z peak at high $\mathrm{f_2\bar{f}_2}$ masses, the details of this mass cut don't matter, as long it is stays far enough from the Z peak and large enough not to cut appreciably into the ISNS$_\gamma$ and FS$_\gamma$ processes. Suitable choices for a fixed mass cut are $M_{\max} = 50$–80 GeV, while for a fractional mass cut $M^2_{\mathrm{f_2\bar{f}_2}}/s < P_{\mathrm{cut}}$ e.g. the values $P_{\mathrm{cut}} = 0.10$ and 0.15 are leading to acceptable ranges of $M_{\max} = 51$–65 GeV and 62–80 GeV for the LEP2 centre-of-mass energies between 161 and 206 GeV.

The advantage of summing many diagrams is that experimental measurements are able to use full 4-fermion MC generators which include all these diagrams and their interferences[22].

Making no distinction between the various diagrams in 4-fermion generators and even including the interchanged SF group leaves no choice for the s' definition other than $s' = M^2_{\mathrm{f_1\bar{f}_1}}$. Only events which fulfil both the above cut-based definition and the s' cut are counted as signal.

Concerning the potential double counting problem the same remarks as for the diagram-based definition hold. In contrast to the diagram-based definition, however, questions arise for four identical fermions, since the correct pairing is usually not known (see also the discussion in the footnote of Section 4.15). This effect is still an open problem, since especially the rejection of ZZ events via the cut on $M_{\mathrm{f_2\bar{f}_2}}$ depends on the chosen pairing. For estimating the size of the effect, we have calculated the amount of cut-based real signal pairs using four different pairing algorithms for qqqq events, simulated with GRC4f. The pairing was chosen to maximize or minimize certain masses or mass sums as detailed in Table 15. For high s' events the maximum observed difference between any two algorithms is ranging from $(0.06 \pm 0.03) \times 10^{-3}$ at 189 GeV to $(0.08 \pm 0.04) \times 10^{-3}$ at 206 GeV, whereas for inclusive events these numbers are $(0.4 \pm 0.1) \times 10^{-3}$ at 189 GeV and $(0.8 \pm 0.2) \times 10^{-3}$ at 206 GeV. Taking this difference as an estimate for the effect of wrong pairing, it increases with centre-of-mass energy as expected from the increasing ZZ cross-section, but stays below 1 per mil even for inclusive hadrons at the highest energies. The uncertainty due to pairing ambiguities can in principle be largely reduced by correcting for the difference of a given pairing algorithm to the true pairing, which can be obtained using the weights of the REW99 library [185] for GRC4f events.

As will be shown in the next subsection, for obtaining the correct 2f+4f selection efficiency and the correct background in experimental measurements, it suffices to separate the 4-fermion final states, i.e. the *real* pairs, into two samples, which form signal and background, respectively. Virtual pair corrections are signal, but their size is irrelevant for the experimental measurements in first order. Real pair signal samples with the above definition can be obtained e.g. with GRC4f or KORALW. In contrast, for obtaining a theoretical prediction the sum of *real and virtual* pair corrections are needed. Due to mass cuts on $M_{\mathrm{f_2\bar{f}_2}}$, this is not possible with ZFITTER or TOPAZ0 for the above cut-based signal definition.

[22] Again one could even go for an additional inclusion of ISS$_\gamma$ and ISS$_Z$ diagrams here, which the 4-fermion generators KORALW and GRC4f offer. This question is of no relevance for large R_{cut} values above 0.4 or so, since the ISS contributions are negligible there. For small R_{cut} values of the order 0.01 the ISS contribution is appreciable (some per cent of the 2-f cross-section). While for ISNS and FS+SF the cut on $M_{\mathrm{f_2\bar{f}_2}}$ nearly exclusively selects the ISNS$_\gamma$ and FS$_\gamma$ contributions, this is not obviously the case for ISS. This might lead to non-negligible differences between the cut-based definition above and the corresponding diagram-based definition ISNS$_\gamma$+FS$_\gamma$+ISS$_\gamma$. Since none of the LEP experiments included the ISS (γ^*/Zee) process in their signal definition so far, this question has not been quantitatively addressed in this workshop.

A new version 2.11 of GENTLE/4fan is able to calculate both real and virtual pair corrections with mass cuts, where the flag setting corresponding to our above definition is IPPS=6, IGONLY=3, and $P_{\rm cut} = 0.10$. Another possibility is to add real pair corrections obtained from KORALW (or GRC4f) to the virtual pair corrections, which have recently been implemented in the new version 4.14 of $\mathcal{KK}$MC.

Table 15: Real hadronic pair cross-sections $\mathrm{qqq'q'}$ in pb, and relative corrections in per mil, obtained from GRC4f for the process $\mathrm{e^+e^-} \to$ hadrons at $\sqrt{s} = 189$ GeV and 206 GeV for four different pairing algorithms applied to the case of four identical quarks in the cut-based definition (2).

$\mathrm{qqq'q'}$	$\sigma^{\rm Real}$	$\delta^{\rm Real}$	$\sigma^{\rm Real}$	$\delta^{\rm Real}$
$R_{\rm cut}$	0.7225		0.01	
algorithm	189 GeV			
$\min(M_{\mathrm{f_2\bar{f}_2}})$	0.0159	0.74	0.585	6.07
$\max(M_{\mathrm{f_1\bar{f}_1}} - M_{\mathrm{f_2\bar{f}_2}})$	0.0173	0.80	0.548	5.69
$\max(M_{\mathrm{f_1\bar{f}_1}})$	0.0173	0.80	0.564	5.85
$\max(M_{\mathrm{f_1\bar{f}_1}} + M_{\mathrm{f_2\bar{f}_2}})$	0.0173	0.80	0.589	6.11
algorithm	206 GeV			
$\min(M_{\mathrm{f_2\bar{f}_2}})$	0.0117	0.68	0.568	7.30
$\max(M_{\mathrm{f_1\bar{f}_1}} - M_{\mathrm{f_2\bar{f}_2}})$	0.0130	0.76	0.509	6.54
$\max(M_{\mathrm{f_1\bar{f}_1}})$	0.0130	0.76	0.541	6.95
$\max(M_{\mathrm{f_1\bar{f}_1}} + M_{\mathrm{f_2\bar{f}_2}})$	0.0130	0.76	0.575	7.39

5.5.3 Background subtraction and efficiency determination

The total 2f+4f signal cross-section has the form

$$\sigma = \sigma^{\rm Born} + \sigma^{\rm Virt} + \sigma^{\rm Real} \equiv \sigma^{\rm Born}(1 + \delta^{\rm Virt} + \delta^{\rm Real}), \tag{28}$$

where $\sigma^{\rm Born}$ is the (ISR convoluted) 2-fermion cross-section, $\sigma^{\rm Real}$ is the (ISR convoluted) cross-section with real pair emission, and $\sigma^{\rm Virt}$ is the (negative) correction due to virtual pairs. The effect of including a part of the 4f final states as pair emission correction is twofold. First, obviously only those 4f events which are not counted as 2f+4f signal contribution are to be subtracted as background. (Subtracting wrongly all 4-fermion events as background which pass the 2-fermion selection, can, depending on the s' cut, easily lead to mismeasurements larger than one per cent.) Second, the influence of the real signal pairs on the selection efficiency has to be taken into account. We call in the following

$$\epsilon_{\rm 2f} = \frac{\sigma^{\rm Born}_{\rm vis}}{\sigma^{\rm Born}}, \tag{29}$$

$$\epsilon_{\rm 4f} = \frac{\sigma^{\rm Real}_{\rm vis}}{\sigma^{\rm Real}}, \tag{30}$$

where the subscript 'vis' denotes the part of the cross-section for the respective process which passes all selection cuts. It is a very good approximation to assume that the vertex corrections don't change the selection efficiency, since they lead to the same final state, so that the efficiency for the 'Born+Virt' part of the cross-section is still $\epsilon_{\rm 2f}$. This leads to a total selection efficiency for the 2f+4f process of

$$\epsilon = \frac{(1 + \delta^{\rm Virt})\epsilon_{\rm 2f} + \delta^{\rm Real}\epsilon_{\rm 4f}}{1 + \delta^{\rm Virt} + \delta^{\rm Real}} \tag{31}$$

$$\approx (1 - \delta^{\rm Real} + \delta^{\rm Real}(\delta^{\rm Real} + \delta^{\rm Virt}))\epsilon_{\rm 2f} + (\delta^{\rm Real} - \delta^{\rm Real}(\delta^{\rm Real} + \delta^{\rm Virt}))\epsilon_{\rm 4f} \tag{32}$$

$$\approx (1 - \delta^{\rm Real})\epsilon_{\rm 2f} + \delta^{\rm Real}\epsilon_{\rm 4f}, \tag{33}$$

where the expression has been expanded up to $\mathcal{O}(\delta^2)$ in the second line and to $\mathcal{O}(\delta)$ in the third line. Since $\delta \sim 0.01$ it is fully sufficient to retain the first order in δ, which means that the experimental measurements need only to know the fraction $\delta^{\rm Real}$ of real pair emission, and are completely insensitive to the virtual pair correction $\delta^{\rm Virt}$.

Even more transparently one can write the efficiency correction $\Delta\epsilon = \epsilon - \epsilon_{\rm 2f} = \delta^{\rm Real}(\epsilon_{\rm 4f} - \epsilon_{\rm 2f})$ which means that the efficiency correction is the product of the real pairs fraction and the difference in efficiencies between events with and without pairs. Moreover, if events with very soft or low-mass pairs have identical selection efficiencies to events without pairs, they need not be explicitly modeled, which justifies cutoffs for soft or low-mass pairs in explicit 4-vector MC generation. Such cutoffs modify $\delta^{\rm Real}$ and $\epsilon_{\rm 4f}$ in such a way that the same efficiency correction emerges.

To give a feeling for the size of the effect of pairs on the selection efficiency, we have listed in Table 16 some typical numbers for pair corrections in hadronic and muonic selection efficiencies, obtained from a real pair simulation with the GRC4f generator at $\sqrt{s} = 189$ GeV using the cuts-based signal definition (2) and the hadronic event selection of the OPAL experiment. The effect for the other LEP experiments is of similar size.

Table 16: Efficiency corrections $\Delta\epsilon$ for the selection of hadrons and muon pairs due to pair emission corrections for the OPAL experiment at $\sqrt{s} = 189$ GeV. The meaning of the variables is given in the text.

	$e^+e^- \to$ hadrons		$e^+e^- \to \mu^+\mu^-$	
$R_{\rm cut}$	0.7225	0.01	0.7225	0.01
$\epsilon_{\rm 2f}$	87.9%	87.4%	89.8%	79.1%
$\epsilon_{\rm 4f}$	83.2%	79.7%	86.4%	54.6%
$\delta^{\rm Real}$	0.006	0.022	0.005	0.015
$\Delta\epsilon$	-0.02%	-0.17%	-0.02%	-0.37%

For the high s' selection the small fraction $\delta^{\rm Real}$ and the small difference between the efficiencies $\epsilon_{\rm 4f}$ and $\epsilon_{\rm 2f}$ results in a very small efficiency correction, well below one per mil. Both numbers are larger for the inclusive selections, so that the relative efficiency changes due to pairs for inclusive hadrons is about 2 per mil (-0.17% absolute) and about 5 per mil for muons (-0.37% absolute). Note, that to obtain these efficiency corrections both ISNS and FS real pairs have to be generated explicitly, which is possible e.g. with the GRC4f or KORALW programs.

5.5.4 Pairs in semianalytical and Monte Carlo tools

For most of the programs, the treatment of pair corrections has been described in Section 4 of this report. We summarize here the essential points in a comparison of all programs. The Feynman diagrams included in the programs, and the availability of possible mass cuts are summarized in Table 17. It is obvious that with the existing programs a large variety of signal definitions would in principle be possible, though many of them would be accessible with one program only.

For our diagram-based and cut-based signal definitions we list here the features needed for predictions and measurements of pair corrections.

- Theoretical prediction of diagram-based definition 1:
  Virtual pairs, ISNS_γ, desirably with common photon-pair exponentiation. For all primary pairs, apart from $f_1\bar{f}_1$ = ee, this is available in ZFITTER, TOPAZ0, GENTLE, and in the combination $\mathcal{KK}$MC+KORALW. For $f_1\bar{f}_1$ = ee only LABSMC has virtual and real pairs for s- and t-channel Bhabhas, yet without photon-pair convolution.

- Experimental measurement of diagram-based definition 1:
  Complete event generation of $ISNS_\gamma$ and FS_γ, separable from other diagrams. For all primary pairs this is possible in KORALW or GRC4f.

- Theoretical prediction of cut-based definition 2:
  Virtual pairs and possibility of mass cuts on secondary pairs for ISNS, FS, and SF, desirably with photon-pair convolution. For all primary pairs, apart from $f_1\overline{f}_1$ = ee, this is possible in GENTLE and $\mathcal{KK}$MC+KORALW. For $f_1\overline{f}_1$ = ee no program with these features exists.

- Experimental measurement of cut-based definition 2:
  Complete event generation of ISNS, FS,and SF separable from other diagrams. For all primary pairs this is possible in KORALW or GRC4f.

Obviously, ISS is needed for none of the two signal definitions above. Initial-final state interference (IFI) of pairs is completely negligible for any signal definition. Both are nevertheless listed for completeness in Table 17.

In the following sections we will give a broad variety of numerical results on pair corrections from several programs. The programs will then be compared for the two 4-fermion signal definitions discussed above.

Table 17: Summary of pair corrections available in various programs. For Feynman diagrams the possibility of mass cuts on the secondary pair is indicated by 'mass'. The convolution of photons and pairs in a common exponentiation is listed in the row γ-pair conv. IFI stands for interference of initial- and final-state pairs. Note that for LABSMC the singlet contribution listed under ISS is in fact the multi-peripheral (MP) diagram ee→eeff, and ISNS, FS and SF refer to both s and t-channel Bhabha scattering. The last four rows indicate for which signal definition theoretical predictions (th) are possible, and for which signal definition a full 4-fermion signal and background event sample for experimental measurements (exp) can be obtained. For the 2f+4f signal definitions 'real' means that only real pairs can be calculated, and have to be combined with another program calculating the virtual part 'virt'.

Program							
	ZFITTER	TOPAZ0	$\mathcal{KK}$MC	KORALW	GRC4f	GENTLE	LABSMC
virtual pairs	yes	yes	yes	no	no	yes	yes
$ISNS_\gamma$	yes	yes	no	mass	mass	mass	yes
$ISNS_Z$	no	no	no	mass	mass	mass	no
FS_γ	mass	no	no	mass	mass	mass	yes
FS_Z	no	no	no	mass	mass	mass	no
SF_γ	no	no	no	mass	mass	mass	no
SF_Z	no	no	no	mass	mass	mass	no
ISS_γ	yes	yes	no	mass	mass	no	yes (MP)
ISS_Z	no	no	no	mass	mass	no	no(MP)
IFI	no	no	no	yes	yes	yes	no
γ-pair conv.	yes	yes	no	yes	no	yes	no
definition 1 (th)	yes	yes	virt	real	real	yes	yes
definition 1 (exp)	no	no	no	yes	yes	no	no
definition 2 (th)	no	no	virt	real	real	yes	no
definition 2 (exp)	no	no	no	yes	yes	no	no

5.5.5 *Numerical results and conclusions from GENTLE*

Numerical results obtained with the use of the code GENTLE_4fan v.2.11 [23] are presented in the tables and figures shown below. They contain $\delta_{\rm pairs}$ defined by Eq. (15) in Section 4.15 for two processes: $e^+e^- \to$ muons and $e^+e^- \to$ hadrons for two cuts on invariant mass of the primary pair $R_{\rm cut} = 0.01$ and 0.7225 and three c.m.s. energies: 189, 200 and 206 GeV. The wide range of the cut on invariant mass of the secondary pair was studied, $P_{\rm cut} = 10^{-4} - 1$. Results for several typical selections of groups of Feynman diagrams (IPPS, IGONLY) are shown.

In Tables 18 and Fig. 22 we show $\delta_{\rm pairs}(P_{\rm cut})$ for the process $e^+e^- \to$ muons for two $R_{\rm cut}$ and three c.m.s. energies. We note drastic dependence on $R_{\rm cut}$, moderate energy dependence and plateau-like $P_{\rm cut}$ dependence in cases when Z exchange is not included. Solid lines show $\delta_{\rm pairs}(P_{\rm cut})$ when only ISPP mediated by γ exchange is taken into account. Adding on top of it the FSPP has practically no influence for $R_{\rm cut} = 0.01$ and gives almost constant negative shift for $R_{\rm cut} = 0.7225$. For the latter case $\delta_{\rm pairs}(P_{\rm cut})$ are very flat, practically no $P_{\rm cut}$ dependence is seen. For $R_{\rm cut} = 0.01$, $\delta_{\rm pairs}(P_{\rm cut})$ exhibits some $P_{\rm cut}$ dependence. Allowing Z exchange we observe an interesting phenomenon which we called *Z opening*. It occurs when two cuts allow resonance production of the Z boson. We emphasize that Z opening has nothing to do with Z radiative return (ZRR). As seen from the last Fig. 22 it takes place in the case when the ISR convolution is ignored. Z opening is expected qualitatively, and from the figures we may easily see its quantitative size. Z opening rapidly grows with energy, reaching half a per cent at 206 GeV. Therefore, it is relatively important and one has to bother about cutting of such events. (Blind use of $P_{\rm cut} = 1$ may be dangerous.)

In Fig. 22 we also show by dots ZFITTER v.6.30 results, which are shown only at $P_{\rm cut} = 1$ since ZFITTER doesn't allow for cutting of ISPP. The agreement between GENTLE and ZFITTER is at the level half a per mil for $R_{\rm cut} = 0.7225$ and — one per mil for $R_{\rm cut} = 0.01$. (Note much better agreement for the case when the ISR is ignored.) It is not surprising since GENTLE and ZFITTER exploit very different approach for the ISR convolution. ZFITTER uses fully expanded, order-by-order additive approach (see Section 4.13.1). As far as pairs is concerned this means:

$$\sigma(QED) = \sigma(photonic) + \sigma(pairs\ \mathcal{O}(\alpha^2)) + \sigma(\mathcal{O}(\alpha^3)) + \sigma(\mathcal{O}(\alpha^4)), \tag{34}$$

with the two last terms computed in Ref. [144] in the LLA (Leading Logarithmic Approximation). The term $\sigma(\mathcal{O}(\alpha^3))$ represents the lowest order QED correction to the Born $\mathcal{O}(\alpha^2)$ pair production.

In the framework of the GENTLE-like 'multiplicative' approach one computes a convolution integral from a $4f$ kernel, which takes into account multiple photon emission. So, the 1 per mil or better agreement between GENTLE and ZFITTER is far from being trivial. Given completely different treatments of ISR convolution we may trade the difference, which arises after convolution, for a measure of the theoretical uncertainty which is due to ISR convolution.

One should note that ISR convolution is very important. Even for $R_{\rm cut} = 0.7225$ it reaches 10% while for $R_{\rm cut} = 0.01$ it changes the result by a factor of three. Here, however, the bulk of the effect is due to ZRR which enhances the denominator of Eq. (15) reducing thereby the factor $\delta_{\rm pairs}(P_{\rm cut})$ drastically.

The quantities $\delta_{\rm pairs}(P_{\rm cut})$ for the process $e^+e^- \to$ hadrons are shown in Tables 19 and Fig. 23. They are very similar to the case of the process $e^+e^- \to$ muons behaviour and actually the same discussion applies for them. We note that the size of the effect is nearly two times bigger as compared to the muon case. This is due to the fact that pair emission contributes strongly to the return to the Z, which has a much larger hadronic branching fraction than the mixture of virtual photon and Z in the s-channel propagator at the full centre-of-mass energy. Another funny feature of $\delta_{\rm pairs}(P_{\rm cut})$'s for the process $e^+e^- \to$ hadrons is much better agreement between GENTLE and ZFITTER leading to an impossibility

[23] Accessible from: /afs/cern.ch/user/b/bardindy/public/Gentle2_11
also from the Gentle/Zeuthen homepage: http://www.ifh.de/∼riemann/doc/Gentle/gentle.html

to see the difference in the case if ISR is ignored. Therefore, in this case the difference seen in the first three figures of Fig. 23 is totally due to ISR convolution.

Table 18: GENTLE/4_fan v.2.11. Process $e^+e^- \to \mu^+\mu^-$. `IPPS - IGONLY` rows. Hadronic language.

`ISR convoluted quantities.`

$E = 189\ GeV$, $\delta(P_{cut})$

P_{cut}	0.0001	0.001	0.010	0.100	0.150	contd.	IPPS	IGONLY
	0.1750	0.200	0.225	0.250	0.300	1.00		
$R_{cut} = 0.01$	5.8156	7.7941	9.5154	10.4482	10.6872	10.7325	1 | 2	
						11.7306	ZFITTER	
	5.8156	7.7941	9.5155	10.4606	10.6070	contd.	1 | 3	
	10.6825	10.8080	11.3911	13.5519	13.7479	13.8411		
	5.3732	7.6951	9.5950	10.5609	10.8012	10.8465	5 | 2	
	5.3732	7.6951	9.5952	10.5627	10.8071	10.8617	6 | 2	
						11.9639	ZFITTER	
	5.3732	7.6951	9.5953	10.5744	10.7219	contd.	6 | 3	
	10.7980	10.9241	11.5095	13.6773	13.8740	13.9673		
$R_{cut} = 0.7225$	-1.7323	-1.4773	-1.3747	-1.3717	-1.3717	-1.3717	(1,2)(1,3)	
						-0.9964	ZFITTER	
	-3.2583	-2.7733	-2.5885	-2.5835	-2.5835	-2.5835	(5,2)(6,2)(6,3)	
						-2.0504	ZFITTER	

$E = 200\ GeV$, $\delta(P_{cut})$

P_{cut}	0.0001	0.001	0.010	0.100	0.150	contd.	IPPS	IGONLY
	0.1750	0.200	0.225	0.250	0.300	1.00		
$R_{cut} = 0.01$	5.8989	7.9395	9.6584	10.6105	10.8783	10.9248	1 | 2	
						11.9984	ZFITTER	
	5.8989	7.9395	9.6585	10.6284	10.8053	contd.	1 | 3	
	10.9482	11.6520	14.9003	15.1863	15.2964	15.3783		
	5.4563	7.8469	9.7404	10.7247	10.9939	11.0405	5 | 2	
	5.4563	7.8469	9.7406	10.7266	10.9999	11.0559	6 | 2	
						12.2349	ZFITTER	
	5.4563	7.8469	9.7407	10.7439	10.9223	contd.	6 | 3	
	11.0660	11.7724	15.0308	15.3178	15.4282	15.5103		
$R_{cut} = 0.7225$	-1.7789	-1.5164	-1.4148	-1.4118	-1.4118	-1.4118	(1,2)(1,3)	
						-1.0255	ZFITTER	
	-3.3345	-2.8336	-2.6500	-2.6451	-2.6451	-2.6451	(5,2)(6,2)(6,3)	
						-2.1047	ZFITTER	

$E = 206\ GeV$, $\delta(P_{cut})$

P_{cut}	0.0001	0.001	0.010	0.100	0.150	contd.	IPPS	IGONLY
	0.1750	0.200	0.225	0.250	0.300	1.00		
$R_{cut} = 0.01$	5.9443	8.0187	9.7355	10.6962	10.9785	11.0267	1 | 2	
						12.1390	ZFITTER	
	5.9443	8.0187	9.7356	10.7181	10.9237	contd.	1 | 3	
	11.1712	14.4038	15.6238	15.7834	15.8827	15.9639		
	5.5007	7.9289	9.8181	10.8106	11.0944	11.1426	5 | 2	
	5.5007	7.9289	9.8182	10.8125	11.1005	11.1582	6 | 2	
						12.3771	ZFITTER	
	5.5007	7.9289	9.8184	10.8339	11.0414	contd.	6 | 3	
	11.2902	14.5337	15.7574	15.9174	16.0172	16.0985		
$R_{cut} = 0.7225$	-1.8034	-1.5368	-1.4358	-1.4329	-1.4329	-1.4329	(1,2)(1,3)	
						-1.0401	ZFITTER	
	-3.3753	-2.8657	-2.6828	-2.6779	-2.6779	-2.6779	(5,2)(6,2)(6,3)	
						-2.1323	ZFITTER	

`No ISR convolution.`

$E = 189\ GeV$, $\delta(P_{cut})$

P_{cut}	0.0001	0.001	0.010	0.100	0.150	contd.	IPPS	IGONLY
	0.1750	0.200	0.225	0.250	0.300	0.990		
$R_{cut} = 0.01$	12.5194	16.4786	20.1024	22.2181	22.8271	22.9431	1 | 2	
						23.6269	ZFITTER	
	12.5194	16.4786	20.1027	22.2473	22.6088	contd.	1 | 3	
	22.8021	23.1311	24.7146	30.7067	31.2377	31.4727		
	11.8957	16.3204	20.2167	22.3954	23.0078	23.1240	5 | 2	
	11.8957	16.3205	20.2170	22.3987	23.0195	23.1592	6 | 2	
						23.8601	ZFITTER	
	11.8957	16.3204	20.2172	22.4270	22.7919	contd.	6 | 3	
	22.9865	23.3172	24.9062	30.9168	31.4496	31.6850		
$R_{cut} = 0.7225$	-1.6117	-1.3290	-1.2093	-1.2053	-1.2053	-1.2053	(1,2)(1,3)	
						-0.8076	ZFITTER	
	-3.0406	-2.5043	-2.2892	-2.2826	-2.2826	-2.2826	(5,2)(6,2)(6,3)	
						-1.8755	ZFITTER	

$E = 200\ GeV$, $\delta(P_{cut})$

P_{cut}	0.0001	0.001	0.010	0.100	0.150	contd.	IPPS	IGONLY
	0.1750	0.200	0.225	0.250	0.300	0.990		
$R_{cut} = 0.01$	12.5073	16.5516	20.1372	22.2697	22.9439	23.0634	1 | 2	
						23.7421	ZFITTER	
	12.5074	16.5516	20.1375	22.3113	22.7416	contd.	1 | 3	
	23.0972	24.9021	33.3764	34.1438	34.4484	34.6566		
	11.8747	16.4011	20.2588	22.4548	23.1322	23.2518	5 | 2	
	11.8747	16.4011	20.2591	22.4581	23.1441	23.2873	6 | 2	
						23.9781	ZFITTER	
	11.8747	16.4011	20.2594	22.4993	22.9333	contd.	6 | 3	
	23.2911	25.1027	33.6027	34.3721	34.6776	34.8862		
$R_{cut} = 0.7225$	-1.6566	-1.3655	-1.2469	-1.2430	-1.2430	-1.2430	(1,2)(1,3)	
						-0.8318	ZFITTER	
	-3.1127	-2.5590	-2.3450	-2.3385	-2.3385	-2.3385	(5,2)(6,2)(6,3)	
						-1.8755	ZFITTER	

$E = 206\ GeV$, $\delta(P_{cut})$

P_{cut}	0.0001	0.001	0.010	0.100	0.150	contd.	IPPS	IGONLY
	0.1750	0.200	0.225	0.250	0.300	0.990		
$R_{cut} = 0.01$	12.5145	16.6099	20.1757	22.3187	23.0222	23.1474	1 | 2	
						23.8252	ZFITTER	
	12.5145	16.6099	20.1760	22.3692	22.8621	contd.	1 | 3	
	23.4732	31.6676	34.7997	35.2219	35.4948	35.7042		
	11.8765	16.4632	20.3007	22.5071	23.2141	23.3393	5 | 2	
	11.8765	16.4632	20.3010	22.5104	23.2262	23.3750	6 | 2	
						24.0627	ZFITTER	
	11.8765	16.4632	20.3013	22.5608	23.0581	contd.	6 | 3	
	23.6725	31.8950	35.0364	35.4600	35.7340	35.9437		
$R_{cut} = 0.7225$	-1.6800	-1.3844	-1.2665	-1.2625	-1.2625	-1.2625	(1,2)(1,3)	
						-0.8437	ZFITTER	
	-3.1510	-2.5877	-2.3748	-2.3683	-2.3683	-2.3683	(5,2)(6,2)(6,3)	
						-1.9433	ZFITTER	

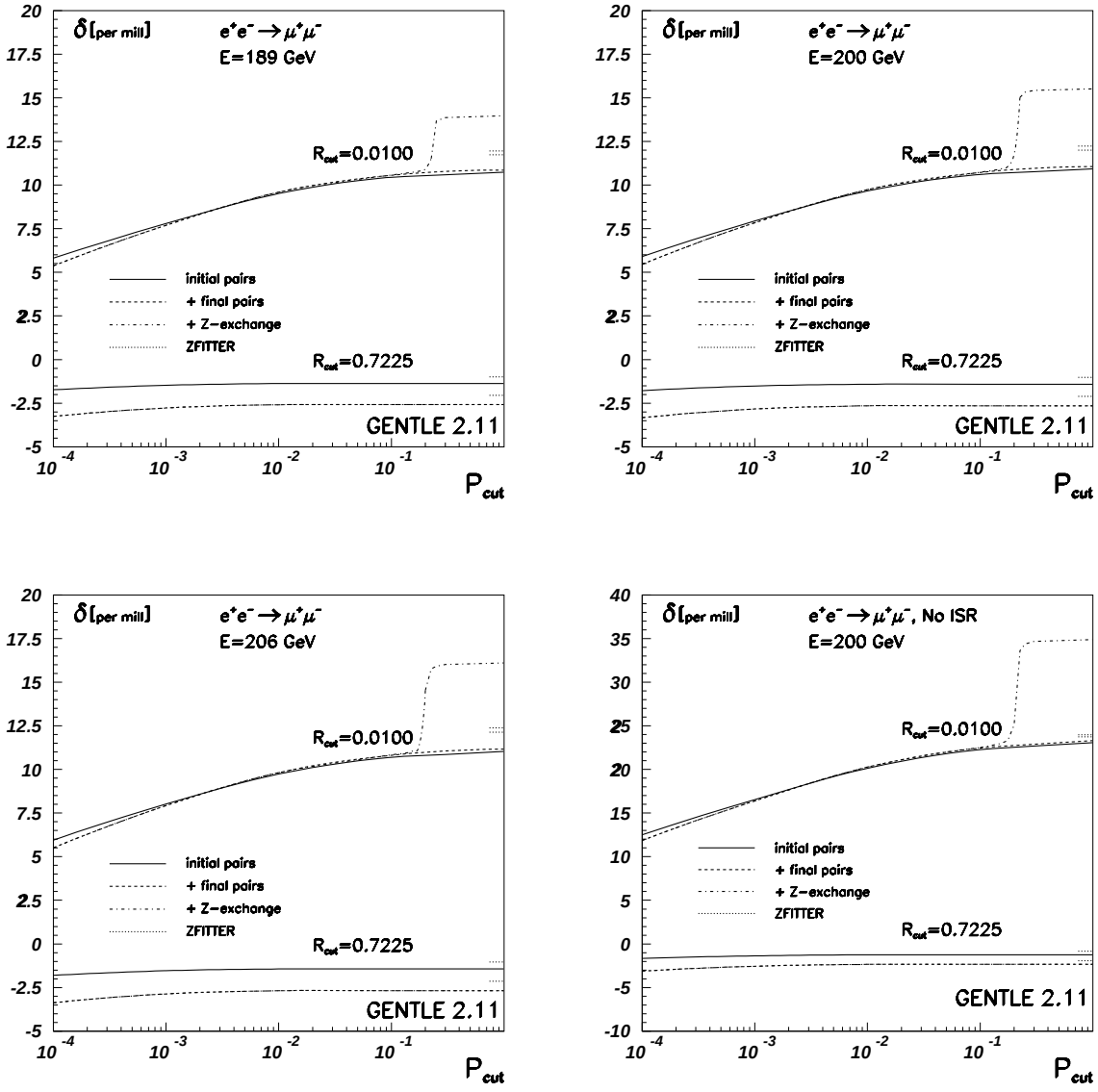

Fig. 22: $\delta_{\rm pairs}(P_{\rm cut})$ for the process $e^+e^- \to$ muons for two $R_{\rm cut}$ and three c.m.s energies. In the fourth figure we show $\delta_{\rm pairs}(P_{\rm cut})$ computed without ISR convolution.

Table 19: GENTLE/4_fan v.2.11. Process $e^+e^- \to$ hadrons. `IPPS - IGONLY` rows. Hadronic language.

ISR convoluted quantities.

$E = 189\ GeV$, $\delta(P_{cut})$

P_{cut}	0.0001	0.001	0.010	0.100	0.150	contd.	IPPS	IGONLY
	0.1750	0.200	0.225	0.250	0.300	1.00		
$R_{cut} = 0.01$	8.3775	10.9339	13.1863	14.4159	14.7064	14.7204	1	2
						15.7608	ZFITTER	
	8.3775	10.9339	13.1865	14.4322	14.6214	contd.	1	3
	14.7171	14.8718	15.5549	17.9327	18.0857	18.1148		
	8.2763	10.9088	13.1993	14.4351	14.7259	14.7399	5	2
	8.2763	10.9088	13.1994	14.4357	14.7276	14.7443	6	2
						15.8172	ZFITTER	
	8.2763	10.9088	13.1997	14.4530	14.6431	contd.	6	3
	14.7392	14.8944	15.5801	17.9650	18.1186	18.1478		
$R_{cut} = 0.7225$	-1.5255	-1.2484	-1.1353	-1.1319	-1.1319	-1.1319	(1,2)(1,3)	
						-0.9179	ZFITTER	
	-1.9329	-1.5916	-1.4556	-1.4516	-1.4516	-1.4516	(5,2)(6,2)(6,3)	
						-1.2044	ZFITTER	

$E = 200\ GeV$, $\delta(P_{cut})$

P_{cut}	0.0001	0.001	0.010	0.100	0.150	contd.	IPPS	IGONLY
	0.1750	0.200	0.225	0.250	0.300	1.00		
$R_{cut} = 0.01$	8.5770	11.2305	13.4972	14.7648	15.1044	15.1198	1	2
						16.2416	ZFITTER	
	8.5770	11.2306	13.4973	14.7887	15.0221	contd.	1	3
	15.2079	16.1080	20.1957	20.5429	20.6588	20.6865		
	8.4766	11.2071	13.5105	14.7840	15.1239	15.1392	5	2
	8.4766	11.2071	13.5105	14.7846	15.1257	15.1438	6	2
						16.2989	ZFITTER	
	8.4766	11.2071	13.5108	14.8099	15.0443	contd.	6	3
	15.2309	16.1338	20.2315	20.5795	20.6958	20.7236		
$R_{cut} = 0.7225$	-1.5804	-1.2971	-1.1862	-1.1829	-1.1829	-1.1829	(1,2)(1,3)	
						-0.9545	ZFITTER	
	-1.9996	-1.6491	-1.5151	-1.5112	-1.5112	-1.5112	(5,2)(6,2)(6,3)	
						-1.2492	ZFITTER	

$E = 206\ GeV$, $\delta(P_{cut})$

P_{cut}	0.0001	0.001	0.010	0.100	0.150	contd.	IPPS	IGONLY
	0.1750	0.200	0.225	0.250	0.300	1.00		
$R_{cut} = 0.01$	8.6811	11.3870	13.6588	14.9441	15.3084	15.3267	1	2
						16.4897	ZFITTER	
	8.6811	11.3870	13.6590	14.9735	15.2478	contd.	1	3
	15.5732	19.7728	21.3411	21.5347	21.6530	21.6851		
	8.5810	11.3643	13.6721	14.9631	15.3277	15.3459	5	2
	8.5810	11.3643	13.6722	14.9636	15.3295	15.3505	6	2
						16.5474	ZFITTER	
	8.5810	11.3643	13.6725	14.9946	15.2703	contd.	6	3
	15.5970	19.8076	21.3796	21.5734	21.6924	21.7246		
$R_{cut} = 0.7225$	-1.6087	-1.3216	-1.2118	-1.2085	-1.2085	-1.2085	(1,2)(1,3)	
						-0.9722	ZFITTER	
	-2.0340	-1.6783	-1.5452	-1.5414	-1.5414	-1.5414	(5,2)(6,2)(6,3)	
						-1.2711	ZFITTER	

No ISR convolution.

$E = 189\ GeV$, $\delta(P_{cut})$

P_{cut}	0.0001	0.001	0.010	0.100	0.150	contd.	IPPS	IGONLY
	0.1750	0.200	0.225	0.250	0.300	1.00		
$R_{cut} = 0.01$	33.2486	42.5376	51.2066	56.3515	57.7553	57.8219	1	2
						57.7690	ZFITTER	
	33.2486	42.5376	51.2073	56.4227	57.2975	contd.	1	3
	57.7612	58.5352	62.1302	75.1478	76.0152	76.1520		
	33.0615	42.4798	51.2250	56.3876	57.7924	57.8590	5	2
	33.0615	42.4798	51.2252	56.3894	57.7988	57.8780	6	2
						57.8345	ZFITTER	
	33.0615	42.4798	51.2263	56.4652	57.3445	contd.	6	3
	57.8094	58.5864	62.1939	75.2450	76.1156	76.2530		
$R_{cut} = 0.7225$	-1.3856	-1.0766	-0.9440	-0.9394	-0.9394	-0.9394	(1,2)(1,3)	
						-0.7095	ZFITTER	
	-1.7690	-1.3889	-1.2294	-1.2241	-1.2241	-1.2241	(5,2)(6,2)(6,3)	
						-0.9957	ZFITTER	

$E = 200\ GeV$, $\delta(P_{cut})$

P_{cut}	0.0001	0.001	0.010	0.100	0.150	contd.	IPPS	IGONLY
	0.1750	0.200	0.225	0.250	0.300	1.00		
$R_{cut} = 0.01$	33.8736	43.5229	52.2574	57.5531	59.1834	59.2584	1	2
						59.1258	ZFITTER	
	33.8736	43.5229	52.2582	57.6572	58.7285	contd.	1	3
	59.6082	64.0254	84.5451	86.3575	87.0043	87.1394		
	33.6820	43.4663	52.2776	57.5912	59.2224	59.2975	5	2
	33.6820	43.4663	52.2778	57.5930	59.2291	59.3171	6	2
						59.1926	ZFITTER	
	33.6820	43.4663	52.2790	57.7031	58.7794	contd.	6	3
	59.6628	64.0929	84.6602	86.4765	87.1252	87.2609		
$R_{cut} = 0.7225$	-1.4406	-1.1251	-0.9951	-0.9905	-0.9905	-0.9905	(1,2)(1,3)	
						-0.7478	ZFITTER	
	-1.8349	-1.4451	-1.2881	-1.2828	-1.2828	-1.2828	(5,2)(6,2)(6,3)	
						-1.0420	ZFITTER	

$E = 206\ GeV$, $\delta(P_{cut})$

P_{cut}	0.0001	0.001	0.010	0.100	0.150	contd.	IPPS	IGONLY
	0.1750	0.200	0.225	0.250	0.300	1.00		
$R_{cut} = 0.01$	34.2037	44.0515	52.8127	58.1865	59.9220	60.0137	1	2
						59.8426	ZFITTER	
	34.2037	44.0515	52.8134	58.3142	59.5569	contd.	1	3
	61.0914	81.4962	89.2448	90.2678	90.8890	91.0531		
	34.0095	43.9954	52.8335	58.2254	59.9618	60.0535	5	2
	34.0095	43.9955	52.8337	58.2272	59.9686	60.0735	6	2
						59.9101	ZFITTER	
	34.0095	43.9955	52.8352	58.3618	59.6105	contd.	6	3
	61.1509	81.6079	89.3740	90.3992	91.0227	91.1875		
$R_{cut} = 0.7225$	-1.4687	-1.1492	-1.0204	-1.0159	-1.0159	-1.0159	(1,2)(1,3)	
						-0.7660	ZFITTER	
	-1.8687	-1.4733	-1.3175	-1.3122	-1.3122	-1.3122	(5,2)(6,2)(6,3)	
						-1.0643	ZFITTER	

The eight Tables 20–21 contain the partial contributions to $\delta_{\rm pairs}$, i.e. separately 20 channels for five primary $\otimes$ four secondary pairs for the process $e^+e^- \to$ hadrons: $d, u, s, c, b \ \otimes$ hadrons, e, μ, τ, for IPPS=5, IGONLY=2 – $[E_{\rm cm} = 189,\ 206\ {\rm GeV}] \otimes [P_{\rm cut} = 1.0,\ 0.7225]$;
for IPPS=6, IGONLY=3 – $[E_{\rm cm} = 189,\ 206\ {\rm GeV}] \otimes [P_{\rm cut} = 0.1,\ 0.7225]$.
The difference between two sets with IPPS=5, IGONLY=2 and IPPS=6, IGONLY=3 is due to $P_{\rm cut}$, which is small owing to the plateau-like dependence, and due to Z exchange, which is also small since Z doesn't open yet for a $P_{\rm cut}$ at 0.10.

Finally, two Tables 22 contain four partial contributions to $\delta_{\rm pairs}$ for the process $e^+e^- \to$ muons for the same set of input parameters. However, we show here both 'ISR off' and 'ISR on' cases and only IPPS=5, IGONLY=2 selection. The 'ISR on' is similar to the process $e^+e^- \to$ hadrons properties and the same discussion applies in this case.

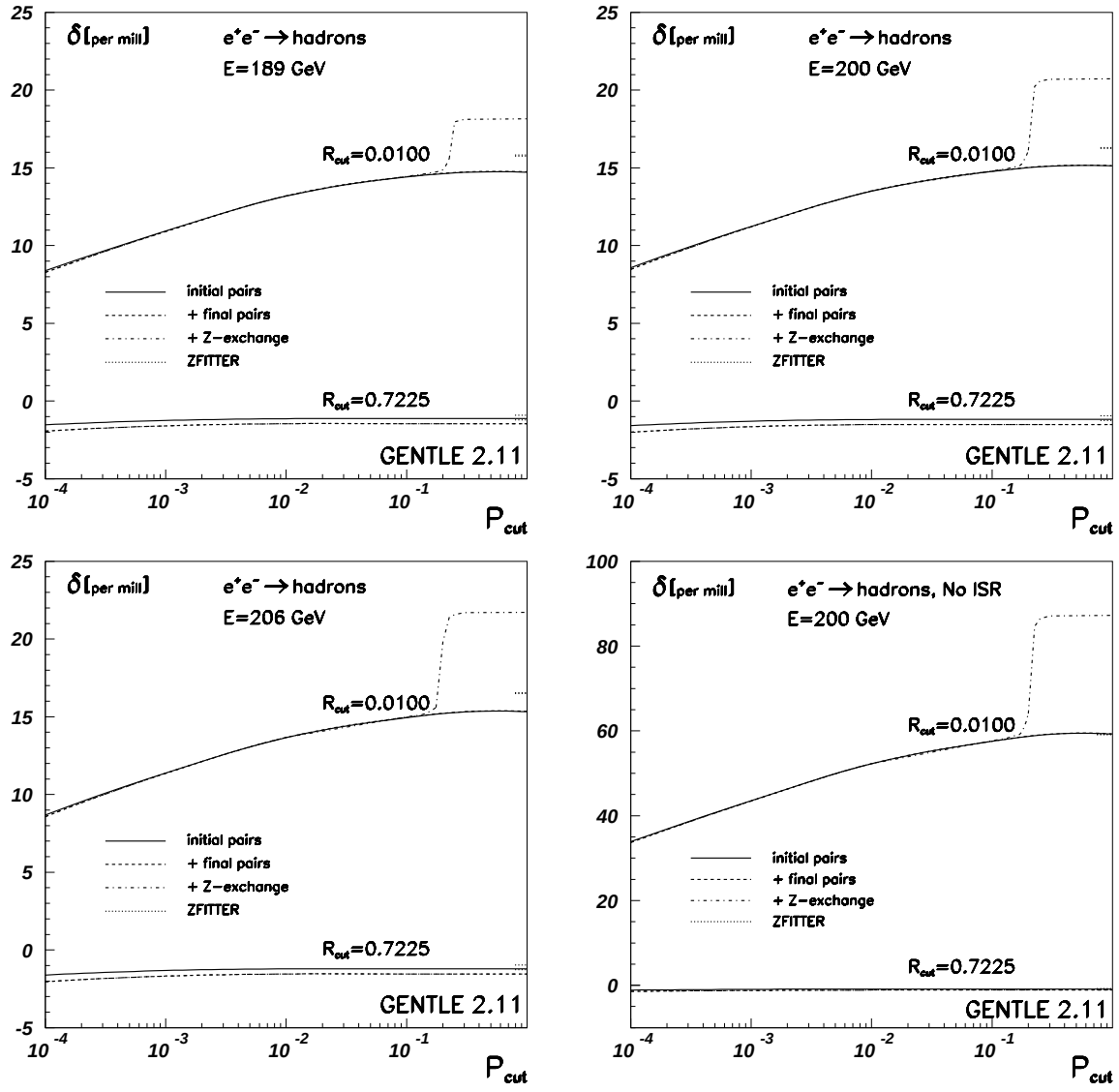

Fig. 23: $\delta_{\rm pairs}(P_{\rm cut})$ for the process $e^+e^- \to$ hadrons for two $R_{\rm cut}$ and three c.m.s energies. In the fourth figure we show $\delta_{\rm pairs}(P_{\rm cut})$ computed without ISR convolution.

Table 20: LEP2: GENTLE_4fan v.2.11, $e^+e^- \to$ hadrons. Partial contributions. I1-primary pair, I2-secondary pair. I1,I2 $= \ 0-hadrons,\ 1-e,\ 2-\mu,\ 3-\tau,\ 4-d,\ 5-u,\ 6-s,\ 7-c,\ 8-b$. Cross-sections in pb, δ's in per mil. The parameters (IPPS,IGONLY)=(5,2) correspond to the diagram-based signal definition with $s' = M^2_{\rm inv}$.

$E = 189\ GeV$, $R_{cut} = 0.01$, $P_{cut} = 1.0$, IPPS=5, IGONLY=2

I1	I2	$\sigma^{\rm Born}$	$\sigma^{\rm Real}$	$\sigma^{\rm Virt}_{\rm ISR}$	$\sigma^{\rm Virt}_{\rm FSR}$	$\delta^{\rm Real}$	$\delta^{\rm Virt}_{\rm ISR}$	$\delta^{\rm Virt}_{\rm FSR}$	$\delta^{\rm total}$
4	0	19.42884	0.12580	-0.01332	-0.00148	6.4748	-0.6857	-0.0762	5.7129
5	0	19.03515	0.11305	-0.01375	-0.00611	5.9391	-0.7223	-0.3210	4.8958
6	0	19.42884	0.12579	-0.01332	-0.00148	6.4746	-0.6857	-0.0762	5.7127
7	0	19.03515	0.11268	-0.01375	-0.00611	5.9197	-0.7223	-0.3210	4.8764
8	0	19.42884	0.12549	-0.01332	-0.00148	6.4587	-0.6857	-0.0762	5.6968
4	1	19.42884	0.20001	-0.05562	-0.00572	10.2945	-2.8628	-0.2943	7.1374
5	1	19.03515	0.19311	-0.05550	-0.02316	10.1447	-2.9156	-1.2166	6.0125
6	1	19.42884	0.19968	-0.05562	-0.00539	10.2776	-2.8628	-0.2772	7.1376
7	1	19.03515	0.18709	-0.05550	-0.01708	9.8284	-2.9156	-0.8975	6.0154
8	1	19.42884	0.19752	-0.05562	-0.00321	10.1665	-2.8628	-0.1653	7.1383
4	2	19.42884	0.04907	-0.00670	-0.00074	2.5254	-0.3447	-0.0383	2.1424
5	2	19.03515	0.04465	-0.00683	-0.00304	2.3454	-0.3589	-0.1595	1.8269
6	2	19.42884	0.04906	-0.00670	-0.00073	2.5252	-0.3447	-0.0375	2.1430
7	2	19.03515	0.04439	-0.00683	-0.00277	2.3322	-0.3589	-0.1453	1.8280
8	2	19.42884	0.04888	-0.00670	-0.00055	2.5161	-0.3447	-0.0286	2.1428
4	3	19.42884	0.01387	-0.00057	-0.00006	0.7141	-0.0296	-0.0033	0.6812
5	3	19.03515	0.01213	-0.00063	-0.00028	0.6374	-0.0332	-0.0147	0.5895
6	3	19.42884	0.01387	-0.00057	-0.00006	0.7141	-0.0296	-0.0033	0.6812
7	3	19.03515	0.01213	-0.00063	-0.00028	0.6372	-0.0332	-0.0147	0.5893
8	3	19.42884	0.01387	-0.00057	-0.00005	0.7137	-0.0296	-0.0025	0.6816
total		96.35682	1.88215	-0.38207	-0.07979	19.5331	-3.9652	-0.8281	14.7399

$E = 189\ GeV$, $R_{cut} = 0.7225$, $P_{cut} = 1.0$, IPPS=5, IGONLY=2

I1	I2	$\sigma^{\rm Born}$	$\sigma^{\rm Real}$	$\sigma^{\rm Virt}_{\rm ISR}$	$\sigma^{\rm Virt}_{\rm FSR}$	$\delta^{\rm Real}$	$\delta^{\rm Virt}_{\rm ISR}$	$\delta^{\rm Virt}_{\rm FSR}$	$\delta^{\rm total}$
4	0	3.50115	0.00262	-0.00349	-0.00039	0.7495	-0.9981	-0.1109	-0.3595
5	0	5.53081	0.00492	-0.00552	-0.00245	0.8903	-0.9985	-0.4438	-0.5519
6	0	3.50115	0.00262	-0.00349	-0.00039	0.7495	-0.9981	-0.1109	-0.3595
7	0	5.53081	0.00491	-0.00552	-0.00245	0.8872	-0.9985	-0.4438	-0.5550
8	0	3.50115	0.00261	-0.00349	-0.00039	0.7451	-0.9981	-0.1109	-0.3639
4	1	3.50115	0.01081	-0.01172	-0.00122	3.0881	-3.3484	-0.3482	-0.6085
5	1	5.53081	0.02090	-0.01852	-0.00779	3.7792	-3.3489	-1.4092	-0.9790
6	1	3.50115	0.01077	-0.01172	-0.00116	3.0773	-3.3484	-0.3311	-0.6022
7	1	5.53081	0.01968	-0.01852	-0.00603	3.5579	-3.3489	-1.0901	-0.8812
8	1	3.50115	0.01049	-0.01172	-0.00077	2.9949	-3.3484	-0.2193	-0.5728
4	2	3.50115	0.00131	-0.00164	-0.00018	0.3732	-0.4692	-0.0521	-0.1481
5	2	5.53081	0.00247	-0.00260	-0.00115	0.4468	-0.4693	-0.2086	-0.2311
6	2	3.50115	0.00131	-0.00164	-0.00018	0.3732	-0.4692	-0.0513	-0.1474
7	2	5.53081	0.00246	-0.00260	-0.00107	0.4439	-0.4693	-0.1944	-0.2198
8	2	3.50115	0.00130	-0.00164	-0.00015	0.3700	-0.4692	-0.0424	-0.1416
4	3	3.50115	0.00012	-0.00020	-0.00002	0.0332	-0.0581	-0.0065	-0.0313
5	3	5.53081	0.00021	-0.00032	-0.00014	0.0380	-0.0581	-0.0258	-0.0459
6	3	3.50115	0.00012	-0.00020	-0.00002	0.0332	-0.0581	-0.0065	-0.0313
7	3	5.53081	0.00021	-0.00032	-0.00014	0.0380	-0.0581	-0.0258	-0.0460
8	3	3.50115	0.00012	-0.00020	-0.00002	0.0332	-0.0581	-0.0057	-0.0306
total		21.56506	0.09994	-0.10512	-0.02613	4.6346	-4.8743	-1.2118	-1.4516

$E = 206\ GeV$, $R_{cut} = 0.01$, $P_{cut} = 1.0$, IPPS=5, IGONLY=2

I1	I2	$\sigma^{\rm Born}$	$\sigma^{\rm Real}$	$\sigma^{\rm Virt}_{\rm ISR}$	$\sigma^{\rm Virt}_{\rm FSR}$	$\delta^{\rm Real}$	$\delta^{\rm Virt}_{\rm ISR}$	$\delta^{\rm Virt}_{\rm FSR}$	$\delta^{\rm total}$
4	0	15.62789	0.10691	-0.01087	-0.00121	6.8407	-0.6955	-0.0773	6.0679
5	0	15.46305	0.09625	-0.01147	-0.00510	6.2248	-0.7420	-0.3298	5.1531
6	0	15.62789	0.10690	-0.01087	-0.00121	6.8405	-0.6955	-0.0773	6.0677
7	0	15.46305	0.09596	-0.01147	-0.00510	6.2056	-0.7420	-0.3298	5.1338
8	0	15.62789	0.10666	-0.01087	-0.00121	6.8247	-0.6955	-0.0773	6.0520
4	1	15.62789	0.16394	-0.04496	-0.00462	10.4900	-2.8766	-0.2958	7.3175
5	1	15.46305	0.15910	-0.04552	-0.01901	10.2889	-2.9440	-1.2293	6.1156
6	1	15.62789	0.16367	-0.04496	-0.00436	10.4731	-2.8766	-0.2787	7.3177
7	1	15.46305	0.15421	-0.04552	-0.01407	9.9729	-2.9440	-0.9101	6.1188
8	1	15.62789	0.16194	-0.04496	-0.00261	10.3621	-2.8766	-0.1669	7.3186
4	2	15.62789	0.04115	-0.00545	-0.00061	2.6329	-0.3485	-0.0387	2.2457
5	2	15.46305	0.03755	-0.00567	-0.00252	2.4284	-0.3666	-0.1629	1.8989
6	2	15.62789	0.04114	-0.00545	-0.00059	2.6327	-0.3485	-0.0379	2.2463
7	2	15.46305	0.03735	-0.00567	-0.00230	2.4152	-0.3666	-0.1487	1.9000
8	2	15.62789	0.04100	-0.00545	-0.00045	2.6236	-0.3485	-0.0290	2.2461
4	3	15.62789	0.01213	-0.00048	-0.00005	0.7760	-0.0306	-0.0034	0.7420
5	3	15.46305	0.01061	-0.00054	-0.00024	0.6862	-0.0351	-0.0156	0.6355
6	3	15.62789	0.01213	-0.00048	-0.00005	0.7760	-0.0306	-0.0034	0.7420
7	3	15.46305	0.01061	-0.00054	-0.00024	0.6860	-0.0351	-0.0156	0.6353
8	3	15.62789	0.01212	-0.00048	-0.00004	0.7756	-0.0306	-0.0026	0.7424
total		77.80978	1.57131	-0.31166	-0.06559	20.1943	-4.0054	-0.8429	15.3459

$E = 206\ GeV$, $R_{cut} = 0.7225$, $P_{cut} = 1.0$, IPPS=5, IGONLY=2

I1	I2	$\sigma^{\rm Born}$	$\sigma^{\rm Real}$	$\sigma^{\rm Virt}_{\rm ISR}$	$\sigma^{\rm Virt}_{\rm FSR}$	$\delta^{\rm Real}$	$\delta^{\rm Virt}_{\rm ISR}$	$\delta^{\rm Virt}_{\rm FSR}$	$\delta^{\rm total}$
4	0	2.74284	0.00215	-0.00289	-0.00032	0.7830	-1.0543	-0.1171	-0.3884
5	0	4.49374	0.00422	-0.00474	-0.00211	0.9381	-1.0546	-0.4687	-0.5852
6	0	2.74284	0.00215	-0.00289	-0.00032	0.7830	-1.0543	-0.1171	-0.3884
7	0	4.49374	0.00420	-0.00474	-0.00211	0.9350	-1.0546	-0.4687	-0.5883
8	0	2.74284	0.00214	-0.00289	-0.00032	0.7786	-1.0543	-0.1171	-0.3928
4	1	2.74284	0.00860	-0.00940	-0.00098	3.1356	-3.4269	-0.3570	-0.6482
5	1	4.49374	0.01732	-0.01540	-0.00649	3.8553	-3.4273	-1.4441	-1.0161
6	1	2.74284	0.00857	-0.00940	-0.00093	3.1248	-3.4269	-0.3399	-0.6419
7	1	4.49374	0.01633	-0.01540	-0.00506	3.6337	-3.4273	-1.1249	-0.9186
8	1	2.74284	0.00834	-0.00940	-0.00063	3.0423	-3.4269	-0.2280	-0.6126
4	2	2.74284	0.00106	-0.00135	-0.00015	0.3867	-0.4907	-0.0545	-0.1586
5	2	4.49374	0.00210	-0.00221	-0.00098	0.4666	-0.4909	-0.2182	-0.2424
6	2	2.74284	0.00106	-0.00135	-0.00015	0.3866	-0.4907	-0.0537	-0.1578
7	2	4.49374	0.00208	-0.00221	-0.00092	0.4637	-0.4909	-0.2039	-0.2311
8	2	2.74284	0.00105	-0.00135	-0.00012	0.3835	-0.4907	-0.0448	-0.1521
4	3	2.74284	0.00010	-0.00017	-0.00002	0.0364	-0.0638	-0.0071	-0.0345
5	3	4.49374	0.00019	-0.00029	-0.00013	0.0422	-0.0638	-0.0284	-0.0500
6	3	2.74284	0.00010	-0.00017	-0.00002	0.0364	-0.0638	-0.0071	-0.0345
7	3	4.49374	0.00019	-0.00029	-0.00013	0.0422	-0.0638	-0.0284	-0.0500
8	3	2.74284	0.00010	-0.00017	-0.00002	0.0364	-0.0638	-0.0063	-0.0337
total		17.21602	0.08205	-0.08670	-0.02189	4.7659	-5.0361	-1.2712	-1.5414

Table 21: LEP2: GENTLE_4fan v.2.11, $e^+e^- \to$ hadrons. Partial contributions. I1-primary pair, I2-secondary pair. I1,I2 = $0-hadrons,\ 1-e,\ 2-\mu,\ 3-\tau,\ 4-d,\ 5-u,\ 6-s,\ 7-c,\ 8-b$. Cross-sections in pb, δ's in per mil. The parameters (IPPS,IGONLY)=(6,3) together with $P_{\rm cut} = 0.10$ correspond to the cut-based signal definition.

$E = 189\ GeV$, $R_{cut} = 0.01$, $P_{cut} = 0.1$, IPPS=6, IGONLY=3

I1	I2	$\sigma^{\rm Born}$	$\sigma^{\rm Real}$	$\sigma^{\rm Virt}_{\rm ISR}$	$\sigma^{\rm Virt}_{\rm FSR}$	$\delta^{\rm Real}$	$\delta^{\rm Virt}_{\rm ISR}$	$\delta^{\rm Virt}_{\rm FSR}$	$\delta^{\rm total}$
4	0	19.42884	0.12204	-0.01332	-0.00148	6.2814	-0.6857	-0.0762	5.5196
5	0	19.03515	0.10954	-0.01375	-0.00611	5.7547	-0.7223	-0.3210	4.7113
6	0	19.42884	0.12204	-0.01332	-0.00148	6.2812	-0.6857	-0.0762	5.5194
7	0	19.03515	0.10917	-0.01375	-0.00611	5.7353	-0.7223	-0.3210	4.6919
8	0	19.42884	0.12173	-0.01332	-0.00148	6.2654	-0.6857	-0.0762	5.5035
4	1	19.42884	0.19928	-0.05562	-0.00572	10.2568	-2.8628	-0.2943	7.0997
5	1	19.03515	0.19242	-0.05550	-0.02316	10.1085	-2.9156	-1.2166	5.9764
6	1	19.42884	0.19895	-0.05562	-0.00539	10.2399	-2.8628	-0.2772	7.0098
7	1	19.03515	0.18640	-0.05550	-0.01708	9.7923	-2.9156	-0.8975	5.9792
8	1	19.42884	0.19679	-0.05562	-0.00321	10.1287	-2.8628	-0.1653	7.1006
4	2	19.42884	0.04835	-0.00670	-0.00074	2.4885	-0.3447	-0.0383	2.1055
5	2	19.03515	0.04397	-0.00683	-0.00304	2.3099	-0.3589	-0.1595	1.7915
6	2	19.42884	0.04834	-0.00670	-0.00073	2.4883	-0.3447	-0.0375	2.1061
7	2	19.03515	0.04372	-0.00683	-0.00277	2.2967	-0.3589	-0.1453	1.7925
8	2	19.42884	0.04817	-0.00670	-0.00055	2.4792	-0.3447	-0.0286	2.1059
4	3	19.42884	0.01316	-0.00057	-0.00006	0.6772	-0.0296	-0.0033	0.6443
5	3	19.03515	0.01146	-0.00063	-0.00028	0.6019	-0.0332	-0.0147	0.5540
6	3	19.42884	0.01316	-0.00057	-0.00006	0.6772	-0.0296	-0.0033	0.6443
7	3	19.03515	0.01145	-0.00063	-0.00028	0.6017	-0.0332	-0.0147	0.5538
8	3	19.42884	0.01315	-0.00057	-0.00005	0.6768	-0.0296	-0.0025	0.6447
total		96.35682	1.85451	-0.38207	-0.07979	19.2463	-3.9652	-0.8281	14.4530

$E = 189\ GeV$, $R_{cut} = 0.7225$, $P_{cut} = 0.1$, IPPS=6, IGONLY=3

I1	I2	$\sigma^{\rm Born}$	$\sigma^{\rm Real}$	$\sigma^{\rm Virt}_{\rm ISR}$	$\sigma^{\rm Virt}_{\rm FSR}$	$\delta^{\rm Real}$	$\delta^{\rm Virt}_{\rm ISR}$	$\delta^{\rm Virt}_{\rm FSR}$	$\delta^{\rm total}$
4	0	3.50115	0.00262	-0.00349	-0.00039	0.7495	-0.9981	-0.1109	-0.3595
5	0	5.53081	0.00492	-0.00552	-0.00245	0.8903	-0.9985	-0.4438	-0.5519
6	0	3.50115	0.00262	-0.00349	-0.00039	0.7495	-0.9981	-0.1109	-0.3595
7	0	5.53081	0.00491	-0.00552	-0.00245	0.8872	-0.9985	-0.4438	-0.5550
8	0	3.50115	0.00261	-0.00349	-0.00039	0.7451	-0.9981	-0.1109	-0.3639
4	1	3.50115	0.01081	-0.01172	-0.00122	3.0881	-3.3484	-0.3482	-0.6085
5	1	5.53081	0.02090	-0.01852	-0.00779	3.7792	-3.3489	-1.4092	-0.9790
6	1	3.50115	0.01077	-0.01172	-0.00116	3.0773	-3.3484	-0.3311	-0.6022
7	1	5.53081	0.01968	-0.01852	-0.00603	3.5579	-3.3489	-1.0901	-0.8812
8	1	3.50115	0.01049	-0.01172	-0.00077	2.9949	-3.3484	-0.2193	-0.5728
4	2	3.50115	0.00131	-0.00164	-0.00018	0.3732	-0.4692	-0.0521	-0.1481
5	2	5.53081	0.00247	-0.00260	-0.00115	0.4468	-0.4693	-0.2086	-0.2311
6	2	3.50115	0.00131	-0.00164	-0.00018	0.3732	-0.4692	-0.0513	-0.1474
7	2	5.53081	0.00246	-0.00260	-0.00107	0.4439	-0.4693	-0.1944	-0.2198
8	2	3.50115	0.00130	-0.00164	-0.00015	0.3700	-0.4692	-0.0424	-0.1416
4	3	3.50115	0.00012	-0.00020	-0.00002	0.0332	-0.0581	-0.0065	-0.0313
5	3	5.53081	0.00021	-0.00032	-0.00014	0.0380	-0.0581	-0.0258	-0.0459
6	3	3.50115	0.00012	-0.00020	-0.00002	0.0332	-0.0581	-0.0065	-0.0313
7	3	5.53081	0.00021	-0.00032	-0.00014	0.0380	-0.0581	-0.0258	-0.0459
8	3	3.50115	0.00012	-0.00020	-0.00002	0.0332	-0.0581	-0.0057	-0.0306
total		21.56506	0.09994	-0.10512	-0.02613	4.6346	-4.8743	-1.2118	-1.4516

$E = 206\ GeV$, $R_{cut} = 0.01$, $P_{cut} = 0.1$, IPPS=6, IGONLY=3

I1	I2	$\sigma^{\rm Born}$	$\sigma^{\rm Real}$	$\sigma^{\rm Virt}_{\rm ISR}$	$\sigma^{\rm Virt}_{\rm FSR}$	$\delta^{\rm Real}$	$\delta^{\rm Virt}_{\rm ISR}$	$\delta^{\rm Virt}_{\rm FSR}$	$\delta^{\rm total}$
4	0	15.62789	0.10304	-0.01087	-0.00121	6.5936	-0.6955	-0.0773	5.8209
5	0	15.46305	0.09275	-0.01147	-0.00510	5.9983	-0.7420	-0.3298	4.9266
6	0	15.62789	0.10304	-0.01087	-0.00121	6.5934	-0.6955	-0.0773	5.8207
7	0	15.46305	0.09245	-0.01147	-0.00510	5.9791	-0.7420	-0.3298	4.9073
8	0	15.62789	0.10280	-0.01087	-0.00121	6.5777	-0.6955	-0.0773	5.8049
4	1	15.62789	0.16320	-0.04496	-0.00462	10.4431	-2.8766	-0.2958	7.2706
5	1	15.46305	0.15843	-0.04552	-0.01901	10.2454	-2.9440	-1.2293	6.0721
6	1	15.62789	0.16294	-0.04496	-0.00436	10.4262	-2.8766	-0.2787	7.2709
7	1	15.46305	0.15354	-0.04552	-0.01407	9.9295	-2.9440	-0.9101	6.0753
8	1	15.62789	0.16121	-0.04496	-0.00261	10.3152	-2.8766	-0.1669	7.2717
4	2	15.62789	0.04043	-0.00545	-0.00061	2.5869	-0.3485	-0.0387	2.1997
5	2	15.46305	0.03689	-0.00567	-0.00252	2.3859	-0.3666	-0.1629	1.8564
6	2	15.62789	0.04042	-0.00545	-0.00059	2.5867	-0.3485	-0.0379	2.2003
7	2	15.46305	0.03669	-0.00567	-0.00230	2.3727	-0.3666	-0.1487	1.8575
8	2	15.62789	0.04028	-0.00545	-0.00045	2.5776	-0.3485	-0.0290	2.2001
4	3	15.62789	0.01141	-0.00048	-0.00005	0.7299	-0.0306	-0.0034	0.6960
5	3	15.46305	0.00995	-0.00054	-0.00024	0.6437	-0.0351	-0.0156	0.5930
6	3	15.62789	0.01141	-0.00048	-0.00005	0.7299	-0.0306	-0.0034	0.6960
7	3	15.46305	0.00995	-0.00054	-0.00024	0.6435	-0.0351	-0.0156	0.5928
8	3	15.62789	0.01140	-0.00048	-0.00004	0.7296	-0.0306	-0.0026	0.6964
total		77.80978	1.54398	-0.31166	-0.06559	19.8430	-4.0054	-0.8429	14.9946

$E = 206\ GeV$, $R_{cut} = 0.7225$, $P_{cut} = 0.1$, IPPS=6, IGONLY=3

I1	I2	$\sigma^{\rm Born}$	$\sigma^{\rm Real}$	$\sigma^{\rm Virt}_{\rm ISR}$	$\sigma^{\rm Virt}_{\rm FSR}$	$\delta^{\rm Real}$	$\delta^{\rm Virt}_{\rm ISR}$	$\delta^{\rm Virt}_{\rm FSR}$	$\delta^{\rm total}$
4	0	2.74284	0.00215	-0.00289	-0.00032	0.7830	-1.0543	-0.1171	-0.3884
5	0	4.49374	0.00422	-0.00474	-0.00211	0.9381	-1.0546	-0.4687	-0.5852
6	0	2.74284	0.00215	-0.00289	-0.00032	0.7830	-1.0543	-0.1171	-0.3884
7	0	4.49374	0.00420	-0.00474	-0.00211	0.9350	-1.0546	-0.4687	-0.5883
8	0	2.74284	0.00214	-0.00289	-0.00032	0.7786	-1.0543	-0.1171	-0.3928
4	1	2.74284	0.00860	-0.00940	-0.00098	3.1356	-3.4269	-0.3570	-0.6482
5	1	4.49374	0.01732	-0.01540	-0.00649	3.8553	-3.4273	-1.4441	-1.0161
6	1	2.74284	0.00857	-0.00940	-0.00093	3.1248	-3.4269	-0.3399	-0.6419
7	1	4.49374	0.01633	-0.01540	-0.00506	3.6337	-3.4273	-1.1249	-0.9186
8	1	2.74284	0.00834	-0.00940	-0.00063	3.0423	-3.4269	-0.2280	-0.6126
4	2	2.74284	0.00106	-0.00135	-0.00015	0.3867	-0.4907	-0.0545	-0.1586
5	2	4.49374	0.00210	-0.00221	-0.00098	0.4666	-0.4909	-0.2182	-0.2424
6	2	2.74284	0.00106	-0.00135	-0.00015	0.3866	-0.4907	-0.0537	-0.1578
7	2	4.49374	0.00208	-0.00221	-0.00092	0.4637	-0.4909	-0.2039	-0.2311
8	2	2.74284	0.00105	-0.00135	-0.00012	0.3835	-0.4907	-0.0448	-0.1521
4	3	2.74284	0.00010	-0.00017	-0.00002	0.0364	-0.0638	-0.0071	-0.0345
5	3	4.49374	0.00019	-0.00029	-0.00013	0.0422	-0.0638	-0.0284	-0.0500
6	3	2.74284	0.00010	-0.00017	-0.00002	0.0364	-0.0638	-0.0071	-0.0345
7	3	4.49374	0.00019	-0.00029	-0.00013	0.0422	-0.0638	-0.0284	-0.0500
8	3	2.74284	0.00010	-0.00017	-0.00002	0.0364	-0.0638	-0.0063	-0.0337
total		17.21602	0.08205	-0.08670	-0.02189	4.7659	-5.0361	-1.2712	-1.5414

Table 22: LEP2: GENTLE_4fan v.2.11, $e^+e^- \to$ muons. Partial contributions. I1-primary pair, I2-secondary pair. Cross-sections in pb, δ's in per mil. Upper part ISR off, lower part ISR on.

$E = 189\ GeV$, $R_{cut} = 0.01$, $P_{cut} = 1.0$, IPPS=5, IGONLY=2									
I1	I2	$\sigma^{\rm Born}$	$\sigma^{\rm Real}$	$\sigma^{\rm Virt}_{\rm ISR}$	$\sigma^{\rm Virt}_{\rm FSR}$	$\delta^{\rm Real}$	$\delta^{\rm Virt}_{\rm ISR}$	$\delta^{\rm Virt}_{\rm FSR}$	$\delta^{\rm total}$
2	0	3.36252	0.03595	-0.00339	-0.00339	10.6901	-1.0086	-1.0086	8.6729
2	1	3.36252	0.05601	-0.01131	-0.01048	16.6584	-3.3633	-3.1155	10.1795
2	2	3.36252	0.01391	-0.00159	-0.00159	4.1376	-0.4732	-0.4724	3.1920
2	3	3.36252	0.00403	-0.00020	-0.00020	1.1979	-0.0591	-0.0591	1.0796
total		3.36252	0.10990	-0.01649	-0.01565	32.6840	-4.9043	-4.6557	23.1240
$E = 189\ GeV$, $R_{cut} = 0.7225$, $P_{cut} = 1.0$, IPPS=5, IGONLY=2									
2	0	3.36252	0.00434	-0.00339	-0.00339	1.2893	-1.0086	-1.0086	-0.7280
2	1	3.36252	0.01778	-0.01131	-0.01048	5.2876	-3.3633	-3.1155	-1.1913
2	2	3.36252	0.00217	-0.00159	-0.00159	0.6442	-0.4732	-0.4724	-0.3015
2	3	3.36252	0.00019	-0.00020	-0.00020	0.0564	-0.0591	-0.0591	-0.0618
total		3.36252	0.02447	-0.01649	-0.01565	7.2774	-4.9043	-4.6557	-2.2826
$E = 206\ GeV$, $R_{cut} = 0.01$, $P_{cut} = 1.0$, IPPS=5, IGONLY=2									
2	0	2.78510	0.03069	-0.00297	-0.00297	11.0197	-1.0651	-1.0651	8.8896
2	1	2.78510	0.04657	-0.00959	-0.00890	16.7229	-3.4419	-3.1941	10.0869
2	2	2.78510	0.01175	-0.00138	-0.00138	4.2203	-0.4949	-0.4940	3.2314
2	3	2.78510	0.00351	-0.00018	-0.00018	1.2611	-0.0649	-0.0649	1.1314
total		2.78510	0.09253	-0.01411	-0.01342	33.2241	-5.0667	-4.8181	23.3393
$E = 206\ GeV$, $R_{cut} = 0.7225$, $P_{cut} = 1.0$, IPPS=5, IGONLY=2									
2	0	2.78510	0.00380	-0.00297	-0.00297	1.3646	-1.0651	-1.0651	-0.7655
2	1	2.78510	0.01508	-0.00959	-0.00890	5.4133	-3.4419	-3.1941	-1.2226
2	2	2.78510	0.00188	-0.00138	-0.00138	0.6755	-0.4949	-0.4940	-0.3134
2	3	2.78510	0.00018	-0.00018	-0.00018	0.0630	-0.0649	-0.0649	-0.0668
total		2.78510	0.02093	-0.01411	-0.01342	7.5165	-5.0667	-4.8181	-2.3683
$E = 189\ GeV$, $R_{cut} = 0.01$, $P_{cut} = 1.0$, IPPS=5, IGONLY=2									
2	0	7.72785	0.04296	-0.00588	-0.00588	5.5589	-0.7608	-0.7608	4.0374
2	1	7.72785	0.08124	-0.02296	-0.02104	10.5132	-2.9704	-2.7226	4.8201
2	2	7.72785	0.01732	-0.00289	-0.00288	2.2416	-0.3739	-0.3730	1.4947
2	3	7.72785	0.00439	-0.00029	-0.00029	0.5682	-0.0370	-0.0370	0.4943
total		7.72785	0.14592	-0.03201	-0.03009	18.8819	-4.1420	-3.8933	10.8465
$E = 189\ GeV$, $R_{cut} = 0.7225$, $P_{cut} = 1.0$, IPPS=5, IGONLY=2									
2	0	3.15567	0.00374	-0.00315	-0.00315	1.1853	-0.9987	-0.9987	-0.8120
2	1	3.15567	0.01605	-0.01057	-0.00979	5.0858	-3.3492	-3.1014	-1.3648
2	2	3.15567	0.00189	-0.00148	-0.00148	0.5984	-0.4694	-0.4685	-0.3396
2	3	3.15567	0.00016	-0.00018	-0.00018	0.0491	-0.0581	-0.0581	-0.0671
total		3.15567	0.02183	-0.01539	-0.01460	6.9186	-4.8754	-4.6267	-2.5835
$E = 206\ GeV$, $R_{cut} = 0.01$, $P_{cut} = 1.0$, IPPS=5, IGONLY=2									
2	0	6.34605	0.03674	-0.00501	-0.00501	5.7896	-0.7900	-0.7900	4.2096
2	1	6.34605	0.06755	-0.01912	-0.01755	10.6447	-3.0133	-2.7655	4.8658
2	2	6.34605	0.01466	-0.00244	-0.00244	2.3101	-0.3853	-0.3844	1.5404
2	3	6.34605	0.00385	-0.00025	-0.00025	0.6064	-0.0398	-0.0398	0.5268
total		6.34605	0.12280	-0.02683	-0.02526	19.3508	-4.2284	-3.9798	11.1426
$E = 206\ GeV$, $R_{cut} = 0.7225$, $P_{cut} = 1.0$, IPPS=5, IGONLY=2									
2	0	2.60959	0.00328	-0.00275	-0.00275	1.2564	-1.0547	-1.0547	-0.8531
2	1	2.60959	0.01359	-0.00894	-0.00830	5.2079	-3.4275	-3.1797	-1.3993
2	2	2.60959	0.00164	-0.00128	-0.00128	0.6281	-0.4909	-0.4901	-0.3528
2	3	2.60959	0.00014	-0.00017	-0.00017	0.0550	-0.0638	-0.0638	-0.0726
total		2.60959	0.01865	-0.01314	-0.01250	7.1474	-5.0370	-4.7883	-2.6779

5.5.6 *Results on pairs from $\mathcal{KK}$MC and KORALW*

There is an intriguing possibility to define and realize with $\mathcal{KK}$MC+KORALW an alternative definition of the $2f$ signal: $\boxed{2f \text{ Experimental Signal} \equiv 2f \text{ signal without any pairs}}$ realized by:

- Eliminating completely all $4f$ background together with other backgrounds and detector efficiency using KORALW.
- Eliminating virtual pair contributions $\sim 1\%$ together with the ISR*FSR interference using $\mathcal{KK}$MC.
- Switching off pairs in ZFITTER or TOPAZ0.

The above scenario was usually not emphasized in the past, because of the potential technical difficulties with the MC integration, and the cancellation of the mass singularities. On the other hand, while constructing the KORALW program, this application was kept in mind [78] and the appropriate coverage of phase space integration was ensured. Together with the recent upgrade of $\mathcal{KK}$MC with the virtual pair form-factors this opens the way to the first exercises in this direction. The cancellation of fermion masses in KORALW+$\mathcal{KK}$MC is expected to be technically and physically as good as in the semi-analytical programs that are compared with them[24].

Note that that the evaluation of the *experimental efficiency* and elimination of the *background* requires running $\mathcal{KK}$MC and KORALW anyway, so complete elimination of the secondary pair effects would come essentially as a byproduct of the above procedure, with little theoretical uncertainty. Before the above scenario could be realized several technical points needed to be checked:

- Even though a lot of technical tests were already performed on KORALW in all corners of $4f$ phase space, also with untagged electrons, additional tests need to be (re)done. As an example of such technical tests we show in Fig. 24 the comparison of KORALW with analytical result of [137] for the $\mu\bar{\mu}\tau\bar{\tau}$ final state as a function of $v_{cut} = 1 - R_{cut}$ for $\sqrt{s} = 189$ GeV. The τ mass is set equal to μ mass. The three histograms correspond to different approximations of matrix element in KORALW: ISNS$_\gamma$ (`ISWITCH=5`), ISNS$_{\gamma+Z}$ (`ISWITCH=2`) and complete 4f (`ISWITCH=1`). Apart from the discrepancy at the Z peak due to finite binning size, the semianalytical and corresponding Monte Carlo results agree within the statistical errors. Another possible test is the comparison with the semianalytical program GENTLE. This comparison is currently under study.
- For the sake of comparisons the option of reducing matrix element of KORALW to ISNS$_\gamma$, FSNS$_\gamma$ etc. has been introduced, as described in Section 4.17 of this Report.
- The virtual ISNS$_\gamma$ and FSNS$_\gamma$ terms have been incorporated into $\mathcal{KK}$MC as described in Section 4.5.4 of this Report.

With both programs updated, as an example of the numerical results, the correction to the process $e\bar{e} \to \mu\bar{\mu}$ due to emission of one real pair has been calculated by `KORALW` with the following cuts:

1. mass of $\mu\bar{\mu}$ pair with highest mass bigger than (A) $0.9\sqrt{s}$ or (B) $0.4\sqrt{s}$ (two cuts);
2. angle of muon from $\mu\bar{\mu}$ pair with highest mass with respect to the beam: $|\cos\theta_\mu| \leq 0.95$;
3. sum of transverse momenta of neutrina less than $0.3(\sqrt{s} - \sum E_\nu)$.

[24] This approach to pairs was already realized in the case of Bhabha scattering in the BHLUMI 2.30 of Ref. [201], where multiple real pairs are generated within the full exclusive phase space and the virtual and real pair corrections cancel numerically.

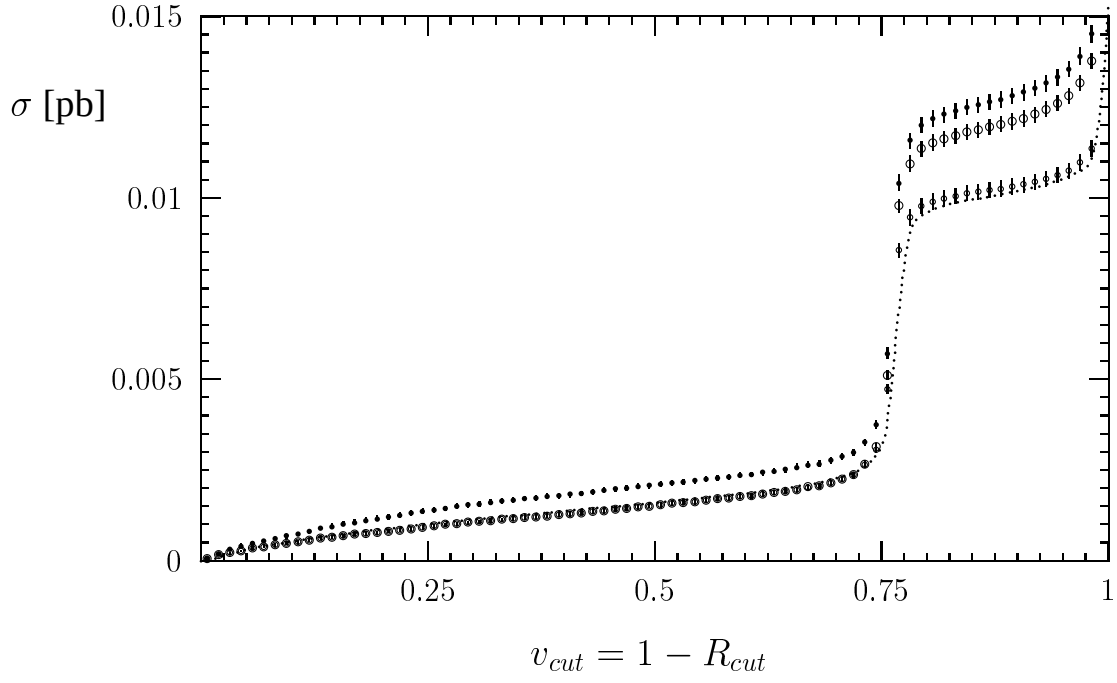

Fig. 24: Total cross-sections [pb] for $e\bar{e} \to \mu\bar{\mu}\tau\bar{\tau}$ from KORALW MC in various approximations of matrix element: ISNS$_{\gamma+Z}$ (big open circles), ISNS$_{\gamma}$ (small open circles), complete 4f (big dots) and semianalytical ISNS$_{\gamma}$ of Ref. [137] (small dots) as a function of $v_{cut} = 1 - R_{cut}$ for $\sqrt{s} = 189$ GeV. Note that m_τ is set equal to m_μ.

The calculation is quite fast and numerically stable. The cuts (A,B) correspond for example to (roughly) **IAleph5**, **IAleph6**. The additional cut on neutrino is based on the L3 realistic cut on secondary pair (Section 2.4). Its aim is to reduce the W-pair production background by requiring transverse energy imbalance to be smaller than 0.3E$_{vis}$. Together with the virtual component calculated by $\mathcal{KK}$MC the results are summarized in Table 23.

Table 23: Pair corrections to $e\bar{e} \to \mu\bar{\mu}$ calculated by KORALW (real) and $\mathcal{KK}$MC (virtual) for $\sqrt{s} = 189$ GeV. All quark and lepton pairs are included. Cuts (A) and (B) are defined in the text.

Cut	$\sigma_{tot}[pb]$	$\mathcal{KK}$MC σ_{virt} [pb]	KORALW σ_{real} [pb]
A	2.67	$-0.025 \pm .001$	$+0.020 \pm .001$
B	6.70	$-0.070 \pm .001$	$+0.497 \pm .006$

The following comments are in order here:

(a) The σ_{real} of KORALW is with *complete* $4f$ matrix element for all fermions $f = d, u, s, c, b, \mu, \tau, \nu's$ and *not* the ISNS signal of the signal definition proposal outlined in Sections 5.5.1 and 5.5.2.

(b) Masses m_f are taken 0.2 GeV for $f = d, u, s$ and PDG values for the rest. Changing m_f of light quarks by factor two induces only $\delta\sigma_{virt}/\sigma = 0.04\%$!

(c) ISR was switched *off* in KORALW and *on* in $\mathcal{KK}$MC.

(d) The virtual pair correction is -0.9% with little dependence on the cut on $M_{\mu\bar{\mu}}$.

(e) The electron channel dominates in real pair contributions.

This project is at the moment unfinished. In particular we have not discussed here the issues related to bremsstrahlung. It is instructive to note in this context that one of the reasons that makes possible numerical cancellation amongst two separate Monte Carlo programs is the fact that bremsstrahlung in both KORALW and $\mathcal{KK}$MC is implemented in the same way, based on the YFS principle. As there are a number of different ways of simulating photonic cascades in different Monte Carlo codes this issue may be a nontrivial one in some cases.

The merits of the above definition of the $2f$ signal are to be judged by LEP experimentalists. The authors of $\mathcal{KK}$MC and KORALW will provide the tools if there is an interest. Finally let us also stress that the tandem KORALW+$\mathcal{KK}$MC can be useful not only for implementing the scenario 'without pairs' decribed in the beginning of this section, but also for implementing any other two-fermion signal and for comparisons with any other semianalytical or Monte Carlo programs. It is an equally important role.

5.5.7 Results on pairs from TOPAZ0

Here we briefly describe the implementation of pairs in TOPAZ0 [25]. Since version 4.4 (April 1999) TOPAZ0 [69] allows the additional value **ONP = 'I'**, where an extension of the Kuraev–Fadin (KF) approach [90] for virtual pairs and for soft and exponentiated ISNS$_\gamma$ pairs is used; the extension is also applicable to hadron pairs, because one uses KKKS results [137] for $\mathcal{O}(\alpha^2)$ and writes it in terms of moments. Then one matches it to KF and generalizes KF to soft and exponentiated hadrons pairs [202].

Next, one uses the generalized KF-approach for virtual $+$ ISNS soft pairs and cut to the same s' value of IS QED radiation, s' being the centre-of-mass energy of the e^+e^- system after initial-state radiation of photons and pairs. This choice, however, is not strictly needed.

Finally, one includes soft pairs only up to some cut Δ that is compatible with $E \gg \Delta \gg 2\,m$, where E is the energy of the incoming electron(positron). Above it one uses ISNS$_\gamma$ hard pairs according to the KKKS formulation but not added linearly, KKKS in convolution with IS QED radiation. The radiator used here is a LL one, with options `ORISPP = 'S'` (second order) and `ORISPP = 'T'` (third order).

An old comparison with `MIZA` in the JMS [142] approach gave a nice agreement for energies around the Z peak, below 0.03 per mil from 88 GeV to 94 GeV.

ISS$_\gamma$ pairs [68], i.e. ISS-pairs where the t-channel exchange is only via a photon, can be included by selecting **OSING = 'SP'**.

After some tuned comparison with GENTLE/ZFITTER, version 4.4 of TOPAZ0 has been slightly upgraded[26] to cure instability problems in virtual pairs and in real τ-pair production for very low values of the s'-cut.

A sample of results is shown in Tables 24–27 where δ (in per mil) is the relative effect of pair production, $\sigma(\mathrm{pairs})/\sigma$. Pair corrections are shown in Tables 24 and 25 for $e^+e^- \to$hadrons and in Tables 26 and 27 for $e^+e^- \to \mu^+\mu^-$ for the two values of s'/s and for $\sqrt{s} = 189$ GeV. Results are shown for all secondary pairs both virtual and real. When compared with GENTLE's predictions in *hadronic* language in Table 20 for hadrons and Table 22 (IPPS,IGONLY)=(5,2), ISR on, for muons we observe a nice agreement everywhere for virtual pairs, with a maximum deviation of 0.1 per mil. When we neglect FS$_\gamma$ pairs, not implemented in TOPAZ0 and compare the real pairs for hadrons with Table 20 it follows that for the total contribution to the hadronic cross-section the differences range from 0.9 per mil when the radiative return is allowed ($s'/s \geq 0.01$) to 0.6 per mil when the radiative return is inhibited ($s'/s \geq 0.7225$). Inclusion of FS$_\gamma$ would increase this difference somewhat. A comparison of the total corrections to the options without FS pairs in GENTLE and ZFITTER in Table 33 shows a maximal

[25] Authors of the report thank G. Passarino for providing numerical results.

[26] (*http://www.to.infn/~giampier/topaz0_v44_rs8_220600.f)*

difference of 1.7 per mil for hadrons. For muons we have a similar 1.5 per mil maximal difference in Table 34. Note also that GENTLE – ZFITTER agreement is $0.5 \div 1$ per mil with ZFITTER closer to TOPAZ0, so that we see a 0.7 per mil maximal difference between TOPAZ0 and ZFITTER.

Table 24: TOPAZ0 predictions for virtual (V), real (R) and total (T) pair-production corrections to $e^+e^- \to$ hadrons at $\sqrt{s} = 189$ GeV and for $s'/s \geq 0.01$. Results are shown for all *secondary* pairs. All δ's are in per mil.

	$\sqrt{s} = 189$ GeV $e^+e^- \to$ hadrons, $s'/s = 0.01$		
	$\delta_{\rm T}^{\rm V,ISR}$	$\delta_{\rm T}^{\rm R,ISR}$	$\delta_{\rm T}^{\rm T,ISR}$
e^+e^-	-2.91	+10.37	+7.46
$\mu^+\mu^-$	-0.35	+2.57	+2.22
$\tau^+\tau^-$	-0.03	+0.72	+0.69
hadrons	-0.71	+6.76	+6.05
all	-4.00	+20.42	+16.42

Table 25: TOPAZ0 predictions for virtual (V), real (R) and total (T) pair-production corrections to $e^+e^- \to$ hadrons at $\sqrt{s} = 189$ GeV and for $s'/s \geq 0.7225$. Results are shown for all *secondary* pairs. All δ's are in per mil.

	$\sqrt{s} = 189$ GeV $e^+e^- \to$ hadrons, $s'/s = 0.7225$		
	$\delta_{\rm T}^{\rm V,ISR}$	$\delta_{\rm T}^{\rm R,ISR}$	$\delta_{\rm T}^{\rm T,ISR}$
e^+e^-	-3.42	+2.93	-0.49
$\mu^+\mu^-$	-0.48	+0.37	-0.11
$\tau^+\tau^-$	-0.06	+0.05	-0.01
hadrons	-1.03	+0.66	-0.37
all	-4.99	+4.01	-0.98

Table 26: TOPAZ0 predictions for virtual (V), real (R) and total (T) pair-production corrections to $e^+e^- \to \mu^+\mu^-$ at $\sqrt{s} = 189$ GeV and for $s'/s \geq 0.01$. Results are shown for all *secondary* pairs. All δ's are in per mil.

	$\sqrt{s} = 189$ GeV $e^+e^- \to \mu^+\mu^-$, $s'/s = 0.01$		
	$\delta_{\rm T}^{\rm V,ISR}$	$\delta_{\rm T}^{\rm R,ISR}$	$\delta_{\rm T}^{\rm T,ISR}$
e^+e^-	-2.98	+8.52	+5.54
$\mu^+\mu^-$	-0.38	+2.04	+1.66
$\tau^+\tau^-$	-0.04	+0.57	+0.53
hadrons	-0.77	+5.30	+4.53
all	-4.17	+16.43	+12.26

Table 27: TOPAZ0 predictions for virtual (V), real (R) and total (T) pair-production corrections to $e^+e^- \to \mu^+\mu^-$ at $\sqrt{s} = 189$ GeV and for $s'/s \geq 0.7225$. Results are shown for all *secondary* pairs. All δ's are in per mil.

	$\sqrt{s} = 189$ GeV $e^+e^- \to \mu^+\mu^-$, $s'/s = 0.7225$		
	$\delta_{\rm T}^{\rm V,ISR}$	$\delta_{\rm T}^{\rm R,ISR}$	$\delta_{\rm T}^{\rm T,ISR}$
e^+e^-	-3.31	+2.79	-0.52
$\mu^+\mu^-$	-0.46	+0.34	-0.12
$\tau^+\tau^-$	-0.06	+0.05	-0.01
hadrons	-0.99	+0.61	-0.38
all	-4.83	+3.80	-1.03

There are unsolved problems that will constitute the bulk of next TOPAZ0 upgrading. They are:

1. double-counting of real pairs and pairing ambiguities in the realistic language of hadrons, i.e. not at the parton level;
2. identical particles in primary and secondary pairs;
3. splitting of real pairs into different channels, i.e. how to define $e^+e^- \to e^+e^-\overline{b}b$, $\overline{b}b$ pair-correction to Bhabha? e^+e^- pair correction to $\sigma_{\rm had}$? Background?
4. flavour misinterpretation;
5. extension to Bhabha scattering, i.e. implementation of pair corrections with realistic cuts, collinearity and energy thresholds, instead of simple s'-cuts.

Cutting on secondary pairs is not a real problem once pairing–double-counting ambiguities are solved in hadronic language via $R_{\rm had}$. The reason why this cut was never implemented is that hadron pairs are easily constructed in the language of moments [137] which requires integrating over the *defined* secondary pair. If one cuts on it the answer is at parton level and should be folded with $R_{\rm had}$ and, presently, there is no routine capable of giving $R_{\rm had}(s)$ for $0 < s < 200\,$GeV without doing some extra work at very low s and around the thresholds [203].

5.5.8 Results on pairs for Bhabhas from LABSMC

With the default version of LABSMC (i.e. without the multi-peripheral contribution) the sum of virtual+real pair effects was determined for the Bhabha observables listed in Table 28. The corrections were calculated with respect to the cross sections, where all other types of RC have already been applied. There is a simple dependence of the size of corrections on the applied cuts. The strongest cuts on real emission are there, the largest (and most negative) effect is coming out. The largest corrections are found for some idealized observables, where also the final-state corrections do give a lot.

Concerning the multi-peripheral two-photon corrections, there are visible contributions only for a few observables. The only large correction is for **IOpal3** because of the wide range of allowed collinearity and a very low energy threshold for electrons (1 GeV). For all other observables, not listed in Table 29, the multi-peripheral reaction is cut away.

The accuracy on the above numbers can be estimated to be about 20%, which is mainly coming from the uncertainty in the description of secondary hadronic pairs.

5.5.9 Comparison of results for hadrons and muons

In the following we shall compare the results of the different signal definitions obtained from various programs for primary hadrons and primary muons. The Bhabha process will be discussed in the next section.

Real pairs

As explained above, only the amount of *real* secondary ISNS plus FS pair $f_2\overline{f}_2$ emission enters the experimental measurements of 2-fermion cross-sections. For all primary pairs apart from $f_1\overline{f}_1$ = ee this contribution can be calculated in GENTLE, KORALW, and GRC4f. Since the checks of the new KORALW code were not completely finished at the time of writing this report, we compare in the following GRC4f and GENTLE, using the cut-based signal definition (2), which is realized in GENTLE via IPPS=6, IGONLY=3, and $P_{\rm cut} = 0.10$. The GRC4f prediction has been obtained with method (A) described in Section 4.16. Using method (B) gives consistent results. The result of the comparison for $qqf_2\overline{f}_2$ corrections to the process $e^+e^- \rightarrow$ hadrons at $\sqrt{s}$=189 GeV is listed in Table 30 and 31. Comparisons at other centre-of-mass energies result in similar numbers.

Table 28: LABSMC corrections due to pairs in per mil of the cross-sections for the respective observables.

obs.	189	200	206 [GeV]
realistic observables			
Aleph3	-2.133	-2.180	-2.130
Aleph4	-2.281	-2.286	-2.287
Delphi3	-2.197	-2.228	-2.257
LT4	-2.618	-2.660	-2.684
LT5	-1.871	-1.894	-1.924
LT6	-0.887	-0.920	-0.889
LT7	-0.482	-0.668	-0.728
LT8	0.206	0.150	0.184
Opal3	0.131	0.014	0.072
Opal4	-2.626	-2.699	-2.706
Opal5	-1.635	-1.669	-1.669
idealized observables			
IAleph3	-5.846	-6.009	-5.994
IAleph4	-6.774	-6.925	-6.967
ILT4	-5.322	-5.427	-5.451
ILT5	-1.867	-1.890	-1.920
ILT6	-0.885	-0.918	-0.887
ILT7	-0.481	-0.666	-0.725
ILT8	0.206	0.150	0.184
IOpal3	0.131	0.014	0.072
IOpal4	-2.716	-2.691	-2.699
IOpal5	-1.628	-1.662	-1.662

Table 29: LABSMC pair corrections due to multi-peripheral two-photon processes.

obs.	189	200	206 [GeV]
Delphi3	0.105	0.106	0.107
IOpal3	2.336	2.359	2.370
IOpal4	0.070	0.069	0.069
IOpal5	0.423	0.426	0.428

Table 30: Real pair cross-sections in pb, and relative corrections in per mil, obtained from GRC4f and GENTLE for the process $e^+e^- \to$ hadrons at $\sqrt{s} = 189$ GeV for **high** s' **events of** $R_{\rm cut} = 0.7225$ according to the cut-based definition (2). The last column lists the difference between GRC4f and GENTLE in per mil of the hadronic cross-section. The errors given are statistical only.

$f_1\bar{f}_1\ f_2\bar{f}_2$	$\sigma^{\rm Real}_{\rm GRC4f}$	$\sigma^{\rm Real}_{\rm GENTLE}$	$\delta^{\rm Real}_{\rm GRC4f}$	$\delta^{\rm Real}_{\rm GENTLE}$	$\Delta\delta^{\rm Real}$
qqee	0.090 ± 0.002	0.073	4.2 ± 0.1	3.4	$+0.8$
qq$\mu\mu + \tau\tau$	0.013 ± 0.002	0.010	0.6 ± 0.1	0.4	$+0.2$
qqqq	0.016 ± 0.002	0.018	0.7 ± 0.1	0.8	-0.1
total qq$f_2\bar{f}_2$	0.119 ± 0.003	0.100	5.5 ± 0.2	4.6	$+0.9$

Table 31: Real pair cross-sections in pb, and relative corrections in per mil, obtained from GRC4f and GENTLE for the process $e^+e^- \to$ hadrons at $\sqrt{s} = 189$ GeV for **inclusive events** of $R_{\rm cut} = 0.01$. The last column lists the difference between GRC4f and GENTLE in per mil of the hadronic cross-section. The errors given are statistical only.

$f_1\bar{f}_1\ f_2\bar{f}_2$	$\sigma^{\rm Real}_{\rm GRC4f}$	$\sigma^{\rm Real}_{\rm GENTLE}$	$\delta^{\rm Real}_{\rm GRC4f}$	$\delta^{\rm Real}_{\rm GENTLE}$	$\Delta\delta^{\rm Real}$
qqee	1.16 ± 0.01	0.97	12.1 ± 0.1	10.1	$+2.0$
qq$\mu\mu + \tau\tau$	0.35 ± 0.01	0.29	3.6 ± 0.1	3.0	$+0.6$
qqqq	0.58 ± 0.03	0.59	6.0 ± 0.3	6.1	-0.1
total qq$f_2\bar{f}_2$	2.09 ± 0.03	1.85	21.7 ± 0.3	19.2	$+2.5$

The results show that for secondary lepton pairs GRC4f has about 20% more real pairs than GENTLE, though the difference is not statistically significant for $\mu\mu$ and $\tau\tau$ in the high s' sample. For hadronic pairs there is perfect agreement, despite the fact that GENTLE uses a pure hadronic approach (in terms of $R_{\rm had}$) to obtain qqqq, while GRC4f calculates partonic corrections (where we have used quark masses of $m_u = m_d = 0.14$ GeV) which have been a posteriori corrected for the effect of the low-mass hadronic $R_{\rm had}$ ratio and of the running $\alpha_{\rm em}$ via re-weighting of the GRC4f events (not available in default GRC4f). These latter corrections have only a small impact on the comparison, since they tend to cancel each other, if $\alpha_{\rm em}(s)$ has been used in the generation of the events, resulting in a total correction of -0.001 pb and -0.01 pb for $\sigma^{\rm Real}_{\rm GRC4f}$(qqqq) for $R_{\rm cut}$ = 0.7225 and 0.01, respectively.

The total real pairs difference between GRC4f and GENTLE in terms of the corresponding hadronic cross-section is 0.9 per mil for the high s' selection and 2.5 per mil for the inclusive selection. A possible source of this difference is the more sophisticated treatment of common photon and pairs emission in GENTLE while GRC4f simply attaches a photon radiator function to the 4-fermion matrix element. Note that the agreement for qq pairs depends on the choice of quark masses in GRC4f.

Comparing with Table 16 it is evident that even in the worst case (inclusive muons) a 20% error on $\delta_{\rm Real}$ means a relative error of 0.1% for the combined 2f+4f efficiency. One can therefore conclude that GRC4f is adequate to calculate the influence of pair emission on the efficiency to better than 0.1%.

Comparison between signal definitions

Since the virtual pair corrections are identical for the above diagram-based (1), and cut-based (2) signal definitions, the total difference between the definitions is given by the difference in the amount of real pairs. Repeating the above calculations with the diagram-based signal definition (1), using the same s' definition [i.e. IPPS=5, IGONLY=2, $P_{\rm cut} = 1.0$ (no cut on secondary pairs) in GENTLE] results in Table 32 of differences in real pair cross-sections.

Table 32: Differences between diagram-based definition (1) and cut-based definition (2) for real pairs in per mil of the hadronic cross-section, obtained from GRC4f and GENTLE for the process $e^+e^- \to$ hadrons at $\sqrt{s} = 189$ GeV for high s' events with $R_{\rm cut} = 0.7225$ and inclusive events with $R_{\rm cut} = 0.01$. For $R_{\rm cut} = 0.7225$ no significant difference was observed within the statistical errors of the comparison in both programs. For qqee the diagram-based definition was not available for GRC4f.

$f_1\bar{f}_1\ f_2\bar{f}_2$	$\Delta\delta^{\rm Real}_{\rm GRC4f}$		$\Delta\delta^{\rm Real}_{\rm GENTLE}$	
$R_{\rm cut}$	0.7225	0.01	0.7225	0.01
qqee	–	–	< 0.0001	0.04
qq$\mu\mu + \tau\tau$	< 0.1	0.02 ± 0.12	< 0.0001	0.07
qqqq	< 0.1	0.31 ± 0.33	< 0.0001	0.18
total qq$f_2\bar{f}_2$	–	–	< 0.0001	0.29

This comparison shows that for inclusive hadrons the difference between the two definitions, as predicted by GENTLE, is of order 10^{-4} for each class of pairs listed, amounting to a total of 2.9×10^{-4}. The results of GRC4f are consistent, though their sensitivity is limited by the statistical error of some 10^{-4}. For high s' hadrons no difference between definitions 1 and 2 is visible even on the level of 10^{-7} in GENTLE.

Comparison of real+virtual pairs

In the following we compare as a typical example the sum of virtual and real pair corrections for primary hadrons and primary muons at $\sqrt{(}s) = 189$ GeV for four different definitions of the secondary pair signal:

A Diagram-based definition (1) with $s' = M^2_{\rm prop}$

B Diagram-based definition (1) with $s' = M^2_{\rm inv}$

C Cut-based definition (2) with $s' = M^2_{\rm inv}$ and $P_{\rm cut} = 0.15$

D Cut-based definition (2) with $s' = M^2_{\rm inv}$ and $P_{\rm cut} = 0.10$

Table 33: Relative virtual + real pair corrections in per mil of the total cross-section for the process $e^+e^- \to$ hadrons at $\sqrt{s} = 189$ GeV for different signal definitions. A – means that this definition is not accessible in the respective program.

Definition	GENTLE	ZFITTER	TOPAZ0	GENTLE	ZFITTER	TOPAZ0
$R_{\rm cut}$	0.01			0.7225		
A) diagram, $s' = M^2_{\rm prop}$	14.72	15.76	16.42	-1.13	-0.92	-0.98
B) diagram, $s' = M^2_{\rm inv}$	14.74	15.82	–	-1.45	-1.20	–
C) cuts, $P_{\rm cut} = 0.15$	14.64	–	–	-1.45	–	–
D) cuts, $P_{\rm cut} = 0.10$	14.45	–	–	-1.45	–	–
$\delta_{\rm B} - \delta_{\rm A}$	0.02	0.06	–	-0.32	-0.29	–
$\delta_{\rm B} - \delta_{\rm C}$	0.10	–	–	< 0.0001	–	–
$\delta_{\rm B} - \delta_{\rm D}$	0.29	–	–	< 0.0001	–	–

Table 34: Relative virtual + real pair corrections in per mil of the total cross-section for the process $e^+e^- \to \mu^+\mu^-$ at $\sqrt{s} = 189$ GeV for different signal definitions. A $-$ means that this definition is not accessible in the respective program.

Definition	GENTLE	ZFITTER	TOPAZ0	GENTLE	ZFITTER	TOPAZ0
$R_{\rm cut}$	0.01			0.7225		
A) diagram, $s' = M^2_{\rm prop}$	10.73	11.73	12.26	-1.37	-1.00	-0.98
B) diagram, $s' = M^2_{\rm inv}$	10.84	11.96	–	-2.58	-2.05	–
C) cuts, $P_{\rm cut} = 0.15$	10.72	–	–	-2.58	–	–
D) cuts, $P_{\rm cut} = 0.10$	10.57	–	–	-2.58	–	–
$\delta_{\rm B} - \delta_{\rm A}$	0.11	0.23	–	-1.21	-1.05	–
$\delta_{\rm B} - \delta_{\rm C}$	0.12	–	–	< 0.0001	–	–
$\delta_{\rm B} - \delta_{\rm D}$	0.27	–	–	< 0.0001	–	–

From these tables several conclusions can be drawn. The comparison between GENTLE, ZFITTER, and TOPAZ0 for the diagram-based definition with $s' = M^2_{\rm prop}$ (A) reveals maximum differences of 1.7 (1.5) per mil for inclusive hadrons (muons) and 0.2 (0.4) per mil for high s' hadrons (muons) between any two of the programs. Differences between cut-based and diagram-based signal definitions are between 1 and 3×10^{-4} for inclusive selections for $P_{\rm cut}$ in the range from 0.10 to 0.15 (compare also Table 32), and below 10^{-7} for the high s' selection, as long s' is defined as $M^2_{\rm inv}$ everywhere. Whereas for the inclusive selections the difference between $s' = M^2_{\rm prop}$ and $s' = M^2_{\rm inv}$ is at most 0.2 per mil, it is about 0.3 (1.1) per mil for high s' hadrons (muons). Compared to the LEP-combined statistical precision of the measurements all these differences are small. Even the 1.7 per mil difference between GENTLE and TOPAZ0 for inclusive hadrons is only about half of the expected LEP-combined statistical error, summed over all centre-of-mass energies, and is thus not far from the precision tag of 1.1 per mil.

5.5.10 Results for Bhabhas

There is only one program, LABSMC, which is able to calculate virtual+real pair effects for $s+t$ channel Bhabha scattering for the signal definition given above. Therefore a comparisons like the one performed above for hadrons and muons cannot be done for primary electron pairs. We just state here that the pair corrections for idealized observables range from +0.2 per mil for **ILT8** to -7.0 per mil for **IAleph4**. Largish corrections between 5 and 7 per mil occur only for observables which cut hard on $M_{\rm inv}$. For them a relative accuracy of 20–30% would be needed to meet the experimental precision tags, which are between 0.13 and 0.21% for the cross-sections. All other corrections are below 3 per mil so that for them a 50% pair correction accuracy would suffice. The author of LABSMC estimates a relative accuracy of 20% for pair corrections, which would mean that all experimental precision requirements are met. Yet, it would be very valuable if the pair corrections in LABSMC could be cross-checked against another code.

5.5.11 Conclusions for pair effects

Shortly before and during this workshop a lot of new code for pair corrections at LEP2 was developed. Before 1999, essentially only the diagram-based pair correction with $s' = M^2_{\rm prop}$, i.e. inclusive FS pairs, could be calculated by ZFITTER and TOPAZ0 for all primary pairs apart from electrons. Common exponentiation of initial-state photons and ISNS$_\gamma$ pairs for energies away from the Z-peak as well as optional ISS$_\gamma$ pairs were implemented in both codes in 1999. ZFITTER has now been upgraded to include explicit FS$_\gamma$ with the possibility of mass cuts. The new GENTLE/4fan offers even more options with mass cuts on all pairs and inclusion of pairs from virtual Z's and swapped FS diagrams. Finally a new powerful combination of $\mathcal{KK}$MC and KORALW is being developed which contributed first numbers to this document. This makes a whole variety of options for pair treatment available.

The main achievements of the pair study described above are:

- A proposal for a signal definition which can be, to better than 0.1% accuracy, defined either based on (experiment oriented) cuts or on (theory oriented) diagrams.
- The determination of efficiency corrections using full event generators has been checked for GRC4f to a precision of 0.1%, from a comparison of real pair cross-sections with GENTLE.
- Double counting of hadronic events has been studied with GRC4f and found to be smaller than 10^{-4}.
- Problems of pairing ambiguities for four identical fermions become increasingly important with the larger ZZ cross-sections at high energies, especially for inclusive measurements with the signal definitions adopted here. From varying pairing algorithms, a worst-case difference of 0.8 per mil was found for inclusive hadrons at 206 GeV.
- Differences for pair corrections between s' definitions via the propagator or primary pair mass in the diagram-based approach have been determined. GENTLE and ZFITTER both find them to be about 0.3 (1.1) per mil for high s' hadrons (muons).
- Maximum differences for the diagram-based pair correction of 1.7 (1.5) per mil for inclusive hadrons (muons) and 0.2 (0.4) per mil for high s' hadrons (muons) between any two of the programs GENTLE, ZFITTER and TOPAZ0 have been found.
- A first complete calculation of pair corrections for Bhabhas has been done by LABSMC.

We conclude that for the proposed signal definition sufficient comparisons have been performed to be confident that the above numbers are limitations of the theoretical uncertainties. With the exception of the 1.7 per mil difference for inclusive hadrons, which is slightly above the respective precision tag of 1.1 per mil, all theoretical uncertainties are well below the experimental precision tags. For other signal definitions, however, uncertainties have not been checked systematically. Some more information is present from the tables presented in this section. It is in any case not advisable to chose a signal definition for pairs that can be calculated by one program only. Especially for the case of Bhabha scattering it would be highly desirable to have more than one code predicting the effects of secondary pairs. Improvements are still expected in GENTLE, TOPAZ0 and $\mathcal{KK}$MC+KORALW.

6 SUMMARY

In this report we have addressed the question of uncertainties of the predictions of *theoretical* calculations for quantities measured in LEP2 experiments (LEP2 observables). We also have studied uncertainties in relating measured quantities to theoretical predictions, via signal definitions and acceptance corrections, especially for the effect of secondary pair radiation, and to a lesser degree wide angle Bhabha scattering. The calculations were contributed by several theoretical groups and are implemented using various techniques and approaches embodied in most cases in Monte Carlos, but also in semi-analytical codes – most of them are already in use in all LEP2 collaborations. We tried to cover all two-fermion processes: production of quark-, muon- and tau-pairs, the Bhabha process. Considerable effort was also invested in the processes with (additional) tagged single and double photons. The neutrino channel and Bhabha channel are of course the most important in this class. The whole analysis of the theoretical prediction was done for the rather complete list of LEP2 observables, which we tried to have as close as possible to the ones used by LEP experiments. Most of the collected theoretical predictions are for simplified experimental acceptances (so called idealized observables), but we also tried, not without some success, to produce and discuss theoretical predictions for *realistic* LEP2 observables.

Already from the beginning of the work of our two-fermion group it was expected that for the full LEP2 statistics the most important issues in the evaluation of the theoretical uncertainties would be:

1. production of secondary pairs,
2. QED initial-final state interference,
3. precise cross-checks of QED initial-state radiation and multi-photon effects,
4. numerical cross-checks of the electroweak corrections.

The QED parts of the calculations have turned out to be under very good control; the biggest and most important contributions from the initial-state radiation (which is up to 200%) is now under control down to 0.2–0.4% (final-state radiation included) in most cases.

The initial-final state interference, which is $\sim 2\%$, is now controlled down to 0.2%.

The above is true for the ordinary two-fermion LEP2 observables, which do not require the presence of one or two visible (tagged) photons. In the case of tagged photons the achieved precision varies with the type of the cut and is typically 4% for the $\nu\bar{\nu}\gamma$ observables, 3% for Bhabha and 1% for $\mu^+\mu^-\gamma$, or $\tau^+\tau^-\gamma$. The initial-final state interference has turned out to be rather important for the observables with tagged photons.

For the Bhabha process the QED bremsstrahlung was found to be one of the main sources of uncertainties for the end-cap observables. For the LEP2 observables relying on the data from the barrel (wide angle) detector only, there is a sizeable contribution from the electroweak part of the calculation. We were unable to explore this subject before the end of the workshop.

In the work of our group we did not have a chance to scrutinize once again the pure electroweak corrections. To some extent it was already done in the earlier LEP workshops, so one could say that it is not really necessary, on the other hand it is always necessary to cross-check the codes like ZFITTER and $\mathcal{KK}$MC used by LEP2 experiments once again, on every possible aspect. We clearly recommend that it should be done in the near future.

As a collorary of the tests of ZFITTER and $\mathcal{KK}$MC we have noticed that the numerical contribution from the so-called electroweak boxes, which is negligible at LEP1, and is still rather small at lower CMS energies of LEP2 like 189 GeV, is, however, already quite large $\sim 2\%$ at higher LEP2 energies like 206 GeV. In other words, as far as electroweak phenomena are concerned, the LEP experiments at the LEP2 top energies start to be in the same situation as the future Linear Colliders!

The production of the secondary pairs was at the top of the list of priorities of this workshop. We have come up with a proposal for a 2-fermion signal definition including pair radiation, which is simple and equally applicable to all final-state fermions, from electrons to hadrons, and to all s' cuts. This signal definition comes in fact optionally as a diagram-based or as a cut-based definition, where the one best suited for the given experimental or theoretical setup can be chosen. All definitions are numerically identical within 0.3 per mil for hadrons and 1.1 per mil for muons for any s' cut.

For this set of signal definitions we have performed a broad variety of comparisons and tests, starting from effects like pairing ambiguities, double counting, and efficiency corrections, eventually leading to a comparison between different theoretical codes for computing real and virtual pair corrections. Uncertainties and biases resulting from these studies were found to range from below 0.1 per mil to at most 1.7 per mil of the 2-fermion cross-sections. This corresponds to up to 20% relative uncertainties on the pair corrections. Some theoretical codes have provided results also for other definitions of pair signals, which are however often calculable by one code, only. This situation is expected to improve with forthcoming upgrades of GENTLE, TOPAZ0 and $\mathcal{KK}$MC+KORALW. For the Bhabha scattering process, only one theoretical calculation of pair effects is available for the proposed signal definition.

In the immediate future after the present workshop we would most urgently recommend cross-checks for the purely electroweak corrections, especially for wide angle Bhabha, and for secondary pair corrections for the Bhabha process.

There seem to be few unresolved problems as far as QED is concerned, except for certain observables with the tagged photons $e^+e^- \to \nu\bar{\nu}\gamma$ and (to a lesser degree) for wide angle Bhabhas, where further improvements of the theoretical precision by a factor 4–10 are necessary.

Table 35: Comparison of the typical theoretical uncertainties with the typical experimental precision tags

class of observables	theoretical uncertainty	experimental precision tag
$e^+e^- \to q\bar{q}(\gamma)$	0.26%	0.1% -0.2%
$e^+e^- \to \mu^+\mu^-(\gamma)$	0.4%	0.4% -0.5%
$e^+e^- \to \tau^+\tau^-(\gamma)$	0.4%	0.4% -0.6%
$e^+e^- \to e^+e^-(\gamma)$ (endcap)	0.5%	0.13%
$e^+e^- \to e^+e^-(\gamma)$ (barrel)	2.0%	0.21%
$e^+e^- \to e^+e^-\gamma$	3%	1.5%
$e^+e^- \to l^+l^-\gamma$	1%	1.5%
$e^+e^- \to \nu\bar{\nu}\gamma$	4%	0.5%

We tried to summarize all of the above information once again in Table 35, where we list the theoretical precisions attained in our study for the LEP2 observables defined in Section 2 in comparison with typical ultimate experimental requirements for combined LEP2 data.

References

[1] ALEPH Collaboration, CERN-EP/99-042 (submitted to Eur. Phys. J. C).

[2] DELPHI Collaboration, P. Abreu *et al.*, EP 99–05 (Accepted by Eur. Phys. J. C).

[3] L3 Collaboration, M. Acciarri *et al.*, *Phys. Lett.* **B370** (1996) 195–210.

[4] L3 Collaboration, M. Acciarri *et al.*, *Phys. Lett.* **B407** (1997) 361–376.

[5] L3 Collaboration, M. Acciarri *et al.*, *Phys. Lett.* **B479** (2000) 101, hep-ex/0002034.

[6] L3 Collaboration, M. Acciarri *et al.*, *Phys. Lett.* **B476** (2000) 40, hep-ex/0002035.

[7] OPAL Collaboration, K. Ackerstaff *et al.*, *Eur. Phys. J.* **C2** (1998) 441, hep-ex/9708024.

[8] OPAL Collaboration, G. Abbiendi *et al.*, *Eur. Phys. J.* **C6** (1999) 1, hep-ex/9808023.

[9] OPAL Collaboration, G. Abbiendi *et al.*, hep-ex/9908008.

[10] L3 Collaboration, M. Acciarri *et al.*, *Phys. Lett.* **B473** (2000) 177–185.

[11] OPAL Collaboration, K. Ackerstaff *et al.*, *Eur. Phys. J.* **C1** (1998) 45–64, hep-ex/9709027.

[12] L3 Collaboration, M. Acciarri *et al.*, *Phys. Lett.* **B470** (1999) 268–280.

[13] OPAL Collaboration, K. Ackerstaff *et al.*, *Eur. Phys. J.* **C2** (1998) 607, hep-ex/9801024.

[14] OPAL Collaboration, G. Abbiendi *et al.*, *Eur. Phys. J.* **C8** (1999) 23, hep-ex/9810021.

[15] OPAL Collaboration, G. Abbiendi *et al.*, *Eur. Phys. J.* **C8** (1999) 191, hep-ex/9811028.

[16] F. Jegerlehner, Hadronic effects in (g-2)(μ) and $\alpha_{QED}(M_Z)$: Status and perspectives, in *Proc. of the 4th Int. Symp. on Radiative Corrections (RADCOR 98): Application of Quantum Field Theory to Phenomenology*, Barcelona, 1998, J. Sola, ed. (World Scientific, Singapore, 1999), pp. 75–89, `hep-ph/9901386`.

[17] S. Eidelman and F. Jegerlehner, *Z. Phys.* **C67** (1995) 585–602, `hep-ph/9502298`.

[18] M. Steinhauser, *Phys. Lett.* **B429** (1998) 158–161, `hep-ph/9803313`.

[19] H. Burkhardt, F. Jegerlehner, G. Penso and C. Verzegnassi, *Z. Phys.* **C43** (1989) 497.

[20] H. Burkhardt and B. Pietrzyk, *Phys. Lett.* **B356** (1995) 398.

[21] R. B. Nevzorov, A. V. Novikov and M. I. Vysotsky, *JETP Lett.* **60** (1994) 399.

[22] B. Geshkenbein and V. Morgunov HEPPH–9407228.

[23] A. Martin and D. Zeppenfeld, *Phys. Lett.* **B345** (1994) 558.

[24] M. Swartz, *Phys. Rev.* **D53** (1996) 5268.

[25] K. Abel and F. Yndurain FTUAM-95-32, September 1995.

[26] R. Alemany *et al.*, *Eur. Phys. J.* **C2** (1998) 123.

[27] M. Davier and A. Höcker, *Phys. Lett.* **B419** (1998) 419.

[28] J. Kühn and M. Steinhanser, *Phys. Lett.* **B437** (1998) 425.

[29] J. K. S. Groote and A. Pivovarov, *Phys. Lett.* **B440** (1998) 375.

[30] M. Davier and A. Höcker, *Phys. Lett.* **B435** (1998) 427.

[31] A. Ballestrero *et al.*, `hep-ph/0006259`.

[32] D. Bourilkov, `hep-ph/0002172`.

[33] D. Bourilkov, *JHEP* **08** (1999) 006, `hep-ph/9907380`.

[34] J. Fujimoto, T. Kaneko, Y. Kurihara, D. Perret-Gallix and Y. Shimizu, *Phys. Lett.* **B304** (1993) 189–192.

[35] Y. Kurihara, J. Fujimoto, T. Ishikawa, Y. Shimizu and T. Munehisa, `hep-ph/9908422`.

[36] S. Jadach, W. Płaczek and B. F. L. Ward, *Phys. Lett.* **B390** (1997) 298.

[37] S. Jadach, O. Nicrosini, *et al.*, Event generators for Bhabha scattering, in *Physics at LEP2*, Eds. G. Altarelli, T. Sjöstrand and F. Zwirner, CERN 96–01, Vol. 2, p. 229.

[38] D. R. Yennie, S. C. Frautschi and H. Suura, *Ann. Phys.* **13** (1961) 379–452.

[39] S. Jadach, E. Richter-Wąs, B. F. L. Ward and Z. Wąs, *Comput. Phys. Commun.* **70** (1992) 305.

[40] M. Bohm, A. Denner and W. Hollik, *Nucl. Phys.* **B304** (1988) 687.

[41] F. A. Berends, R. Kleiss and W. Hollik, *Nucl. Phys.* **B304** (1988) 712.

[42] W. Beenakker, F. Berends and S. C. van der Marck, *Nucl. Phys.* **B349** (1991) 323.

[43] F. A. Berends *et al.*, *Nucl. Phys.* **B206** (1982) 61.

[44] W. Płaczek, S. Jadach, M. Melles, B. Ward and S. Yost, Precision calculation of Bhabha scattering at LEP, in *Radiative Corrections: Applications of Quantum Field Theory to Phenomenology*, Barcelona, 1998, J. Sola, ed. (World Scientific, Singapore, 1999), p. 325.

[45] W. Płaczek, talk given at the meeting of the LEP2MC Workshop CERN, 12 Oct. 1999.

[46] F. A. Berends and R. Kleiss, *Nucl. Phys.* **B228** (1983) 537.

[47] S. Jadach, W. Płaczek, E. Richter-Wąs, B. F. L. Ward and Z. Wąs, *Comput. Phys. Commun.* **102** (1997) 229.

[48] A. B. Arbuzov, `hep-ph/9907298`.

[49] S. Jadach, Z. Wąs and B. F. L. Ward, preprint DESY-99-106, CERN-TH/99-235, UTHEP-99-08-01, Comput. Phys. Commun. in press, `hep-ph/9912214`.

[50] S. Jadach, B. F. L. Ward and Z. Was, *Comput. Phys. Commun.* **124** (2000) 233, `hep-ph/9905205`.

[51] A. Jacholkowska, J. Kalinowski and Z. Was, *Eur. J. Phys* **C6** (1999) 485.

[52] S. Jadach, B. Ward and Z. Wąs, *Phys. Lett.* **B257** (1991) 213.

[53] Z. Wąs, *Acta Phys. Polon.* **B18** (1987) 1099.

[54] S. Jadach, B. F. L. Ward and Z. Wąs, *Comput. Phys. Commun.* **66** (1991) 276.

[55] S. Jadach, B. F. L. Ward and Z. Wąs, *Comput. Phys. Commun.* **79** (1994) 503–522.

[56] S. Jadach and B. F. L. Ward, *Comput. Phys. Commun.* **56** (1990) 351.

[57] S. Jadach and B. F. L. Ward, *Phys. Lett.* **B274** (1992) 470.

[58] S. Jadach and Z. Wąs, *Phys Lett.* **219** (1989) 103; J.H. Kühn, S. Jadach, R.G. Stuart and Z. Wąs, *Z. Phys.* **C38** (1988) 609; J.H. Kühn and R. G. Stuart, *Phys. Lett.* **B200** (1988) 360.

[59] S. Jadach and Z. Wąs, *Phys. Rev.* **D41** (1990) 1425.

[60] P. Colas, R. Miquel, and Z. Wąs, *Phys. Lett.* **B246** (1990) 541.

[61] T. Paul, J. Swain and Z. Wąs, `hep-ph/9905207`.

[62] A. Jacholkowska, J. Kalinowski and Z. Wąs, *Comput. Phys. Commun.* **124** (2000) 238, `hep-ph/9905225`.

[63] S. Jadach, B. Ward and Z. Was, *Phys. Lett.* **B408** (1997) 281.

[64] R. Decker, S. Jadach, J. H. Kühn and Z. Wąs, *Comput. Phys. Commun.* **76** (1993) 361.

[65] E. Barberio and Z. Wąs, *Comput. Phys. Commun.* **79** (1994) 291.

[66] S. Jadach, B. F. L. Ward and Z. Wąs, preprint CERN-TH/2000-087, UTHEP-99-09-01, `hep-ph/0006359`.

[67] S. Jadach, B. F. L. Ward and Z. Wąs, *Phys. Lett.* **B449** (1999) 97–108, `hep-ph/9905453`.

[68] F. A. Berends, G. Burgers and W. L. van Neerven, *Nucl. Phys.* **B297** (1988) 429; E: ibid., **B304** (1988) 921.

[69] G. Montagna, O. Nicrosini, F. Piccinini and G. Passarino, Fortran program TOPAZ0, v.4.4 available from
http://www.to.infn.it/~giampier/topaz0.html, see also [204–206].

[70] R. Kleiss and W. J. Stirling, *Nucl. Phys.* **B262** (1985) 235.

[71] R. Barbieri, J. Mignaco and E. Remiddi, *Nuovo Cimmento* **11A** (1972) 824, 865.

[72] M. Igarashi and N. Nakazawa, *Nucl. Phys.* **B288** (1987) 301.

[73] S. Yost, private communication.

[74] D. Bardin, M. Bilenky, P. Christova, T. Riemann, M. Sachwitz and H. Vogt, *Comput. Phys. Commun.* **59** (1990) 303.

[75] D. Bardin, P. Christova, M. Jack, L. Kalinovskaya, A. Olshevski, S. Riemann and T. Riemann, ZFITTER v.6.21: A semi-analytical program for fermion pair production in e^+e^- annihilation, DESY 99–070 (1999), submitted to Comput. Phys. Commun., hep-ph/9908433.

[76] S. Jadach, B. Ward and Z. Was, Global positioning of spin GPS scheme for half-spin massive spinors, CERN preprint CERN-TH/98-235 (1998).

[77] G. J. H. Burgers, *Phys. Lett.* **B164** (1985) 167.

[78] S. Jadach, W. Placzek, M. Skrzypek, Z. Wąs and B. F. L. Ward, Monte Carlo program koralw v. 1.42 for all four-fermion final states in e^+e^- collisions, CERN preprint CERN-TH/98-242, 1998.

[79] *Z-PHYSICS at LEP1*, Eds. G. Altarelli, R. Kleiss and C. Verzegnassi, CERN 89–08, 3 Vols., (CERN, Geneva, 1989).

[80] F. Berends, R. Kleiss and S. Jadach, *Comput. Phys. Commun.* **29** (1983) 185.

[81] S. Jadach and Z. Wąs, *Comput. Phys. Commun.* **85** (1995) 453.

[82] R. Miquel, C. Mana and M. Martinez, *Z. Phys.* **C48** (1990) 309–314.

[83] S. Jadach, M. Skrzypek and B. F. L. Ward, *Phys. Lett.* **B257** (1991) 173.

[84] A. B. Arbuzov, hep-ph/9910280.

[85] A. B. Arbuzov *et al.*, *JHEP* **10** (1997) 001, hep-ph/9702262.

[86] M. Skrzypek, *Acta Phys. Polon.* **B23** (1992) 135.

[87] A. B. Arbuzov, hep-ph/9908361.

[88] A. B. Arbuzov *et al.*, *Nucl. Phys.* **B485** (1997) 457–502, hep-ph/9512344.

[89] D. Bardin *et al.*, hep-ph/9908433.

[90] E. Kuraev and V. Fadin, *Sov. J. Nucl. Phys.* **41** (1985) 466–472.

[91] A. B. Arbuzov, E. A. Kuraev, N. P. Merenkov and L. Trentadue, *Nucl. Phys.* **B474** (1996) 271–285.

[92] A. B. Arbuzov, E. A. Kuraev, N. P. Merenkov and L. Trentadue, *Phys. Atom. Nucl.* **60** (1997) 591–600.

[93] A. B. Arbuzov, E. A. Kuraev and B. G. Shaikhatdenov, *J. Exp. Theor. Phys.* **88** (1999) 213, hep-ph/9805308.

[94] T. Ishikawa, T. Kaneko, K. Kato, S. Kawabata, Y. Shimizu and H. Tanaka, GRACE manual, KEK report 92–19, 1993.

[95] T. Munehisa, J. Fujimoto, Y. Kurihara, and Y. Shimizu, *Prog. Theor. Phys.* **95** (1996) 375.

[96] W. Beenakker *et al.*, WW cross-sections and distributions, in *Physics at LEP2*, Eds. G. Altarelli, T. Sjöstrand and F. Zwirner, CERN 96–01, Vol. 1, p. 79.

[97] F. A. Berends, G. J. H. Burgers, C. Mana, M. Martinez and W. L. van Neerven, *Nucl. Phys.* **B301** (1988) 583.

[98] F. Berends, G. Burgers and W. van Neerven, *Phys. Lett.* **B177** (1986) 191.

[99] M. Igarashi and N. Nakazawa, *Nucl. Phys.* **B288** (1987) 301.

[100] G. Montagna, M. Moretti, O. Nicrosini and F. Piccinini, *Nucl. Phys.* **B541** (1999) 31–49, hep-ph/9807465.

[101] K. Hagiwara, R. D. Peccei, D. Zeppenfeld and K. Hikasa, *Nucl. Phys.* **B282** (1987) 253.

[102] G. Montagna, O. Nicrosini and F. Piccinini, *Comput. Phys. Commun.* **98** (1996) 206–214.

[103] G. Passarino, *Nucl. Phys.* **B237** (1984) 249.

[104] F. Caravaglios and M. Moretti, *Phys. Lett.* **B358** (1995) 332–338, hep-ph/9507237.

[105] T. Ohl, *Comput. Phys. Commun.* **101** (1997) 269–288, hep-ph/9607454.

[106] D. Bardin *et al.*, Forward–backward asymmetries, in *Proc. of Workshop on Z Physics at LEP*, Geneva, 1989, Eds. G. Altarelli, R. Kleiss and C. Verzegnassi, report CERN 89–08 (1989), Vol. 1, pp. 201–234.

[107] D. Bardin *et al.*, Z line shape, in *Proc. of Workshop on Z Physics at LEP*, Geneva, 1989, Eds. G. Altarelli, R. Kleiss and C. Verzegnassi, CERN 89–08 (1989), Vol. 1, pp. 89–128.

[108] E. Accomando *et al.*, Standard Model processes, in *Physics at LEP2*, Eds. G. Altarelli, T. Sjöstrand and F. Zwirner, CERN 96–01 (1996), pp. 207–248, hep-ph/9601224.

[109] D. Bardin *et al.*, Electroweak working group report, in *Reports of the Working Group on Precision Calculations for the Z Resonance*, Eds. D. Bardin, W. Hollik and G. Passarino, CERN 95–03 (1995), pp. 7–162, hep-ph/9709229.

[110] D. Bardin and G. Passarino, Upgrading of precision calculations for electroweak observables, preprint CERN-TH/98–92 (1998), hep-ph/9803425 v.2.

[111] D. Bardin, M. Grünewald and G. Passarino, Precision calculation project report, hep-ph/9902452 (1999).

[112] P. Christova, M. Jack, S. Riemann and T. Riemann, Predictions of ZFITTER v.6 for fermion-pair production with acollinearity cut, DESY preprint 99–037 (1999), hep-ph/9908289.

[113] M. Jack, QED radiative corrections to $e^+e^- \to \bar{f}f$ with realistic cuts at LEP energies and beyond, talk given at 14th *Int. Workshop on High Energy Physics and Quantum Field Theory (QFTHEP 99)*, Moscow, Russia, 27 May – 2 Jun 1999, preprint DESY 99–166 (1999), hep-ph/9911296.

[114] P. Christova, M. Jack, S. Riemann and T. Riemann, Radiative corrections to $e^+e^- \to \bar{f}f$, ECFA/DESY note LC-TH-2000-008 (2000), contrib. to: Proc. of 2nd Joint ECFA/DESY Study on Physics and Detectors for a Linear Electron–Positron Collider, held at Orsay, Lund, Frascati, Oxford, and Obernai from April 1998 until Oct. 1999, to appear as DESY report 123F, *Physics Studies for a Future Linear Collider*, Eds. R. Heuer, F. Richard and P. Zerwas, `hep-ph/0002054`.

[115] D. Bardin, M. Bilenky, A. Chizhov, A. Sazonov, O. Fedorenko, T. Riemann and M. Sachwitz, *Nucl. Phys.* **B351** (1991) 1–48.

[116] D. Bardin, M. Bilenky, A. Sazonov, Y. Sedykh, T. Riemann and M. Sachwitz, *Phys. Lett.* **B255** (1991) 290–296.

[117] P. C. Christova, M. Jack and T. Riemann, *Phys. Lett.* **B456** (1999) 264, `hep-ph/9902408`.

[118] D. Bardin, P. Christova and O. Fedorenko, *Nucl. Phys.* **B175** (1980) 435.

[119] D. Bardin, P. Christova and O. Fedorenko, *Nucl. Phys.* **B197** (1982) 1.

[120] A. Akhundov, D. Bardin and T. Riemann, *Nucl. Phys.* **B276** (1986) 1.

[121] D. Bardin, S. Riemann and T. Riemann, *Z. Phys.* **C32** (1986) 121.

[122] D. Bardin, M. S. Bilenky, G. Mitselmakher, T. Riemann and M. Sachwitz, *Z. Phys.* **C44** (1989) 493.

[123] I. N. Silin, Fortran subroutine `SIMPS`.

[124] Y. Sedykh, Fortran subroutine `FDSIMP`.

[125] D. Bardin, A. Leike, T. Riemann and M. Sachwitz, *Phys. Lett.* **B206** (1988) 539–542.

[126] T. Riemann, The Z boson resonance parameters, in *Irreversibility and Causality, Proc. of the 21st Int. Colloquium on Group Theoretical Methods in Physics*, Goslar, 1996, Eds. A. Bohm, H. Doebner and P. Kielanowski, Lecture Notes in Physics, Vol. 504 (Springer, Berlin, 1998), pp. 157–177, `hep-ph/9709208`.

[127] A. R. Bohm and N. L. Harshman, On the mass and width of the Z-boson and other relativistic quasistable particles, Texas Univ. preprint (2000), `hep-ph/0001206`.

[128] T. Matsuura, Fortran subroutines `TRILOG` and `S12`.

[129] F. Jegerlehner, Fortran function `hadr5` (Feb 1995) see Ref. [17].

[130] G. Degrassi, Fortran package `m2tcor` (Oct 1996) see Refs. [167, 171].

[131] A. Arbuzov, Fortran packages `pairho` and `funang` (March 2000) see Ref. [144].

[132] B. Kniehl, Fortran package `bkqcdl5_14.f` (1990) see Ref. [207].

[133] G. Bonneau and F. Martin, *Nucl. Phys.* **B27** (1971) 381–397.

[134] M. Greco, G. Pancheri-Srivastava and Y. Srivastava, *Nucl. Phys.* **B101** (1975) 234–262.

[135] M. Greco, G. Pancheri-Srivastava and Y. Srivastava, *Phys. Lett.* **56B** (1975) 367.

[136] M. Greco, G. Pancheri-Srivastava and Y. Srivastava, *Nucl. Phys.* **B171** (1980) 118–140; E: *Nucl. Phys.* **B197** (1982) 543–546.

[137] B. A. Kniehl, M. Krawczyk, J. H. Kühn and R. G. Stuart, *Phys. Lett.* **209B** (1988) 337.

[138] M. Bilenky and A. Sazonov, QED corrections at Z^0 pole with realistic kinematical cuts, Dubna preprint JINR-E2-89-792 (1989).

[139] W. Beenakker, F. Berends and W. van Neerven, Applications of renormalization group methods to radiative corrections, in *Proc. of the Int. Workshop on Radiative Corrections for e^+e^- Collisions*, Schloß Ringberg, Tegernsee, 1989, Ed. J. H. Kühn (Springer, Berlin, 1989), p. 3.

[140] G. Montagna, O. Nicrosini and L. Trentadue, *Phys. Lett.* **231** (1989) 492.

[141] G. Montagna, O. Nicrosini and L. Trentadue, *Nucl. Phys.* **B357** (1991) 390.

[142] S. Jadach, M. Skrzypek and M. Martinez, *Phys. Lett.* **B280** (1992) 129–136.

[143] G. Montagna, O. Nicrosini and F. Piccinini, *Phys. Lett.* **B406** (1997) 243–248, `hep-ph/9611463 v.2`.

[144] A. Arbuzov, Light pair corrections to e^+e^- annihilation at LEP/SLC, `hep-ph/9907500`.

[145] G. Källén and A. Sabry, *K. Dan. Vidensk. Selsk., Mat.-Fys. Medd.* **17** (1955) 29.

[146] S. M. Berman, *Phys. Rev.* **112** (1958) 267.

[147] T. Kinoshita and A. Sirlin, *Phys. Rev.* **113** (1959) 1652–1660.

[148] G. Källén, *Springer Tracts in Modern Physics* **46** (1968) 67–132.

[149] M. Dine and J. Sapirstein, *Phys. Rev. Lett.* **43** (1979) 668.

[150] K. G. Chetyrkin, A. L. Kataev and F. V. Tkachev, *Phys. Lett.* **85B** (1979) 277.

[151] W. Celmaster and R. J. Gonsalves, *Phys. Rev. Lett.* **44** (1980) 560.

[152] G. Mann and T. Riemann, *Annalen Phys.* **40** (1984) 334.

[153] J. van der Bij and M. Veltman, *Nucl. Phys.* **B231** (1984) 205.

[154] J. J. van der Bij, *Nucl. Phys.* **B248** (1984) 141.

[155] A. Djouadi and C. Verzegnassi, *Phys. Lett.* **195B** (1987) 265.

[156] J. J. van der Bij and F. Hoogeveen, *Nucl. Phys.* **B283** (1987) 477.

[157] A. Djouadi, *Nuovo Cim.* **100A** (1988) 357.

[158] D. Bardin and A. Chizhov, On the $O(\alpha_{em}\alpha_s)$ corrections to electroweak observables, in *Proc. Int. Topical Seminar on Physics of e^+e^- Interactions at LEP Energies*, JINR Dubna, 1988, JINR preprint E2-89-525 (1989), Eds. D. Bardin *et al.*, pp. 42–48.

[159] S. Gorishny, A. Kataev and S. Larin, *Phys. Lett.* **B273** (1991) 141–144.

[160] A. L. Kataev, *Phys. Lett.* **B287** (1992) 209–212.

[161] A. B. Arbuzov D. Bardin, and A. Leike, *Mod. Phys. Lett.* **A7** (1992) 2029–2038,; E, **A9** (1994) 1515.

[162] J. Fleischer, O. V. Tarasov, F. Jegerlehner and P. Raczka, *Phys. Lett.* **B293** (1992) 437–444.

[163] R. Barbieri, P. Ciafaloni and A. Strumia, *Phys. Lett.* **B317** (1993) 381.

[164] L. Avdeev, J. Fleischer, S. Mikhailov and O. Tarasov, *Phys. Lett.* **B336** (1994) 560–566; E, **B349** (1995) 597, hep-ph/9406363.

[165] K. Chetyrkin, J. Kühn and A. Kwiatkowski, QCD corrections to the e^+e^- cross-section and the Z boson decay rate, in *Reports of the Working Group on Precision Calculations for the Z Resonance,* Eds. D. Bardin, W. Hollik and G. Passarino, CERN 95–03 (1995), pp. 175–263, hep-ph/9503396.

[166] G. Degrassi, P. Gambino and A. Vicini, *Phys. Lett.* **B383** (1996) 219–226, hep-ph/9603374.

[167] G. Degrassi, P. Gambino and A. Sirlin, *Phys. Lett.* **B394** (1997) 188–194, hep-ph/9611363.

[168] T. van Ritbergen and R. G. Stuart, *Phys. Lett.* **B437** (1998) 201, hep-ph/9802341.

[169] T. van Ritbergen and R. G. Stuart, *Phys. Rev. Lett.* **82** (1999) 488, hep-ph/9808283.

[170] R. Harlander, T. Seidensticker, and M. Steinhauser, *Phys. Lett.* **B426** (1998) 125–132, hep-ph/9712228.

[171] G. Degrassi and P. Gambino, Two loop heavy top corrections to the Z^0 boson partial widths, Padua Univ. preprint DFPD-99-TH-19 (1999), hep-ph/9905472.

[172] D. Bardin and G. Passarino, *The Standard Model in the Making: Precision Study of the Electroweak Interactions* (Clarendon, Oxford, 1999).

[173] A. Leike, T. Riemann and J. Rose, *Phys. Lett.* **B273** (1991) 513–518, hep-ph/9508390.

[174] T. Riemann, *Phys. Lett.* **B293** (1992) 451–456, hep-ph/9506382.

[175] M. Grünewald, S. Kirsch and T. Riemann, Fortran Program SMATASY v.6.10 (27 May 1999); obtainable from
/afs/cern.ch/user/g/gruenew/public/smatasy/smata6_10.fortran
or from http://l3www.cern.ch/homepages/gruenew/welcome.html.

[176] S. Riemann, Fortran Program ZEFIT v. 5.0 (1997);
obtainable from http://www.ifh.de/~riemanns/uu/zefit5_0.uu.

[177] J. H. Field and T. Riemann, *Comput. Phys. Commun.* **94** (1996) 53–87, hep-ph/9507401.

[178] A. Arbuzov, D. Bardin, J. Blümlein, L. Kalinovskaya and T. Riemann, *Comput. Phys. Commun.* **94** (1996) 128, hep-ph/9511434.

[179] A. Arbuzov, in preparation.

[180] M. Greco, *Phys. Lett.* **B240** (1990) 219.

[181] A. H. Hoang, J. H. Kuhn and T. Teubner, *Nucl. Phys.* **B455** (1995) 3–20, hep-ph/9507255.

[182] D. Bardin *et al.*, *Comput. Phys. Commun.* **104** (1997) 161, hep-ph/9612409.

[183] M. W. Grunewald *et al.*, hep-ph/0005309.

[184] D. Bardin, A. Leike and T. Riemann, *Phys. Lett.* **B344** (1995) 383–390, hep-ph/9410361.

[185] M. Verzocchi, Rew99: a library of routines for reweighting four-fermion Monte Carlo samples based on the grc4f matrix elements, OPAL-TN 618, August 1999, OPAL Technical Note, unpublished.

[186] S. Jadach, W. Placzek, M. Skrzypek, B. F. L. Ward and Z. Wąs, *Comput. Phys. Commun.* **119** (1999) 272–311, hep-ph/9906277.

[187] M. Skrzypek, S. Jadach, W. Płaczek and Z. Wąs, *Comput. Phys. Commun.* **94** (1996) 216.

[188] M. Skrzypek, S. Jadach, M. Martinez, W. Płaczek and Z. Wąs, *Phys. Lett.* **B372** (1996) 289.

[189] W. Beenakker and A. Werthenbach, hep-ph/0005316.

[190] J. H. Kuhn, A. A. Penin and V. A. Smirnov, hep-ph/0005301.

[191] P. Ciafaloni and D. Comelli, *Phys. Lett.* **B476** (2000) 49, hep-ph/9910278.

[192] M. Melles, hep-ph/0006077.

[193] M. Greco and A. F. Grillo, *Nuovo Cim. Lett.* **15** (1976) 174.

[194] B. W. Lynn and R. G. Stuart, *Nucl. Phys.* **B253** (1985) 216.

[195] J. H. Kühn and R. G. Stuart, *Phys. Lett.* **200B** (1988) 360.

[196] P. Holt, *Z. Phys.* **C72** (1996) 31.

[197] P. Holt, *Acta Phys. Pol.* **B25** (1997) 689.

[198] E. A. Kuraev and V. S. Fadin, *Yad. Fiz.* **41** (1985) 733–742 (in Russian).

[199] G. Passarino, The PP-LEP2Poll, transparencies, 8 December 1999, **www** page at http://www.to.infn.it/∼giampier/latex/pp_quest.ps.

[200] OPAL Collaboration, See Ref. [7], and also: http://home.cern.ch/∼mkobel/lep2mc/index.html.

[201] S. Jadach, M. Skrzypek and B. Ward, *Phys. Rev.* **D55** (1997) 1206.

[202] G. Passarino, unpublished.

[203] T. Teubner, private communication.

[204] G. Montagna, F. Piccinini, O. Nicrosini, G. Passarino and R. Pittau, *Nucl. Phys.* **B401** (1993) 3–66.

[205] G. Montagna, F. Piccinini, O. Nicrosini, G. Passarino and R. Pittau, *Comput. Phys. Commun.* **76** (1993) 328–360.

[206] G. Montagna, O. Nicrosini, F. Piccinini and G. Passarino, *Comput. Phys. Commun.* **117** (1999) 278, hep-ph/9804211.

[207] B. Kniehl, *Nucl. Phys.* **B347** (1990) 86--104.